Using Multi-Parametric Imaging and Multi-Nuclear Cardiac Magnetic Resonance to Investigate Novel Treatment Strategies for Heart Failure

Moritz Jens Hundertmark

MD

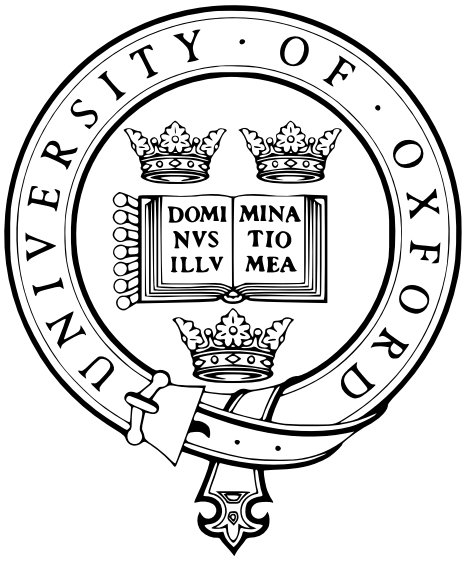

St. Catherine's College

Division of Cardiovascular Medicine

Radcliffe Department of Medicine

University of Oxford

A thesis submitted for the degree of

Doctor of Philosophy in Medical Sciences

Hilary Term 2022

Declaration

This Thesis and all results herein are entirely my own work, unless otherwise indicated. The present results have not been submitted, either wholly or substantially, for another degree at this university, or for a degree at any other institution. I have acknowledged assistance from colleagues and collaborators where relevant.

The total word count is 41424 words (excluding front matter, abstract and bibliography).

Abstract

Heart failure (HF) remains the leading cause for hospitalisation in patients over the age of 65 years in industrialised nations. Furthermore, prognosis of HF remains poor and lags behind the improvements observed for similar chronic conditions like cancer, despite efforts for new therapies. However, these therapies are mostly available for patients with HF and a reduced ejection fraction (HFrEF), whereas prognostically relevant therapies for patients with HF and a preserved ejection fraction (HFpEF) have been absent for more than 20 years and this only changed very recently with the results of the *EMPEROR-preserved* trial[1] investigating treatment with empagliflozin (10 mg once daily) in patients with HFpEF. Equally, a significant improvement of quality of life and physical limitations has been shown for patients with HFpEF following treatment with dapagliflozin in PRESERVED-HF.[2]

An increasing amount of evidence describes more subtypes of the complex and rather arbitrarily classified syndrome of HF and thus, there is a growing need for comprehensive, non-invasive imaging techniques to identify and individually phenotype patients affected. Furthermore, the same approach could be used to assess novel treatments as well as identify treatment responders, further tailoring individual patient management and aid efforts to improving prognosis. Additionally, use of a model imaging technique may lower the exponential costs of

drug development by reducing the numbers of subjects needing to be enrolled and increasing reproducibility of findings.

Cardiovascular magnetic resonance (CMR) fulfils many of the demands for a model imaging technique in the context of HF-phenotyping and -drug development. Firstly, CMR is the gold standard method to assess cardiac structure and function. More importantly, it allows examination of imaging and metabolic parameters alike and, with novel techniques like dynamic nuclear polarisation (i.e. hyperpolarized MR spectroscopy), even direct assessments of molecular cellular pathways. Thirdly, HF is a syndrome affecting multiple organ systems and thus, has complex and incompletely understood links in need of exploration. MR offers the possibility of multi-organ assessment in the same session and therefore, is perfectly placed to gather information on the biological interplay in HF.

The underlying mechanism for the observed benefits of sodium glucose like transporter 2 inhibitors (SGLT2i) like empagliflozin in HFrEF are not yet understood. One of the leading hypotheses brought forward was that SGLT2i may induce changes in myocardial substrate selection via increased availability of ketone bodies which may serve as an additional energy source for the failing heart. Thus, I sought to investigate whether empagliflozin treatment (10mg per day) would enhance myocardial energetics in patients with HFrEF (phosphocreatine to adenosine triphosphate ratio, PCr/ATP). In this randomised controlled trial (RCT), patients did not improve measures of resting or dobutamine stress myocardial energetics (**Chapter 3**) and empagliflozin treatment neither altered a panel of 19 serum metabolites assessed by targeted metabolomic analysis. However, there were interesting changes to the amount of triglycerides stored in the heart, myocardial

cell volume and hypertrophy as well as markers of fibrosis and quality of life (QoL). This exemplifies the usefulness of CMR in the interrogation of novel treatments and likewise emphasises that the broad range of indications for SGLT2i (diabetes, chronic kidney disease, heart failure) is possibly mirrored by a multi-organ rather than a single cardio-specific effect in patients with HFrEF.

As it was unclear until very recently if patients with HFpEF would equally benefit from treatment with SGLT2i, I further integrated a HFpEF cohort into the RCT and investigated the identical variety of parameters as for the HFrEF patients (**Chapter 4**). Similarly to the findings in the HFrEF cohort (**Chapter 3**), I could not observe any changes to myocardial energetics (resting PCr/ATP as primary endpoint) or whole-body substrate usage (targeted metabolomics). Interestingly, I detected certain similarities nevertheless as myocardial triglycerides reduced in the treatment arm but not in the placebo group. Furthermore, systolic function (peak circumferential and radial strain) and measures of pulmonary function improved. This was also paralleled by a numerically improved walking distance in the six-minute walk test (6MWT) and increased QoL (assessed by the Kansas City Cardiomyopathy Questionnaire; KCCQ). The present results reinforce the need for mechanistic experiments in human subjects *in-vivo*, as they highlight the disparity of results from animal models that previously showed a metabolic effect following treatment with SGLT2i. Furthermore, more research is needed into effects of drugs in different HFpEF subtypes (e.g. diabetic, obese) to improve risk stratification and adequate treatment.

To explore novel, non-pharmacological treatments targeting unique subgroups under the '*HFpEF-umbrella'*, I aimed to explore whether a lifestyle intervention of weight loss is an effective treatment for patients with obesity and HFpEF (**Chapter 5**). Accordingly, I enrolled patients with a clinical diagnosis of HFpEF and observed cardio-metabolic effects following 10 weeks of a very low energy diet (VLED). Assessments included exercise CMR and dobutamine stress phosphorus magnetic resonance spectroscopy (^{31}P-MRS). While cardiac energetics at rest or during dobutamine stress did not change, prognostic serum markers (n-terminal pro-BNP; NT-proBNP) and symptom burden (New York Heart Association; NYHA) improved significantly and cardiac structure (LV-mass) as well as function (diastolic function on echo and RV function at rest and during exercise) ameliorated. The results emphasise that lifestyle treatments in select patient groups are underutilised yet cost-efficient, safe and successful. Furthermore, the obesity paradox (describing the observation that mild obesity appears to be protective in HF) may not equally apply to the group of severely obese HFpEF patients (BMI>30 kg/m^2) and thus, this should be investigated in larger trials.

Finally, I was interested to examine the feasibility of CMR in the context of early (phase IIa) cardio-metabolic drug development. In **Chapter 6**, I enrolled 22 patients with type 2 diabetes (T2D) but no underlying HF and investigated the effects of ninerafaxstat, a novel drug intended to enhance myocardial substrate metabolism via restoring metabolic flexibility in the heart. Here I show that the drug's proposed mechanism of action can indeed be successfully investigated by using [1-^{13}C]pyruvate hyperpolarized MRS. The pyruvate dehydrogenase (PDH) flux was improved in the majority of subjects (7/9). Furthermore, this resulted in

significantly improved PCr/ATP and reduced myocardial steatosis. Diastolic function and early LV-filling also improved following drug treatment for 4 or 8 weeks. Based on these results, hyperpolarized MRS is a suitable tool to investigate the mechanism of action in early drug development in humans with reduced sample sizes. The broader implication is certainly that, similar to treatments for immune modulation (e.g. canakimumab), patient selection is key for metabolic assessments in clinical trials.

To summarise, this Thesis examines cardio-metabolic effects of different pharmacological and lifestyle treatments in distinct populations and further demonstrates the suitability of CMR as an investigational tool for drug development. While the results underpin the importance of substrate selection and implications on cardiac structure and function, improved patient selection is key for demonstrating these effects with statistical significance. Furthermore, refuting the '*fuel hypothesis'* theory as the main contributor to SGLT2i's mode of action, I provide evidence for multi-organ effects of SGLT2i being likely responsible for the benefits observed in HF. Secondly, I add to the existing evidence that intentional weight loss is a safe and effective treatment in obese HFpEF patients.

Publications

Manuscripts Contributing to DPhil Thesis

1. **Hundertmark, M. J**., Agbaje, O. F., Coleman, R., George, J. T., Grempler, R., Holman, R. R., ... & Neubauer, S. (2021). Design and rationale of the EMPA-VISION trial: investigating the metabolic effects of empagliflozin in patients with heart failure. ESC Heart Failure, 8(4), 2580-2590
2. **Hundertmark M. J.*,** Burrage MK*, Valkovič L, Watson WD, Rayner J, Sabharwal N, Ferreira VM, Neubauer S, Miller JJ[#], Rider OJ[#], Lewis AJM[#]. Energetic basis for exercise-induced pulmonary congestion in heart failure with preserved ejection fraction. Circulation. (Ahead of Print) *contributed equally, [#]contributed equally

Other Publications During DPhil

1. Frantz, S., **Hundertmark, M. J**., Schulz-Menger, J., Bengel, F. M., & Bauersachs, J. (2022). Left ventricular remodelling post-myocardial infarction: pathophysiology, imaging, and novel therapies. *European Heart Journal*.
2. Raman, B., Tunnicliffe, E. M., Chan, K., Ariga, R., **Hundertmark, M.,** Ohuma, E. O., ... & Neubauer, S. (2021). Association Between Sarcomeric Variants in Hypertrophic Cardiomyopathy and Myocardial Oxygenation: Insights From a Novel Oxygen-Sensitive Cardiovascular Magnetic Resonance Approach. *Circulation*, 144(20), 1656-1658.

3. Apps, A., Valkovič, L., Peterzan, M., Lau, J. Y., **Hundertmark, M**., Clarke, W., ... & Schmid, A. I. (2021). Quantifying the effect of dobutamine stress on myocardial Pi and pH in healthy volunteers: A 31P MRS study at 7T. *Magnetic resonance in medicine*, 85(3), 1147-1159.
4. Peterzan, M.A., Clarke, W.T., Lygate, C.A., Lake, H.A., Lau, J.Y., Miller, J.J., Johnson, E., Rayner, J.J., **Hundertmark, M.J**., Sayeed, R. and Petrou, M., 2020. Cardiac energetics in patients with aortic stenosis and preserved versus reduced ejection fraction. *Circulation*, 141(24), 1971-1985.
5. **Hundertmark, M**. (2020). Should CMR be the default imaging modality in clinical trials for heart failure?. *Cardiovascular Diagnosis and Therapy*, 10(3), 554.
6. Clarke, W.T., Peterzan, M.A., Rayner, J.J., Sayeed, R.A., Petrou, M., Krasopoulos, G., Lake, H.A., Raman, B., Watson, W.D., Cox, P. and **Hundertmark, M.J**., 2019. Localized rest and stress human cardiac creatine kinase reaction kinetics at 3 T. *NMR in Biomedicine*, 32(6), p.e4085.
7. **Hundertmark, M**., Williams, T., Vogel, A., Moritz, M., Bramlage, P., Pagonas, N., ... & Sasko, B. (2019). Capnocytophaga canimorsus as cause of fatal sepsis. *Case reports in infectious diseases*, 2019.
8. **Hundertmark, M.,** & Wicks, E. (2018). Diabetes mellitus and heart failure: insights from a toxic relationship. *Practical Diabetes*, 35(4), 112-116b.

Table of Contents

List of Figures

List of Tables

List of Abbreviations

^{1}H	proton/hydrogen
3D-CSI	three dimensional chemical shift imaging
6-MWT	six-minute walk test
^{18}F	fluorine 18
^{31}P	phosphorus
°C	degrees Celsius
µg	microgram
Acetyl-CoA	acetyl coenzyme A
ADP	adenosine diphosphate
AE	adverse event
AF	atrial fibrillation
AHA	American Heart Association
AIF	arterial input function
AMP	adenosine monophosphate
AMPK	adenosine monophosphate activated protein kinase
ANCOVA	analysis of covariance
ANOVA	analysis of variance
AS	aortic stenosis
ATP	adenosine triphosphate
AUC	area under the curve
β-OHB	beta hydroxybutyrate
BCAA	branched-chain amino acids
BMI	body mass index
BMIPP	^{123}I-βmethyl-P-iodophenylpentadecanoic acid

BP	blood pressure
bpm	beats per minute
bSSFP	balanced steady-state free precession
Ca^{2+}	Calcium
CABG	coronary artery bypass grafting
CAD	coronary artery disease
CHF	chronic heart failure
CI	confidence interval
CK	creatine kinase
CK_{MB}	myofibrillar creatine kinase
CK_{mito}	mitochondrial creatine kinase
CKD	chronic kidney disease
CMR	cardiovascular magnetic resonance
CoQ	coenzyme Q
CPET	cardiopulmonary exercise test
CPT1	carnitine palmitoyl transferase 1
CRT	cardiac resynchronization therapy
CT	computed tomography
CTCA	computed tomography coronary angiography
CVD	cardiovascular disease
CW	continuous wave
DCA	dichloroacetate
DCM	dilated cardiomyopathy
DICOM	Digital Imaging and Communications in Medicine
DPG	diphosphoglycerate
DRESS	depth resolved surface coil spectroscopy
ECG	electrocardiogram
ECV	extracellular volume
EDV	end-diastolic volume
EDTA	ethylenediaminetetraacetic acid
EF	ejection fraction

eGFR	estimated glomerular filtration rate
EOS	end of study
EOT	end of treatment
EPA	electron paramagnetic agent
EQ-5D5L	5 level EQ-5D
ESV	end-systolic volume
ETC	electron transport chain
FA	fatty acid
$FADH_2$	dihydro flavin adenine dinucleotide
FAO	fatty acid oxidation
FAT / CD36	fatty acid translocase
FDG	fluorodeoxyglucose
FEV_1	forced expiratory volume at 1 second
FFA	free fatty acid
FLASH	fast low-angle shot
FOV	field of view
FVC	forced vital capacity
GBCA	gadolinium-based contrast agent
Gd	gadolinium
GI	gastro-intestinal
GLUT	glucose transporter
GP	general practitioner
GRAPPA	generalized auto-calibrating partially parallel acquisition
GRE	gradient echo
HbA1c	glycated haemoglobin A1c
HF	heart failure
HFpEF	heart failure with a preserved ejection fraction
HFrEF	heart failure with a reduced ejection fraction
HLA	horizontal long axis
HR	heart rate

ICA	invasive coronary angiography
IHD	ischaemic heart disease
IMP	investigational medicinal product
IQR	interquartile range
IR	inversion recovery
IV	intravenous
Kcal	kilocalorie
LAVI	left atrial volume index
LC	liquid chromatography
LDH	lactate dehydrogenase
LGE	late gadolinium enhancement
LV	left ventricle/ventricular
LVEDVi	left ventricular end diastolic volume index
LVEF	left ventricular ejection fraction
LVMi	left ventricular mass index
LVOT	left ventricular outflow tract
MACE	major adverse cardiovascular event
MBF	myocardial blood flow
MBV	myocardial blood volume
MCT4	monocarboxylate transporter 4
mg	milligram
Min	minute/minutes
ml	millilitre
mmHg	millimetre mercury
MOCO	motion correction
MPI/MPS	myocardial perfusion imaging/scan
MR	magnetic resonance
MRI	magnetic resonance imaging
MRP	meal replacement product
MRS	magnetic resonance spectroscopy
ms	millisecond

MS	mass spectroscopy
MTG	myocardial triglyceride/triglycerides
NADH	nicotinamide adenine dinucleotide
NHS	National Health Service
NMR	nuclear magnetic resonance
NOE	nuclear Overhauser effect
NPV	negative predictive value
NR	nicotinamide riboside
NRES	national research ethics service
NYHA	New York Heart Association
OCDEM	Oxford Centre for Diabetes, Endocrinology and Metabolism
OCMR	Oxford Centre for Clinical Magnetic Resonance Research
OMT	optimal medical treatment
OUH	Oxford University NHS Hospitals Foundation Trust
PCI	percutaneous coronary intervention
PCr	phosphocreatine
PCr/ATP	phosphocreatine to adenosine triphosphate ratio
PDE	phosphodiester
PDFF	proton density fat fraction
PET	positron emission tomography
Pg	picogram
PLS-DA	partial least-squares discriminant analysis
PPA	phenylphosphonic acid
PPAR	peroxisome proliferator activated receptors
PPS	per protocol set
PRESS	point-resolved spectroscopy
PW	pulsed wave
QC	quality control
QoL	quality of life

RAAS	renin angiotensin aldosterone system
REC	research ethics committee
RER	respiratory exchange ratio
RF	radiofrequency
ROC	receiver operating characteristic
ROI	region of interest
ROS	reactive oxygen species
RS	randomised set
SA	short axis
SAR	specific absorption rate
SBP	systolic blood pressure
SD	standard deviation
SE	standard error
SEM	standard error of the mean
SFP	sterile fluid pathway
SCMR	Society for Cardiovascular Magnetic Resonance
SCOT	succinyl-CoA:3-oxoacid-CoA-transferase
SD	standard deviation
SGLT2i	sodium glucose transporter 2 inhibitor
ShMOLLI	Shortened Modified Look-Locker Inversion recovery
SPECT	single-photon emission computed tomography
STEAM	stimulated echo acquisition mode
SV	stroke volume
T	Tesla
T1	longitudinal or spin-lattice relaxation
T2	transverse or spin-spin relaxation
T1D	type 1 diabetes mellitus
T2D	type 2 diabetes mellitus
TD	trigger delay
TCA	tricarboxylic acid cycle

TE	echo time
TI	inversion time
TR	repetition time
TTE	transthoracic echocardiography
UTE	ultra-short echo time
UK	United Kingdom
USA	United States of America
V	volt
VLA	vertical long axis
VLED	very low energy diet
W	watt
WOCBP	woman/women of childbearing potential

Acknowledgements

The pandemic has expedited the digitalisation of Medicine and Academia. I would like to contribute to positive change and thus, have decided to make my acknowledgements available without any barriers by following the QR-code below.

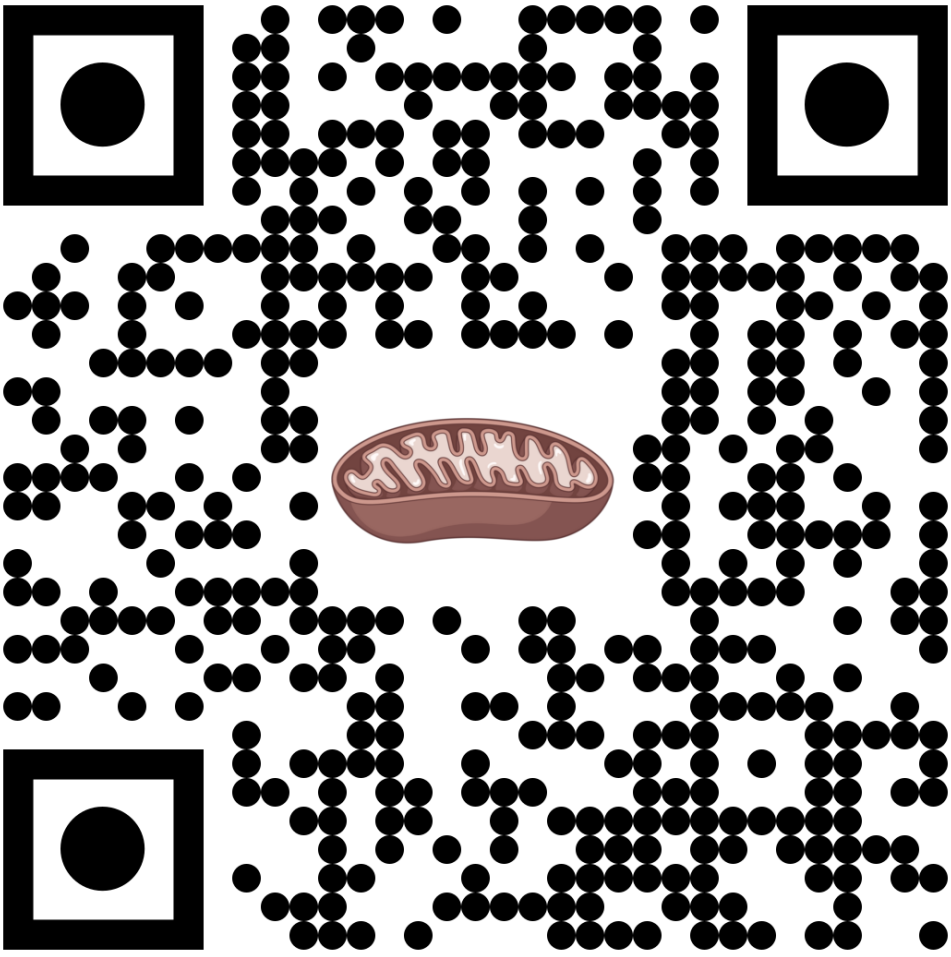

1 Introduction

1.1 Overview

Chronic heart failure (CHF) is a clinical syndrome with significant consequences for the individual but also society as a whole. Globally, it generates costs of more than $100 billion and in the UK alone accounts for more than 2% of all healthcare-related annual spending.[3] HF prevalence is continuously rising while its incidence remains broadly unaffected, despite available drug and device management.[4] For the last decade, the number of patients with HFpEF have increased steadily and HFpEF is now the most common form of HF.[5]

Currently, HF is categorised following the arbitrary measure of left ventricular ejection fraction (LVEF), which is a result of the early availability of echocardiography for the first therapeutic clinical trials of vasodilating agents in HF[6] rather than reflection of pathophysiological links. As such, there is continuous debate whether this emphasis on a measure of ventricular output is adequate to mirror the pathophysiological changes underlying HF.[7]

The heart has an unmitigated need for energy provision as systolic contraction and diastolic relaxation are active consumers of adenosine triphosphate (ATP). As a result, almost 30 % of the cardiomyocyte volume is reserved for mitochondria in which energy in form of ATP is generated under use of oxygen (oxidative phosphorylation).[8] Substrates for this process are fat, carbohydrates, branched chain

amino acids (BCAA), ketones and lactate which are converted into acetyl coenzyme A (acetyl-CoA) before entering the tricarboxylic acid cycle (TCA). HF and metabolic diseases like type 2 diabetes (T2D) and obesity share common features of derangements in energy metabolism. However, each of these conditions has a distinct signature of adverse metabolic alterations. Thus, in the first part of the introductory chapter, I will review existing evidence on changes of metabolism in the normal heart and conversely, elaborate on distinct changes in cardio-metabolic diseases.

Therapeutic modulation of energy metabolism is the central topic of this thesis hence, I will examine the available literature on pharmacological and lifestyle interventions and their effects on substrate metabolism in the failing heart.

Cardiovascular magnetic resonance (CMR) is perfectly suited to investigate metabolic and functional changes of the heart muscle in health and disease. However, other techniques to investigate metabolism exist and thus, the last part of this chapter will be devoted to review the potential advantages and drawbacks of the different available techniques.

1.2 Physiological energy metabolism in the heart

The heart is frequently described as an epicurean of all forms of available energy. Generating around three grams of ATP per heartbeat it has a vast demand of continuous energy supply.[9,10] Overall, three important (main) steps can be singled out of the process of supplying incessant energy:

1. Energetic substrates are shuffled into the cell
2. Conversion of substrates into Acetyl-CoA before entering the tricarboxylic acid cycle (TCA) generating reducing equivalents to fuel the reaction of oxidative phosphorylation in the mitochondria[11]
3. Replenishing the ATP pool by transferring energy-containing phosphate bonds from ADP to ATP

Myocardial energy supply, under resting conditions and with sufficient availability of oxygen, is mainly secured by use of fat (70 %) and glucose (20 %) while the other 10% are a mix of ketone bodies, lactate, pyruvate and BCAAs.[12] The ability to swiftly switch between different substrates according to demands and availability has been termed 'metabolic flexibility' and represents one of the core features of the healthy heart (**Figure 1.1**).[13]

Figure 1.1: Physiological Cardiac Energy Metabolism

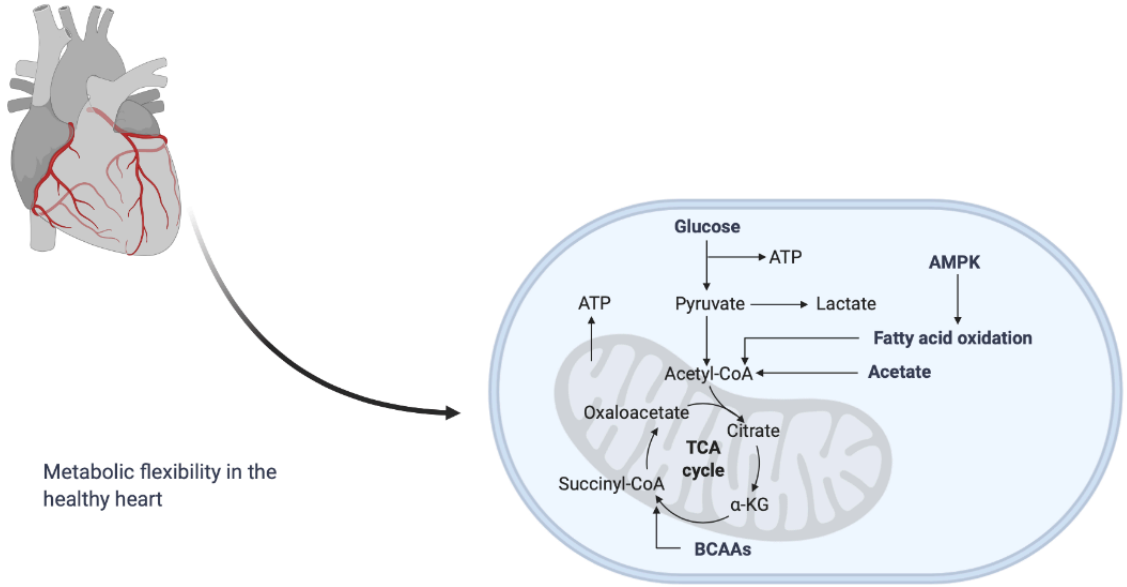

***Figure 1.1: Physiological Cardiac Energy Metabolism**. The healthy heart uses a variety of available substrates concomitantly and can momentarily switch from one to the other.*

*This metabolic flexibility is one of the hallmarks of the healthy heart's energy metabolism. **α**-KG=alpha ketoglutarate; Acetyl-Coa=acetyl coenzyme A; AMPK=adenosine monophosphate activated protein kinase; ATP=adenosine triphosphate; BCAA=branched-chain amino acids; Succinyl CoA=succinyl coenzyme A*

1.2.1 Myocardial substrates

Lipids, in the form of fatty acids, bound to albumin or triglycerides as part of very low-density lipoproteins (VLDL) reach cardiomyocytes via the bloodstream. Cellular uptake is generally passive although the process is often facilitated by a complex in the cellular membrane called fatty acid translocase (FAT or CD36; **Figure 1.2**).[14] When inside the cell, the rate limiting enzyme carnitine palmitoyl transferase 1 (CPT-1) facilitates formation of long chain acylcarnitine which then enters the mitochondria. Here, a series of chemical reactions called 'beta-oxidation' converges this further into acetyl-CoA which enters the TCA and generates proton donors ($FADH_2$ and NADH) for the respiratory chain and thus, ATP replenishment. This finely tuned process is orchestrated and tightly regulated. CPT-1 for example is inhibited by malonyl-CoA which is only accumulated in higher concentrations if there is an oversupply of acetyl-CoA. Upstream regulation occurs via peroxisome proliferator activated receptors (PPAR) which are activated by triglycerides.[15] The energy yield from fatty acid oxidation (FAO) is the greatest of all substrates but likewise uses the most oxygen hence, paradoxically, fatty acids are the least efficient energy substrates when comparing the amount of ATP produced per mol of oxygen consumed.[16]

Glucose on the other hand, is considered the most efficient carbon substrate fuel for ATP generation as it has a favourable amount of oxygen consumption due to the

fact that its glycolytic conversion to pyruvate can occur anaerobically, producing lactate.[17,18] Glucose is taken up by the cardiomyocyte largely via glucose transporter 4 (GLUT4) which facilitates glucose shuffling in an insulin-dependent manner while GLUT1 enables insulin independent translocation.[19] In order to keep the glucose in the cytoplasm, the enzyme 'hexokinase' phosphorylates it to glucose-6-phosphate which may be converted to glycogen for storage or enter glycolysis to produce pyruvate. Pyruvate can be converted to lactate (in case of hypoxic environments) or enter the mitochondria via mitochondrial pyruvate carriers (MPC) and is then oxidised to acetyl-CoA via pyruvate dehydrogenase (PDH) before entering the TCA. Equally to FA usage, energy production from glucose has multiple regulating steps. PDH is inhibited by a surplus of acetyl-CoA and NADH from beta-oxidation resulting in inhibition of activity via PDH-kinase.[20]

Glucose and lipid metabolism are co-dependent on one another and regulate each other via a process called the 'Randle cycle'.[21] In short, this process is designed to link substrate usage to availability (**Figure 1.2**).

Figure 1.2: Glucose- and Fatty Oxidation Pathways

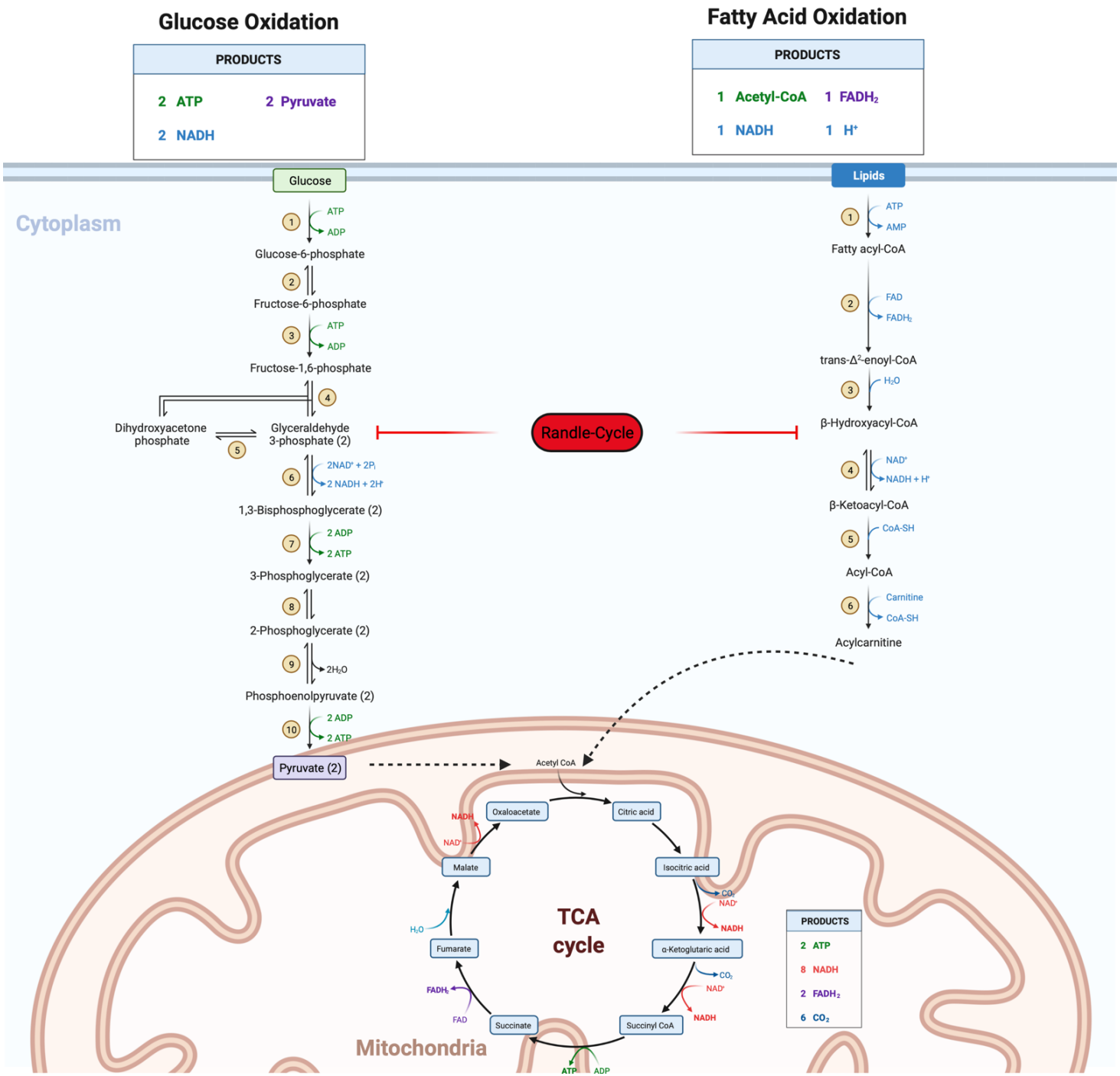

Figure 1.2: Glucose and Fat Oxidation pathways. *Schematic overview of the individual steps required for translocation of glucose (left) and fatty acids (right) into the mitochondria to feed into the tricarboxylic acid cycle.*

Lactate, under conditions of higher levels in the bloodstream, can be taken up by the heart via monocarboxylate transporter 4 (MCT4) and reversibly be converted to pyruvate via lactate dehydrogenase (LDH) which then enters the mitochondria where it is used for ATP-generation (see above).[18]

Recently, it was shown that ketone bodies as substrates can contribute to ATP-production considerably if general ketone levels are elevated.[22] beta-hydroxybutyrate (β-OHB) and acetoacetate are the two main ketone isoforms circulating in the blood stream and the heart preferentially uses β-OHB as a substrate. Uptake into cardiomyocytes occurs via MCT1 (SLC16A1) and the rate limiting enzyme for conversion into acetyl-CoA is succinyl-CoA:3-oxoacid-CoA-transferase (SCOT). Regulation is currently poorly understood and ketone bodies also appear to have signalling properties hence, more research is needed to elucidate this complex procedural network.[23]

Branched-chain amino acids (BCAA) can be oxidised in the heart and thus, represent a potential source of ATP generation (usually < 2 %).[24] More importantly, BCAAs appear to have a substantial function in modulating cardiac signalling pathways and as such may be promoting insulin resistance via leucine induced impairment of insulin receptors and/or accumulation of potentially toxic BCAA intermediates.[25]

1.2.2 Oxidative phosphorylation

The vast majority of energy generated (95% under resting conditions) results from a process whereby electrons are shuffled through a series of enzymatic complexes (electron transport chain, ETC) located in the inner mitochondrial membrane under the use of reducing equivalents (NADH / FADH).[8] As there is a proton gradient across the inner mitochondrial membrane which is created by electron donation of reducing equivalents ($FADH_2$ and NADH) created from metabolic substrates feeding into the TCA[11], a hydrogen gradient drives the electron transfer to oxygen and thus the ATP-synthase creating ATP from ADP (**Figure 1.3**).[8] Importantly not all substrates create an equal amount of usable, free energy (ΔG ATP) as reducing equivalents enter the ETC in different locations. As such, $FADH_2$ entering the ETC in complex II will provide a lower energetic gradient, resulting in a lower amount of ATP generated.[26,27]

Figure 1.3: Electron Transport Chain

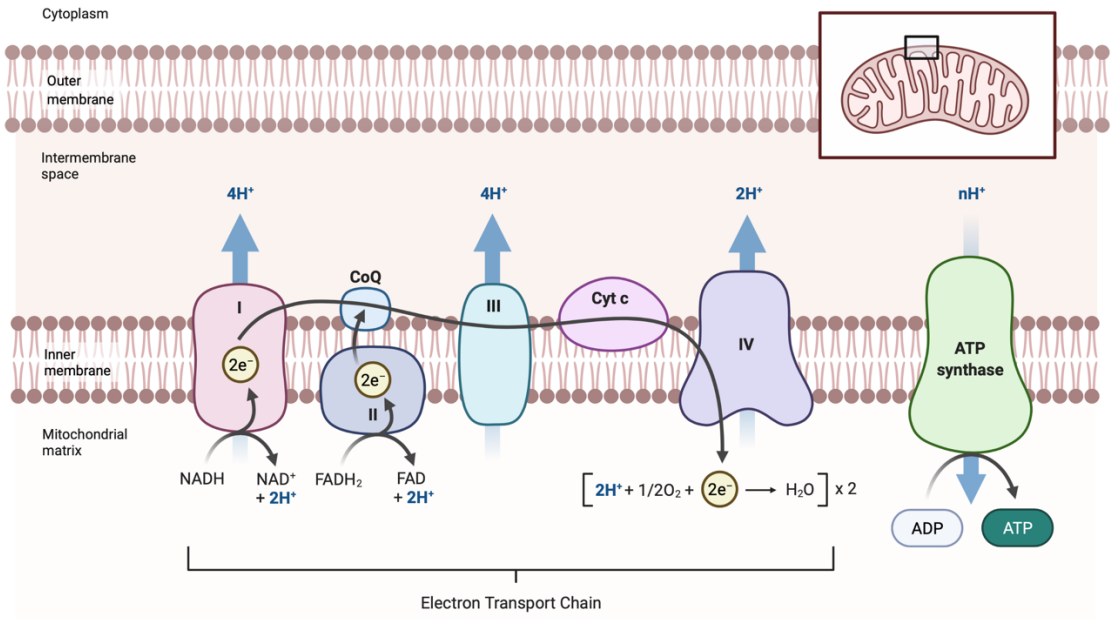

***Figure 1.3: Electron Transport Chain**. Graphic of the outer (top layer) and inner (bottom layer) mitochondrial membrane and intermembrane space. The electron transport chain (ETC) consists of four complexes that transfer hydrogen (H^+) from reducing equivalents ($NADH_2$ / FADH) and shuffle them into the intermembrane space while transferring electrons (e^-) to oxygen (O_2). This creates a gradient which fuels the ATP-synthase creating adenosine triphosphate (ATP).*

FAO produces twice as much NADH than $FADH_2$ while the generation of NADH from glucose oxidation and oxidation of ketones is four times greater.[28] Furthermore, ketones increase the redox potential between complex I and II of the ETC by oxidising Coenzyme Q and thus, increase ΔG from ATP-hydrolysis.[29]

1.2.3 Phosphotransfer

Because the heart would run out of ATP exceptionally quickly if only relying on the turnover rate of the mitochondrial ETC, it needs an energy reserve.[30,31] In the adult heart, phosphocreatine (PCr) content is twice as high as ATP.[32] The enzyme creatine kinase (CK) facilitates the reversible transfer of the γ-phosphoryl group of ATP to creatine and thus, creates PCr and ADP.[33] As ATP is polar and relatively big, it cannot move quickly within the cardiomyocyte to reach areas in higher demand of energy. As such, the phosphotransfer reactions ensure constant ATP levels and likewise adequate spatial distribution of high-energy phosphates. Due to the fact that CK exists in two different isoforms, mitochondrial CK (CK_{mito}) and myofibrillar CK (CK_{MB}), the reaction has a polarity and its equilibrium rests on the site of ATP-creation (**Figure 1.4**).

Figure 1.4: The Creatine Kinase System

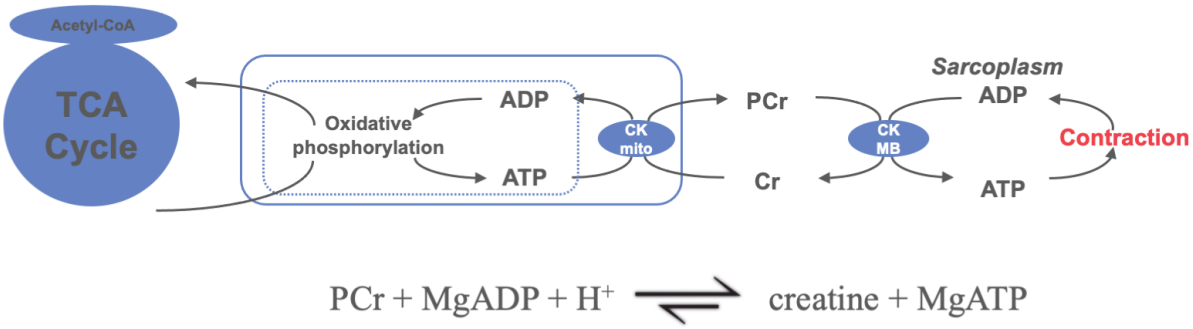

Figure 1.4: The Creatine Kinase System. *Top row shows the spatial distribution of high-energy phosphates by means of the creatine kinase (CK) system from mitochondria (left top row) using mitochondrial CK (CK_{mito}) to facilitate production of phosphocreatine (PCr) and shuttle it to the myofibrils (right, top row) where myofibrillar CK (CK_{MB}) is used to generate ATP. The bottom row shows the CK-reaction in which the equilibrium is on the right side.*

1.3 Metabolic alterations in different diseases

Alterations in substrate metabolism but also in ATP-generation and the creatine kinase system are a hallmark of various forms of cardio-metabolic diseases, including and especially HF, and often precede structural remodelling and clinically overt disease.[34] Correspondingly, patients with HF[9,35-37], T2D[38,39] and obesity[40] exhibit lower concentrations of ATP and PCr *in-vivo,* respectively. Nevertheless, despite sharing the overall reduced amount myocardial energy, each syndrome presents with certain distinct metabolic derangements hence, the following part of the introduction will review these in more detail.

1.3.1 Heart failure with reduced ejection fraction

In HFrEF, the heart loses its ability to swiftly shift from one fuel source to a different one. This process, termed 'metabolic flexibility', is a key characteristic of the adult, healthy heart and as such, losing it has wide-ranging consequences.[13] The heart gradually but progressively and in correlation to the severity of HF, loses up to a third of ATP content.[32,41,42] Importantly, the failing, non-ischaemic heart is not a hypoxic environment [43] and likewise well supplied with metabolic substrates. Thus, the energetic failure is deemed a mismatch between ATP-synthesis and degradation pathways.[44] This mismatch also affects the high phosphate energy transfer and buffering via PCr as the total creatine content in HF is reduced by around two-thirds of normal and expression of creatine transporters as well as CK isoenzymes is lower, too.[45] Many mechanisms may contribute to the end-result of reduced oxidative phosphorylation. Increased oxidative stress by reactive oxygen species (ROS) was described to damage mitochondrial DNA, increases lipid peroxidation and overall reduce ATP-synthesis.[46,47] Additionally, an impaired mitochondrial Ca^{2+}-equilibrium contributes substantially to mitochondrial dysfunction as too low levels of Ca^{2+} can reduce mitochondrial enzyme function while an elevation may turn mitochondria into 'death machines' by inducing apoptotic pathways.[48] Lastly, mitochondrial biogenesis is reduced and degradation of damaged mitochondria (mitophagy) increased in HF with post-translational modification of mitochondrial proteins being insufficient all these mechanisms contribute to mitochondrial dysfunction in HF.[49,50]

On a substrate level, uptake of FA into cardiomyocytes[51] and FAO are decreased in HFrEF and its main transcriptional regulator, peroxisome proliferator activator

alpha (PPARα), is repressed.[52,53] The reduction in myocardial FAO escalates the energetic deficit, in turn increasing HF-severity.[16]

While glucose oxidation (relative to FAO) is overall decreased in the failing heart[54], glucose uptake via GLUT1[55] and glycolysis are reportedly increased.[56] Interestingly, this matches observations from deleterious mouse models where mice developed diastolic and systolic dysfunction following GLUT4 and PDH-deletion, respectively.[57,58] Of note, insulin resistance is a frequent phenomenon (even in non-diabetic) HF and as insulin is required for GLUT4-mediated glucose uptake, it will equally contribute to reduced glucose uptake.[59]

In recent years, a growing interest in ketone body metabolism revealed that circulating ketones and myocardial ketone body oxidation are substantially increased in HF.[22,60] Momentarily, it is unclear if these effects are seen as salutary or disadvantageous. Contrary to pyruvate (from glucose oxidation), ketones are not anaplerotic substrates and can thus lead to dysfunction of the TCA and knock-on effects on glucose oxidation. Furthermore, FAO seems to be inhibited by increased rates of ketone body oxidation.[61,62]

Levels of BCAAs increase in HFrEF and this might be due to an impairment of BCAA oxidation.[63,64] Accumulation of BCAAs might be a driver of adverse remodelling in HF via stimulation of the mammalian target of rapamycin (mTOR). This hypothesis would be in keeping with the observation that mTOR-inhibition with rapamycin improves cardiac function while further supplementation with BCAAs worsens it in HF.[65,66] Similarly, accumulation of BCAA-intermediates

appears to contribute to insulin resistance in HF which in turn may promote LV hypertrophy and metabolic and contractile dysfunction.[67-69]

1.3.2 Heart failure with preserved ejection fraction

Regrettably, the metabolic and molecular changes underlying HFpEF are incompletely investigated and thus remain poorly understood. Furthermore, there is a lack of appropriate animal models reflecting the true, admittedly very complex, aetiology of this syndrome.[70,71] Typically, experiments aiming to increase the mechanistic understanding of metabolic changes in HFpEF make use of volume and pressure overload, aortic banding, obesity and T2D. However, these models are restricted to a single causal aetiology which in human HFpEF, is rarely the case. Only recently, a novel porcine multifactorial model of HFpEF was created hence, results of studies are eagerly awaited.[72]

Patients with HFpEF have a similar state of energy depletion seen in HFrEF.[73,74] It has been established that increased circulating concentrations of FA increase the risk of HFpEF-development however it is unclear whether this implication holds true for patients with already established HFpEF.[75] FAO is increased in patients with diabetic and/or obese HFpEF[76,77] and transgenic murine models of FAO-inhibition also display cardiac hypertrophy and impairment of cardiac function.[78,79]

It is unclear what role glucose oxidation plays in the development and worsening of HFpEF. While it is generally thought to be decreased[80,81] a study in rodents exposed to transverse aortic constriction (TAC) inducing HFpEF exhibited increases in glucose oxidation and glycolysis.[82]

More work is required regarding alterations and possible contribution of ketones and BCAAs metabolism in HFpEF.[24,83] Generally, increased levels of circulating substrates (both ketones and BCAAs) have been observed in HFpEF which led to the assumption that oxidation of these metabolites is likely increased.[84] However, despite this association it is unclear whether these metabolites carry a causal role in the aggravation of HFpEF.[16]

1.3.3 Type 2 diabetes and obesity

Obesity and T2D are mutually related as the vast majority of T2D patients are obese. Equally, obesity is not a disease occurring in isolation and as such, metabolic changes observed are not unique to obesity.[85] Correspondingly, a 'metabolic' phenotype of normal weight and BMI exists who exhibit classical features of obesity emphasising that not only weight itself but lipid distribution seems to be of relevance.[86]

The presence of cardiac dysfunction in the absence of typical aetiologies (CAD, valvular heart disease, overt hypertension) other than diabetes is currently described as 'diabetic cardiomyopathy'. A myriad of potential pathological mechanisms have been described and these include inflammation, RAAS-activation, cardiac autonomic neuropathy (overactivation of sympathetic nervous system promoting hypertrophy, fibrosis and dysfunction), microvascular dysfunction and oxidative stress.[87-89] At present, there is no established marker of disease to predict cardiac dysfunction in patients with T2D and no specific disease management strategies exist.

Further to the aforementioned, T2D and obesity induce certain metabolic derangemens: Rates of FA-uptake and FAO are elevated in obese and diabetic humans and this is thought to contribute to the accrual and storage of lipids in the myocardium.[77,90] Myocardial steatosis induces accumulation of FAO intermediates such as long-chain acyl CoA, diacylglycerol as well as ceramides and these contribute to metabolic dysfunction, a process termed 'lipotoxicity'.[91,92] The increase in FAO further inhibits glucose oxidation via the Randle cycle, thus contributing to reduced metabolic flexibility and over-reliance on lipids.[21] On a molecular level, obese and diabetic patients show an overly active AMP-activated protein kinase (AMPK) which regulates FA-synthesis and oxidation and also promotes insulin resistance and downregulation of glucose oxidation.[93] The shuttling and buffering of high-energy phosphates via the CK-system is upregulated in obese patients but under higher workloads, cannot compensate for increased demand and thus, might lead to exercise intolerance and blunted cardiac adaptation to stress.[40]

1.4 Therapeutic modulation of energy metabolism in heart failure

As outlined above, the mechanistic evidence generated for HF and other metabolic cardiomyopathies offers plenty of intriguing metabolic targets. Unfortunately, most potential treatments do not make it into clinical development and thus, metabolic modulation is an underdeveloped therapeutic research area. Further to this, animal data is frequently conflicting. This part of the introduction of this Thesis will thus focus on available human evidence for metabolic modulators in HF.

1.4.1 Pharmacological agents

Targeted therapies to improve mitochondrial function have rarely been translated to trials in patients. However, some human evidence exists for myocardial effects of treatment with Coenzyme Q (CoQ).[94] Furthermore, *Q-SYMBIO*, randomising 420 patients with HFrEF to treatment with CoQ and following them up prospectively for more than 2 years, did show impressive improvements in CV-mortality and MACE as well as improved symptom burden.[95] However, this treatment has never been implemented into routine care and no larger outcome trial was performed to replicate these results.

Elamipretide, a small molecule aiming to improve mitochondrial biodynamics by associating to cardiolipin in the inner mitochondrial has shown success in various animal models of mitochondrial dysfunction. A first trial in 8 patients with chronic HFrEF was encouraging as it did reduce markers of adverse remodelling.[96]

In HFrEF and HFpEF alike, derangements in the redox state of NADH have been reported and mouse models have successfully demonstrated that administration of Nicotinamide riboside (NR) slowed development of HF.[97,98] Interestingly, patients with a naturally high NAD+-precursor rich diet also appear to have lower rates of CV-disease and overall mortality.[99] As a result, this novel therapeutic approach has now been translated to clinical trials in patients with HF (ClinicalTrials.gov NCT04528004) although results are yet outstanding.

Another agent currently under investigation is resveratrol, a naturally occurring polyphenol which appears to have effects on ROS in mitochondria.[100] In a clinical trial enrolling 40 adults with previous myocardial infarction, resveratrol improved

diastolic and endothelial function.[101] Trials with HF patients (ClinicalTrials.gov NCT03525379 and NCT01914081) are currently underway and results will hopefully shed more light on resveratrol's potential in this population.

Dichloroacetate (DCA) inhibits PDH-kinase (PDK) which effectively increases glucose oxidation. In the HF setting, particularly with increasing reliance on FAO, this appears to be beneficial.[13] Small pilot trials testing DCA have elicited conflicting results with one reporting improved cardiac function but another one not showing statistically valid improvements.[102,103] As outlined before, patient selection appears to be key to demonstrate salutary effects.

Inhibiting FAO in patients with HF conversely increases glucose oxidation via the Randle cycle. Etomoxir and perhexiline, two inhibitors of the rate-limiting enzyme for FAO (carnitine palmitoyltransferase 1, CPT1), have been tested in patients with HF *in-vivo*. While both etomoxir and perhexiline demonstrated improvements in cardiac function, output and symptom burden[104-106], perhexiline also improved energy metabolism.[107,108] Sadly, hepatotoxicity was observed and thus, impeded further testing and development. Interestingly, isolated downregulation of FA uptake without compensatory increase of glucose oxidation with the lipolysis-inhibitor Acipimox resulted in decreased myocardial function in patients with DCM.[109] These results emphasise the continuous need for energy provision in the heart and underscore the interconnected metabolic network in which homeostasis is required.

Trimetazidine has been used as an anti-anginal agent in over 100 countries for a significant amount of time. Concerning substrate metabolism, trimetazidine inhibits

the final enzyme of beta-oxidation (3-ketoacyl CoA thiolase) and thus reverses overreliance on FAO in HF.[110] In HF patients, trimetazidine treatment on top of optimal medical treatment (OMT), improved cardiac function and energetics.[111,112] The mechanism is thought to be beneficial in T2D and obesity and thus, has been investigated in this Thesis (**Chapter 6**).

Allopurinol is another pharmacological agent that has demonstrated enhancing metabolic effects in patients with HF. By inhibiting xanthine oxidase, a critical enzyme in the degradation of purines and ATP, inhibition resulted in reduced amounts of ROS in animal studies. Interestingly, high-energy phosphotransfer via the CK-reaction was acutely improved in non-ischaemic HF patients.[113]

1.4.2 Dietary interventions

A considerable lack exists on data from human subjects regarding the effects of intentional weight loss in HF. No large-scale outcome trial has investigated intentional, supervised weight loss for patients with chronic HF. Small-scale, largely retrospective evidence exists often resulting in detection of increased all-cause mortality with weight loss (obesity paradox in HF).[114] However, these studies do not distinct between fat distribution, weight loss due to underlying concomitant diseases (e.g. cancer) and often include a survivorship bias.

Increasing evidence describes a distinct HFpEF phenotype typically female, characterised by obesity, T2D and inflammation and this ‘metabolic cardiomyopathy’ subgroup appears to react differently to treatments compared to other HF phenogroups.[115,116]

A recent RCT enrolling 100 patients with a mean BMI of almost 40 kg/m^2 and a diagnosis of chronic HFpEF, a patient group frequently omitted from outcome trials in HF, showed that caloric restriction (i.e. weight loss) and exercise both increase quality of life (QoL) exercise capacity (peak $\dot{V}O_2$) and importantly have an additive effect when combined.[117] In a similar patient group of subjects with severe obesity and HFrEF, patients undergoing bariatric surgery was associated with significantly improved LVEF and NYHA class.[118]

In a very recent study, 41 patients with obesity and HFpEF (mean BMI 40.8 kg/m^2) underwent a 26-week weight management program. Following the intervention, QoL and exercise tolerance had improved. Importantly, measurable improvements in diastolic function E/e' were only seen after 26 weeks.[119] Given the evidence outlined above and the findings in this thesis (**Chapter 5**) outlining that filling pressures, cardiac structure and adaptation to exercise significantly improve in HF patients with substantial obesity, it appears odd that international guidelines do not even comment on the possibility of weight management in selected patients with HF.[120,121]

1.5 Investigation of cardiac metabolism

Various technologies exist to interrogate energy metabolism.[122] However, most of these methods require invasive assessments (like withdrawal of blood from the aorta and coronary sinus) and thus pose a significant risk as well as logistical challenges, or pose a possible health hazard as they employ radioactivity on the human body which carries stochastic radiation effects irrespective of the radiation dose.

CMR is the gold-standard for most accurate and reproducible assessment of cardiac mass, volumes and function.[123-125] Its reliable image quality allows reproducible evaluation of cardiac structure, image quality is not adversely affected by body habitus, and it does not involve ionising radiation or radioactive isotopes. One of its main advantages is the fact that different nuclei, other than hydrogen (^{1}H) used for imaging, can be utilised to investigate certain metabolites and also energetic equivalents. Other nuclei (besides ^{1}H) include ^{31}Phosphorus (^{31}P), ^{17}Oxygen, ^{13}Carbon (^{13}C) and principally ^{2}H (Deuterium).

1.5.1 ^{1}H-MRS

Protons (^{1}H) are naturally abundant in most body tissues and also considerably sensitive to magnetisation. As such, ^{1}H-magnetic resonance spectroscopy (MRS) enables detection of metabolites such as creatine, lactate, carnitine, taurine and lipids.[126,127]

Use of ^{1}H-MRS in this thesis concerned assessment of ectopically stored fat in the myocardium (myocardial steatosis) and this has been correlated with diastolic dysfunction, inflammation and adverse remodelling.[128,129]

Human use of this technique usually involved single-voxel techniques such as a stimulated echo acquisition mode (STEAM) or point-resolved spectroscopy (PRESS) which are usually ECG-gated and typically acquired during a breath hold to compensate for respiratory motion.[130,131] Using these techniques assessing myocardial steatosis in humans typically generates a spectrum of water and triglycerides as well as total creatine (**Figure 1.5**).

Figure 1.5: Assessment of Myocardial Steatosis with ^{1}H-MRS

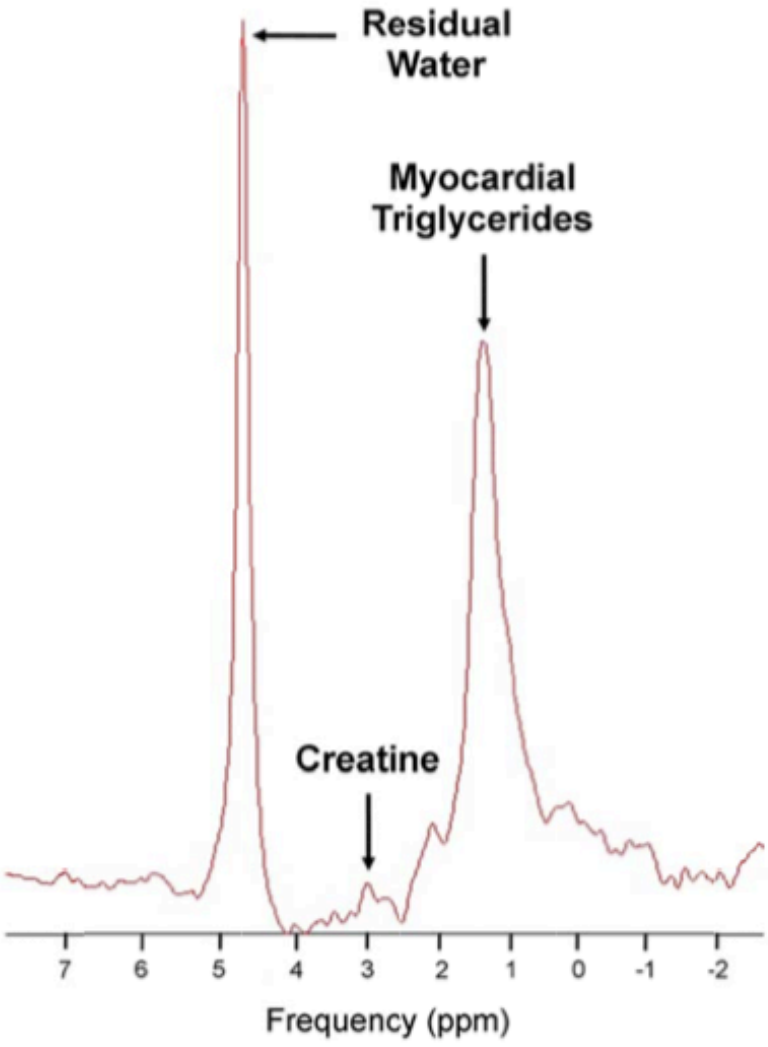

Figure 1.5: Assessment of myocardial steatosis with ^{1}H-MRS. Representative spectrum generated by stimulated echo acquisition mode (STEAM) proton magnetic resonance spectroscopy (^{1}H-MRS). Adapted from Taegtmayer et al.[122]

Limitations in the signal-to-noise ratio as well as arrhythmia, which is frequently seen in patients with T2D, obesity and HFpEF, adds to the complexity of avoiding reliable chemical information *in-vivo*.

1.5.2 ^{31}Phosphorus MRS

^{31}P-MRS enables assessment of ATP and PCr separately due to a phenomenon commonly referred to as 'chemical shift'.[132] This principle describes that the precise resonance frequency of a nucleus is dependent on its chemical milieu and as such, the ^{31}P-nucleus in PCr has a different resonance frequency than those bound in ATP. This is emphasised in a typical ^{31}P-MRS spectrum (**Figure 1.6**).

Figure 1.6: ^{31}P-MRS Spectrum

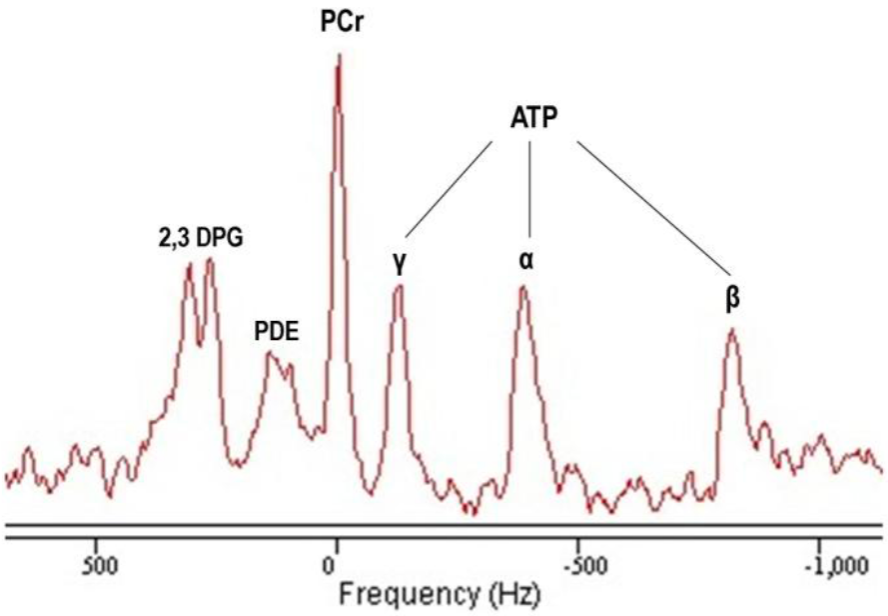

***Figure 1.6: Spectrum obtained with ^{31}P-MRS**. Representative spectrum obtained from the myocardium of a healthy volunteer. The ratio of phosphocreatine (PCr) and the three (**γ, α, β**) ATP peaks (left to right). 2, 3 DPG = diphosphoglycerate;l PDE=phosphodiester; adapted from Taegtmayer et al.[122]*

Different varieties within the field of ^{31}P-MRS exist which all have certain advantages and drawbacks. Depth resolved surface coil spectroscopy (DRESS) uses a single slice within the myocardium in parallel to the surface receiver coil.[133] Its main advantage is the reduced time to acquire the spectrum which is usually 3-4 minutes. The technique of choice nowadays, which has also been applied in this Thesis, is three-dimensional chemical shift imaging (3D-CSI).[134] The sequence employed herein makes use of phase encoding to differentiate signal received spatially. This method enables creation of a matrix of individual voxels (**Figure 1.7**) which improves spatial localisation however, acquisition times are substantially longer (around 13 minutes) and a small voxel size for each individual voxel leads to a relatively low signal to noise ratio and furthermore makes contamination from neighbouring voxels more likely.[135] An important point is the application of saturation bands to avoid signal contamination from the liver (high PDE but no PCr) and skeletal muscle (higher PCr/ATP than myocardium).[136]

Figure 1.7: ^{31}P-MRS 3D-CSI Voxel Matrix

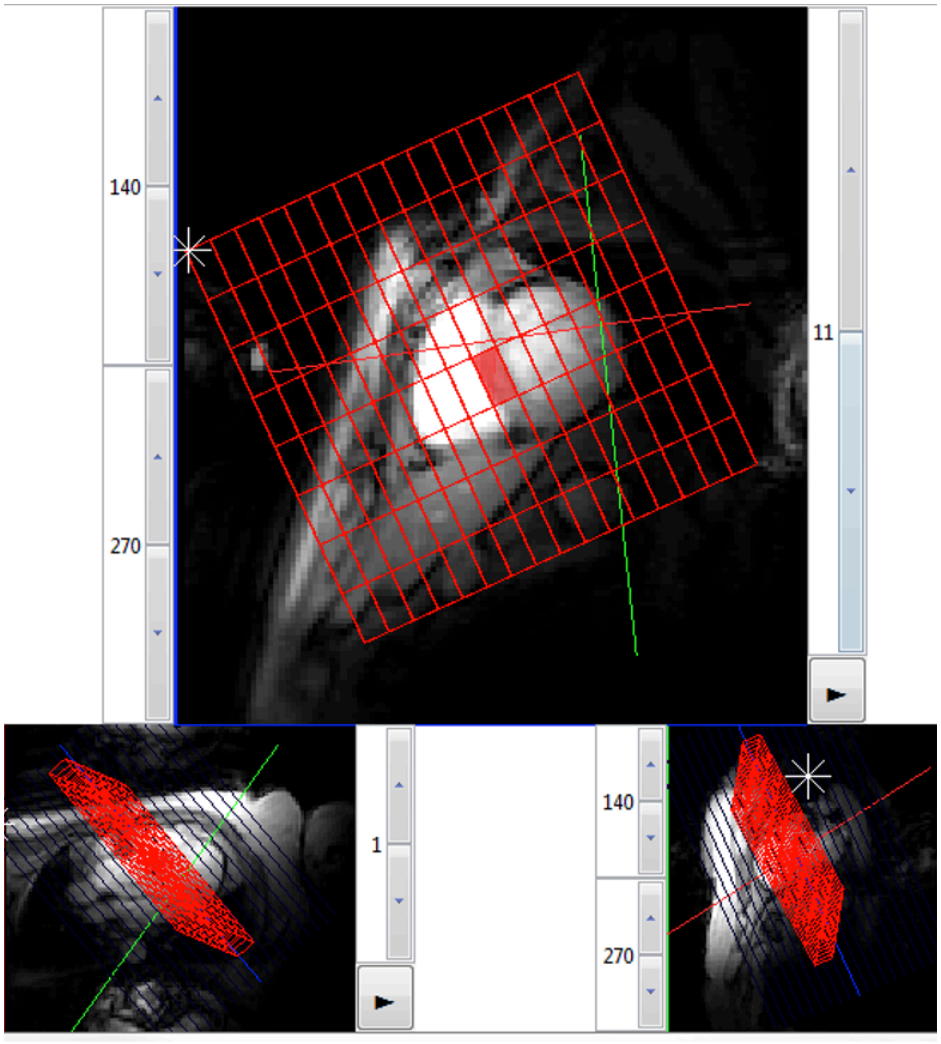

***Figure 1.7: ^{31}P-MRS 3D-CSI Voxel Matrix**. Matrix of voxels created by using three-dimensional chemical shift imaging (3D-CSI) which enables individual voxel selection; here in the middle part of the interventricular septum highlighted in red (upper picture). The lower two pictures show the localisation of the voxel matrix in different views (HLA left; VLA right).*

Whole heart analysis, instead of a single voxel in the interventricular septum, would be possible with methods allowing for creation of a non-cuboidal voxel matrix such as spatial localization with optimal point spread function (SLOOP).[137]

Similarly to quantification of PCr/ATP, ^{31}P-MRS can be used to investigate the CK-system and especially the reaction speed of transferring high-energy phosphates from mitochondria to the myofibrils. This 'CK flux' investigation is useful as the majority of immediate energy provision and buffering of higher workloads is covered by this system. By saturating the magnetisation of γ-ATP, the PCr-signal is reduced due to both substances being near equilibrium through the CK-reaction. This reduction of the PCr peak is proportional to the rate constant of the forward flux in the CK-reaction. Knowing this and the tissue PCr-content, it enables calculation of total CK-flux.[138]

Importantly, ^{31}P-MRS can easily be combined with pharmacological stress to assess the myocardial energy reserve under states of increased stress. Dobutamine has been used frequently in this context. It is a sympathomimetic catecholamine with strong beta1-adrenergic receptor activity, and mild alpha1- and beta2-receptor activity. This results in marked inotropic effects at low doses (<10 µg/kg/min), with increased chronotropic effects alongside increased myocardial oxygen demand and myocardial work at higher doses (20-40 µg/kg/min). Dobutamine is rapidly metabolised (half-life approximately two minutes) thus, effects decaying quickly and can be antagonised by beta blockade making it suitable for stress testing.[139] It is administered as an intravenous (IV) infusion, typically commenced at a dose of 5 µg/kg/min followed by an increase to 10 µg/kg/min after 3 minutes and then in 10 µg/kg/min increments every 3 minutes thereafter to a maximum dose of 40 µg/kg/min. A typical endpoint is achievement of a target heart rate of 65% of maximal predicted heart rate (Age in years – 220).

1.5.3 Hyperpolarized CMR

By labelling a metabolite (pyruvate, beta hydroxybutyrate) with ^{13}C, it will be detectable against the background of carbon structures in the myocardium. However, ^{13}C has a very low polarity as such, is difficult to detect with MRS. By hyperpolarizing the so-called 'probe', a hugely complex process involving cooling the substance to < -272 °C, it increases the susceptibility to magnetisation by a factor of 10.000. This enables detection of individual metabolites (for example pyruvate) but also downstream products and thus, live visualisation of metabolic substrate pathways in-vivo (**Figure 1.8**). **Chapter 6** in this Thesis uses this modality for the first time in the context of a human phase II two trial with a novel IMP.

Figure 1.8: Hyperpolarized [1-^{13}C]pyruvate MRS

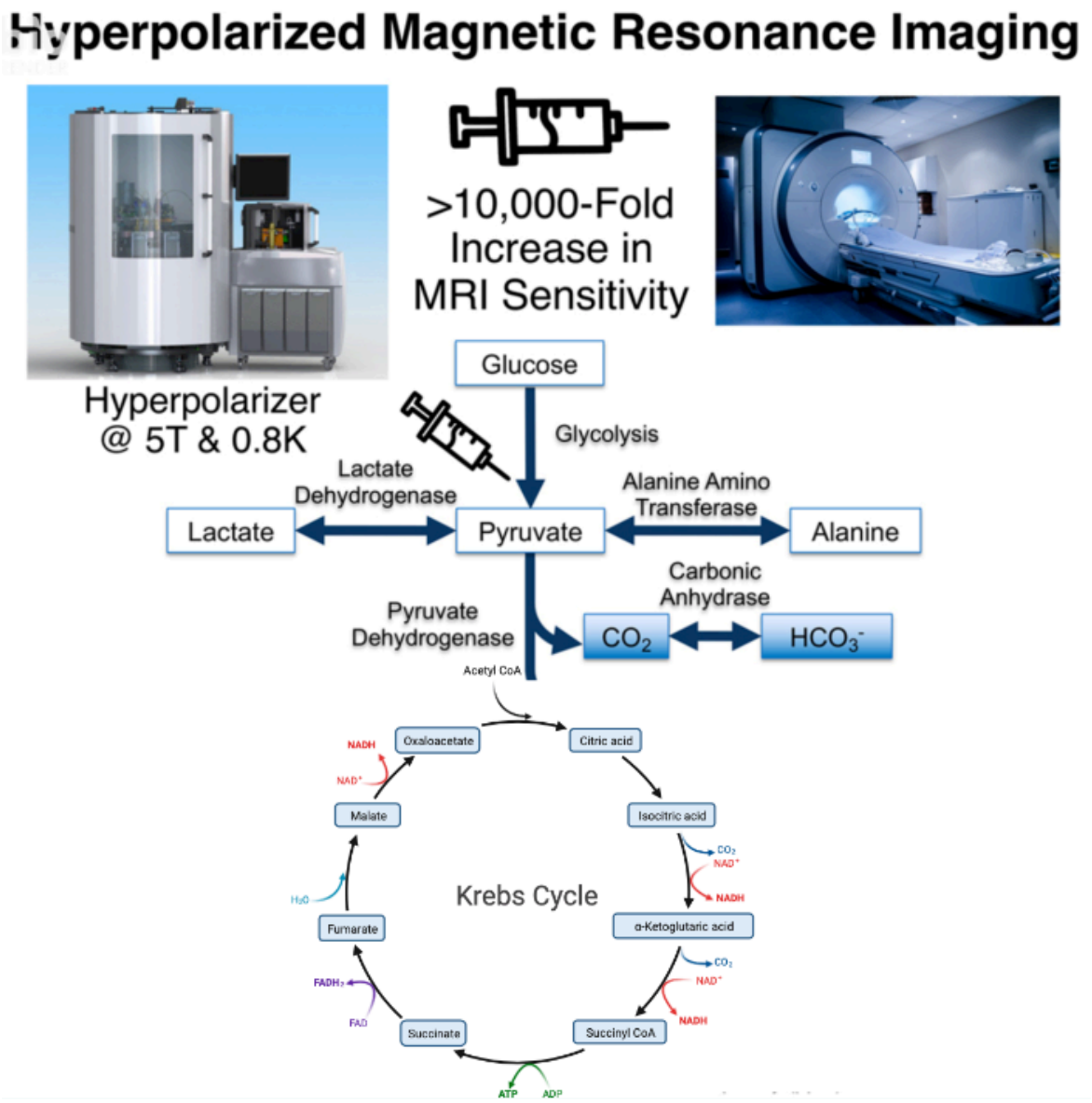

Figure 1.8: Hyperpolarized [1-^{13}C]pyruvate MRS. *To hyperpolarize a sample, the ^{13}C labelled molecule is mixed with a stable radical, placed in a high magnetic field (>3.35 T) and cooled to <1.4 K. At this temperature, the electron spins of the radical are almost completely polarised. Irradiation with microwaves near to the resonant frequency of the electron spin transfers this polarisation to the ^{13}C nuclei. A superheated, pressurised buffer is used to rapidly melt the molecule, and return it to near room temperature with 30–50% polarisation, which then decays exponentially over the next 2–3 minutes. This rapid decay means there is only a short time to administer the pyruvate to the subject under test and acquire spectra before signal is lost. Figure amended according to Rider et al.*[140] *; used with author permission.*

1.5.4 Nuclear metabolic imaging

Positron emission tomography (PET) uses radiolabelled substrates (tracers) which are taken up by the target organ, in this case the heart, and can then be visualised in place of their accumulation.[141,142] Use of positron emitting radioisotopes improves spatial resolution and contrast however, the technique is rather expensive and thus has lost importance as more metabolic assessments are now performed with single-photon emission computed tomography (SPECT). SPECT detects γ-radiation emitted from radiotracers which have a significantly longer half-life compared to positron emitting tracers. This substantially improves logistics and as such, reduces costs but also makes the modality more widely available.[141] Unfortunately, SPECT-specific radiotracers for assessment of glucose metabolism are not currently available. Consequently, its main use is the assessment of fatty acid metabolism by using tracers such as ^{123}I-βmethyl-P-iodophenylpentadecanoic acid (BMIPP) which is retained in the cellular triglyceride pool and thus offers good image quality.[143,144]

Myocardial glucose metabolism is still principally assessed with PET as this technique remains the gold-standard for this application. The. Typical radiotracer used for assessment is ^{18}F-Fluorodeoxyglucose (^{18}F-FDG).[145] A major disadvantage of ^{18}F-FDG is the need for a mathematical correction called the 'lump constant' which limits accuracy and the inability to assess glucose metabolism downstream as FDG does not follow the same metabolic fate as naturally occurring glucose.[146]

1.6 Important previous work on CMR and metabolism

Essentially all of the CMR techniques used in this thesis would never have been imaginable 100 years ago and even today, are only used by few centres around the planet. Being able to use these sophisticated techniques is a special privilege and would not have remotely been possible without the pioneers in the field making these methods accessible to the broader scientific community. A variety of scientists over a broad period of time have contributed to these discoveries and naturally, only very few have had the privilege of being awarded with the most coveted scientific honours, the Nobel Prize. Nevertheless, the following Nobel Laureates have contributed to the CMR techniques used in this thesis and thus, are mentioned separately:

Otto Stern won the Nobel Prize in Physics in 1943 for discovering the magnetic momentum of the proton, essentially laying the foundation for using NMR for diagnostic purposes by demonstrating that certain nuclei of atoms interact with magnetic fields.

Building on Stern's work, *Isidor I. Rabi* received the Nobel Prize in Physics in 1944 for proving that a magnetic field is able to change the state of the magnetic moment of an atomic nuclei (Rabi Oscillation).

Felix Bloch (Bloch equations) discovered an equation to calculate the nuclear magnetisation in a magnetic field. Together with the discoveries of *Edward Mills Purcell* this enabled material's compositions using NMR. Their work was distinguished by the Nobel Committee in 1952 with a Nobel Prize in Physics.

Richard R. Ernst proved in 1966 that the sensitivity of NMR spectroscopy could be dramatically improved when using radiofrequency pulses and thus, laid the basis of modern-day NMR spectroscopy. His work was awarded with a Nobel Prize in Chemistry in 1991.

In 2002, *Kurt Wüthrich* was awarded a Nobel Prize in Chemistry for making it possible to use NMR for determining a three-dimensional structure in solution (for example proteins in a cellular environment).

The Nobel Prize in Physiology or Medicine in 2003 was awarded jointly to *Sir Peter Mansfield* and *Paul C. Lauterbur*. Their discoveries made MRI usable for diagnostic purposes and thus, contributed significantly to the exponential use of non-invasive imaging techniques for diagnostics and medical research.

Equally important were the discoveries surrounding cellular (energy) metabolism. Although a total of 24 Nobel Prizes in different categories have been awarded to scientist investigating important parts of cellular metabolism (carbohydrates and lipids) as well as enzymes and vitamins, a few especially relevant Laureates for the context of this thesis are listed in the following section.

In 1922, *Otto Fritz Meyerhof* and *Archibald Vivian Hill* received the Nobel Prize in Physiology or Medicine for their discoveries around energy conversions in anaerobic conditions (e.g. exercise) and the conversion of carbohydrates to lactate as well the need for oxygen for using lactate during exercise recovery.

Otto Heinrich Warburg provided compelling evidence on the importance of iron and hemoglobin as a respiratory enzyme and its subsequent involvement in cellular ‘respiration’. Another important observation, despite not being honoured

with a Nobel Prize, was the process of ‘aerobic glycolysis’ in tumour cells, an effect used today for diagnostic purposes in a PET scan.

Important discoveries relating to anaerobic cellular metabolism were made by Carl Ferdinand and Gerty Theresa Cori. Amongst findings relating to the catalytic breakdown of glycogen they showed that lactate, produced during anerobic glycolysis in cells, is transported to the liver where it is used for gluconeogenesis before being returned to the cells. This work received the Nobel Prize in Physiology or Medicine in 1947.

All metabolic substrates are converged to a single compound (acetyl-CoA) which undergoes cyclic transformation to deliver reducing equivalents for oxidative phosphorylation in the mitochondria. This process, called the tricarboxylic acid cycle, and the necessary enzyme for this catalytic conversion (coenzyme A), were discovered by *Hans Adolf Krebs* and *Fritz Lipmann* whose achievements were honoured with a Nobel Prize in Physiology or Medicine in 1953.

Their work regarding how fatty acid and cholesterol metabolism are orchestrated and regulated won *Konrad Bloch* and *Feodor Lynen* the Nobel Prize in Physiology or Medicine in 1964.

ATP is the universal energetic currency of all living organisms and was discovered by Karl Lohmann in 1929. Interestingly, it was *Fritz Lipmann* (see above) who also discovered that ‘energy-rich phosphate bonds’ in ATP are the provider of chemical energy in living cells. *Peter Mitchell* was honoured with the Nobel Prize in Chemistry for his investigations concerning the process of oxidative phosphorylation and thus, creation of ATP via the electron transport

chain in the mitochondria. In 1997, the Nobel Prize in Chemistry was awarded to *Paul D. Boyer* and *John E. Walker* for the discovery of the enzyme ATP-synthase and how it regenerates ATP from ADP and inorganic phosphate.

All of the work mentioned here can be found on the official Nobel Committee website.[147]

1.7 Current knowledge gaps

It is clear from the evidence summarised in this introductory Chapter that many processes in the metabolic network in patients with HF and metabolic cardiomyopathies are poorly explored. It is particularly evident, that the currently used approach to phenotype HF patients according to their LVEF needs significant improvements as it has become clear with the rise of HFpEF that distinct subgroups exist within the broad umbrella of clinical HF-syndromes and importantly, these respond to treatment differently. Exploring novel treatments in the context of myocardial substrate metabolism may provide valuable insights and promote broader understanding of mechanisms involved thus, promoting further development of novel therapies. Subsequently, I sought to address the topics outlined above over the course of this Thesis and cogently, the following topics will be explored:

1.7.1 Effects of SGLT2-inhibition in patients with HFrEF

Evidence from many, mostly rodent, animal models supported the hypothesis that SGLT2i such as empagliflozin may enhance myocardial energy metabolism as they

induce a mild hyperketonaemia. With increasing amount of circulating ketone bodies, the heart appears to increase its use for energy generation. Yet, nothing is known about the metabolic effects of SGLT2i in patients with HFrEF *in-vivo*. Whether a measurable increase in energy metabolism can be detected and what other structural, functional and physiological parameters might be affected to explain SGLT2is salutary effects in HFrEF will be investigated in **Chapter 3**.

1.7.2 Effects of SGLT2-inhibition in patients with HFpEF

HFpEF is now the most prevalent HF-phenotype and efforts to characterise these patients have revealed marked differences compared to patients with HFrEF. Notably, all established HFrEF therapies trialled in patients with HFpEF have elicited negative results in large outcome trials. Thus, there is a considerable unmet medical need combined with an extensive lack of mechanistic understanding of metabolic processes involved in HFpEF. **Chapter 4** pursued to explore if SGLT2i effects differ in patients with HFpEF.

1.7.3 Effects of weight loss in patients with HFpEF

Observational studies have determined the existence of a so-called 'obesity paradox' in HF. This describes the paradoxical finding that mild obesity may be protective and protect from mortality in HF. On the other hand, severe obesity, often associated with T2D, is now the most frequent comorbidity in HFpEF and a distinct obese HFpEF phenotype has been described. As such, it is surprising that no prospective data exists on metabolic and functional changes of weight loss in this cohort. Hence, **Chapter 5** aims to provide evidence for use of this

underutilised resource by investigating the effects of a VLED in patients with obesity and HFpEF.

1.7.4 Effects of metabolic substrate inhibition in patients with diabetic cardiomyopathy

The final chapter (**Chapter 6**) of this Thesis examines the novel cardiac mitotrope ninerafaxstat in a phase IIa trial with obese diabetic patients. Numbers of patients affected by T2D are constantly rising and presence of T2D has a direct detrimental impact on development but also aggravation of HF. Metabolic derangements are frequently observed in T2D and thus re-balancing substrate metabolism may be a promising strategy for patients with diabetic cardiomyopathy. Notably, as the obese HFpEF phenotypes shares many similarities with obese T2D, this may also shed some light on general mechanisms which could be exploited for novel therapeutics in HFpEF.

Chapter 2 Methods

2.1 Ethical considerations

All investigations carried out in this thesis received a favourable opinion from the South Central – Oxford A Research Ethics Committee (REC reference: 13/SC/0376) of the National Research Ethics Service (NRES) representing the NRES Directorate within the National Patient Safety Agency and Research Ethics Committees in England. Further to this, each project involving an IMP likewise was approved by the Medicines and Healthcare products regulatory Agency. Thirdly, the Healthcare Research Authority and Oxford University Hospitals NHS Foundation Trust (OUH) permitted carrying out this research work. All procedures were carried out in accordance with institutional procedures and the Declaration of Helsinki. All participants gave written informed consent for participation, and such was obtained prior to any study investigations taking place. Data was recorded in an anonymised fashion and stored on a high-compliance server off-site with independent backups in different locations. Written confidential data was kept in locked filing cabinets on our study site.

2.2 Study participants

Patients with Heart Failure with a reduced Ejection Fraction (HFrEF)

Patients with chronic and thus, stable HFrEF, on OMT referred to Oxford University Hospitals NHS Foundation Trust for assessment in the HF clinic, the general practitioner (GP) cardiology service or clinical cardiac MRI between April 2018 and May 2020 were screened for eligibility. Patients satisfying the inclusion criteria and without any exclusion criteria present were provided with a patient information leaflet and invited to take part in the study. Patients who provided written informed consent were then invited for a screening visit and, given eligibility, subsequently enrolled and randomised to treatment (see **Chapter 3**).

Patients with Heart Failure with a preserved Ejection Fraction (HFpEF)

Patients with clinically diagnosed HFpEF undergoing routine clinical assessments in OUH were screened for eligibility. Data from patients meeting the inclusion criteria and without any exclusion criteria and who provided written informed consent were invited for a screening visit and, if eligible, enrolled and randomised to treatment (see **Chapter 4**).

Patients with Obesity and Heart Failure with a preserved Ejection (HFpEF)

Patients with obesity (BMI $\geq$ 30 kg/m^2) and an established diagnosis of HFpEF were recruited for this longitudinal study when attending MRI appointments at the John Radcliffe Hospital (Oxford, UK) as part of an NHS investigation or after

having been involved in other observational studies on site if they consented to be contacted for further research projects. After providing informed consent, eligible patients were enrolled on the study and received the proposed intervention (see **Chapter 5**)

Patients with Obesity and Type 2 Diabetes

Patients with obesity (BMI ≥ 30kg/m^2) and type 2 diabetes (T2D; HbA1c ≥ 6,5%) were recruited from various sources within OUH NHS Foundation Trust (Diabetes Clinics Churchill Hospital) as well as research collaborators (Thames Valley Clinical Research Network Primary Care Database, Oxford Centre for Diabetes, Endocrinology and Metabolism – OCDEM) and domestic databases (Oxford Biobank, NIHR BioResource, University of Oxford). Patients who expressed interest in taking part in the trial were invited to attend a screening visit. Following provision of their written informed consent, eligible patients were enrolled and allocated treatment (see **Chapter 6).**

2.2.1 Inclusion criteria

The following inclusion criteria provide an overview of the general criteria applied for each respective study. For further details, the reader is advised to kindly refer to the individual chapters in the results section of this thesis.

All subjects

- Male or female, between 18 and 75 years of age
- Able and willing to give informed consent for participation in the study and able to comply with all study requirements

Patients with HFrEF for SGLT2i (Chapter 3)

- Patients referred to Oxford University Hospitals NHS Foundation Trust for assessment for HF:
    - Chronic HF diagnosed at least 3 months before informed consent
    - NYHA II-IV at screening
    - LVEF ≤ 40% measured by TTE at screening
    - Elevated NT-proBNP (> 125pg/ml in patients in sinus rhythm or > 600pg/ml in patients with AF)
    - Stable doses of OMT for HF

Patients with HFpEF for SGLT2i (Chapter 4)

- Patients referred to University of Oxford Centre for Clinical Magnetic Resonance Research (OCMR) for clinical assessment of HF:
    - Chronic HF diagnosed at least 3 months before informed consent
    - NYHA II-IV at screening
    - LVEF ≥ 50%

- Structural left heart disease (LAVI ≥ 34 ml/m^2; LVMI ≥ 115 g/m^2 for males and ≥ 95 g/m^2 for females)
- NT-proBNP > 125pg/ml for patients in sinus rhythm or > 600pg/ml for patients in AF

Patients with Obesity and HFpEF (Chapter 5)

Patients with clinically diagnosed chronic HFpEF and obesity (BMI ≥ 28.5kg/m^2) with no documented previous ischaemic heart disesase (IHD) or any symptoms suggesting active ischaemia were recruited.

Patients with Obesity and T2D (Chapter 6)

Patients with obesity (BMI ≥ 30 but ≤ 40kg/m^2) and T2D (HbA1c ≥ 6.5%) who were registered with the Oxford Biobank (OCDEM,Oxford, UK) or research active GP surgeries within the Thames Valley clinical research network (CRN) were invited to enrol in the study if the following criteria applied:

- Preserved LVEF of ≥ 50% on echo
- Preserved renal function (eGFR ≥ 60ml/min)
- Stable antidiabetic therapy within the last 3 months before informed consent
- No SGLT2i or insulin

2.2.2 Exclusion criteria

All subjects

- Age < 18 or > 75 years old
- Inability to give informed consent
- Significant valvular heart disease (particularly moderate or severe aortic stenosis)
- Severe outflow tract obstruction (hypertrophic cardiomyopathy)
- Uncontrolled arterial hypertension (persistently > 180/100 mmHg)
- Uncontrolled arrhythmias
- Significant renal impairment (creatinine clearance < 30 ml/min) will be excluded for CMR scans involving intravenous contrast agent administration (but can still safely undergo CMR scans which do not involve contrast administration)
- Contraindications to dobutamine
- Woman of childbearing potential (WOCBP) who is pregnant, lactating, or planning pregnancy during the course of the study
- Inability to tolerate CMR scanning (claustrophobia, inability to lie flat)
- Contraindications to CMR scanning (implantable devices or other metallic implants, cardiac pacemaker, internal cardioverter-defibrillator, cranial aneurysm clips, metallic ocular foreign bodies, hypersensitivity to gadolinium or other study drugs)

- Any other significant disease or disorder which may put the participant at risk or affect the participant's ability to participate in the study, or may influence the reliability of the study results as determined by the Investigator

2.3 Clinical assessment

On the day of scanning, all subjects underwent a focused clinical assessment. This included history for:

- Inclusion and exclusion criteria as above
- MRI safety screening questionnaire
- Drug history including allergies
- History of recent caffeine intake and fasting (subjects were required to have had no food or fluid intake other than water for at least 6 hours prior)

The following study procedures were also performed in selected studies and are listed in the respective Methods section of each chapter.

- Height (cm) and weight (kg) using calibrated scales
- Blood pressure measurement
- Resting 12-lead electrocardiogram (ECG)
- Intravenous cannulation and blood sampling for biochemical analysis
- Blood sample processing for serum metabolomic analysis
- Resting transthoracic echocardiogram (TTE) for assessment of LV volumes and systolic and diastolic function

- Cardio-pulmonary exercise testing (CPET) including basic spirometry to assess cardio-respiratory fitness
- Six-minute walking test (6-MWT) for assessment of walking distance and exercise symptoms (Borg-Scale)
- Assessment of patient reported outcomes via Kansas City Cardiomyopathy Questionnaire (KCCQ) and EQ-5D5L.

2.4 Cardiac CT

Participants underwent research coronary computed tomography coronary angiography (CTCA) to rule out significant coronary artery disease (CAD) if no clinical CTCA or ischemia testing (for example myocardial perfusion scan) had been performed within 6 months prior to informed consent.

CTCA scans were performed on a 320-slice CT scanner (Canon Medical Systems Ltd, Crawley, UK) in accordance with performance guidelines outlined by the Society of Cardiovascular Computed Tomography.[148] Patients received beta-blockade (IV metoprolol tartrate) to achieve a heart rate (HR) of < 60 bpm as well as glycerol trinitrate for coronary vasodilation. Intravenous iodine contrast was administered via a cannula placed in a peripheral vein followed by a saline flush. The acquisition covered a region from 2cm above the left main coronary artery to 2cm below the cardiac apex in a single breath hold. CT image reconstruction and analysis followed international recommendations.[149]

2.5 CMR protocols

A variety of different CMR techniques were used in each of the four experiments in this thesis however, these consisted of:

1) Phosphorus magnetic resonance spectroscopy for investigation of cardiac energy metabolism at rest and during pharmacological dobutamine stress
2) [1-^{13}C]pyruvate hyperpolarized magnetic resonance spectroscopy to assess pyruvate dehydrogenase flux
3) Proton magnetic resonance spectroscopy for assessment of myocardial steatosis (via myocardial triglycerides)
4) Left ventricular volumes and function at rest and during pharmacological dobutamine stress as well as physiological exercise
5) Native and post-contrast T1-mapping for tissue characterisation and estimation of extracellular volume
6) Short axis myocardial tagging to investigate left ventricular myocardial deformation (strain)
7) Rest perfusion imaging to assess for quantification of myocardial blood flow
8) Late gadolinium enhancement (LGE) to assess for focal areas of cellular necrosis/fibrosis

CMR examinations were performed using two 3-Tesla MRI scanners (Magnetom PRISMA and Magnetom TRIO, Siemens Healthineers, Erlangen, Germany) as well as a General Electric SpinLab System for dynamic nuclear polarisation (described respectively below). Imaging and ^{1}H-MRS were performed using an 18-channel

phased-array surface coil with the participant supine, whereas ^{31}P-MRS was performed by use of a dual channel heart liver coil in prone position. Hyperpolarized MRS spectra were generated using a two channel transmit, eight channel receiver array (Rapid Biomedical, Rimpar, Germany). Careful skin preparation included cleaning of the skin with a special abrasive skin gel to enhance electrical conduction. Electrodes were positioned carefully to ensure good ECG quality and a large R-wave to T-wave ratio, to reduce the risk of mistriggering during acquisitions. Images were typically acquired during a breath hold at the end of expiration to minimise respiratory motion effects and enable standardised slice positioning.

2.5.1 Phosphorus magnetic resonance spectroscopy

All participants underwent cardio-metabolic assessments in fasting state, defined as having been at least 6 hours without solid food or any drinks other than water. Scans were performed on a 3T MR scanner (Magnetom TRIO, Siemens Healthineers, Erlangen, Germany). A Siemens Heart/Liver ^{31}P coil was used consisting of a large outer element (26 x 28 cm) which acts as ^{1}H transmit-receive and ^{31}P transmit, with a smaller loop/butterfly receive pair (12 x 15 cm loop and 23 x 12 cm butterfly) receiving the ^{31}P signal.

Subjects laid prone with their left ventricle positioned over the center of the coil at the magnet isocentre. Proton localisers were used to position the subject correctly. Ten free induction decay inversion recovery (IR-FID) curves (1 ms hard inversion) with increasing inversion delay (100 – 3000 ms) are acquired, along with locations of phenylphosphonic acid (PPA) fiducial and cod-liver oil phantoms.

Pilot images were taken to position the CSI matrix. Piloting was performed in vertical long axis (VLA), horizontal long axis (HLA) and short axis planes, where a stack of 20 slices was obtained. Fast low-angle shot (FLASH) images were used: slice thickness 10 mm, TR 7 ms, TE 3.37 ms, FOV 400 x 340 mm.

A 3D acquisition-weighted chemical shift imaging (CSI) was used with an acquisition matrix size measuring 16 x 8 x 8 and a field of view of 240 x 240 x 200 mm resulting in a nominal voxel size of 11.25 ml. The grid was oriented to place voxels in the inter-ventricular septum. Two saturation bands were placed over the skeletal muscle in the chest wall and one over the liver in order to minimise signal contamination.

The acquisition was non-gated with TR around 910-1010 ms depending upon the specific absorption rate (SAR). The acquisition delay was reduced to a minimum (TE* = 0.3 ms) using the ultra-short echo time (UTE-CSI) technique to maximise acquired signal and reduce first order phase effects (therefore reducing artefact). The optimised RF pulse (duration 2.4 ms) was centred between γ and α peaks of ATP (usually by subtracting 250 Hz from the observed phosphocreatine frequency) to ensure uniform excitation over the entire spectral bandwidth. Nuclear Overhauser effect (NOE) enhancement was used to increase the signal-to-noise ratio in acquired spectra: five pulses, length 2.5 ms, inter-pulse delay 80.5 ms, pulse voltage 222.5 V and average flip angle 150°.

2.5.1.1 Dobutamine stress phosphorus magnetic resonance spectroscopy

Prior to any stress investigations, participants were asked to withhold their beta blockers for at least 24 hours, if not clinically contra-indicated. For protocols where

participants underwent stress imaging or -spectroscopy an infusion pump and a long line of extension tubing was used so that the participant could remain in the magnet bore following successful acquisition of the resting part of the protocol. Dobutamine was administered at incremental rates as a continuous intravenous infusion via a syringe driver (Perfusor, B. Braun Medical Ltd, Sheffield, UK). Starting dose initially at 10 µg/kg/min but increased up to a maximum of 40 µg/kg/min depending on presence of a satisfactory haemodynamic response. This was defined as 65 % of the age maximum (220-age in years) heart rate which was subsequently maintained at the elevated rates for the duration of the acquisition (approximately 11 minutes). Heart rate and blood pressure were measured at baseline and at two-to-three-minute intervals during and after pharmacological stress, until the indices returned to normal or near-normal figures (i.e., baseline results). Wherever possible, additional cine imaging in HLA, VLA and a mid-short axis slice were acquired to measure myocardial function during peak stress. For logistical reasons, this had to be performed without moving the patient out of the scanner and thus, the images were acquired using an individually created GRE-sequence with the integrated scanner receiver coil. As such, the images were significantly more prone to artefacts and generally of a lower quality.

2.5.1.2 Spectral analysis

The basal septal voxel was selected for analysis: this was the only user-dependent part of the process, the rest being fully automated. In-house Matlab software ($OXSA^{150}$) determined the flip angle for the selected voxel by co-registering the short axis images with the spectral data. Flip angle variation due to coil loading effects was calculated by the use of acquired inversion recovery data and the

localizer containing the locations of cod liver oil capsules in fixed positions in the coil.

Pre-processing (baseline correction) was undertaken before fitting spectral peaks using the AMARES (advanced method of accurate, robust and efficient spectroscopic fitting) method. Peaks for phosphocreatine, α, β, γ - ATP, 2,3-diphosphoglycerate and phosphodiesters were fitted using prior knowledge of relative peak frequencies, J-coupling constants for ATP, relative peak amplitudes, relative phases and assumed Lorentzian line shapes along with acquisition parameters (central frequency, bandwidth, TR and calculated flip angles at various depths). Peak areas were corrected for RF partial saturation effects using the recorded excitation flip angle, T1 values (PCr 3.8 s, γ-ATP 2.4 s, α-ATP 2.5 s, β-ATP 2.7 s, 2,3-DPG 1.39 s, PDE 1.11 s) and spectral overlap with the NADH peak. The value of the ATP peak was corrected for blood contamination by subtracting 11 % of the DPG peak area[151].

PCr/ATP was calculated using the average of the three ATP peaks. The quality of spectral fit was assessed using the coefficient of variation in the coefficient of variation in the measured PCr/ATP, based on Cramer-Rao lower bounds (an indicator of signal to noise ratio in the sample) and standard error propagation formulae. Samples with a greater than 35 % coefficient of variation were excluded.

2.5.2 Hyperpolarized magnetic resonance spectroscopy

2.5.2.1 Sterile pathway production and injection

Sterile fluid pathways (SFPs) were assembled in a Grade A sterile environment containing 1.47 g [1-^{13}C]pyruvic acid (Sigma Aldrich, Gillingham, UK) and 15 mM AH111501 (Syncom, Groningen, Netherlands) as the electron paramagnetic agent (EPA). SFPs were loaded into a General Electric SpinLab system (GE Healthcare, Chicago, USA) which was used for the process of Dynamic Nuclear Polarisation. Sufficient polarisation levels were achieved after 2-3 hours. Dissolution was undertaken using 38.5 g of sterile water heated to 130 °C under pressure, released through the pyruvate containing vial into a receiver vessel containing 17.7 g of trometamol buffer solution (600 mM NaOH, 333 mM Tris base, and 333 mg/L disodium EDTA [as the chelating agent], Royal Free Hospital, London, UK) and a further 19.5 g of sterile water. The EPA was removed by filtration prior to the receiver vessel, with the final product for injection drawn from the receiver vessel into a 50 ml injection syringe (Bayer, Indianola, USA) via a further 0.2 μm sterilization filter (Saint-Gobain, Gaithersburg, USA). Rigorous quality control (QC) of the final filtered sodium [1-^{13}C]pyruvate solution was undertaken prior to human injection. This consisted of both online measurements (pyruvate concentration, residual EPA concentration, temperature, polarization, volume) directly from the SpinLab inbuilt QC console, with further 'offline' pH measurement (RQflex 10, Merck, Darmstadt, Germany) and visual inspection of the product (for visible particulates and appearance) undertaken manually prior to release. Pathways were only released for human injection if the following criteria were met: pH 6.7-8.4, temperature 25.0-37.0 °C, polarization ≥ 15 %, [pyruvate]

220-280 mM, [EPA] ≤ 3.0 μM, appearance: clear, colourless solution with no visible particulate matter. Pathways not meeting these release criteria were rejected. Hyperpolarized [1-^{13}C]pyruvate solution was administered through a venous cannula inserted in a sufficiently sized peripheral vein, at a dose of 0.4 ml/kg, followed by a 25 ml 0.9 % normal saline flush. Injections were performed at a rate of 5 ml per second using a MEDRAD® power injector system (Bayer, Berlin, Germany).

2.5.2.2 Spectral acquisition and analysis

Patients were positioned supine on the scanner table with a two channel transmit, 8 channel surface-receive array (Rapid Biomedical, Rimpar, Germany). Hyperpolarized data were obtained from a 10mm mid-ventricular, short axis slice of the heart using a single slice-selective excitation spectroscopy sequence which acquired gated to the R-wave and acquiring data with every heartbeat during and up to a total of 4 minutes after the injection of the pyruvate pathway. As the ratios of certain metabolites (bicarbonate, alanine, lactate) are known to correlate linearly with the kinetic rate constants of the PDH-reaction, metabolite-to-pyruvate ratios were calculated by summing the first 60-90 s of spectral data acquired following the initial appearance of the hyperpolarized pyruvate resonance in the acquired spectra.

Multi-coil data were recombined in MATLAB using the Whitened Singular Value Decomposition algorithm, with coil combination weights calculated for spectra with the highest SNR subsequently applied to the entire dataset. Spectra were background-subtracted prior to quantification with the AMARES algorithm, with

appropriate prior knowledge. Total integrated metabolite-to-pyruvate ratios were calculated from the data available.

2.5.3 Proton magnetic resonance spectroscopy

Patients were positioned supine on the scanner table using an 18-channel surface coil (Siemens Healthineers, Erlangen, Germany) array. Anatomical images in keeping with the slice positioning for cine imaging (see **Chapter 2.5.4** below) were used and spectral acquisition performed from the inter-ventricular septum of a mid-short axis slice using a stimulated echo sequence (STEAM) as previously described.[127] Spectroscopic acquisitions were performed using an ECG-trigger at end-diastole and in expiration to best reduce motion artefacts. To be able to correctly perform spectral quantification of the data, water-suppressed and unsuppressed spectra were obtained. Water suppressed spectra were collected over 5 breath holds, encompassing 5 acquisitions each, i.e. 25 measurements combined. Next three measurements of water unsuppressed spectra were acquired for internal reference in a single breath hold. Sequence parameters were as follows: echo time 10 ms, mixing time 7 ms, and repetition time at least 750 ms for water-suppressed scans and at least 4,000 ms for non–water-suppressed scans with acquisitions synchronized to the patients' ECG

2.5.3.1 Spectral analysis

Spectral quantification was again performed using the AMARES algorithm included in the OXSA toolbox.[150] The amplitude of the lipid resonance at 1.3 ppm (-CH_2-) from the spectra was then selected for myocardial lipid quantification within the selected voxel. The lipid content is expressed as a percentage relative to

water (proton density fat fraction, PDFF) with the amplitude of the lipid peak divided by the amplitude of the water peak and subsequently multiplied by 100.

2.5.4 Cine imaging for cardiac volumes and function

After standard planning, cine images were acquired in three long axis views (horizontal long axis, HLA; vertical long axis, VLA; left ventricular outflow tract view, LVOT) and in short axis slices covering the whole left ventricle (LV) using balanced steady-state free precession cine imaging. Scan parameters were typically: TR/TE = 40.5/1.14 ms, flip angle = 55°, FOV = 380 x 380 mm, voxel size = 2.0 x 2.0 x 8.0 mm, slice thickness = 8.0 mm, GRAPPA = 3, reference lines = 24, segments = 15, measurements = 1, bandwidth = 930 Hz/Px. Cines were acquired using retrospective ECG gating for participants in sinus rhythm at the time of the scan. For patients in atrial fibrillation/flutter or with frequent ectopy and where acceptable images could not be obtained, prospectively triggered cines were acquired instead.

Image analysis for biventricular indices was performed offline in accordance with Society for Cardiovascular Magnetic Resonance (SCMR) guidelines[125], using cvi42 post-processing software (version 5.10.1, Circle Cardiovascular Imaging Inc., Calgary, Canada). Epicardial and endocardial borders on LV short axis images were manually contoured at end-diastole; endocardial contours were also placed at end-systole. End-systolic (ESV) and end-diastolic (EDV) volumes were used to calculate stroke volume (SV) as SV = EDV – ESV. Ejection fraction (EF) was calculated as EF = SV/EDV. Papillary muscles were included as part of the LV volume but excluded from LV mass. LV mass results from the difference between

the total epicardial volume (sum of epicardial cross-sectional areas multiplied by the sum of the slice thickness and interslice gap) minus the total endocardial volume, multiplied by the specific density of myocardium (1.05 g/ml).

2.5.4.1 Free-breathing exercise cine acquisition

A retrospectively gated, four-fold accelerated, compressed sensing, free-breathing 2D cine imaging sequence was used to acquire a short axis stack covering the entire heart, including both atria. This BEAT-2CV sequence was based on a modified bSSFP sequence, with a variable-density trajectory, and reconstructed using the open-source toolkit Gadgetron, as described previously.[152,153]

Exact sequence parameters were optimised on a per-patient basis, but these were typically a TR of 42–43 ms, determined to be minimal but subject to dynamically evolving SAR and FOV constraints; TE 1.17 ms, determined by a desire for a fixed readout bandwidth of 1302 Hz/Px, flip angle 30–40°, slice thickness 8 mm, FOV typically 340 × 340 mm^2 (but increased on a per-patient basis to avoid spatial aliasing). The base resolution was 160 points with a 77% phase resolution with a 6/8 the phase partial Fourier scheme, corresponding to the acquisition of 92 reconstructed to a matrix size of 160 × 120, and a typical spatial resolution 1.8 × 1.8 mm, with 25 cardiac phases.

Exercise stress was then performed using a CMR-compatible stepping ergometer in the supine position (Cardio Step, Ergospect GmbH, Innsbruck, Austria; (**Figure 2.1**). The exercise protocol comprised a fixed workload of 20 W for 6 minutes. Repeat whole-heart cine images were acquired during the final minute of the exercise period.

Figure 2.1: Exercise CMR

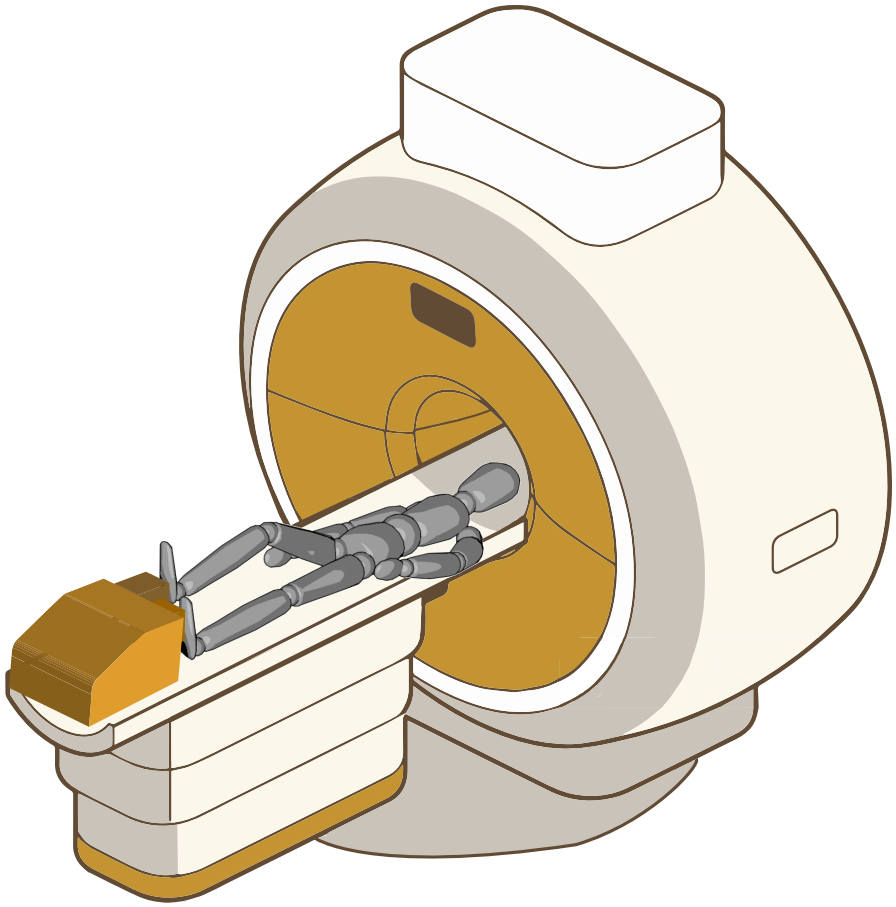

Figure 2.1: Exercise CMR. *Schematic illustration of the setup for exercise CMR investigations using a CMR-compatible pedal ergometer.*

2.5.5 T1-mapping (native)

Myocardial T1-mapping was performed using the ShMOLLI 5(1)1(1)1 sequence as previously published.[154] Typical scan parameters were: TR/TE = 378.98/1.07 ms, flip angle = 35°, FOV read = 360 mm, FOV phase = 75 %, interpolated voxel size = 0.9 x 0.9 x 8.0 mm, slice thickness = 8.0 mm, trigger delay (TD) = 260 ms,

TI 260 ms, measurements = 1, bandwidth = 898 Hz/Px. T1-maps were acquired in the basal, mid-ventricular, and apical slices as described above.

Specific modifications to the typical ShMOLLI sequence described above were undertaken to permit application in the presence of atrial fibrillation or flutter.[155] Briefly, the trigger delay (TD) was reduced to permit readout in systole, thereby reducing the risk of mistriggering that is often encountered when applying the standard diastolic readout (TD = 260 ms) sequence in the presence of tachycardia.

Quality assessment of ShMOLLI T1-maps was performed by visually inspecting the (R^2) maps (**Figure 2.2)**, which were immediately available in-line at time of acquisition.[154,156] R^2 maps are a tool to assess the quality of T1-maps generated, identify compromised acquisitions and re-acquire maps of insufficient quality.[157]

Offline post-processing of T1-maps was conducted in the OCMR imaging corelab using dedicated in-house software (MC-ROI) developed by Professor Stefan K Piechnik (Interactive Data Language v6.1, Exelis Visual Information Solutions, Boulder, Colorado, USA). Endocardial and epicardial contours were placed using dedicated automated software[158] and manually checked for errors and corrected in compliance with internal training standards.[159] Care was taken to minimise contamination of the myocardium by blood-pool and extra-myocardial structure partial volume effects (**Figure 2.2**).

Figure 2.2: T1-Map Analysis

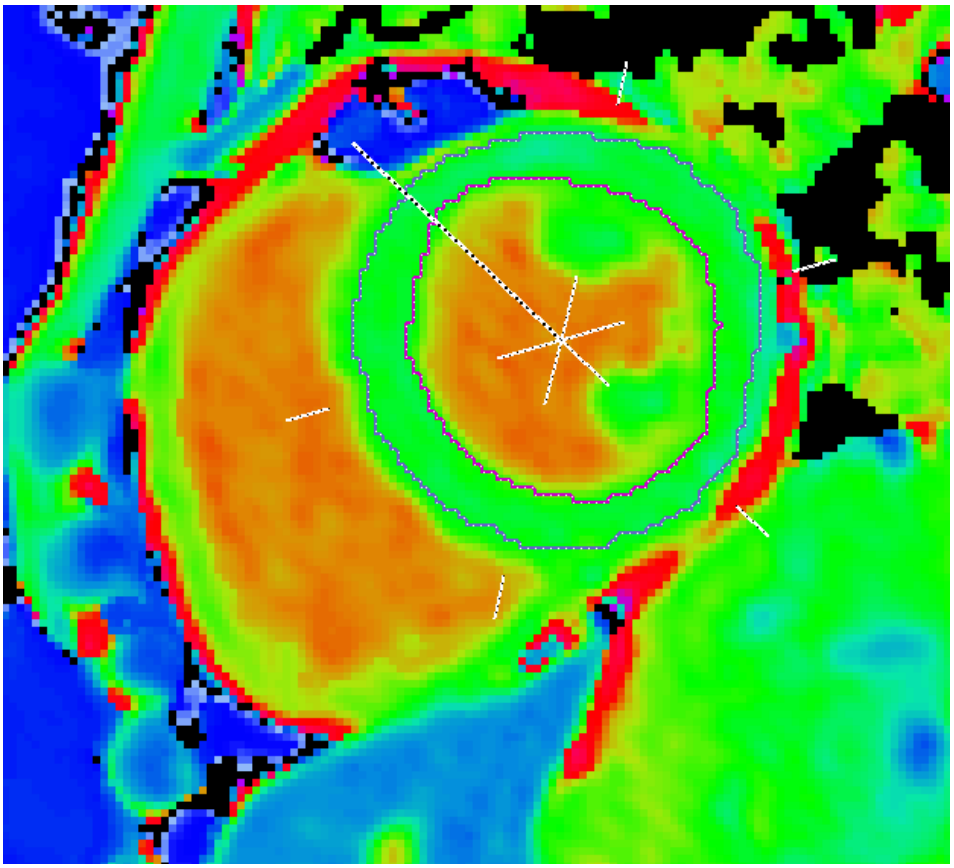

Figure 2.2: T1-map analysis from a mid-ventricular slice using MC-ROI software. *The anterior right ventricular/ left ventricular insertion point is annotated, while endocardial and epicardial contours are placed within the myocardium to avoid contamination from extra-myocardial tissues and partial volume effects.*

2.5.6 Myocardial tagging

Tagged MR images were obtained before administration of gadolinium contrast agents for measurement of LV-strain, using an ECG-triggered segmented k-space fast gradient echo sequence with spatial modulation of magnetization in orthogonal planes creating a square grid of parallel tag lines, as previously described.[160] Three short axis (basal, mid and apical slice respectively) and one long axis (horizontal)

images were obtained. The scan parameters were typically as follows: voxel size 2.1 x 1.4 x 8.0 mm, field of view = 360 x 292 mm, matrix 141 x 256, TR/TE = 40.45/3.89 ms, flip angle 14°, segments = 9, phases = 16, grid tag distance = 7mm, bandwidth = 184 Hz/Px.

Post-processing analysis was performed by an independent analysist blinded to treatment status and patient details using CIM software (CIMTag2D, Auckland, New Zealand). Semi-automated analysis was performed by aligning a grid to the myocardial tagging planes in end-diastole. End-systole was then determined visually, and tags adjusted at each frame throughout the cardiac cycle to derive peak systolic circumferential strain for the mid-ventricular slice, which is expressed as a percentage change from end-diastole. Normal strain has previously been described as -19 ± 234; impaired myocardial contractility is indicated by a more positive value.

2.5.7 Resting perfusion

An intravenous cannula with a three-way tap was placed into a suitable peripheral vein to allow administration of a bolus of gadolinium-based contrast agent.

Perfusion imaging was performed every cardiac cycle (over 60 heart beats) during the first pass of an intravenous gadolinium-based contrast agent using a T1-weighted fast (spoiled) gradient echo sequence. Typical scan parameters were: TR/TE = 142/1.04 ms, flip angle = 50°, FOV read = 360 mm, FOV phase = 75%, voxel size = 1.9 x 1.9 x 8.0 mm, slice thickness = 8.0 mm, TI = 105 ms, GRAPPA = 3, measurements = 60, segments = 37, phases = 1, bandwidth = 1085 Hz/Px.

First-pass perfusion imaging was performed on matching short axis slices (basal, mid-ventricular, apical) to the T1-maps. A 0.05 mmol/kg intravenous bolus injection of a gadolinium contrast agent (gadobutrol, Gadovist) was administered, immediately followed by a 15-20 ml saline flush, both dispensed at 4-6 ml/sec via a power injector (Medrad, Bayer, Leverkusen, Germany). This injection was manually triggered after an interval of 8 heart beats from the initiation of image acquisition. Automated inline pixel-wise perfusion maps were immediately generated, which provide absolute quantification of MBF based on the AHA 16-segment model.[161-163]

Offline perfusion analysis was performed using cvi42 post-processing software (version 5.10.1, Circle Cardiovascular Imaging Inc., Calgary, Canada). First-pass stress and rest perfusion images were carefully analysed for the presence of reversible perfusion defects. Quality assessment of the dual AIF sequence approach was performed based on correct positioning of the region of interest (ROI) within the LV blood pool, as well as heart rate mistriggering. Global and segmental quantitative myocardial blood flow measurements were derived from rest and stress pixel-wise perfusion maps (**Figure 2.3**).

Figure 2.3: Pixel-wise Perfusion Analysis

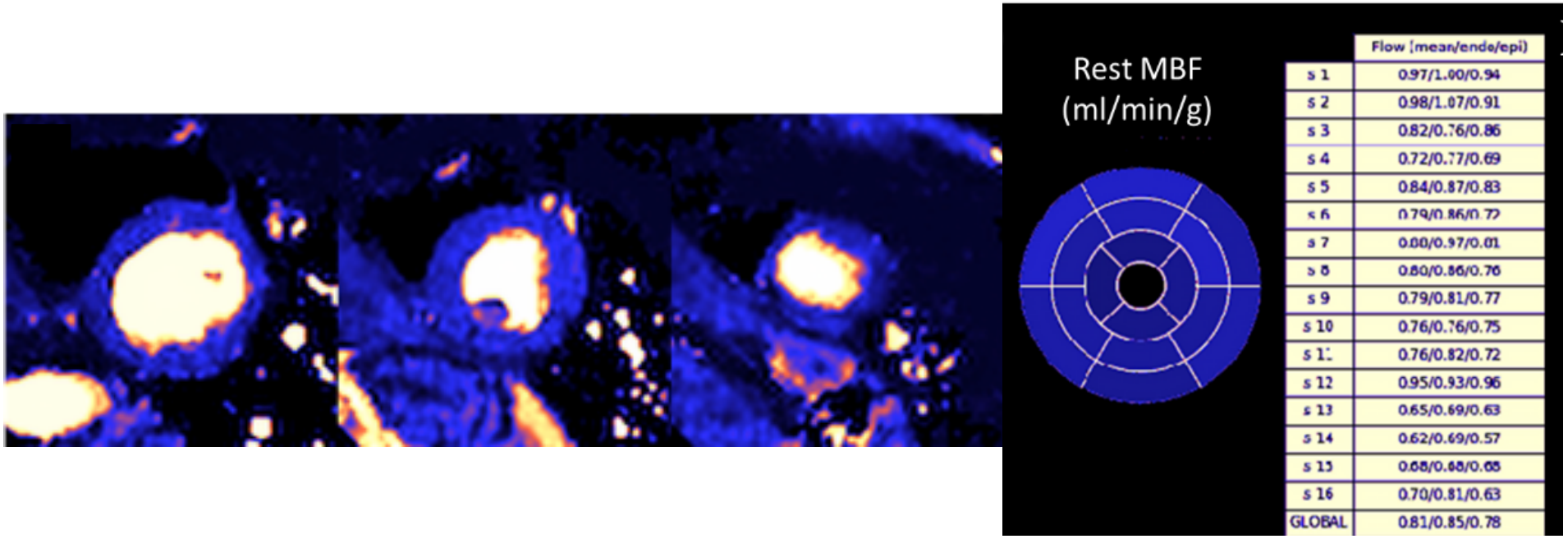

***Figure** 2.3: Pixel-wise perfusion maps for quantification of myocardial blood flow. Examples of perfusion maps at rest acquired in the basal, mid-ventricular, and apical slice positions. This visualises the quantitative estimates of myocardial blood flow (MBF) measurements with both segmental and global estimates.*

2.5.8 Late gadolinium enhancement

Late gadolinium enhancement (LGE) images were acquired using a prospectively triggered T1-weighted phase-sensitive inversion recovery sequence approximately 8-10 minutes after administration of a top up of the same intravenous gadolinium-based contrast agent (Gadovist, 0.1 mmol/kg). The inversion time (TI) was adjusted for optimal nulling of remote normal myocardium. LGE images were acquired in standard long and short axis slices covering the whole LV. Typical scan parameters were TR/TE = 750/3.38 ms, flip angle = 25°, FOV read = 380 mm, FOV phase = 75%, voxel size = 1.5 x 1.5 x 8.0 mm, slice thickness = 8.0 mm, GRAPPA = 2, reference lines = 24, measurements = 1, segments = 25, phases = 1, bandwidth = 130 Hz/Px.

Images were evaluated qualitatively and quantitatively in cvi42 post-processing software (version 5.10.1, Circle Cardiovascular Imaging Inc., Calgary, Canada) for the presence or absence, pattern (subendocardial, mid-wall, subepicardial, transmural), and regional distribution of LGE areas. LGE suspected on short axis imaging was confirmed with additional imaging in long axis views or perpendicular to the lesion.

2.5.9 Post-contrast T1-mapping and ECV estimation

Post-contrast T1-maps were acquired following administration of an intravenous gadolinium-based contrast agent. Slice position and sequence parameters were essentially unchanged to those used for native T1-mapping.

Offline post-processing of post-contrast T1-maps was conducted using the same methods as outline for native T1-maps. R1 of blood and myocardium was calculated as R1 = 1/T1 for both native and post-contrast maps. Haematocrit was measured on a blood sample drawn on the same day, immediately prior to the CMR scan.

Extracellular volume (ECV) was calculated as per the following formula[164]:

$$\text{ECV} = (1 - \text{haematocrit}) \times (\frac{\Delta R1_{myocardium}}{\Delta R1_{blood}})$$

2.6 Echocardiography

Patients were assessed by two-dimensional (2D) transthoracic echocardiography (TTE, **Figure 2.4**) using a standardised imaging protocol as laid out by the British Society of Echocardiography.[165]

All patients underwent TTE assessments at rest, in supine position and importantly before any demanding physical activity or pharmacological stress investigations. Apical four- and two chamber images were acquired to calculate left ventricular ejection fraction (LVEF) using the biplane method proposed by Simpson.[166] Pulsed-wave (PW) Doppler of the mitral valve, tissue Doppler of the basal septum and basal lateral wall were obtained to assess left ventricular diastolic function. PW Doppler of the right and left ventricular outflow tract, continuous wave (CW) doppler of the aortic and pulmonary valves and continuous wave (CW) Doppler of the main pulmonary artery and the aortic root in parasternal short axis at vessel level

were acquired to rule out any major valve or vascular disease. Images were contoured in keeping with official recommendations[167] by an operator blinded to treatment status on a Philips IntelliSpace Cardiovascular analysis platform (Philips Healthcare, Farnborough, UK)

A B

Figure 2.4: Representative Echocardiography Images

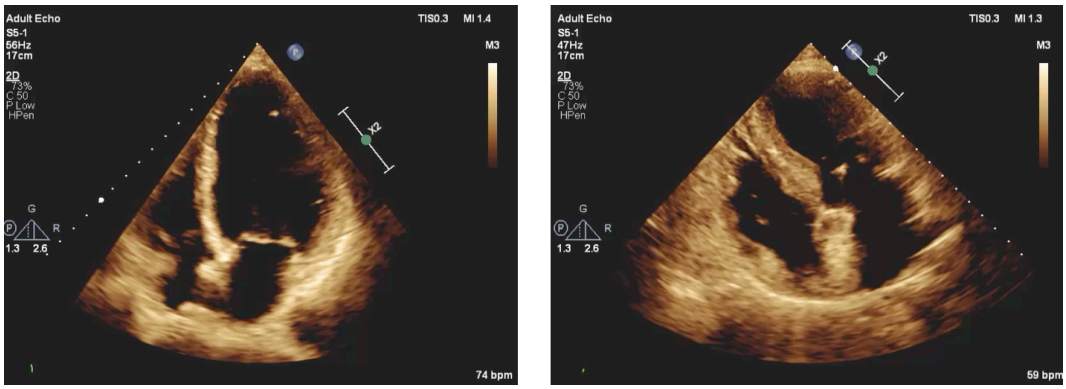

Figure 2.4: Echocardiography. *Representative four chamber / horizontal long axis images of a patient with HFrEF (A) and HFpEF (B).*

2.7 Cardiopulmonary exercise testing and spirometry

Participants enrolled in experiments involving an ergometer exercise protocol (see **Chapters 3 and 4**) were asked to complete a peak cardiopulmonary exercise test using a stationary cycle ergometer (Ergoline GmbH, Bitz, Germany) and breath-by-breath respiratory gas analyser (Metalyzer 3B, Cortex Biophysik, Leipzig, Germany) with a predefined, standardised incremental exercise protocol with an initial load of 20W and incremental 10W stages per minute.

Before any testing, calibration was conducted using a 3.0-L calibration syringe (Futuremed, Granada Hills, California, USA). After a rest period of 3 minutes, workloads were increased according to a ramp protocol of 10 watts (W) every

minute with breath-by-breath gas exchange and heart rate being measured throughout the test. Peak oxygen uptake (peak $\dot{V}O_2$) was determined at baseline (Visit 2) and EOT (Visit 4) after achieving a respiratory exchange ratio (RER) of >1.1. Blood pressure, oxygen saturation, capillary lactate (finger prick or earlobe) and rated perceived exertion score[168] were measured at rest and subsequently every 2-3 minutes. Patients were encouraged to reach a level of maximum effort but were told to stop at the discretion of the supervising investigator if there were any exercise-related adverse effects. Analysis of the exercise data was carried out in an automated, reproducible fashion on a dedicated workstation with the necessary software for analysis (MetaSoft Studio, Cortex Medical, Cortex Biophysik GmbH, Leipzig, Germany). The investigator carried out scrupulous data quality checks on each dataset.

All participants mentioned above were likewise undergoing standardised spirometry using the identical equipment (Metalyzer 3B) before any exercise testing was carried out. Participants remained in a seated position wearing a nose clip and using a mouthpiece with lips tightly sealed around this. At least three acceptable forced in- and expirations, carefully checking recorded waveforms, were acquired enabling analysis of forced expiratory volume at 1 second (FEV_1) and forced vital capacity (FVC).

2.8 Six-minute walk test

Participants enrolled in the respective studies (see **Chapters 3 and 4**) performed a six-minute walk test (6-MWT) independently at their own pace along a dedicated, 20-meter-long corridor. The institution's standard protocol as well as previously

published guidance[169] were followed for conducting the test. Total distance covered, rating of perceived exertion[168] as well as HR and BP were recorded prior to and after the test.

2.9 Electrocardiogram

12-lead Electrocardiograms (ECG) were performed at different timepoints with paper traces collected for each time point. In the event of an adverse event with any cardiac symptoms (for example arrhythmia or chest pain), additional ECGs were recorded. Any clinically relevant changes in the ECG were reported as adverse event (AE) and followed up until resolved.

2.10 Patient reported outcomes

2.10.1 Kansas City Cardiomyopathy Questionnaire

The Kansas City Cardiomyopathy Questionnaire (KCCQ) is a 23-item, self-administered tool designed to evaluate physical limitations, symptoms (frequency, severity, changes over time), social limitations, self-efficacy and QoL in HF patients.[170] Patients had access to a separated, quiet area where they were given sufficient time unsupervised to record their answers on the questionnaires in a pen and paper format. In instances where a patient could not give or decide upon a response, no response was recorded.

2.10.2 EQ-5D-5L

The 5 level EQ-5D is a standardised instrument for use of measuring health related QoL. Patients had to self-report the questionnaire which consists of two pages. Firstly, the ‘descriptive system’ which comprises 5 dimensions of overall health

(mobility, self-care, usual activities, pain/discomfort, anxiety/depression) that can be graded in 5 levels (no problems to unable to perform activity). Secondly, the 'visual analogue scale' on which patients rate their health status from 0 (worst) to 100 (best).

2.11 Blood sampling

Venous blood samples were collected at different time points of each experiment (see details in the Methods section in the respective Chapter). All samples were drawn from patients who were fasting unless indicated otherwise. Generally, a variety of biomarkers relating to the investigational medicinal product (IMP) or the respective interventions were assessed.

In addition, blood samples for a targeted analysis of serum metabolomics (**Chapters 3 and 4**) were taken from the patients prior to and after treatment.

Processing of blood samples took place on site according to domestic standard operating procedures and expert advice. Blood samples where then either sent for analysis at the John Radcliffe Hospital or frozen (-20 or -80 °C) and shipped to a contractor where the subsequent analyses took place (Labcorp Drug Development, Geneva, Switzerland).

Metabolomic samples were pre-processed by centrifugating at 3.000 rpm for 15 minutes at 4 °C and subsequently frozen and stored on site until shipped to an academic collaborator (Prof. Julian Griffin, Imperial College London/University of Aberdeen, UK) for further analysis. Statistical analysis of results was conducted by a blinded investigator in OCMR and then repeated unblinded in OCMR by a different investigator. Serum samples were injected onto a liquid chromatography

(LC) column for adequate separation of individual metabolites before being further separated by application of mass spectrometry (MS) **(Figure 2.5**)

Figure 2.5: Targeted Metabolomics Processing

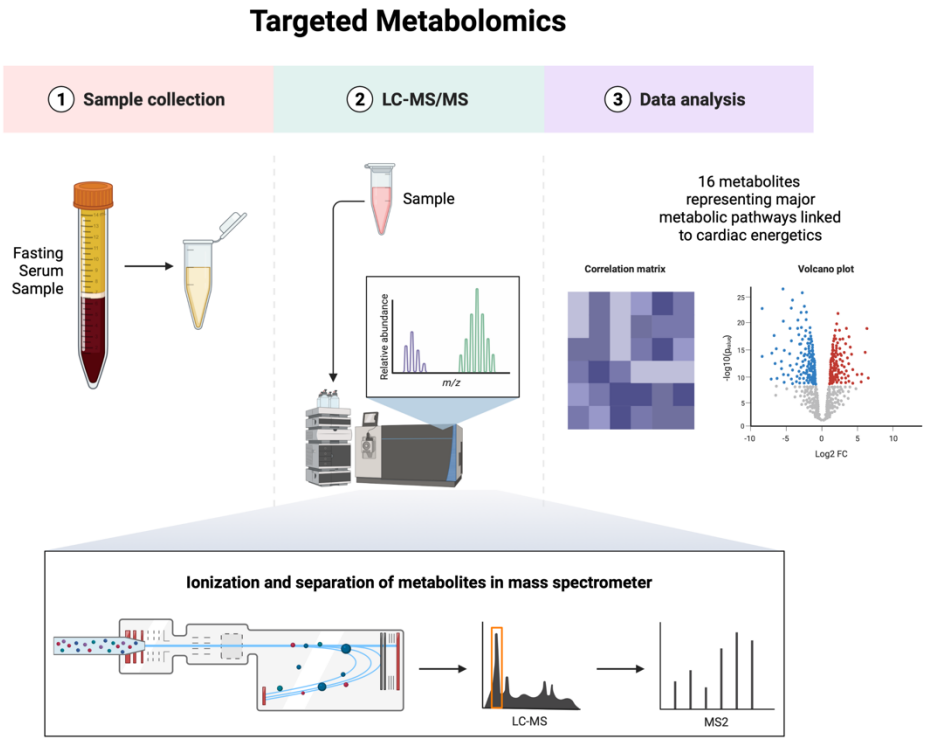

Figure 2.5: Targeted Metabolomics. *Simplified overview of sample processing and analysis: 1: venous blood samples are collected from fasting patients and then centrifuged to collect the supernatant serum only. 2: Liquid chromatography (LC) and mass spectrometry (MS) are used to achieve separation of metabolites followed by identification of the metabolites in a separate MS step. 3: Statistical analysis and visualisation using correlation matrix, volcano plots and principal component analysis (PCA) are used to indicate results.*

2.12 Study interventions

2.12.1 SGLT2i in patients with HFrEF

Empagliflozin (10 mg) and matching placebo were supplied as film-coated tablets produced by Boehringer Ingelheim Pharma GmbH & Co. KG, Biberach/Riss, Germany. Batch release of trial kits was performed by Development Quality and Records Management of Boehringer Ingelheim Pharma GmbH & Co. KG Biberach/Riss, Germany. Patients were advised to take one tablet of empagliflozin (10 mg) or matching placebo at the same time every day (preferably morning) with or without food for the duration of the trial.

2.12.2 SGLT2i in patients with HFpEF

Empagliflozin (10 mg) and matching placebo were supplied as film-coated tablets produced by Boehringer Ingelheim Pharma GmbH & Co. KG, Biberach/Riss, Germany. Batch release of trial kits was performed by Development Quality and Records Management of Boehringer Ingelheim Pharma GmbH & Co. KG Biberach/Riss, Germany. Patients were advised to take one tablet of empagliflozin (10 mg) or matching placebo at the same time every day (preferably morning) with or without food for the duration of the trial.

2.12.3 VLED in patients with HFpEF

Patients were encouraged to follow a strict diet with a reduced energy intake of 800 kilocalories (kcal) per day. To achieve substantial weight loss in the observation period and ensure patient adherence, normal meals were replaced with nutritionally complete (200 kcal per sachet; 59 % carbohydrates, 26 %

protein, 13 % fat, 3 % fibre) meal replacement products (MRP) for the time of the dietary intervention. The MRP was purchased via and supplied by Counterweight Ltd. (Glasgow, UK.)

2.12.4 Ninerafaxstat in patients with obesity and T2D

Ninerafaxstat was supplied by Imbria pharmaceuticals (Boston, Massachusetts, USA) as a modified release tablet formulation containing 200 mg of active ingredient. Patients were self-administering the IMP twice daily at home at the same time each day and kept a dosing diary recording the date, time and amount of IMP taken each day for the duration of the study (4 or 8 weeks).

2.13 Summary

All methods described in this chapter were the mainstay of experiments for the work conducted in this DPhil Thesis. In addition, there is a brief description of the specific methods for every individual chapter providing further details and clarification on the specific techniques and methods used for the respective experiment.

3 *Effects of SGLT2-inhibition in HFrEF*

3.1 Abstract

3.1.1 Background

Following their incidental discovery as potential HF drugs, sodium glucose co-transporter-2 inhibitors (SGLT2i) have now been proven to be an effective treatment to reduce hospitalisations and improve quality of life (QoL) in patients with heart failure (HF). Nevertheless, a conclusive mechanism of action, which would enable deeper understanding of specific patient phenotypes benefiting the most as well as allow development of novel targeted medicines to treat HF, has not yet been identified. Derangements in cardiac energy metabolism are considered a hallmark of HF and it was proposed early that SGLT2i may translate their beneficial effects via enhancing cardiac energy production. Thus, this trial sought to assess if empagliflozin treatment (10 mg OD) leads to detectable changes in PCr/ATP a sensitive marker of cardiac energetics and myocardial energy reserve.

3.1.2 Methods

In this prospective, randomized, double-blind, placebo controlled, mechanistic trial, patients with chronic HF with a reduced ejection fraction (HFrEF; n=36) were randomly assigned to empagliflozin treatment (10 mg OD) or matched placebo for

12 weeks (mean treatment duration 84 days (±6.9)). Symptomatic patients with established HF with a reduced ejection fraction (HFrEF; LVEF ≤ 40%), confirmed by a significantly elevated NT-proBNP (> 125 pg/ml in sinus rhythm or > 600 pg/ml in atrial fibrillation) and echocardiogram at screening, on optimal medical treatment (OMT) were enrolled. We excluded patients in New York Heart Association class <II. The primary endpoint was the change in phosphocreatine to adenosine triphosphate ratio (PCr/ATP) from baseline to week 12 determined by phosphorus magnetic resonance spectroscopy (^{31}P-MRS). No secondary endpoints were prespecified but a list of various exploratory endpoints defined (see **Methods**).

3.1.3 Results

There was no significant difference between empagliflozin and placebo regarding the primary endpoint of change in resting PCr/ATP from baseline to week 12 (-0.25 ± 0.16; 95 % CI: -0.58, 0.09; p=0.14). Equally, there was no significant difference regarding change in PCr/ATP during dobutamine stress (-0.13 ± 0.11; 95 % CI: -0.35, 0.09; p=0.23). Myocardial steatosis expressed by myocardial triglycerides (MTG) measured by ^{1}H-MRS decreased on average in the empagliflozin group (-0.21 ± 0.17) but increased in the placebo group (0.23 ± 0.19) (-0.44 ± 0.26; 95 % CI: -0.97, 0.08; p=0.09). Treatment with empagliflozin led to significant anti-hypertrophic effects expressed in reduced LV-mass (-9.65g ± 3.83; 95 % CI: -17.5, -1.81; p=0.02), cardiac cell volume (-9.179ml ± 2.639; 95 % CI: -14.88, -3.478; p=0.0041) and native threshold T1 (-0.11ms; 95 % CI: -0.20, -0.01; p=0.03) compared to placebo. Measures of cardiopulmonary exercise testing (CPET) were not notably different between empagliflozin and placebo (peak VO_2, VE/VCO_2

slope, VT, RER lactate, exercise time, maximal workload), neither did the walking distance in the 6-MWT increase. Quality of life determined by KCCQ showed superior improvements in the empagliflozin group compared to placebo in all test dimensions. Biomarker analysis of the Renin-Angiotensin-Aldosterone System (RAAS) showed neurohormonal elevations in the treatment arm.

3.1.4 Conclusions

In patients with chronic HFrEF, treatment with 10mg of empagliflozin once daily for 12 weeks, did not lead to measurable improvement of PCr/ATP, at rest or during dobutamine stress, compared to placebo. However, exploratory endpoint analyses suggested favourable structural cardiac changes and anti-fibrotic effects as well as improved measures of QoL and changes in RAAS physiology. These would be consistent with an anti-fibrotic mechanism of action. Given our restrictions on sample size, our results are to be considered hypothesis generating. Nevertheless, they are encouraging for investigation in larger outcome trials.

3.2 Introduction

HF is a clinically complex, multi-organ syndrome which has a plethora of possible causes and with a multifaceted pathophysiology, remains incompletely understood. Despite an overall decreasing incidence over the last three decades, the improvements in therapy, and resultant survival, have led to constantly rising HF prevalence, particularly noticeable in our progressively aging society.[171] Consequentially, perennial hospitalisations, increasing morbidity and frequent comorbid conditions add to the heavy burden for patients and healthcare systems alike. With projections of HF prevalence to possibly affect up to 9 % of all Americans aged 65 and older while cardiovascular drug development remains stagnant[172], novel treatments are urgently needed.[173] This situation is similar on the European continent, where up to 10 % of the population aged 70 and over are affected and frequent hospital admissions and care requirements are leading to an alarming estimated annual cost of almost €30 billion.[3]

Following their serendipitous discovery as novel heart failure drugs[174], the anti-diabetic sodium glucose co-transporter 2 inhibitors (SGLT2i) have risen to become a cornerstone for treatment of HFrEF.[121,175] Beneficial effects include a reduced risk of dying from cardiovascular cause or being hospitalised for HF, major adverse cardiac events (MACE) and improvements of quality of life (QoL).[176,177] Importantly, these effects were consistently seen in patients with and without type 2 diabetes (T2D) at baseline as well as across the spectrum of different SGLT2i hence, can be considered a class-effect of SGLT2i regardless of their selectivity.[178-180]

Nonetheless, it remains elusive how a drug inhibiting transport proteins absent on the cardiomyocyte membrane[181] may lead to a substantially reduced risk for hospitalisation for HF or CV death, evident only months after treatment onset. Preliminary data derived from *in-vitro* studies and animal models suggested a possible effect on myocardial energetics (ATP metabolism) however, the published literature is overall conflicting with some studies describing improvements and others describing no metabolic treatment effects. Generation in pre-clinical models frequently entails disease models of a single etiology (e.g. transverse aortic constriction, volume overload, infarction) which makes generalisation of results and transfer into human HF, with or without T2D, challenging.[182-186]

Administration of SGLT2i induces glucosuria and thus, leads to an energy deficit of at least 250 kcal per day.[187] As a compensatory measure, this results in an increase of free fatty acid (FFA) oxidation and slight hyperketonaemia leading to measurably increased levels of beta hydroxybutyrate (β-OHB), an energy source avidly used by the failing heart.[22] A 'thrifty substrate hypothesis'[188] was put forward to explain the surprising results of *EMPA-REG OUTCOME*[174], where a reduction of hospitalisation for HF was observed in patients with T2D and a high cardiovascular risk, and subsequently, following manuscripts reported improvements in cardiac energy metabolism. Importantly, most studies were in-vitro experiments or utilised animal models, often in an *ex-vivo* approach to assess cardiac energy metabolism. Additionally, many of the studies elicited conflicting results, sometimes even from the same group.[182,183]

Of note and to the best of our knowledge, only two studies have reported *in-vivo* investigation of SGLT2i-treatment in patients however, both enrolled exclusively

type 2 diabetes (T2D) patients and neither was conducted in a randomised, double-blind fashion.[189,190] Despite different CMR and echo imaging studies investigating HFrEF patients, no prior study investigated metabolic effects of SGLT2i in patients with chronic HFrEF, irrespective of presence or absence of T2D, *in-vivo*.

Consequently, *EMPA-VISION* is the first prospective, randomised, double-blind, placebo-controlled trial assessing the effects of empagliflozin treatment on cardiac energy metabolism and physiology.

3.3 Methods

3.3.1 Randomisation

During their baseline visit (Visit 2, see **Figure 3.1**), eligible patients were randomly assigned to either 10mg of empagliflozin or matching placebo per day over a period of 12 weeks. Randomisation occurred in a 1:1 fashion and the drug assignment was carried out using an interactive web response system. The randomisation list involved a pseudo-random number generator ensuring the resulting treatment was both reproducible and non-predictable with a block size of 4.

3.3.2 Study visit schedule

Patients deemed eligible after a meticulous pre-screening process were invited for a screening visit (Visit 1) to determine their eligibility status. From their attendance at this visit, there was a 21-day window to invite them for their subsequent randomisation visit (Visit 2, day 1 of treatment) and perform the randomisation to treatment (see 3.3.1 for details). As a safety precaution, patients were invited for a

safety visit (Visit 3, 14±1 days of treatment) before attending their EOT visit (Visit 4, 84±4 days of treatment). To ensure safety, an additional phone call (Visit 5, days 7-14 after Visit 4) was conducted to ensure uncomplicated withdrawal from the study drug. **Figure 3.1** provides an overview of the visit schedule and timelines for *EMPA-VISION*.

Figure 3.1: Visit Timeline EMPA-VISION HFrEF

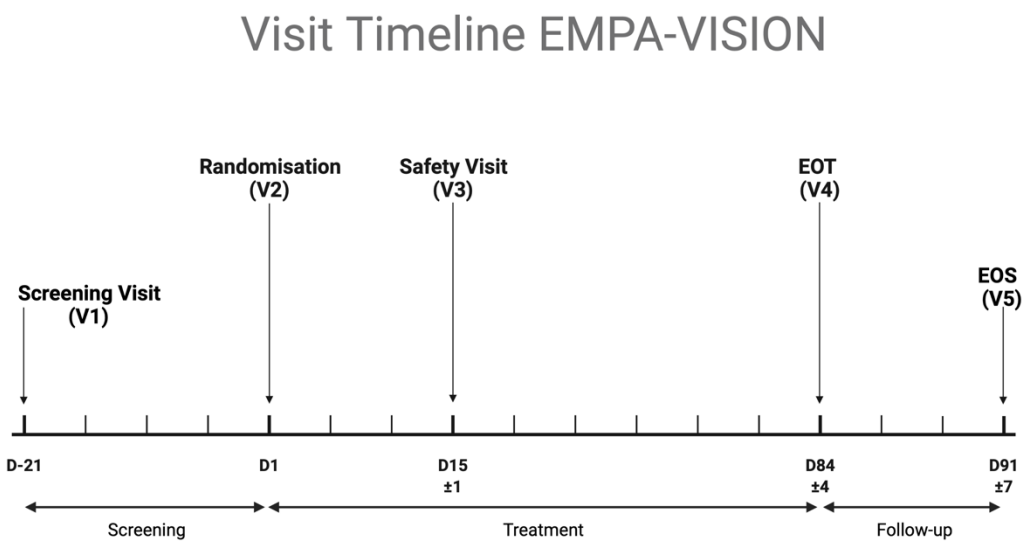

Figure 3.1: Visit Timeline EMPA-VISION HFrEF. *Schematic overview of EMPA-VISION's HFrEF study design: After screening (Visit 1; Day -21) and determination of their eligibility, participants will be invited for randomisation and baseline assessments (Visit 2; Day 1). A safety assessment will be conducted after 15 days (± 1) of treatment (Visit 3; Day 15 ± 1). Following treatment for 12 weeks, baselines assessments were repeated (Visit 4; Day 84 ± 4). A final follow-up was carried out via telephone (Visit 5; Day 91 ± 7). EOS=end of study; EOT=end of treatment.*

3.3.3 Study population

Generally, trial patients were considered eligible if they had an established diagnosis of non-ischaemic, chronic HFrEF with typical signs (NT-proBNP > 125

pg/mL in patient with sinus rhythm or > 600 pg/mL in patients with AF) and symptoms (NYHA II-IV), as well as a left ventricular ejection fraction (LVEF) ≤ 40 % (measured by echocardiography at screening) and appropriate doses of medical HF therapy. Patients with active ischaemia, implanted devices, recent (within 1 week prior to screening visit) decompensated HF, severely impaired renal function (creatinine clearance < 30mL/Min by Cockcroft-Gault formula) were considered ineligible. A comprehensive list of inclusion (**Table 3.1**) and exclusion criteria (**Table 3.2**) are provided below.

Table 3.1:Inclusion Criteria EMPA-VISION HFrEF

Inclusion Criteria HFrEF
•CHF ≥ 3 months •NYHA II-IV at screening •BMI < 40 kg/m^2 •Age ≥ 18 years •Written informed consent LVEF < 40 % (measured by Echocardiogram) •NT-proBNP (> 125 pg/mL) no AF •NT-proBNP (> 600 pg/mL) if diagnosed AF •Optimal medical therapy

Table 3.1: Inclusion Criteria EMPA-VISION HFrEF. *Detailed inclusion criteria from EMPA-VISION HFrEF; AF=atrial fibrillation; BMI=body mass index; CHF=chronic heart failure; LVEF=left ventricular ejection fraction; NT-proBNP=n-terminal pro b-type natriuretic peptide*

Table 3.2: Exclusion Criteria EMPA-VISION HFrEF

Exclusion Criteria HFrEF
•Stroke or TIA < 6 months •Scars or non-viable myocardium in the interventricular septum, unstable angina pectoris due to CAD, major CV surgery (investigator opinion) •Any contraindication for CMR, CPET, dobutamine stress test •Heart transplant recipient or listed for heart transplant •Cardiomyopathy based on infiltrative diseases (e.g. amyloidosis), accumulation diseases (e.g. Haemochromatosis, Fabry's disease), muscular dystrophies,

cardiomyopathy with reversible causes (e.g. stress cardiomyopathy), hypertrophic obstructive cardiomyopathy or known pericardial constriction •Moderate to severe uncorrected primary valvular heart disease •Acute decompensated HF (exacerbation of CHF) requiring IV diuretics, IV inotropes or IV vasodilators, or LVAD or hospitalisation •SBP ≥ 180 mmHg at screening. If SBP > 150 mmHg and < 180mmHg at screening on antihypertensive triple therapy •Symptomatic hypotension and/or a SBP < 100 mmHg at screening •Uncontrolled AF •Untreated ventricular arrhythmia with syncope documented within the 3 months prior to informed consent in patients without ICD •Diagnosis of cardiomyopathy induced by chemotherapy or peripartum < 12 months prior to informed consent •Symptomatic bradycardia or second or third-degree heart block in need of a pacemaker after adjusting beta-blocker therapy or any other negative inotropic agents •Significant chronic pulmonary disease •Indication of liver disease, defined by serum levels of either ALT, AST, or AP above 3 x upper limit of normal •Impaired renal function (Creatinine Clearance < 30 mL/min and/or dialysis) •Haemoglobin < 10 g/dL •T1DM •History of ketoacidosis •Major surgery < 3 months prior or scheduled within trial •GI surgery or significant GI disorder •Active or suspected malignancy or history of malignancy within 2 years prior to informed consent •Any other disease than HF with a life expectancy of < 1 year •Any drug considered likely to interfere with the safe conduct of the trial •Requirement for treatment with empagliflozin •Treatment with any SGLT2i or combined SGLT1- and SGLT2i •Currently enrolled in another investigational device or drug study, or < 30 days between randomisation and ending the other investigational trial •Known allergy or hypersensitivity to empagliflozin or other SGLT2-i •Chronic alcohol or drug abuse •Women who are pregnant, breastfeeding, or who plan to become pregnant while in the trial

***Table 3.2**: **Detailed exclusion criteria for EMPA-VISION HFrEF**. AF, atrial fibrillation; ALT, alanine aminotransferase; AP, alkaline phosphatase; AST, aspartate aminotransferase; BMI, body mass index; CAD, coronary artery disease; CHF, chronic heart failure; CMR, cardiovascular magnetic resonance; CPET, cardiopulmonary exercise testing; CRT, cardiac resynchronization therapy; CV, cardiovascular; GI, gastrointestinal; HF, heart failure; HFpEF, heart failure with preserved ejection fraction; HFrEF, heart failure with reduced ejection fraction; ICD, implantable cardioverter defibrillator; IV, intravenous; LAVI, left atrial volume index; LVAD, left ventricular assist device; LVEF, left ventricular ejection fraction; LVMI, left ventricular mass index; NT-*

proBNP, N-terminal pro-B-type natriuretic peptide; NYHA, New York Heart Association; SBP, systolic blood pressure; SGLT1-i, sodium-glucose co-transporter-1 inhibitor; SGLT2-i, sodium-glucose co-transporter-2 inhibitor; T1DM, type 1 diabetes mellitus; TIA, transitory ischaemic attack

3.3.4 Data acquisition

3.3.4.1 Cardiac CT

If clinical ischaemia testing was not performed within the last 6 months prior to their screening visits, participants underwent a research cardiac CT scan to determine eligibility. The purpose was to assess presence and quantify extent of any possible CAD (see **Chapter 2.4**).

3.3.4.2 CMR

CMR imaging was performed using two different 3-Tesla MRI scanners (Magnetom PRISMA and TRIO, Siemens Healthineers, Erlangen, Germany) as described in **Chapter 2.5**. **Figure 3.2** provides an overview of timings and the detailed scan protocol.

Figure 3.2: CMR Protocol EMPA-VISION HFrEF

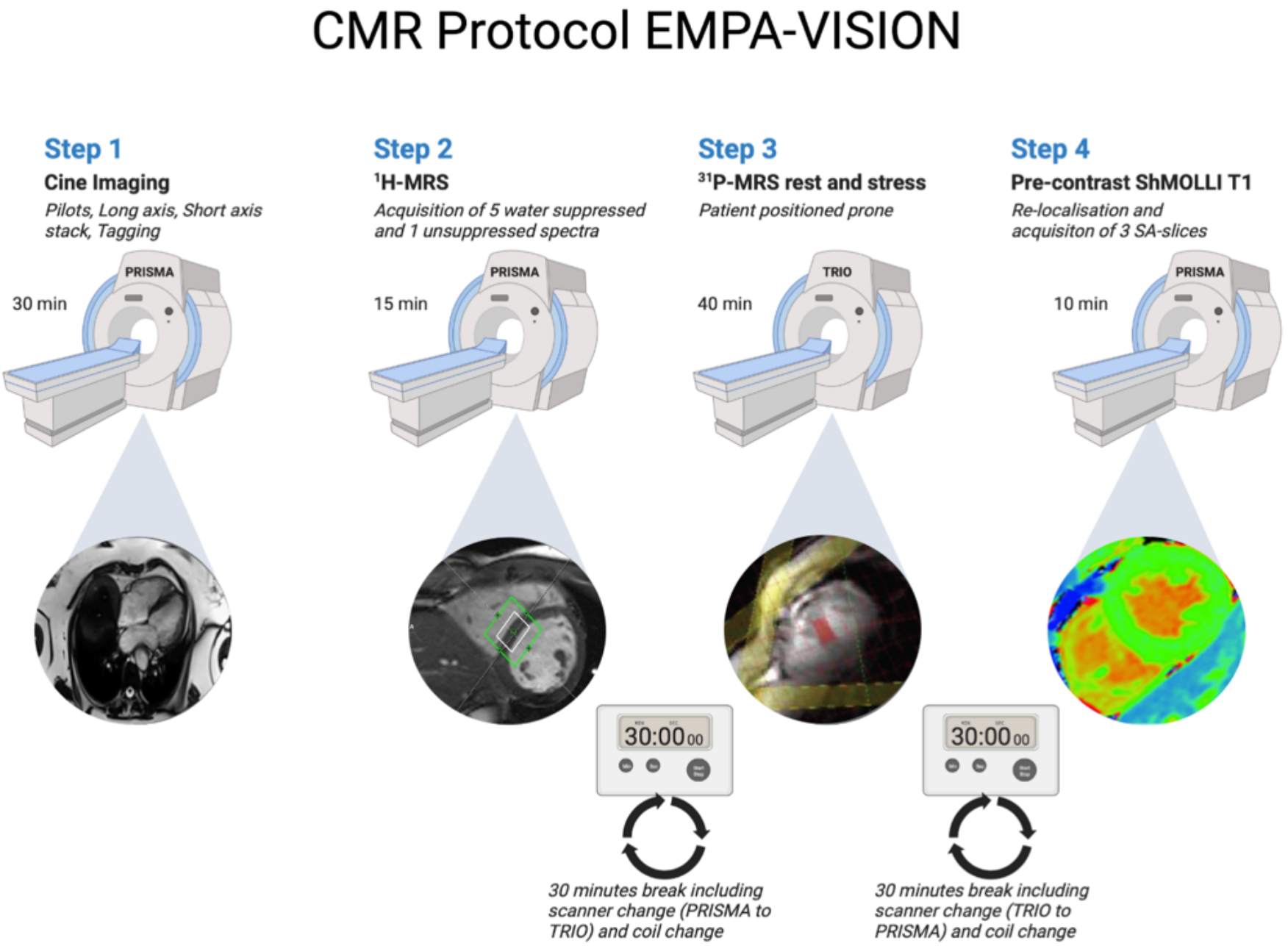

Step 5

Resting Perfusion

Myocardial Blood Flow

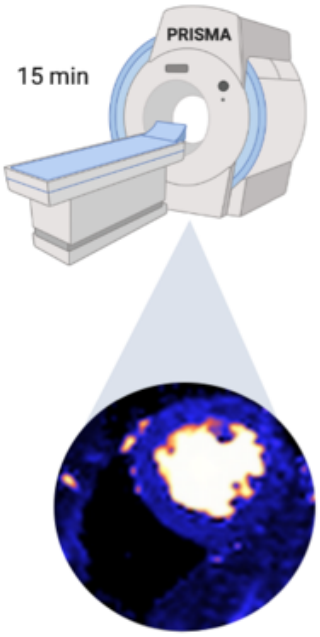

Step 6

LGE 1/2

SA-Stack

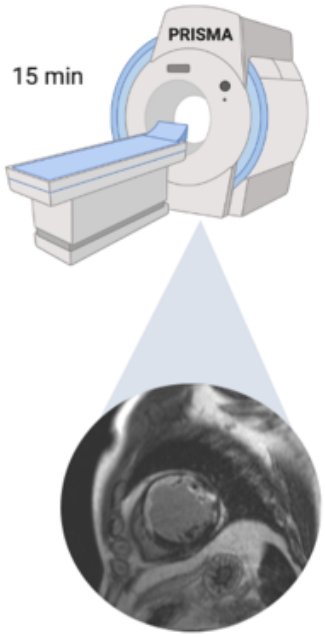

Step 7

Post-Contrast ShMOLLI-T1

Idential slice positioning as before

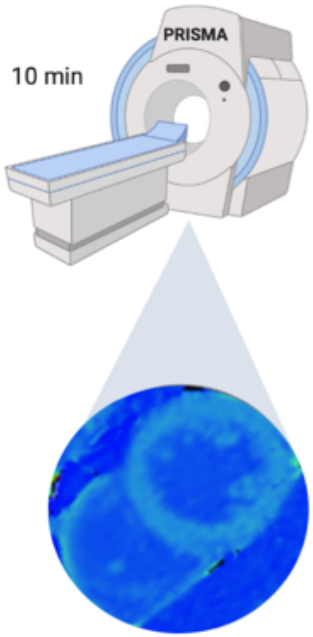

Step 8

LGE 2/2

HLA, VLA, LVOT

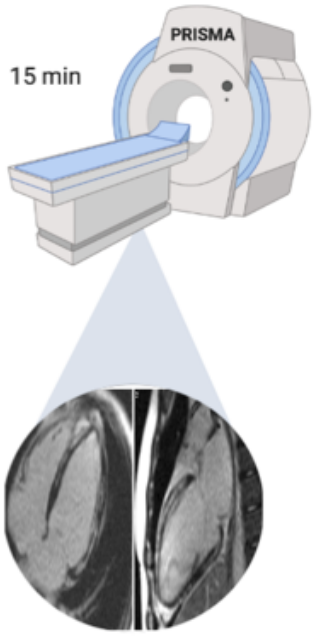

***Figure 3.2**: **EMPA-VISION HFrEF CMR scanning protocol.** The first imaging and MRS sections were acquired on the 3T Siemens PRISMA MR-Scanner. After anatomical planning and pilot acquisition, long and short axis cines as well as myocardial tagging were performed. Then, myocardial triglyceride content (MTG) was assessed using ^{1}H-MRS. After a scanner (to the Siemens 3T TRIO) and coil change, myocardial energetics (PCr/ATP) at rest and during dobutamine stress (65% age-maximal HR) were obtained. Following another break and change back to the Siemens 3T PRISMA, native T1-mapping was performed at rest using ShMOLLI,. Rest perfusion imaging was performed immediately after gadolinium injection (0.05 mmol/kg). followed immediately by short axis (SA) late gadolinium enhancement (LGE) acquisitions. After 15min, post-contrast ShMOLLI was acquired, followed by the last missing long axis LGE-images.*

Using an 18-channel phased-array coil with the participant resting supine on the spine coil array, initial planning pilots and cine images were acquired in two long axis views (HLA, VLA) and in short axis slices covering the whole LV using retrospectively ECG-gated balanced steady-state free precession cine imaging or prospective gating in patients with atrial fibrillation (AF).[125,191] T1-maps were acquired in two matching short-axis slices based on the ShMOLLI sequence as previously described.[154]

Resting perfusion imaging was performed with an IV bolus injection of gadolinium (Gd) contrast (0.1 ml/kg, gadobutrol, Gadovist, Bayer AG, Sheffield, UK) followed by a 15-20 ml saline flush, both administered at 4-6 ml/sec. Pixel-wise perfusion maps were generated automatically using inline perfusion mapping software as previously described, to allow quantitative assessment of myocardial blood flow (MBF).[162]

Late gadolinium enhancement (LGE) imaging was performed in long and short axis views to exclude myocardial infarction or other types of scarring, as per SCMR guidelines.[125,191] **Figure 3.3** presents an overview of CMR-sequences used.

Figure 3.3: CMR Sequences EMPA-VISION HFrEF

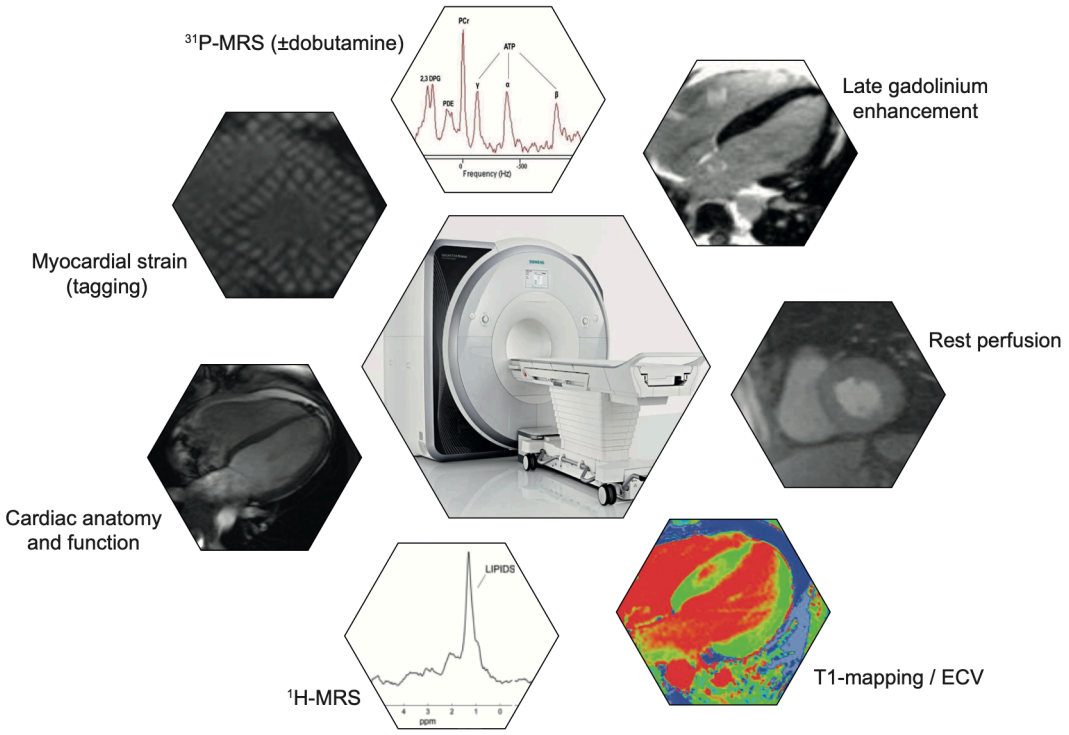

***Figure 3.3**: **CMR Sequences EMPA-VISION** HFrEF. Overview of cardiovascular magnetic resonance (CMR) sequences used for the EMPA-VISION trial. All sequences were performed on scanners by the same vendor (Siemens Healthineers, Erlangen, Germany) and identical field strength (3 Tesla). ^{1}H-MRS=proton magnetic resonance spectroscopy; ^{31}P-MRS=phosphorus magnetic resonance spectroscopy; ECV=extracellular volume.*

3.3.4.3 Dobutamine stress

Dobutamine was administered as a continuous intravenous infusion at incremental rates in order to achieve a significant haemodynamic effect. The infusion was commenced initially at 10 µg/kg/min but increased to a maximum of 40 µg/kg/min, depending on presence of a satisfactory haemodynamic response, which was defined as 65 % of the age maximum heart rate (HR; 220-age). This elevated HR was then maintained for the duration of the acquisition. HR and blood pressure (BP)

were measured at baseline and at one-minute intervals during and after pharmacological stress until normalisation to pre-examination levels. Wherever feasible, stress cines were acquired in a mid-short axis slice as well as VLA and HLA. Due to logistical considerations, the stress-imaging was conducted as part of the ^{31}P-MRS acquisition hence used a different 3T-scanner (Magnetom TRIO, Siemens Healthineers, Erlangen, Germany) and had to be acquired using a locally created gradient echo-sequence (GRE) by means of the integrated scanner receiver coils which resulted in a lower image quality and more susceptibility to movement artefacts.

3.3.4.4 Magnetic resonance spectroscopy

Bi-nuclear magnetic resonance spectroscopy (^{31}P- and ^{1}H-MRS) was used to assess different aspects of myocardial metabolic function. Firstly, cardiac energetics (expressed as PCr/ATP) were assessed using ^{31}P-MRS at rest and during dobutamine stress at 65% age-maximal HR (see **Chapter 2.5.1**) with patients resting in prone position over the centre of a dual-channel ^{31}P Heart/Liver coil (Siemens Healthineers, Erlangen, Germany). Furthermore, myocardial steatosis was assessed via ^{1}H-MRS (see **Chapter 2.5.3**) using an 18-channel surface coil supine in end-diastole and expiration. This enabled acquisition of water suppressed and water unsuppressed lipid spectra allowing for calculation of myocardial triglycerides.

3.3.4.5 Echocardiography

Transthoracic echocardiography (TTE) was used to evaluate cardiac structure and function according to recommendations outlined by the British Society of

Echocardiography.[165] The following clinical information was recorded and analysed on a Philips Healthcare ISCV analysis station:

- LVEF, LVEDV and -ESV, LVMi
- Diastolic function
- LV wall thickness and wall motion status
- Haemodynamic status (cardiac output)
- Valve status

3.3.4.6 Cardiopulmonary exercise testing and spirometry

Patients were seated on a stationary exercise bike (Ergoline GmbH, Bitz, Germany) for resting spirometry (see **Chapter 2.7**) and a cardiopulmonary exercise test (CPET) using breath-by-breath respiratory gas analysis (Metalyzer 3B, Cortex Biophysik, Leipzig, Germany). A standardised incremental exercise protocol was use, and patients encouraged to exercise until a RER of ≥1.1 was reached. SpO_2, capillary lactate and subjective exertion (Borg Scale) were assessed every 2 minutes and peak VO_2 measured at maximal exhaustion (see **Chapter 2.7** for details).

3.3.4.7 Six-minute walk test

Participants performed a six-minute walk test (6-MWT) at their own paced along a 20-meter corridor. Total distance covered, rating of perceived exertion as well as HR and BP were recorded prior to and after the test (see **Chapter 2.8**).

3.3.4.8 Blood sampling and analysis

A variety of biomarkers for assessment of safety (**Table 3.3**) and efficacy were measured in venous blood samples from patients fasting for at least 6 hours (see **Chapter 2.11**).

Table 3.3: Safety Bloods EMPA-VISION HFrEF

Haematology	
• Haematocrit • Haemoglobin • Reticulocyte count • Red blood cells (RBC) / erythrocytes	• White blood cells (WBC) / Leukocytes • Platelet count / thrombocytes • Differential automatic (relative and absolute count): Neutrophils, eosinophils, basophils, monocytes, lymphocytes
Clinical chemistry	
• Albumin • Alkaline phosphatase • GGT (gamma-glutamyl transferase) • ALT (alanine transaminase) • AST (aspartate transaminase) • Bicarbonate • Bilirubin total, fractionated if increased • Calcium • Chloride • Creatinine	• Creatine kinase (CK) • Hs Troponin I (reflex tests if CK is elevated) • Glucose • Magnesium • Phosphate • Potassium • Protein total • Sodium • Urea (BUN) • Uric acid
Lipids	
• Cholesterol (total) • HDL cholesterol • Calculated LDL cholesterol • Triglycerides (reflex test for direct measurement of LDL cholesterol triggered if triglycerides are >400 mg/dL or 4.52 mmol/L)	

Table 3.3: Safety Bloods EMPA-VISION HFrEF*. List of biochemical substances analysed for assessment of safety in EMPA-VISION's HFrEF cohort.*

Biomarker efficacy assessment

- Aceto-acetate
- Aldosterone
- Angiotensin II
- Beta-hydroxybutyrate
- Brain natriuretic peptide
- Erythropoietin
- Fasting plasma glucose
- Free Fatty Acids
- HbA1c

- NT-proBNP
- Renin activity
- Direct renin concentration

Serum metabolomics

- 2,3-phosphoglycerate
- Aconitate
- Adenosine
- Adenosinemonophosphate
- Alphaketobutyrate
- Alphaketoglutarate
- Bis-phosphoglycerate
- Citrate
- Dimethylglycine
- Fructosebisphosphate
- γ-amino butyric acid (GABA)
- Glucose
- Isocitrate
- Inosine
- Lactate
- Malate
- S-Adenosylhomocystein (SAH)
- Succinate
- Pyruvate

3.3.5 Data analysis

3.3.5.1 CMR

Image analysis for cardiac indices was performed in an anonymised fashion offline in accordance with SCMR guidelines[125], using cmr42 post-processing software by

an independent operator who was blinded to patient treatment status (see **Chapter 2.5** for details). Spectroscopy analysis and reconstruction for ^{31}P-MRS was performed using the OXSA Toolbox[150] with explicit calculation of both flip angle and peak partial saturation, correcting for the differing T1 of each metabolite given a particular TR, prior to fitting the phosphorus spectrum via AMARES, as described in detail elsewhere.[150]

3.3.5.2 Echocardiography

Analysis of TTE images was conducted on an ISCV workstation as outlined before (see **Chapter 2.6**).

3.3.5.3 CPET and spirometry

Breath-by-breath respiratory gas analysis to calculate peak $\dot{V}O_2$ and other indices as well as spirometry analysis of FEV1 and FVC was conducted on a workstation after every individual exercise test (see **Chapter 2.7**).

3.3.5.4 Biomarker and metabolomic analysis

Fasting venous bloods for efficacy and safety analyses were processed locally in keeping with official and in-house working instructions and then snap-frozen before being sent to the analysing laboratory (LabCorp, Geneva, Switzerland). Metabolomic processing from fasting serum samples was conducted in a dedicated facility with vast experience in the field (Prof. Griffin Lab, Imperial College London/University of Aberdeen, UK) while analysis and visualisation were performed in OCMR using statistical analysis software (R Core Team 2022, R Foundation for Statistical Computing, Vienna, Austria).

3.3.6 Statistical analysis

Statistical analyses of efficacy data were conducted at the Diabetes Trials Unit (The Oxford Centre for Diabetes, Endocrinology and Metabolism, University of Oxford, UK) following a prespecified statistical analysis plan (see the statistical analysis plan in the Data Supplement). Independent repetition of analyses was carried out for the purpose of this thesis. Due to the lack of specific data describing the impact of SGLT2i on measures of energy metabolism in patients with HF, the sample size was calculated using an effect size based on previously published literature.[107,112,134] Consequently, detecting a treatment difference of 0.3 with a β of 0.8, an estimated effect size of 1.07 and a two-sided significance level of 0.05, the minimum sample size was determined to be a minimum number of n=30 participants. Allowing for a maximum dropout rate of 30%, it was anticipated to recruit a maximum possible number of 43 patients. The primary endpoint analysis was performed using the per protocol set (PPS) of patients with valid PCr/ATP measurements available at baseline and Week 12 and no important protocol violation relevant to the primary endpoint. Protocol violations were reviewed before the database lock. The analytical procedure included a descriptive summary and a formal (inferential) statistical summary, analysis of variance (ANOVA), for the primary endpoint hypothesis testing.

All patients randomised to study treatment, in line with the intention-to-treat principle, were defined as the randomised set (RS) which was set to be employed for a sensitivity analysis to check for an unbiased estimation of the primary endpoint result if a substantial number of protocol violations resulted in a reduced sample size used for the primary endpoint estimates. The analysis of exploratory endpoints

was performed on the RS of patients with available data using descriptive statistics or analysis of covariance (ANCOVA). All summaries were produced for both cohorts and performed on the RS using all available data.

Subgroup analyses were performed to assess the homogeneity of treatment effects on changes in the PCr/ATP ratio in different subgroups (eGFR [< 60 vs. ≥ 60 mL/min/1.73 m^2], diabetes mellitus [yes / no], and atrial fibrillation [yes / no] subgroups). The same ANOVA model as used for the primary endpoint was employed with the addition of subgroup term (if not already fitted) and the treatment by subgroup interaction term.

3.4 Results

Patient recruitment took place in a single centre (OCMR, Oxford, UK) from March 2018 until May 2020. A total of 101 patients performed a screening visit of which 36 patients were enrolled eventually and randomised to treatment.

3.4.1 Study population

One participant in the placebo group withdrew from treatment due to cardiac decompensation shortly before his EOT visit (Visit 4). Overall, 35 (97.2 %) patients successfully finished their trial participation of which 18 were assigned to placebo and 17 assigned to empagliflozin.

The mean duration of exposure to treatment was 83.6 days (SD 10.7) for the empagliflozin group and 84.5 days (SD 3.1) for the placebo group and overall treatment compliance was 99.4 % (SD 1.1). 63.9 % of patients were male, all

patients were White (100 %) and their mean age was 66 years (SD 13.3). All patients had a LVEF ≤ 40 % pre-treatment while a higher proportion of empagliflozin patients had more severe HF (NYHA III) at baseline (29.4 % empagliflozin vs. 5.3 % placebo). The mean eGFR was 71.2 ml/min/m^2 (SD 24.3) and geometric mean NT-proBNP was 801.1 pg/ml (gSD 3.26) and 626.7 pg/ml (gSD 2.93), for the empagliflozin and placebo groups, respectively. **Table 3.4** summarises the general baseline characteristics of the randomised set of patients whereas CMR characteristics at baseline can be found in **Table 3.5.**

Table 3.4: Baseline Patient Characteristics

Characteristic	**Empagliflozin (n=17)**	**Placebo (n=19)**	**p-value**
Age, mean (SD), years	64.7 (12.7)	67.5 (14.1)	
Sex, n (%)			
Male	10 (58.8)	13 (68.4)	
Female	7 (41.2)	6 (31.6)	
Race, n (%)			
White	17 (100)	19 (100)	
BMI (kg/m^2), mean (SD)	30.8 (9.1)	29.4 (4.5)	
SBP (mmHg), mean (SD)	123.4 (24.8)	120.1 (16.1)	
DBP (mmHg), mean (SD)	70.5 (15.4)	69.3 (8.7)	
eGFR (ml/min/1.73 m^2), mean (SD)	73.6 (19.7)	69.1 (28.2)	
NT-proBNP (pg/ml), gMean (gSD)	801.1 (3.26)	626.7 (2.93)	
Minimum, maximum	156.3, 4631.1	126.0, 8922.1	
ECG Parameters			
Heart rate (bpm), mean (SD)	69.1 (10.1)	70.4 (12)	
Sinus rhythm , n (%)	12 (70.6)	13 (68.4)	
Atrial fibrillation, n (%)	5 (29.4)	6 (31.6)	
NYHA classification, n (%)			
I	0	0	
II	12 (70.6)	18 (94.7)	
III	5 (29.4)	1 (5.3)	
IV	0	0	
Medical history, n (%)			
T2D	2 (11.8)	3 (15.8)	
Hypertension	4 (23.5)	4 (21.1)	
Stroke	1 (5.9)	1 (5.3)	
Medications, n (%)			
β-Blockers	14 (82.3)	19 (100)	
Ivabradine	2 (11.8)	0 (0.0)	
ACE-I / ARB	12 (70.6)	16 (84.2)	
Sacubitril / Valsartan	4 (23.5)	3 (15.8)	
MRA	14 (82.3)	12 (63.2)	
Diuretics	9 (52.9)	9 (47.4)	

ns

Anticoagulants	5 (29.4)	6 (31.6)	
Metformin	2 (11.8)	3 (15.8)	

***Table 3.4**: **Baseline characteristics for all patients randomised to treatment**. eGFR=estimated glomerular filtration rate (calculcated using Cockcroft-Gault formula), ACE-i=angiotensin converting enzyme inhibitor, ARB=angiotensin II receptor blocker, bpm=beats per minute, ECG=electrocardiogram, DBP=diastolic blood pressure, MRA=mineralocorticoid receptor antagonist, β-Blockers=betablockers, T2D=type 2 diabetes, NYHA=New York Heart Association, SBP=systolic blood pressure, mmHg=millimetre mercury, pg=picogram, ml=millilitre,*

Table 3.5:Baseline CMR Characteristics EMPA-VISION HFrEF

	Placebo	Empa 10 mg
Randomised patients, N (%)	19 (100.0)	17 (100.0)
PCr/ATP ratio, mean (SD)		
At rest	1.924 (0.354)	1.889 (0.407)
Under dobutamine stress	1.676 (0.402)	1.739 (0.418)
Rest - stress	0.248 (0.436)	0.164 (0.281)
Cramer-Rao bound on PCr/ATP ratio [% of PCr/ATP], mean (SD)		
At rest	14.46 (6.34)	14.32 (7.84)
Under dobutamine stress	14.29 (7.74)	12.56 (5.74)
Myocardial triglyceride ratio (lipids / water) [%], mean (SD)	1.726 (0.849)	1.685 (0.955)
Peak systolic strain [%], mean (SD)		
Circumferential	-11.79 (2.20)	-10.76 (3.39)
Longitudinal	-10.72 (2.49)	-10.82 (3.40)
Radial	20.17 (5.44)	21.31 (7.31)
Peak diastolic strain rate [%/sec], mean (SD)		
Circumferential	48.09 (15.09)	35.69 (10.69)
Longitudinal	28.17 (13.17)	25.24 (9.29)
Torsion [degree], mean (SD)	5.08 (2.10)	4.46 (3.24)
LV end diastolic volume [mL], mean (SD)	223.16 (77.15)	241.79 (78.47)
LV end systolic volume [mL], mean (SD)	138.70 (64.94)	156.49 (66.50)
Stroke volume [mL], mean (SD)	84.47 (25.88)	85.32 (25.14)
Ejection fraction [%], mean (SD)	39.35 (9.84)	36.76 (9.24)
LV mass [g], mean (SD)	143.48 (40.20)	146.58 (33.09)
LV mass index [g/m^2], mean (SD)	68.91 (18.61)	75.43 (18.82)
Native T1 [ms], mean (SD)		
Average	1189.92 (57.47)	1190.11 (43.45)
Threshold	0.40 (0.33)	0.36 (0.25)
Lesions	1232.30 (65.16)	1241.44 (35.83)
Extracellular volume fraction [%], mean (SD)	30.34 (3.76)	30.32 (2.10)
Resting myocardial blood flow [mL/min/g], mean (SD)	1.27 (0.46)	1.11 (0.52)
Quantification of non-ischaemic pattern of LGE (fibrosis) [%], mean (SD)	8.19 (4.27)	6.88 (4.43)

***Table 3.5**: **Baseline CMR-characteristics during rest and dobutamine stress in patients with HFrEF**. LGE=late gadolinium enhancement; LV=left ventricular; SD=standard deviation.*

3.4.2 Primary outcome

3.4.2.1 Resting ^{31}P-MRS

Following 12 weeks of treatment with 10mg of empagliflozin, there was no significant difference regarding the change in resting PCr/ATP compared to placebo. The mean change was -0.179 (SE 0.117) for empagliflozin vs. 0.068 (SE 0.114) for placebo with an adjusted mean treatment difference of -0.247 (SE 0.164; 95 % CI: -0.582, 0.087; p=0.142). These results were further consistent when performing sensitivity analyses (ANCOVA) including baseline PCr/ATP as a covariate for the per protocol set (PPS) of patients (adjusted mean change -0.201 (SE 0.099) for empagliflozin vs. 0.088 (SE 0.096) for placebo; adjusted mean treatment difference -0.289 (SE 0.139. 95 % CI: -0/572, -0.006; p=0.047). Thus, including the baseline covariate led to a slightly increased precision in favour of placebo treatment which resulted in a significant p-value (<0.05).

Figure 3.4: Resting PCr/ATP EMPA-VISION HFrEF

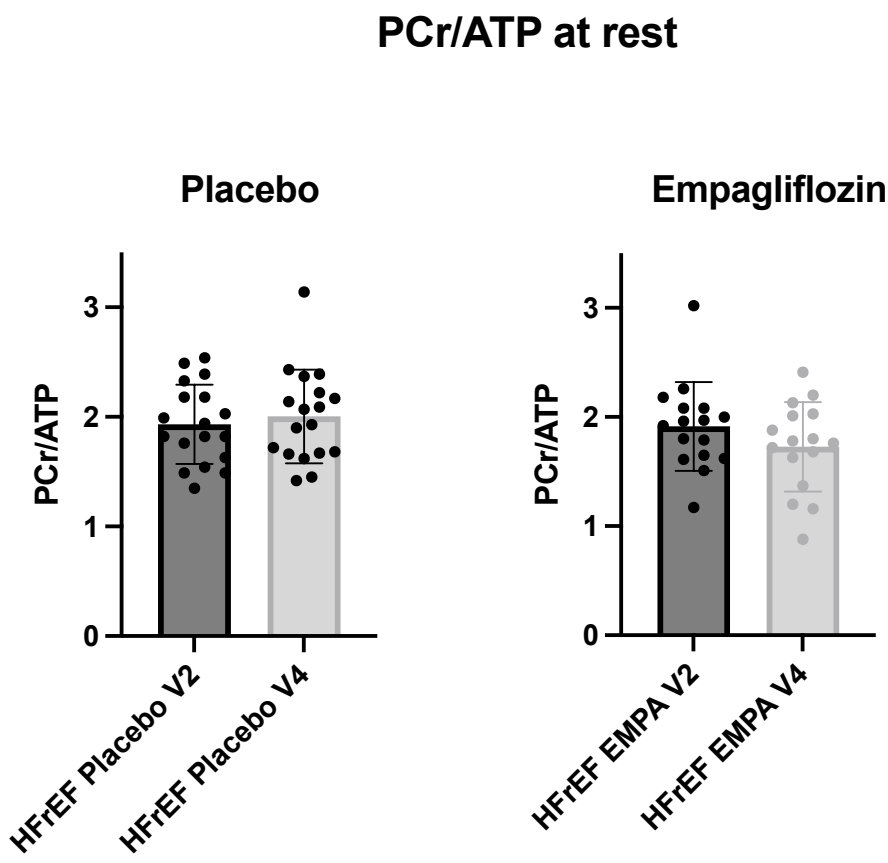

Figure 3.4: Resting PCr/ATP EMPA-VISION HFrEF*. Individual data points for the placebo (left) and empagliflozin treatment arms (right) at baseline (V2) and 12-week follow-up (V4).*

3.4.2.2 Subgroup analyses

To assess treatment homogeneity on changes in the PCr/ATP, we conducted subgroup analyses regarding existing kidney disease (eGFR < 60 ml/Min/1.73m^2 vs. > 60 ml/Min/1.73m^2), diabetes status (T2D yes vs .no) and presence of AF (yes vs. no).

As before, results were consistent with the primary analysis (**Figure 3.5**).

Figure 3.5: Forest Plot Subgroups EMPA-VISION HFrEF

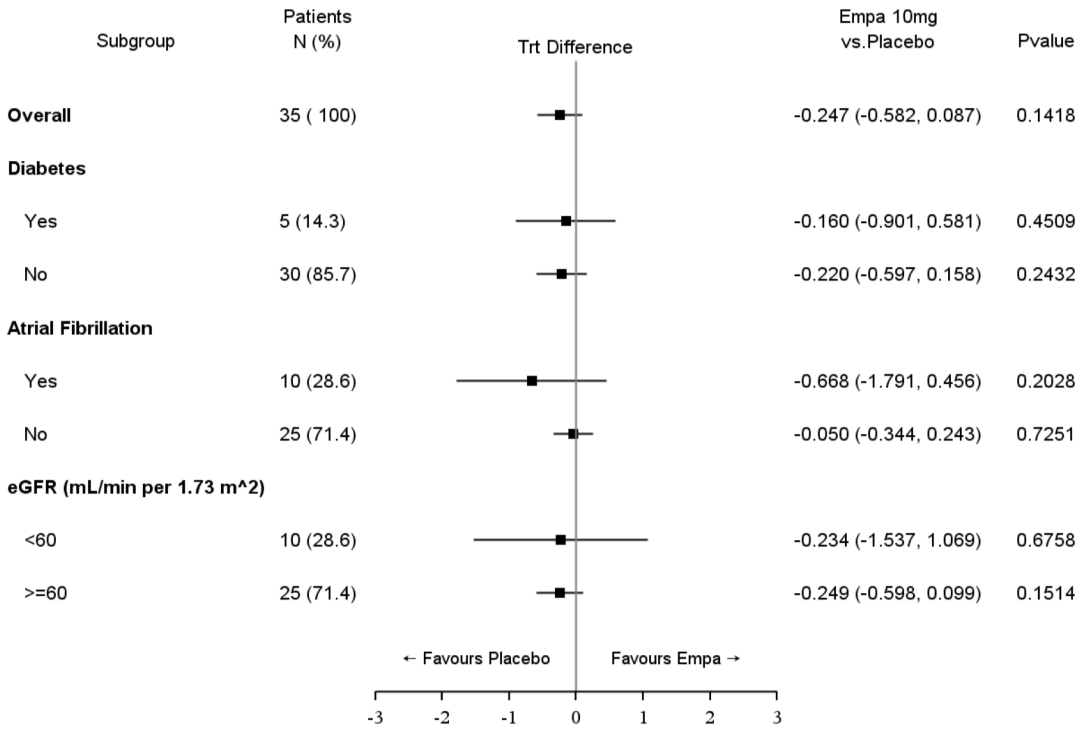

Figure 3.5: Subgroup Analysis EMPA-VISION HFrEF. *Forest plot providing a visual display of 95 % CI according to selected subgroups in the per protocol set of HFrEF patients regarding the change of resting PCr/ATP from baseline to week 12.*

3.4.3 Exploratory outcomes

3.4.3.1 Dobutamine stress ^{31}P-MRS

The adjusted mean change of PCr/ATP during dobutamine stress was -0.055 (SE 0.079) for empagliflozin vs. 0.078 (SE 0.072) for placebo resulting in an adjusted mean treatment difference of -0.132 (SE 0.107; 95 % CI: -0.352, 0.087; p=0.23). Individual data points, divided by treatment cohort (placebo vs. empagliflozin) are presented below (**Figure 3.6**).

Figure 3.6: Dobutamine Stress PCr/ATP EMPA-VISION HFrEF

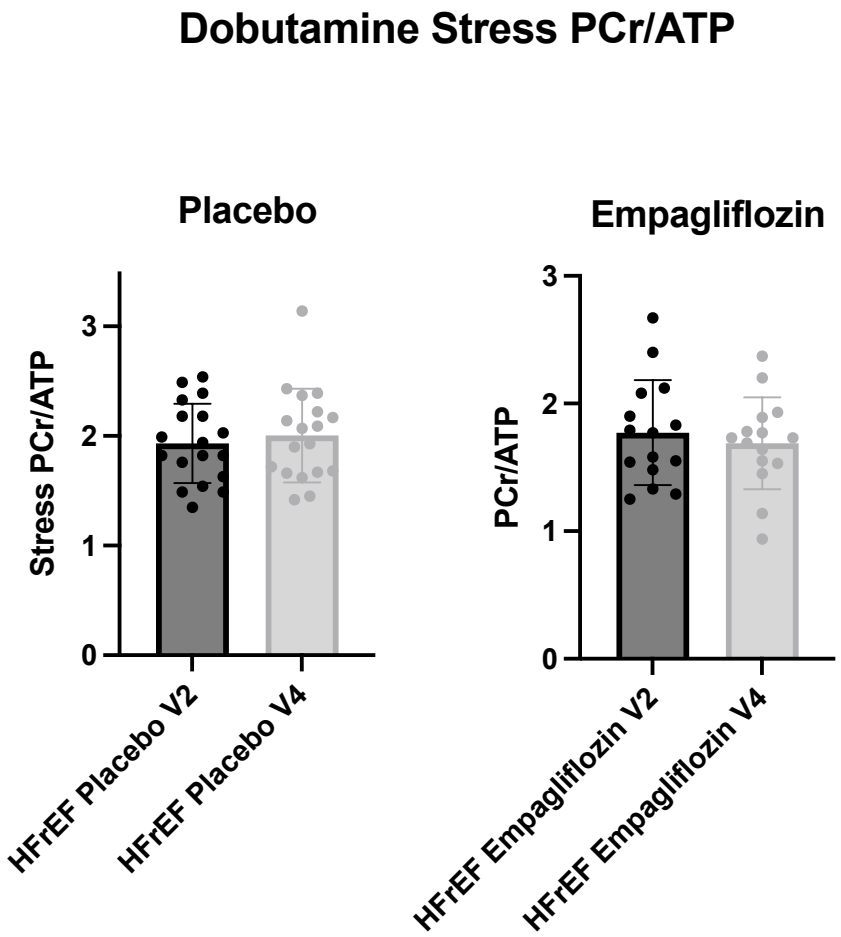

Figure 3.6: Stress PCr/ATP EMPA-VISION HFrEF*. Scatterplot of individual patient values for PCr/ATP during dobutamine stress with bar and standard errors for the placebo and empagliflozin group separately.*

Equally, comparing the change in the difference between rest and stress (Δ PCr/ATP) from baseline to week 12 elicited similar results with an adjusted mean treatment difference of -0.146 (SE 0.124; 95 % CI: -0.401, 0.108: p=0.25). Individual data points are present in **Figure 3.7** below.

Figure 3.7: Delta (rest-stress) PCr/ATP EMPA-VISION HFrEF

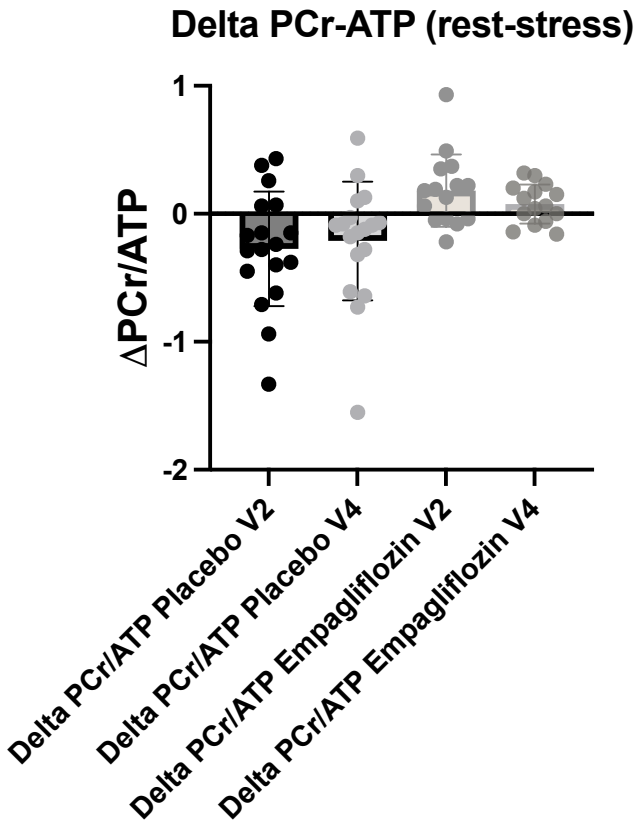

Figure 3.7: Delta PCr/ATP (rest-stress) EMPA-VISION HFrEF. *Scatterplot with bars and standard error of delta PCr/ATP (rest-stress) for individual patients in respective cohorts at baseline (V2) and end of treatment (V4).*

3.4.3.2 Assessment of myocardial steatosis via ^{1}H-MRS

Myocardial steatosis was reduced to a greater extent in the empagliflozin group (-0.209, SE 0.170) compared to placebo (0.234, SE 0.189) which is also expressed in the adjusted mean treatment difference of -0.444 (SE 0.256; 95 % CI: -0.972, 0.084; p=0.0957). Individual patient values are shown below (***Figure 3.8***)

Figure 3.8: Myocardial Triglycerides EMPA-VISION HFrEF

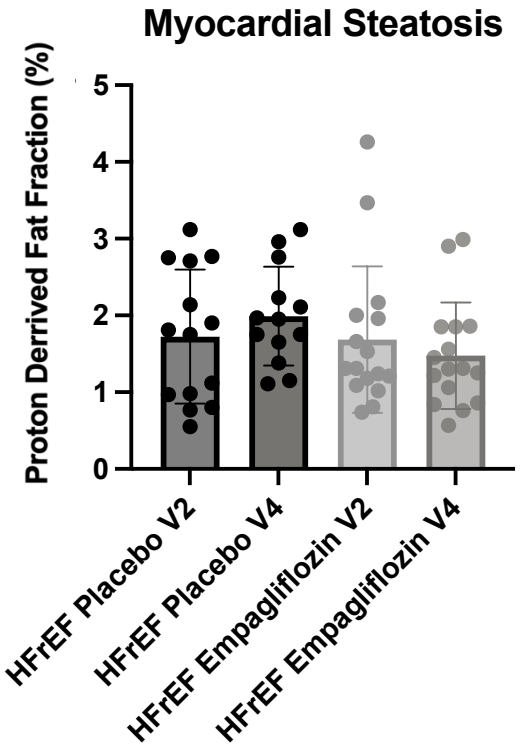

Figure 3.8: Myocardial Triglycerides EMPA-VISION HFrEF*. Scatterplot with bars and standard error of myocardial triglycerides (assessed with ^{1}H-MRS) for individual patients in respective HFrEF cohorts at baseline (V2) and end of treatment (V4).*

3.4.3.3 Serum metabolomics

The effects of empagliflozin and placebo treatment on a set of 19 targeted metabolomic markers were investigated. As expected in biological networks, a correlation matrix (**Figure 3.9 A**) analysis showed correlations between many of

the substances. No change induced by treatment with empagliflozin vs. placebo could be observed when analysing the data with Wilcoxon ranked t-tests (**Figure 3.9 B** for statistical significance vs. magnitude of change). A partial least-squares discriminant analysis (PLS-DA) confirmed the neutral effect of treatment (see **Figure 3.9 C**).

Figure 3.9: Correlation Matrix EMPA-VISION HFrEF

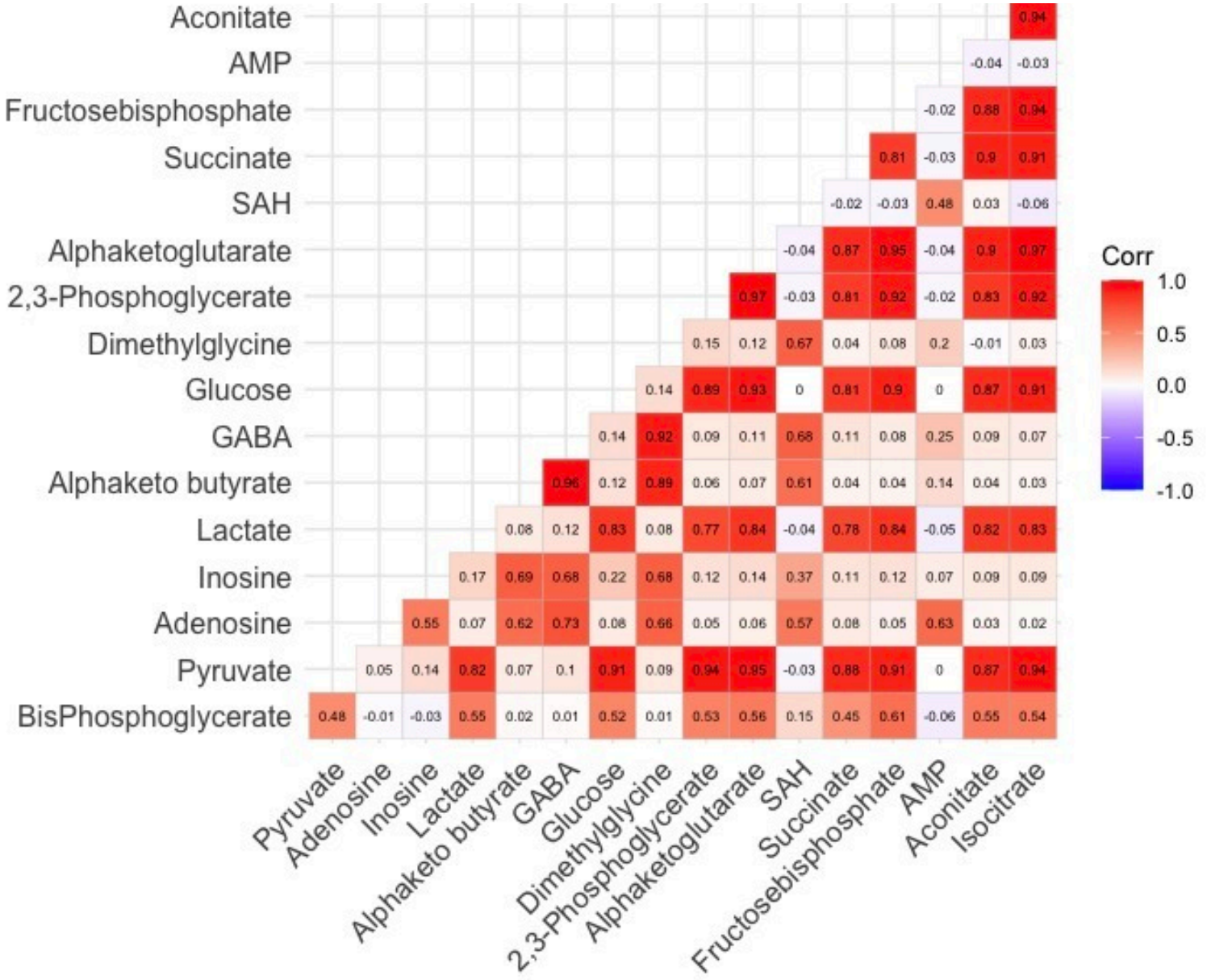

Figure 3.9 A: Correlation Matrix EMPA-VISION HFrEF. *Correlation matrix visualising the degree of correlation between different metabolites with red indicating a high degree of correlation. AMP=adenosine monophosphate; GABA=γ-Aminobutyric acid; SAH=S-Adenosyl-L-homocysteine*

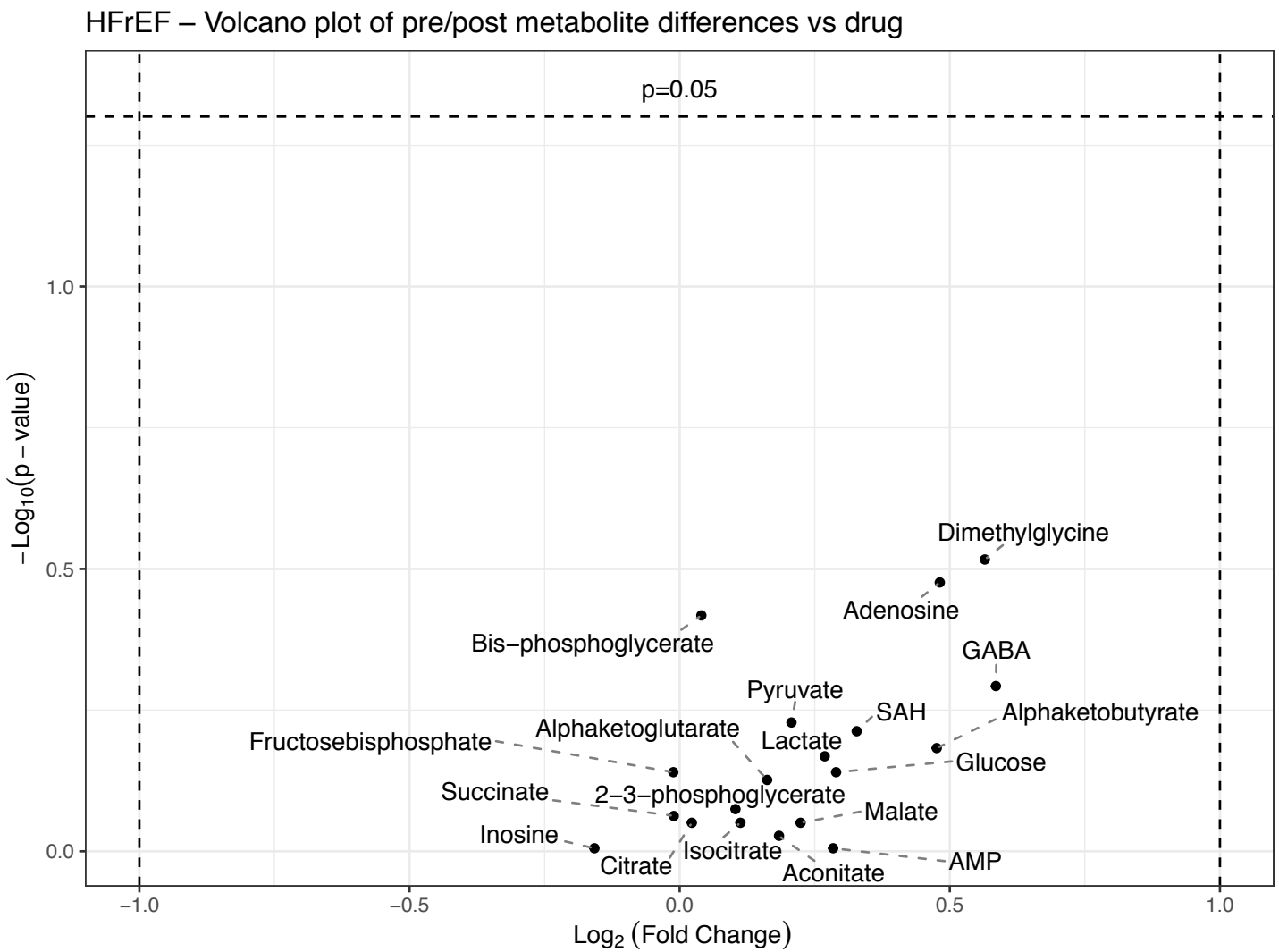

Figure 3.9 B: Volcano plot EMPA-VISION HFrEF. *Volcano plot visualising the degree of statistical significance on the y-axis versus the magnitude of change (fold change) on the x-axis. AMP=adenosine monophosphate; GABA=γ-Aminobutyric acid; SAH=S-Adenosyl-L-homocysteine*

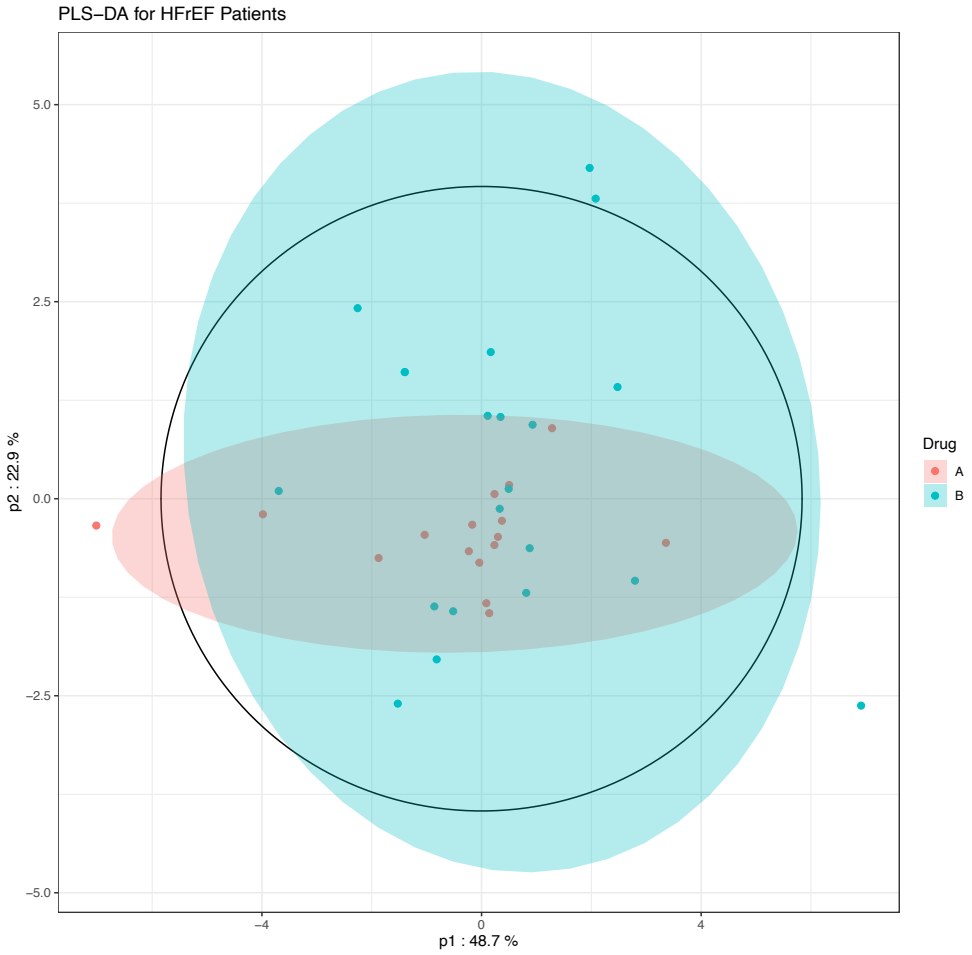

Figure 3.9 C: PLS-DA EMPA-VISION HFrEF. *Partial least-squares determinant analysis (PLS-DA) showing no separation of groups when applying clustering according to treatment status (A=empagliflozin, B=placebo).*

3.4.3.4 Changes in LV structure and function

As presented below in **Table 3.6**, notable changes were seen on assessment of LV mass and LV mass index (LVMI) in the empagliflozin group following 12 weeks of treatment. The adjusted mean reduction of LV mass was -10.81 g (SE 2.78) for empagliflozin and -1.16 g (SE 2.62) for placebo with an adjusted mean treatment difference of -9.65 g (SE 3.83, 95 % CI: -17.49, -1.81; p=0.018) which was equally

evident when indexed to body surface area (LVMI: -4.46 g/m^2, SE 1.94; 95 % CI: -8.42, -0.5; p=0.029).

Table 3.6: Change CMR Parameters EMPA-VISION HFrEF

Parameter Treatment	N	N analysed	Mean baseline (SE)	Adj. mean change (SE)	Adj. mean difference (95% CI)	P value
Peak systolic circumferential strain [%]						
Empagliflozin	17	14	-10.76 (0.91)	-0.75 (0.54)	-0.44 (-2.01, 1.13)	0.5685
Placebo	19	15	-12.20 (0.53)	-0.31 (0.52)		
Peak systolic longitudinal strain [%]						
Empagliflozin	17	14	-10.82 (0.91)	-0.67 (0.55)	-0.15 (-1.75, 1.45)	0.8478
Placebo	19	15	-11.00 (0.60)	-0.52 (0.54)		
Peak systolic radial strain [%]						
Empagliflozin	17	14	21.31 (1.95)	-0.80 (2.08)	-2.97 (-8.85, 2.91)	0.3086
Placebo	19	16	19.88 (1.42)	2.17 (1.94)		
Peak circumferential diastolic strain rate [%/sec]						
Empagliflozin	17	13	35.90 (3.08)	2.09 (3.28)	2.03 (-7.72, 11.78)	0.6711
Placebo	19	16	45.23 (3.31)	0.06 (2.91)		
Peak longitudinal diastolic strain rate [%/sec]						
Empagliflozin	17	13	25.40 (2.67)	-3.16 (2.93)	-5.29 (-13.48, 2.89)	0.1943
Placebo	19	16	27.29 (3.28)	2.14 (2.64)		
Torsion [degree]						
Empagliflozin	17	14	4.46 (0.87)	-0.18 (0.43)	0.29 (-0.94, 1.51)	0.6337
Placebo	19	16	5.15 (0.52)	-0.47 (0.40)		
Stroke volume [mL]						
Empagliflozin	17	16	85.32 (6.28)	-0.55 (3.14)	1.63 (-7.22, 10.48)	0.7901
Placebo	19	18	86.22 (6.00)	-2.19 (2.96)		
EF [%]						
Empagliflozin	17	16	36.76 (2.31)	3.41 (1.23)	1.87 (-1.63, 5.37)	0.2829
Placebo	19	18	40.06 (2.27)	1.53 (1.16)		
LV mass [g]						
Empagliflozin	17	16	146.58 (8.27)	-10.81 (2.78)	-9.65 (-17.49, -1.81)	0.0176
Placebo	19	18	142.01 (9.62)	-1.16 (2.62)		
LV mass index [g/m^2]						
Empagliflozin	17	16	75.43 (4.71)	-4.90 (1.39)	-4.46 (-8.42, -0.50)	0.0286
Placebo	19	18	67.99 (4.41)	-0.44 (1.31)		

Table 3.6: Change from baseline to week 12 of selected CMR parameters EMPA-VISION HFrEF. *EF=LV ejection fraction, mL=millilitres.*

There were further no significant changes in measures of diastolic function, systolic function, or stroke volume during either rest or at peak-dobutamine stress, as determined by CMR (see details in **Table 3.7 A and B** below).

A

Table 3.7: ANCOVA CMR EMPA-VISION HFrEF

Parameter Treatment	N	N analysed	Mean baseline (SE)	Adj. mean change (SE)	Adj. mean difference (95% CI)	P value
Peak circumferential diastolic strain rate during rest [%/sec]						
Empagliflozin	17	12	77.44 (13.06)	-15.07 (5.33)	-8.32 (-22.95, 6.31)	0.2512
Placebo	19	16	69.23 (4.81)	-6.74 (4.61)		
Peak longitudinal diastolic strain rate during rest [%/sec]						
Empagliflozin	17	10	64.96 (13.80)	-5.41 (7.34)	10.38 (-9.78, 30.55)	0.2947
Placebo	19	14	57.76 (10.64)	-15.80 (6.19)		
Peak circumferential systolic strain during rest [%]						
Empagliflozin	17	12	-10.40 (1.53)	0.99 (1.00)	2.12 (-0.61, 4.85)	0.1216
Placebo	19	16	-10.04 (0.67)	-1.13 (0.86)		
Peak longitudinal systolic strain during rest [%]						
Empagliflozin	17	10	-6.80 (1.40)	1.01 (0.91)	1.95 (-0.58, 4.48)	0.1230
Placebo	19	14	-8.29 (1.07)	-0.94 (0.77)		
Peak systolic radial strain during rest [%]						
Empagliflozin	17	12	16.13 (3.12)	-1.63 (1.94)	-2.83 (-8.14, 2.47)	0.2804
Placebo	19	16	16.54 (1.42)	1.20 (1.68)		
Stroke volume during rest [mL]						
Empagliflozin	17	11	70.37 (8.90)	-3.82 (6.36)	-4.24 (-22.27, 13.79)	0.6289
Placebo	19	14	84.90 (6.21)	0.42 (5.61)		
Ejection fraction during rest [%]						
Empagliflozin	17	11	41.54 (3.20)	-0.24 (2.83)	-3.00 (-10.95, 4.96)	0.4411
Placebo	19	14	44.08 (1.82)	2.76 (2.50)		

B

Peak circumferential diastolic strain rate during stress [%/sec]						
Empagliflozin	17	9	76.61 (13.08)	14.64 (9.02)	12.20 (-13.83, 38.23)	0.3336
Placebo	19	11	85.55 (15.79)	2.45 (8.15)		
Peak longitudinal diastolic strain rate during stress [%/sec]						
Empagliflozin	17	9	76.63 (13.07)	6.49 (10.78)	15.15 (-17.78, 48.07)	0.3406
Placebo	19	10	64.18 (9.10)	-8.65 (10.18)		
Peak circumferential systolic strain during stress [%]						
Empagliflozin	17	9	-8.82 (1.98)	-0.71 (1.19)	0.32 (-3.04, 3.68)	0.8425
Placebo	19	12	-7.94 (0.91)	-1.03 (1.02)		
Peak longitudinal systolic strain during stress [%]						
Empagliflozin	17	9	-5.77 (1.36)	0.21 (0.92)	1.18 (-1.65, 4.02)	0.3862
Placebo	19	10	-5.58 (1.16)	-0.97 (0.87)		
Peak systolic radial strain during stress [%]						
Empagliflozin	17	9	13.17 (3.16)	-0.12 (2.13)	-0.94 (-6.97, 5.08)	0.7442
Placebo	19	12	13.22 (2.01)	0.82 (1.84)		
Stroke volume during stress [mL]						
Empagliflozin	17	10	61.22 (6.42)	-2.56 (5.45)	0.36 (-16.53, 17.25)	0.9644
Placebo	19	11	79.77 (7.35)	-2.92 (5.17)		
Ejection fraction during stress [%]						
Empagliflozin	17	10	44.85 (3.26)	1.57 (1.57)	0.31 (-4.44, 5.07)	0.8907
Placebo	19	11	47.79 (3.48)	1.26 (1.49)		

***Table 3.7**: **ANCOVA of CMR Changes EMPA-VISION HFrEF**. Changes from baseline to week 12 in selected measures of left ventricular function and volumes during rest (A) and peak dobutamine stress (B).*

3.4.3.5 Pre- and post-contrast T1-mapping

The change in ShMOLLI-T1-derived measures for myocardial tissue characterisation (native, lesions and threshold) were all numerically greater in the empagliflozin group with the threshold T1 reaching statistical significance (**Table 3.8**).

Table 3.8: ShMOLLI T1 EMPA-VISION HFrEF

Parameter Treatment	N	N analysed	Mean baseline (SE)	Adj. mean change (SE)	Adj. mean difference (95% CI)	P value
Native T1 - average [ms]						
Empagliflozin	17	15	1190.11 (11.22)	-17.56 (6.70)	-8.41 (-28.08, 11.25)	0.3865
Placebo	19	15	1195.49 (14.16)	-9.15 (6.70)		
Native T1 - threshold [ms]						
Empagliflozin	17	14	0.33 (0.06)	-0.14 (0.03)	-0.11 (-0.20, -0.01)	0.0279
Placebo	19	17	0.43 (0.08)	-0.03 (0.03)		
Native T1 - lesions [ms]						
Empagliflozin	17	7	1237.48 (15.12)	-18.23 (15.57)	-11.95 (-59.73, 35.83)	0.5930
Placebo	19	9	1240.77 (22.73)	-6.28 (13.54)		
Quantification of non-ischaemic pattern of LGE fibrosis [%]						
Empagliflozin	17	10	7.48 (1.37)	-0.26 (0.84)	0.85 (-1.37, 3.08)	0.4341
Placebo	19	16	8.19 (1.07)	-1.11 (0.66)		

Table 3.8**: **Change from baseline to week 12 in ShMOLLI-T1 parameters in EMPA-VISION HFrEF. ms=milliseconds

Overall, active treatment reduced the ECV-fraction numerically but did not meet nominal statistical significance. Surprisingly, when deriving LV-cellular and -matrix volume separately as previously described[192], the change in cellular volume in the empagliflozin group (-8.6 g, SE 2.004) compared to placebo (-1.1 g, SE 2.466) (see **Figure 3.10** below) became significant. LV matrix volume showed a greater, albeit no significant, reduction in the empagliflozin group.

Figure 3.10: LV-Cell and -Matrix Volume EMPA-VISION HFrEF

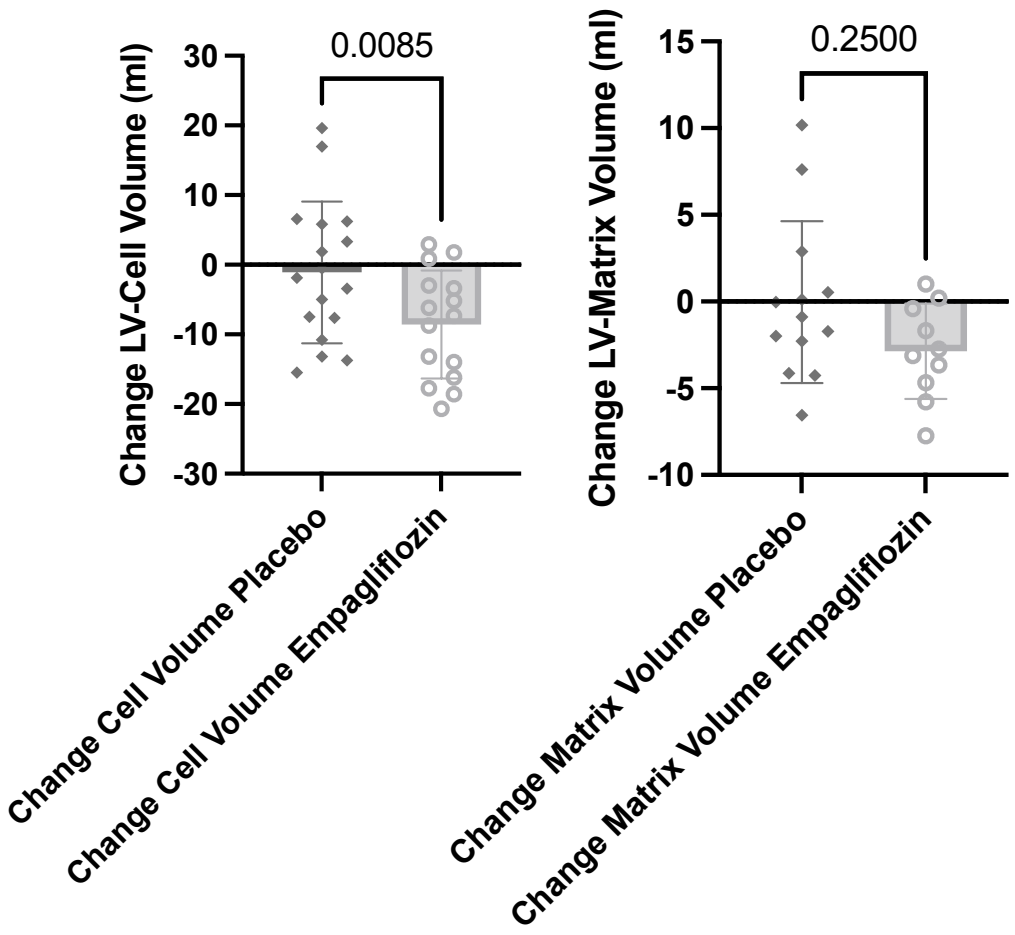

***Figure 3.10**: **LV Cell- and Matrix Volume EMPA-VISION HFrEF**. Changes in LV-Cell and -Matrix volume (baseline to week 12) according to treatment status (placebo vs. empagliflozin).*

3.4.3.6 Echocardiography

There were no notable changes in echo parameters except for LVMI for which there was a mean decrease of -15.4 g/m^2 (SD 28.05) in the empagliflozin but a mean increase of 6.3 g/m^2 (SD 42.26) in the placebo group. **Table 3.9** lists the changes in echo parameter over time underneath.

Table 3.9: Echocardiography Results EMPA-VISION HFrEF

	Placebo						Empa 10mg				
Cohort A:HFrEF	N	Mean	SD	Q1	Median	Q3	N	Mean	SD	Q1	Median	Q3
Number of patients in the analysis set	19						17					
LVEF (%)												
Baseline	18	34.5	4.40	31.6	34.3	39.1	17	31.9	8.39	24.5	34.2	38.0
Week 12	18	41.0	7.71	35.0	41.1	47.3	17	40.8	7.86	32.5	45.3	46.7
Change from baseline at week 12	18	6.5	5.63	1.7	7.9	11.0	17	9.0	6.16	6.7	8.8	11.3
LV end-diastolic volume (mL)												
Baseline	18	148.7	53.04	126.1	138.1	166.0	17	179.4	70.35	132.2	166.0	217.5
Week 12	18	134.7	46.39	114.1	126.9	153.8	17	156.4	79.68	101.4	150.1	182.6
Change from baseline at week 12	18	-14.0	30.99	-26.4	-19.7	2.6	17	-23.0	62.27	-46.7	-21.8	7.2
LV end-systolic volume (mL)												
Baseline	18	97.9	36.51	82.1	90.9	106.4	17	122.8	57.82	77.1	122.1	154.8
Week 12	18	81.3	35.87	61.5	71.0	91.1	17	95.1	58.68	54.7	90.0	106.0
Change from baseline at week 12	18	-16.7	21.39	-27.4	-18.7	-4.3	17	-27.7	44.54	-45.1	-26.7	-8.6
LV mass index (g/m2)												
Baseline	18	115.2	37.56	94.9	110.0	144.7	17	132.3	35.17	117.0	130.1	138.1
Week 12	18	121.5	36.35	98.6	116.3	131.2	17	116.9	27.04	95.7	104.0	141.1
Change from baseline at week 12	18	6.3	46.26	-14.8	-0.7	21.2	17	-15.4	28.05	-38.2	-14.4	9.6
E/e ratio												
Baseline	18	10.4	3.74	7.1	9.2	13.7	17	12.1	4.35	7.9	11.4	15.6
Week 12	18	10.8	4.47	6.9	9.4	13.3	17	9.5	2.91	8.0	8.9	10.0
Change from baseline at week 12	18	0.4	3.61	-1.1	0.1	1.4	17	-2.6	4.46	-4.9	-1.4	0.3
Left atrial volume index (mL/m2)												
Baseline	18	39.9	14.68	27.9	41.2	48.3	17	51.0	29.55	31.7	41.2	62.5
Week 12	18	38.9	14.37	25.9	36.9	48.2	17	45.8	24.18	30.6	41.2	56.1
Change from baseline at week 12	18	-1.1	12.36	-6.2	1.3	7.5	17	-5.2	16.62	-11.7	-9.4	4.3
Chamber thickness (cm)												
Baseline	18	1.2	0.24	1.1	1.3	1.4	17	1.2	0.25	1.0	1.1	1.3
Week 12	18	1.2	0.27	1.1	1.2	1.3	17	1.3	0.18	1.1	1.2	1.4
Change from baseline at week 12	18	-0.0	0.35	-0.2	0.0	0.2	17	0.0	0.24	-0.2	0.1	0.1
Haemodynamic status (cardiac output) (L/min)												
Baseline	18	4.3	1.06	3.6	4.2	4.8	17	4.3	1.52	3.0	3.8	5.4
Week 12	18	4.2	1.27	3.3	4.1	5.1	17	4.1	1.23	3.3	3.8	4.5
Change from baseline at week 12	18	-0.1	1.08	-1.0	0.2	0.6	17	-0.2	1.70	-1.7	0.2	1.1
Septal e-velocity (cm/sec)												
Baseline	18	6.3	2.52	4.1	5.9	8.1	17	5.6	2.06	4.5	5.1	6.5
Week 12	18	5.5	2.09	3.8	5.0	6.8	17	5.5	2.41	3.9	5.0	6.2
Change from baseline at week 12	18	-0.8	2.09	-1.2	-0.8	0.6	17	-0.1	1.76	-1.0	-0.1	1.1
Lateral e-velocity (cm/sec)												
Baseline	18	9.5	4.18	6.7	9.0	10.8	17	8.7	4.23	5.2	8.1	11.6
Week 12	18	9.0	4.40	5.6	8.6	11.3	17	9.6	4.09	5.7	11.0	12.5
Change from baseline at week 12	18	-0.5	2.68	-1.8	-0.4	1.8	17	0.9	3.39	-0.9	0.6	2.6

Table 3.9: *Baseline values, Week 12 values and changes in echocardiographic parameters over time as mean (with SD) and IQR. N=number of patients*

3.4.3.7 Cardiopulmonary exercise testing and spirometry

Surrogates of cardio-respiratory fitness showed numerical increases following treatment with empagliflozin compared to placebo (**Figure 3.11**) but overall, none of those were statistically significant. Systolic blood pressure during peak exercise decreased by -10.94 mmHg (SE 3.52) for empagliflozin contrary to a change of 1.45 mmHg (SE 3.21) for placebo (-12.39 mmHg, SE 4.79; 95% CI: -22.20, -2.58; p=0.0152).

Figure 3.11: Change in CPET Parameters EMPA-VISION HFrEF

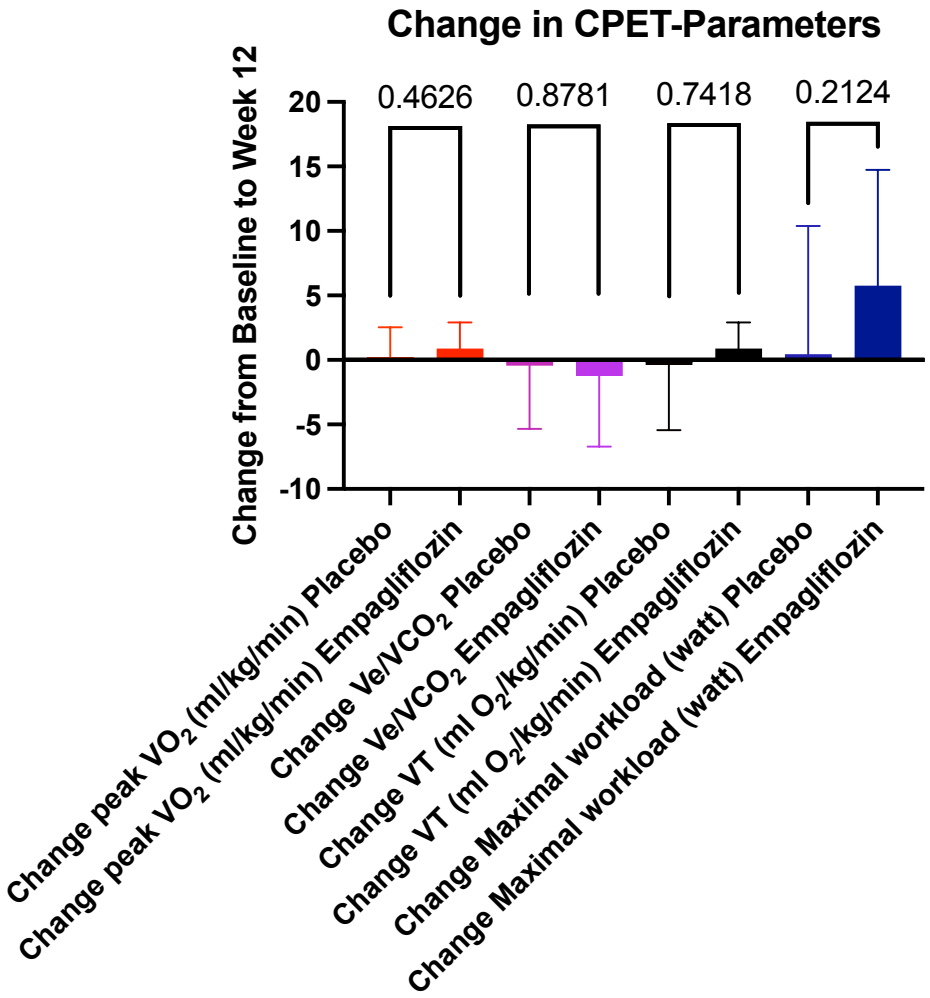

Figure 3.11: CPET Results EMPA-VISION HFrEF*. Median changes of respective CPET-measures with Wilcoxon-ranked t-tests to determine significance.*

3.4.3.8 Six-minute walk test

There was no notable difference between empagliflozin and placebo regarding the change from baseline to week 12 in total distance covered (empagliflozin 17.06 m [SE 7.34] vs. placebo 19.78 m [SE 10.37], *Borg* dyspnoea score (empagliflozin: -0.4 [SD 1.29] vs. placebo -0.2 [SD 1.31]) and fatigue score (-0.9 [SD 1.61] vs. -0.6 [SD 1.74]) in the empagliflozin and placebo treatment groups.

3.4.3.9 Patient reported outcomes

Except for the self-efficacy in the empagliflozin group (mean change -4.41, SD 19.23) and symptom stability in the placebo group (mean change -1.39, SD 26.39), all items of the KCCQ showed some improvement (increased score) from baseline in both the empagliflozin and placebo treatment groups, although relative changes were consistently greater in the empagliflozin group (**Figure 3.12**). Mean changes in the overall summary score from baseline at Week 12 were 9.81 (SD 12.16) for the empagliflozin treatment group and 4.24 (SD 14.33) for the placebo group. Mean changes in the overall clinical summary score from baseline at Week 12 followed the same pattern as changes in the overall summary score. Mean changes in the overall clinical summary score from baseline at Week 12 were 12.33 (SD 12.48) for the empagliflozin treatment group and 6.55 (SD 13.57) for the placebo group.

Figure 3.12: Change in Patient Reported Outcomes EMPA-VISION HFrEF

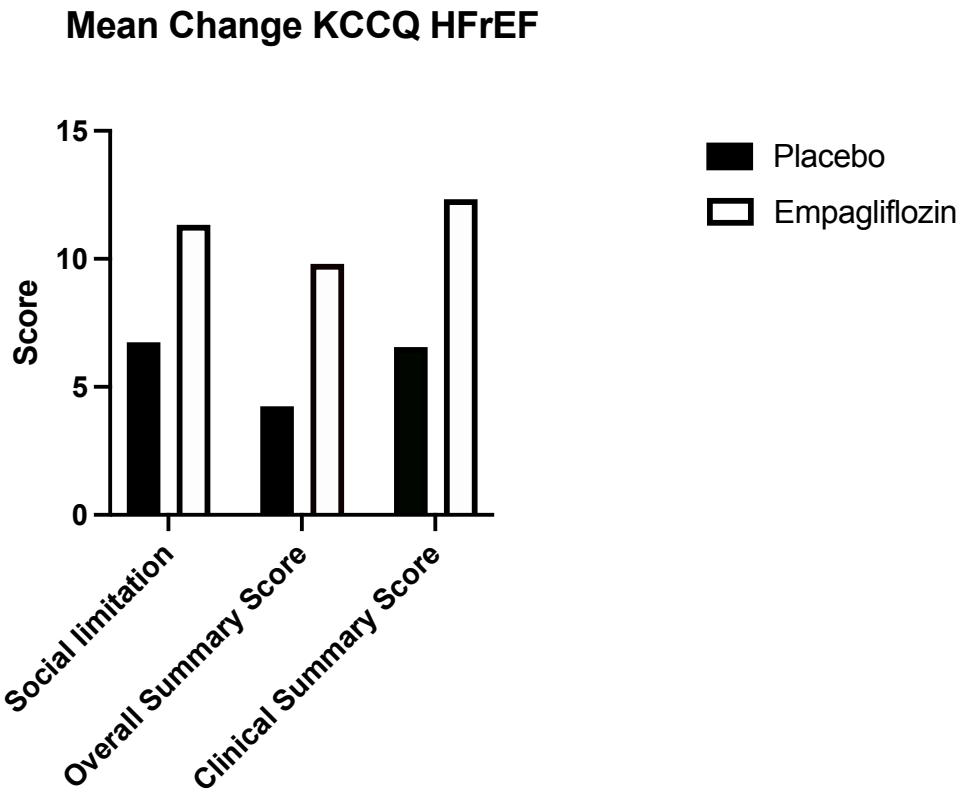

Figure 3.12: Patient Reported Outcomes EMPA-VISION HFrEF. *Mean changes in the respective symptom scores of the KCCQ between the placebo and the empagliflozin groups.*

Responses in the EQ-5D did not show any notable differences between the groups with an increased EQ-VAS score in both the empagliflozin (mean change 7.8; SD 13.6) and placebo group (mean change 5.9; SD 16.9).

3.4.3.10 Biomarker analysis

For most biomarkers we observed no notable difference in change from baseline to last value on treatment between the empagliflozin and placebo groups. For renin, angiotensin II, and renin activity there were increases from baseline to week 12 in the empagliflozin group compared to a decrease in the placebo group. Relative

changes from baseline to week 12 for BNP and NT-proBNP were also comparable in the empagliflozin and placebo treatment groups (**Table 3.10**).

Table 3.10: Biomarker Changes EMPA-VISION HFrEF

Parameter Treatment	N	N analysed	Mean baseline (SD)	Mean change (SD) at last value on treatment
Hba_{1c} [%]				
Empagliflozin	17	16	5.78 (0.59)	-0.08 (0.23)
Placebo	19	18	6.39 (1.78)	-0.06 (0.24)
Acetoacetic acid [µmol/L]				
Empagliflozin	17	2	127.4 (27.7)	49.0 (27.7)
Placebo	19	0	-	-
Beta-hydroxybutyrate [mmol/L]				
Empagliflozin	17	17	0.208 (0.152)	-0.036 (0.134)
Placebo	19	18	0.143 (0.079)	-0.013 (0.082)
Fasting plasma glucose [mmol/L]				
Empagliflozin	17	17	5.54 (0.80)	0.05 (0.65)
Placebo	19	18	6.39 (2.31)	0.43 (1.52)
Free fatty acid [mmol/L]				
Empagliflozin	17	17	0.74 (0.44)	0.04 (0.54)
Placebo	19	18	0.63 (0.26)	0.02 (0.43)
Aldosterone [pmol/L]				
Empagliflozin	17	17	370.461 (247.621)	100.531 (270.644)
Placebo	19	17	363.528 (333.439)	69.423 (253.851)
Angiotensin II [ng/L]				
Empagliflozin	17	16	57.4 (54.9)	79.4 (139.7)
Placebo	19	18	42.8 (32.1)	3.4 (37.8)
Erythropoietin [U/L]				
Empagliflozin	17	16	8.8 (5.9)	2.5 (3.0)
Placebo	19	18	10.2 (4.2)	-0.9 (3.3)
Renin activity [ng/L/h]				
Empagliflozin	17	14	12.56 (13.89)	18.46 (22.96)
Placebo	19	16	13.51 (21.05)	-2.75 (17.32)
Renin [ng/L]				
Empagliflozin	17	14	118.14 (140.66)	326.15 (392.69)
Placebo	19	17	178.54 (262.60)	-82.68 (191.60)
			gMean (gCV %) at baseline	Relative change from baseline gMean ratio (gCV %)
BNP [ng/L]				
Empagliflozin	17	17	113.29 (199.93)	0.79 (65.19)
Placebo	19	18	115.31 (89.05)	0.84 (49.09)
NT-proBNP [pg/mL]				
Empagliflozin	17	17	643.04 (201.24)	0.73 (60.30)
Placebo	19	18	650.03 (138.76)	0.73 (58.56)

Table 3.10: Biomarker Results EMPA-VISION HFrEF*. Change from baseline to week 12 (or last value on treatment) for selected exploratory biomarkers from fasting venous blood.*

Selected changes in blood markers used for efficacy analyses are visualised in ***Figure 3.13.***

Figure 3.13: Relative Biomarker Changes EMPA-VISION HFrEF

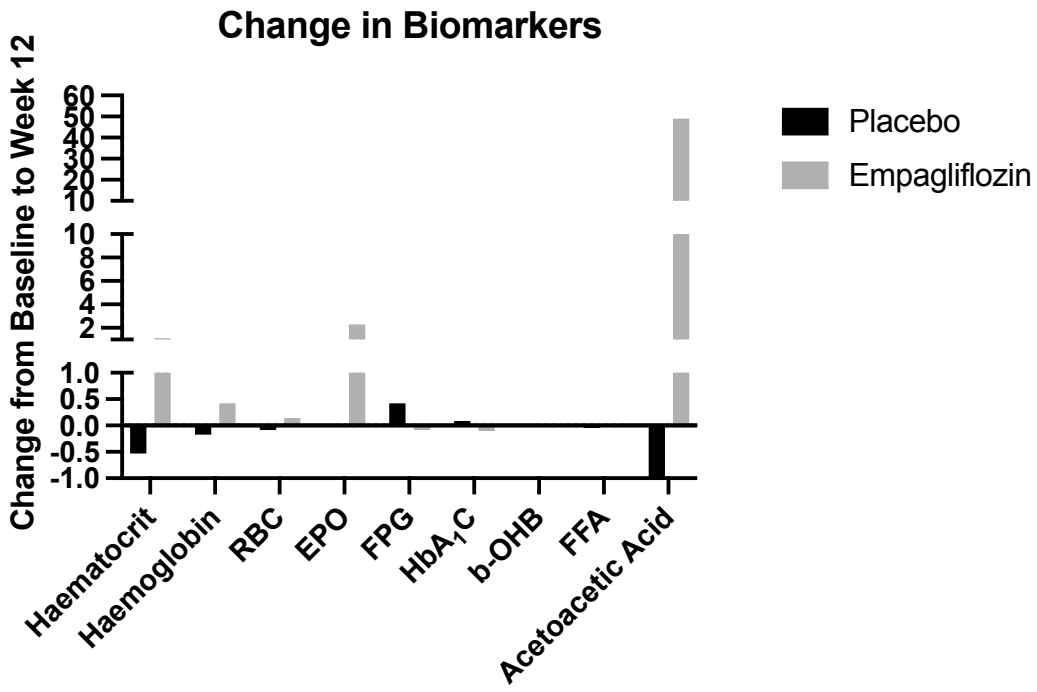

Figure 3.13: Relative Biomarker Changes EMPA-VISION HFrEF. *Visualised summary of changes in selected biomarkers in the empagliflozin and placebo groups, respectively.*

3.5 Discussion

This is the first randomised controlled, placebo controlled study to investigate metabolic effects of empagliflozin in patients with HFrEF with or without T2D *in-vivo*. Furthermore, with a variety of exploratory outcomes and imaging investigations, it enables deeper mechanistic understanding of how SGLT2i exert their beneficial effects in patients with HFrEF. The principal findings of this study are that:

1) SGLT2i treatment did not result in significant enhancement in cardiac energetics, neither when measured *in-vivo* via ^{31}P-MRS at rest or during dobutamine stress, nor when measuring serum metabolites related to overall energy production, *ex-vivo*.

2) Empagliflozin treatment induces anti-fibrotic changes expressed via reduced LVM and LVMI, myocardial cellular volumes and native ShMOLLI T1. Furthermore, there was a near significant reduction of MTG, a marker of cardiac steatosis.

3.5.1 Changes in myocardial energy metabolism

Derangements in myocardial energy metabolism represent a deep link between cardio-metabolic risk factors (e.g. obesity, pre-diabetes), established concomitant diseases (e.g. T2D and hypertension) as well as overt HF and can thus be useful tools for patients risk stratification.[9,193,194] The failing heart's capacity to synthetise energy (i.e. ATP) from substrates like glucose or lipids (and others*)* as well as buffer periods of increased demand (via the CK system) is significantly blunted and when chronic, termed 'metabolic remodelling'.[195] In the chronically failing heart, the available pool of ATP is gradually, but progressively reduced by about 30% and this reflects a mismatch between synthesis and degradation in a generally well-oxygenated tissue. The healthy heart is able to use macronutrients such as fat, glucose, ketones and branched chained amino acids (BCAA) interchangeably and this 'metabolic flexibility' is what the failing heart lacks.[13] As a result, the perfectly balanced metabolic machinery in the heart is failing and logically, repleting the energetic equivalents appears like a valuable target when considering novel

approaches for HF treatments especially when considering that metabolism and cardiac function are indivisibly connected (see **Chapter 1**).

SGLT2i induce glucosuria which leads to a caloric deficit of roughly 250 kcal per day. This in turn lowers the insulin to glucagon ratio and stimulates lipolysis which prompts hepatic production of ketone bodies. It was previously found that the failing heart is an avid utilizer of ketone bodies and that infusion of β-hydroxybutyrate increased myocardial blood flow and cardiac function as well as output in patients with HFrEF.[22,196] It has to be noted that the study by Nielsen et. al. used isotonic glucose infusions and insulin in parallel for both, placebo and β-hydroxybutyrate infusion but the rate of glucose infusions appears to have been substantially higher following the cross-over from placebo to β-hydroxybutyrate and vice versa lower from β-hydroxybutyrate to placebo (only-only Data Supplement).[196] Furthermore, the use of PET instead of hyperpolarized MR makes it impossible to analyse the cellular fate of the 11C-acetate used as a tracer abd this might have biased analyses slightly. Nevertheless, ketones have previously been touted myocardial 'superfuels' that might boost myocardial efficiency.[188,197] As such, it appears reasonable to hypothesise that the beneficial clinical effects observed might (partly) be elicited by enhancing myocardial energetics.

Indeed, early murine experiments presented positive results supporting this hypothesis. [182,184,186] Importantly, rodent HF models have well-known limitations and their generalisability to human HFrEF is restricted.[71] Similar effects were seen in a porcine HF-model where empagliflozin treatment following myocardial infarction improved energetics, largely by increased myocardial ketone utilisation.[185] Nevertheless, the HF model used in this study was purely ischaemic

and due to the experimental set-up, infarcted pigs were anaesthetised and also treated with amiodarone and atropine which might exert independent effects on cardiac energetics.[198] Lastly, a human longitudinal cohort study in patients with T2D reported an increase in cardiac energy reserve (PCr/ATP) following treatment with empagliflozin for 12 weeks.[189] In this study, resting PCr/ATP increased by 0.24 following 12 weeks of treatment with empagliflozin. Notably, this study was not randomised or placebo controlled.[199] Additionally, a prospective observational metabolomics study in diabetics treated with empagliflozin showed an improvement in metabolites associated to BCAA-metabolism.[200] Whether or not these effects are equally present in patients with HFrEF irrespective of underlying T2D was unclear.

The current (randomised controlled) study did not detect an improvement of myocardial energetics (i.e. PCr/ATP) at rest or during peak dobutamine stress from baseline to week 12 in patients with HFrEF treated with empagliflozin vs. placebo. Furthermore, a panel of 19 metabolites relating to intracellular energy production underpinned our neutral results, showing no significant changes (see **Chapter 3.4.3.3**). Although serum metabolomics in HF rather reflect systemic metabolic perturbations than cardio-specific ones, these are still considered disease specific for HF and as such should have provided changes in the metabolite panel in case of detectable changes in high-energy phosphate metabolism.[201] A previous study in advanced (transplant listed) HF patients showed metabolite changes pre- and post LV assist device implantation however, 80% of the patients investigated had an ischaemic aetiology which increases the variability and comparability to our cohort.[202] Human evidence on metabolic effects following SGLT2i treatment

remains scarce but one other randomised controlled trial in patients with T2D likewise did not show any effect on cardiac energetics following 12 weeks of treatment with empagliflozin.[190] The findings presented here were robustly present in sensitivity and subgroup analyses alike, although the limitations in sample size warrant caution when interpreting these. Interestingly, following adjustment for PCr/ATP at baseline, (ANCOVA) the treatment difference indicates a potentially negative effect on (-0.289, SE 0.139) cardiac energetics which would be in keeping with the idea that acetyl-CoA from ketones competes for entry into the TCA with pyruvate from glucose and thus, reduce rates of glucose oxidation via inhibition of PDH.[203] Remarkably, two studies using positron emission tomography (PET) in patients with T2D confirmed a reduced myocardial glucose uptake following empagliflozin and dapagliflozin therapy, respectively.[204,205] Furthermore, a very recent study investigated whether ketone ester supplementation in healthy individuals has any effects on cardiac or skeletal muscle energetics. Despite a drop in glucose and FFA in the patient's blood and induction of a mild hyperketonaemia (similar to SGLT2i treatment) no effects on PCr/ATP in the heart or skeletal muscle were seen.[206] However, whether or not this effect is an epiphenomenon and equally present in non-diabetic HFrEF patients after longer term treatment remains enigmatic and is worthy of further investigation.

3.5.2 Changes in LV-structure and function

The findings in this trial demonstrate a significant anti-hypertrophic (reduced LV mass and indexed mass) and anti-fibrotic (lower native ShMOLLI T1, reduced cardiac cell volume, numerically decreased myocardial triglycerides) but no effects on LV-volumes, -systolic or -diastolic function. These results are equally present in

two different imaging modalities (CMR and echocardiogram) and favour the effect of empagliflozin over placebo.

Notably, these findings are in accordance with previous literature investigating empagliflozin treatment for 6 months in patients with T2D via CMR.[207] In patients with HFrEF and concomitant diabetes, a reverse remodelling effect with reduction of LV-systolic volumes following empagliflozin treatment for 6 months was present.[208] In non-diabetic patients with HFrEF, similar results were obtained including an improvement of LVEF.[209] Importantly, these trials enrolled very selected patient populations including a higher percentage of ischaemic heart failure aetiology, where adverse remodelling is more prevalent and certainly carries higher impact on prognosis.[210] It is established that ketones act as intracellular signal molecules and can inhibit histone deacetylases (HDAC's) which potentially leads to antihypertrophic effects upstream and on the cellular protein level.[211] Furthermore, it was recently proposed that empagliflozin might stimulate autophagy, thereby contributing to reverse-remodelling.[212] This mechanism, despite being hypothetical, could explain the reduction of LV cell volume, but not extracellular matrix, evident in this trial (**Chapter 3.4.3.5**). An observation already made in a cohort of patients with T2D following empagliflozin treatment.[189] Aligned with this finding in our study is the numerically reduced myocardial steatosis in the empagliflozin group (**Chapter 3.4.3.2**). A hallmark of HF, even preceding systolic dysfunction, are reduced rates of FAO while circulating FFAs are typically increased.[213,214] Over time, this leads to deposition of lipids and lipid-metabolism intermediates, further impairing energy generation, increasing inflammation and leading to increase in cellular volumes.[215] Hence, reversing these

adverse changes is an attractive target and, as shown here, can also lead to a reduction in adverse remodelling which might explain the beneficial class effect of SGLT2i in patients with HFrEF.[216] As with other medications for HFrEF, patient selection for this effect to develop might be the key to success as another randomised trial with dapagliflozin (10mg per day for 1 year) in T2D with mild cardiac dysfunction (baseline LVEF 46%) did not show effects on adverse remodelling.[217]. Consequentially, a recent imaging trial investigating the effects of sacubitril/valsartan on adverse remodelling in patients with asymptomatic LV dysfunction (ALVSD) was futile[218] while in another population of patients with ischaemic or idiopathic HFrEF, the treatment reduced adverse remodelling.[219]

3.5.3 Changes in cardiorespiratory fitness and patient reported outcomes

Despite favouring empagliflozin treatment numerically, measures of cardio-respiratory fitness in CPET and spirometry did not show statistically significant improvements (**Chapter 3.4.3.7**) in this trial. Equally, administration of dapagliflozin (10mg per day for 12 weeks) did not result in any measurable enhancement of peak VO_2.[220] Thus far, only one other trial enrolling HFrEF patients investigated cardio-respiratory fitness following SGLT2i treatment (*EMPA-TROPISM*) and this reported significant improvements in peak VO_2 as well as 6MWT distance.[209] *EMPA-VISION* was designed as a mechanistic experiment investigating metabolism primarily. Our results differ insofar as they indicate the effect on walking distance in the 6MWT was comparable between empagliflozin and placebo. This might well be a result of our smaller sample size but similarly can be a reflection of distinct patient characteristics (EMPA-VISION: non-ischaemic HFrEF exclusively). Crucially, two other markedly larger randomised

controlled trials investigating 6MWT in patients with HFrEF as a co-primary outcome could not show significant improvements following treatment with Dapagliflozin (*DETERMINE-reduced*) and empagliflozin (*EMPERIAL-reduced*).[221,222] There is growing criticism for the 6MWT, initially a tool to explore respiratory disease, as a tool to investigate novel HF therapies and patient reported outcomes (such as KCCQ and/or EQ5D) are considered more useful and reproducible.[223] In EMPA-VISION, more patients reported significant improvements in their QoL in the empagliflozin group compared to placebo (**Chapter 3.4.3.9**) which tallies with results of supplementary trials investigating different SGLT2i in patients with HF (canagliflozin[224], dapagliflozin[176], sotagliflozin[180] and empagliflozin[177]).

Of note, peak systolic blood pressure during exercise showed a significant reduction in the empagliflozin group however, no evidence exists on whether lowering exercise related hypertension (a physiological response) is beneficial as blood pressure increase during exercise in HFrEF appears to be driven by contractile reserve, which is a positive prognostic sign.[225] Irrespective of its value, this effect is rather explained by a combination of optimised pre-and afterloading as well as direct vascular effects of SGLT2i peripherally or on the sympathetic nervous system (SNS) centrally.[226-228]

3.5.4 Changes in biomarkers

Biomarkers like BNP, NT-proBNP and Troponin (amongst others) are one of the cornerstones of diagnosis and stratifying risk as well as oversee treatment response in patients with HFrEF.[229] While SGLT2i induce a certain degree of osmotic and natriuretic diuresis, they do not appear to dramatically lower prognostic biomarkers

in patients with acute[230] or chronic[176] HFrEF. Interestingly, SGLT2i like empagliflozin, canagliflozin and dapagliflozin have frequently been found to reduce natriuretic peptides by a magnitude of around 5-13%[179,231-233] which is negligible compared to a near 30% reduction with sacubitril/valsartan in *PARADGIM-HF* and *PROVE-HF*.[234,235] These smaller reductions of natriuretic peptides are uncoupled from reductions of HF hospitalisation which were greater in EMPEROR-reduced (30% relative risk reduction; empagliflozin) than PARADIGM-HF (21% relative risk reduction; sacubitril/valsartan).[178,236] Concordant with these results, there were no major effects on HF-related biomarkers (**Chapter 3.4.3.10**) in EMPA-VISION. Both, placebo and empagliflozin groups, showed a small decrease in NT-proBNP and BNP. Taken together, this suggests a different mechanism of action from traditional diuretic or haemodynamic drug effects in HF.

As expected, there were mild changes relating to empagliflozin's pharmacodynamic profile. Haematocrit, Erythropoetin, fasting plasma glucose and ketones (specifically acetoacetic acid) were elevated (see **Figure 3.13** 'Change in Biomarkers'), mirroring the excellent levels of treatment compliance of patients enrolled. Renin, renin activity and angiotensin II, all neurohormones of the renin-angiotensin-aldosterone (RAAS) system, increased in the empagliflozin group but decreased with placebo. These effects, likely relating to plasma volume contraction, have been shown to be transient and return to normal after one year of treatment in a study with the SGLT2i ertugliflozin.[237]

3.6 Limitations and future directions

Despite the methods used in this study represent the gold standard and metabolic assessment was carried out via in-vivo, spectroscopic and ex-vivo metabolomic analysis, there are several potential limitations.

The population screened and enrolled in this trial all derived from one centre (Oxford University NHS Hospitals Foundation Trust, Oxford, UK) and as such is less diverse than the HF population intended to be treated with SGLT2i. A majority of participants were male (58.8%) and all of them were white. As such, this reduces the generalisability of our results and observed effects of this trial might have been different in patients with other ethnic backgrounds and/or sex.[238,239] Furthermore, patients with an ischaemic aetiology of HF and/or devices were excluded. The majority of HFrEF cases are still caused by ischaemia thus, the results obtained here might not be true for all patients with HF especially as metabolic perturbations in an ischaemic (i.e. hypoxic) environment are distinctly dissimilar from the well oxygenated, non-ischaemic failing heart.[240]

Due to randomisation effects in a small cohort, disease severity in the empagliflozin arm was higher (NT-proBNP, NYHA class, LV-volumes, LVEF). Accordingly, this may have interfered with our outcome analyses. Additionally, empagliflozin is available in two strengths (10mg and 25mg) and this trial exclusively investigated treatment with the lower dose.

As this is the first trial assessing metabolic changes following treatment with SGLT2i in a HF population, power calculations had to be inferred from similar experiments yet with different patient populations enrolled.[107,111,241] It remains

ambiguous if the minimally required number of 30 patients (i.e. 15 per cohort) was large enough to detect a treatment difference. In addition, the treatment difference anticipated in this study might in reality be smaller. Furthermore, the mean BMI of patients enrolled was 30 kg/m^2 which reduces the signal to noise ratio of MRS hence, might further contribute to less reliable results.

The approach to metabolomics included a targeted subset of pre-defined metabolites which carries potential for bias.

Active treatment was only provided for 12 weeks, as this timepoint was previously observed in *EMPAREG-OUTCOME* for beneficial effects on HF outcomes. Given that previous metabolic treatments in HF populations were usually administered for at least 12 months or longer[95] and all positive imaging trials with SGLT2i in HF observed patients for at least 6 months[207-209], it remains a possibility that a longer treatment protocol would have provided different results.

Recently, novel interest has sparked to explore potential metabolic modulation in order to re-orchestrate the perturbed metabolic machinery in patients with HFrEF. Considering SGLT2i in HFrEF, a plethora of animal (small and large animal models, see **Chapter 3.5.1**) exists demonstrating success of metabolic pharmacological intervention with SGLT2i however, little is known on metabolic interplay and differences of HF-aetiology on metabolic phenotypes. Per se, it is likely that a combination of multi-level data is needed to identify possible treatment effects in patient cohorts. The integration of (epi)genetic, and metabolomic data providing targets for key enzyme modulation is likely to hold more success. While certain key enzyme inhibitors like etomoxir have been tested in HF patients, it is

now possible to non-invasively interrogate cell pathways with dynamic nuclear polarisation or hyperpolarized MRS.[242] Given the puzzling data around metabolic effects of SGLT2i, this study appears to be of value and thus, should be conducted in the near future.

3.7 Conclusions

In this trial, 12 weeks of treatment with empagliflozin in patients with HFrEF was safe and well-tolerated but did not improve myocardial energetics at rest or during dobutamine stress (PCr/ATP). However, exploratory outcome analysis suggests an anti-hypertrophic and -fibrotic effect which is in keeping with other trials investigating this treatment in this patient population. Exploring the effects on cardiac energetics and myocardial steatosis in a larger population of patients with less narrow aetiology might be of interest in future.

4 *Effects of SGLT2-inhibition in HFpEF*

4.1 Abstract

4.1.1 Background

SGLT2i have emerged as versatile treatments for patients with T2D, HFrEF as well as CKD. Until recently, it was unclear whether the same would hold true for patients with HFpEF, who tend to be older and presenting with a significantly higher disease heterogeneity. Until recently, all trials investigating pharmacological treatment effects on outcomes in patients with HFpEF were futile however, the EMPEROR-preserved trial demonstrated an overall benefit for usage of SGLT2i for this patient population. The primary outcome, cardiovascular (CV) death or HF hospitalisation, for empagliflozin vs. placebo, was 13.8% vs. 17.1% (hazard ratio [HR] 0.79, 95% confidence interval [CI] 0.69-0.90, $p < 0.001$). Secondary outcomes like change in eGFR and total hospitalisations were also significantly lower in the treatment arm.

Despite these positive results, there is ongoing debate whether the generally positive findings can be attributed to all phenotypes of HFpEF patients alike. Furthermore, it remains unclear by which mechanism, SGLT2i translate their beneficial effects and if this differs from patients with HFrEF. By enrolling patients with a clinical diagnosis of HFpEF and a truly preserved systolic function

(LVEF≥50%), this trial pursued to investigate effects of SGLT2i on cardiac energetics (PCr/ATP) and direct cardiac effects as well as effects on exercise physiology and multi-organ effects.

4.1.2 Methods

In this prospective, randomised, double-blind placebo-controlled mechanistic trial, patients with stable HFpEF (LVEF≥50%, n=36) were enrolled and randomly allocated to empagliflozin (10mg OD) or matching placebo for a duration of 12 weeks. Subjects with typical signs (NT-proBNP>125pg/ml in SR or >600pg/ml in AF) and symptoms (NYHA II-IV) of HF as well as structural cardiac alterations (LVMi≥115g/m^2 in males or ≥95g/m^2 in females OR LAVi>34ml/m^2) were considered eligible. The primary endpoint was defined as the change in resting PCr/ATP from baseline to week 12, determined by MRS. A plethora of other endpoints (see Chapter) were considered exploratory.

4.1.3 Results

As a result of the unprecedented global COVID-19 pandemic and far-reaching effects of national lockdowns, all face-to-face research activities in our single centre (OCMR, Oxford, UK) were suspended from 24th March 2020 onwards. This inability to conduct EOT visits following 12 weeks of treatment led to an exclusion of 13 (36.1%) patients from the randomised set (RS) and a subsequent size reduction of the per protocol set (PPS) to 13 patients on empagliflozin and 11 on placebo. As a result, certain imbalances across treatment groups, with a higher

disease burden in the empagliflozin group (elevated LVMi and LAVi; higher peak diastolic strain rate) compared to the placebo group became apparent.

In brief, there was no significant difference in the difference PCr/ATP from baseline (visit 2) to week 12 (visit 4) (-0.16 ± 0.21; 95% CI: -0.60, 0.29; p=0.47). Equally, no notable difference between the empagliflozin and placebo group were seen regarding the change of PCr/ATP during dobutamine stress (-0.22 ± 0.21; 95% CI: -0.66, 0.23; p=0.32). Interestingly, we observed a numerical decrease of myocardial steatosis (measured as MTG via ^{1}H-MRS) in the empagliflozin group (-0.41 ± 0.29 adjusted mean change) but not in the placebo group (0.02 ± 0.34) (adjusted mean treatment difference -0.427 ± 0.45; 95% CI: -1.39, 0.54; p=0.36). Measures of systolic function at rest significantly improved with SGLT2i [(Peak circumferential systolic strain: -5.28 ± 2.2; 95% CI: -10.04, -0.53; p=0.03), (Peak systolic radial strain: 10.68 ± 4.4; 95% CI: 1.16, 20.19; p=0.03)]. Intriguingly, patients in the empagliflozin group had significantly improved pulmonary function measures (FVC 0.34L.± 0.15, p=0.03; FEV_1=0.14L ±0.06, p=0.04) and further improved walking distance in the six-minute walk test (28.23m ± 14.19; 95% CI: -1.46, 57.93; p=0.06).

4.1.4 Conclusions

Despite the extensive difference between the RS of patients and the eventual PPS, due to the unprecedented global COVID-19 pandemic, this trial revealed that patients with chronic HFpEF who are treated with empagliflozin for 12 weeks do not improve their cardiac energetics at rest or under dobutamine stress. Exploratory endpoint analyses exhibit improved cardiac mechanics, walking distance and

measures of cardiorespiratory fitness as well as a reduced HF-related symptom burden. These results are encouraging for further exploration of responder analyses in selected HFpEF-phenotypes.

4.2 Introduction

Heart failure with a preserved ejection fraction (HFpEF) is an increasing burden globally and has now overtaken the '*classical*' HFrEF as leading HF-phenotype.[4] Due to the frequent expanse of cardio-metabolic diseases (T2D, obesity) and their detrimental cardiac and multi-organ effects, this number is projected to increase significantly in future. Patients with HFpEF tend to be multi-morbid including a higher proportion of frailty and a high prevalence of concomitant conditions, which makes treatment highly complex. Until recently, HFpEF remained a condition without effective treatment options and thus, symptomatic treatment was the mainstay of therapy. The mounting problem of patients with a traditionally higher LVEF but similar or even worse symptom burden than the typical HFrEF patient was acknowledged in 1984 already.[243] However, it took almost 20 years before the first RCT for patients with HFpEF tested the efficacy of candesartan (*CHARM-preserved*) in this population.[244] Frustratingly, all of the pharmacological treatments exhibiting prognostic benefits on outcomes in HFrEF, have proven futile in HFpEF (**Figure 4.1**).

Figure 4.1: Outcome Trials in HFpEF

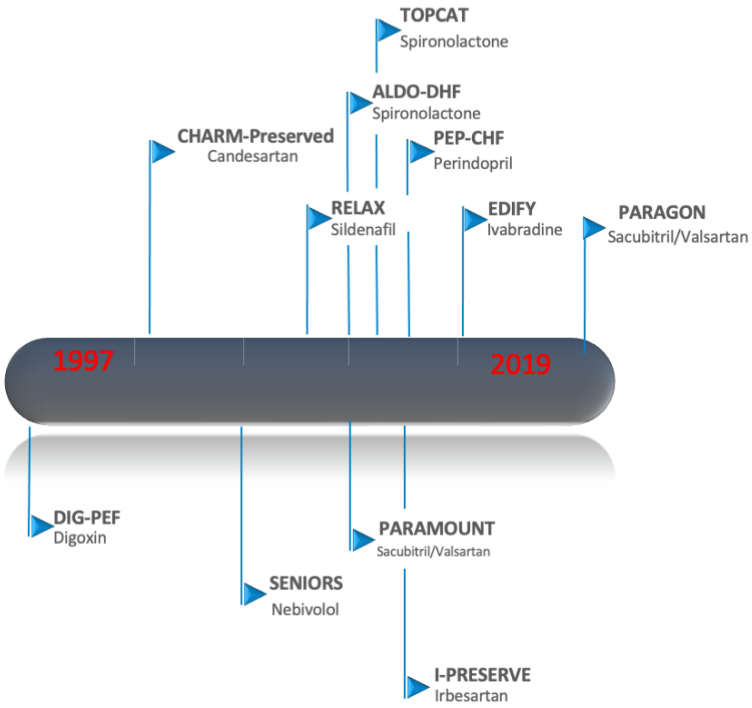

Figure 4.1: Outcome Trials in HFpEF. *Chronologic overview of pharmacologic treatments in randomised controlled trials (RCT) investigated for diastolic HF/HFpEF.*[244-254] *Trial designations written in capital letters and bold with treatment names below.*

Alas, almost another two decades went past before it was demonstrated, for the first time, that empagliflozin reduces the risk for a combination of hospitalisation for HFpEF and cardiovascular death.[1] Nevertheless, a problem in these trials is that, over time, the definition for HFpEF have been inconsistent and trials for a long time have included patients with an EF >40% or 45% and labelled them as HFpEF. This emphasises the problem of phenotypisation in a severely heterogenous disease population.[5]

It was demonstrated previously that patients with HFpEF have an energetic deficit similar to patients with other forms of HF.[73,74] The heart in patients with HFpEF is stiffer and thus, restricted when filling with blood during systole despite a preserved

ejection fraction. This problem is significantly more evident during exercise hence why the hallmark of HFpEF is a severely blunted stress reserve.

Little is known about metabolic alterations of HFpEF patients as most data focused on obese or diabetic patients with LVH and a deranged diastolic function rather as a bystander. Nevertheless, diastolic function requires energy and thus, enhancing energy production in a state of deficit is an attractive novel target in patients with HFpEF. In addition, studies examining mitochondrial function and genetic expression related to energy production indicated a distinct pattern different to metabolic signatures in HFrEF.[255,256] Hence, this trial sought to investigate the effects of 12 weeks of treatment with the SGLT2i empagliflozin on myocardial energy reserve at rest and during dobutamine stress. Furthermore, multiple exploratory endpoints relating to imaging parameters and cardiorespiratory fitness will enable improved understanding of mechanistic effects in this patient population.

4.3 Methods

Due to the nature of *EMPA-VISION*, assessments in the HFpEF group were identical to assessments in the HFrEF group (**Chapter 3**) hence, the methods described below are identical to the descriptions in the previous chapter.

4.3.1 Randomisation

During their baseline visit (Visit 2, **Figure 4.2**), eligible patients were randomly assigned to receive either 10mg of empagliflozin or matching placebo per day over a period of 12 weeks. Randomisation occurred in a 1:1 fashion and the drug assignment was carried out using an interactive web response system. The

randomisation list involved a pseudo-random number generator ensuring the resulting treatment was both reproducible and non-predictable with a block size of 4.

4.3.2 Study visit schedule

Patients deemed eligible after a meticulous pre-screening process were invited for a screening visit (Visit 1) to determine their eligibility status. From their attendance at this visit, there was a 21-day window to invite them for their subsequent randomisation visit (Visit 2, day 1 of treatment) and perform the randomisation to treatment (see 4.3.1 for details). As a safety precaution, patients were invited for a safety visit (Visit 3, 14±1 days of treatment) before attending their EOT visit (Visit 4, 84±4 days of treatment). To ensure safety, an additional phone call (Visit 5, days 7-14 after Visit 4) was conducted to ensure uncomplicated withdrawal from the study drug.

Figure 4.2: Visit Timeline EMPA-VISION HFpEF

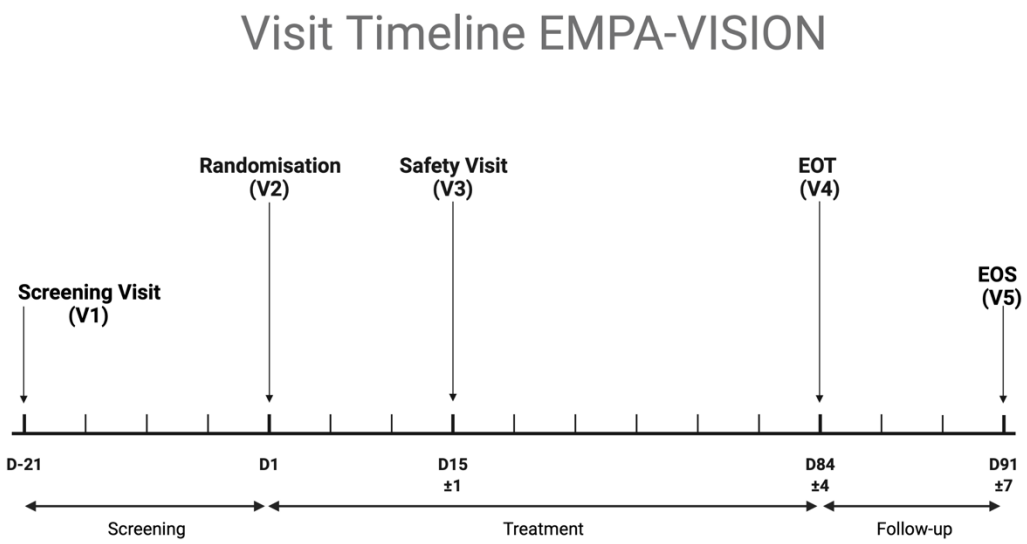

Figure 4.2: Visit Timeline EMPA-VISION HFpEF*. Schematic overview of EMPA-VISION's HFpEF study design: After screening (Visit 1; Day -21) and determination of their eligibility, participants will be invited for randomisation and baseline assessments (Visit 2; Day 1). A safety assessment will be conducted after 15 days (± 1) of treatment (Visit 3; Day 15 ± 1). Following treatment for 12 weeks, baselines assessments were repeated (Visit 4; Day 84 ± 4). A final follow-up was carried out via telephone (Visit 5; Day 91 ± 7). EOS=end of study; EOT=end of treatment.*

4.3.3 Study population

Subjects were considered eligible with an established clinical diagnosis of chronic HFpEF with typical signs (NT-proBNP>125pg/mL in patient with sinus rhythm or >600pg/mL in patients with AF; LVMi >115g/m^2 in males / >95g/m^2 in females; LAVi >34ml/m^2) and symptoms (NYHA II-IV), as well as a preserved LVEF (≥50%) (measured by echocardiography at screening). Patients with active ischaemia, implanted devices, recent (within 1 week prior to screening visit) decompensated HF, or recently changed diuretic dosing as well as a severely

impaired renal function (creatinine clearance <30mL/min by Cockcroft-Gault formula) were excluded. A comprehensive list of inclusion (**Table 4.1**) and exclusion criteria (**Table 4.2**) are provided below.

Table 4.1: Inclusion Criteria EMPA-VISION HFpEF

Inclusion Criteria HFpEF
•CHF ≥ 3 months •NYHA II-IV at screening •BMI < 40 kg/m^2 •Age ≥ 18 years •Written informed consent •LVEF ≥50% •NT-proBNP (> 125 pg/mL) if free from AF •NT-proBNP (> 600 pg/mL) if diagnosed AF •LAVI > 34 mL/m^2 •LVMI > 115 g/m^2 (males) or > 95 g/m^2 (females) •Stable dose of oral diuretics > 1 week

***Table 4.1**: **Detailed inclusion criteria for EMPA-VISION HFpEF**; AF=atrial fibrillation; BMI=body mass index; CHF=chronic heart failure; LVEF=left ventricular ejection fraction; NT-proBNP=n-terminal pro b-type natriuretic peptide*

Table 4.2: Exclusion Criteria EMPA-VISION HFpEF

Exclusion Criteria HFpEF
•Stroke or TIA < 6 months •Scars or non-viable myocardium in the interventricular septum, unstable angina pectoris due to CAD, major CV surgery (investigator opinion) •Any contraindication for CMR, CPET, dobutamine stress test •Heart transplant recipient or listed for heart transplant •Cardiomyopathy based on infiltrative diseases (e.g. amyloidosis), accumulation diseases (e.g. Haemochromatosis, Fabry's disease), muscular dystrophies, cardiomyopathy with reversible causes (e.g. stress cardiomyopathy), hypertrophic obstructive cardiomyopathy or known pericardial constriction •Moderate to severe uncorrected primary valvular heart disease •Acute decompensated HF (exacerbation of CHF) requiring IV diuretics, IV inotropes or IV vasodilators, or LVAD or hospitalisation •SBP ≥ 180 mmHg at screening. If SBP > 150 mmHg and < 180mmHg at screening on antihypertensive triple therapy •Symptomatic hypotension and/or a SBP < 100 mmHg at screening •Uncontrolled AF •Untreated ventricular arrhythmia with syncope documented within the 3 months prior to informed consent in patients without ICD

•Diagnosis of cardiomyopathy induced by chemotherapy or peripartum < 12 months prior to informed consent
•Symptomatic bradycardia or second or third-degree heart block in need of a pacemaker after adjusting beta-blocker therapy or any other negative inotropic agents
•Significant chronic pulmonary disease
•Indication of liver disease, defined by serum levels of either ALT, AST, or AP above 3 x upper limit of normal
•Impaired renal function (Creatinine Clearance < 30 mL/min and/or dialysis)
•Haemoglobin < 10 g/dL
•T1DM
•History of ketoacidosis
•Major surgery < 3 months prior or scheduled within trial
•GI surgery or significant GI disorder
•Active or suspected malignancy or history of malignancy within 2 years prior to informed consent
•Any other disease than HF with a life expectancy of < 1 year
•Any drug considered likely to interfere with the safe conduct of the trial
•Requirement for treatment with empagliflozin
•Treatment with any SGLT2i or combined SGLT1- and SGLT2i
•Currently enrolled in another investigational device or drug study, or < 30 days between randomisation and ending the other investigational trial
•Known allergy or hypersensitivity to empagliflozin or other SGLT2i
•Chronic alcohol or drug abuse
•Women who are pregnant, breastfeeding, or who plan to become pregnant while in the trial

***Table 4.2**: **Detailed Exclusion Criteria for EMPA-VISION HFpEF**. AF, atrial fibrillation; ALT, alanine aminotransferase; AP, alkaline phosphatase; AST, aspartate aminotransferase; BMI, body mass index; CAD, coronary artery disease; CHF, chronic heart failure; CMR, cardiovascular magnetic resonance; CPET, cardiopulmonary exercise testing; CRT, cardiac resynchronization therapy; CV, cardiovascular; GI, gastrointestinal; HF, heart failure; HFpEF, heart failure with preserved ejection fraction; HFrEF, heart failure with reduced ejection fraction; ICD, implantable cardioverter defibrillator; IV, intravenous; LAVI, left atrial volume index; LVAD, left ventricular assist device; LVEF, left ventricular ejection fraction; LVMI, left ventricular mass index; NT-proBNP, N-terminal pro-B-type natriuretic peptide; NYHA, New York Heart Association; SBP, systolic blood pressure; SGLT1-i, sodium-glucose co-transporter-1 inhibitor; SGLT2-i, sodium-glucose co-transporter-2 inhibitor; T1DM, type 1 diabetes mellitus; TIA, transitory ischaemic attack*

4.3.4 Data acquisition

4.3.4.1 Cardiac CT

If clinical ischaemia testing was not performed within the last 6 months prior to their screening visits, participants underwent a research cardiac CT scan to determine eligibility. The purpose was to assess presence and quantify extent of any possible CAD (see **Chapter 2.4**).

4.3.4.2 CMR

CMR imaging was performed using two 3-Tesla MRI scanners (Magnetom PRISMA and TRIO, Siemens Healthineers, Erlangen, Germany). **Figure 4.3** provides an overview of timings and the detailed scan protocol.

Figure 4.3: CMR Protocol EMPA-VISION HFpEF

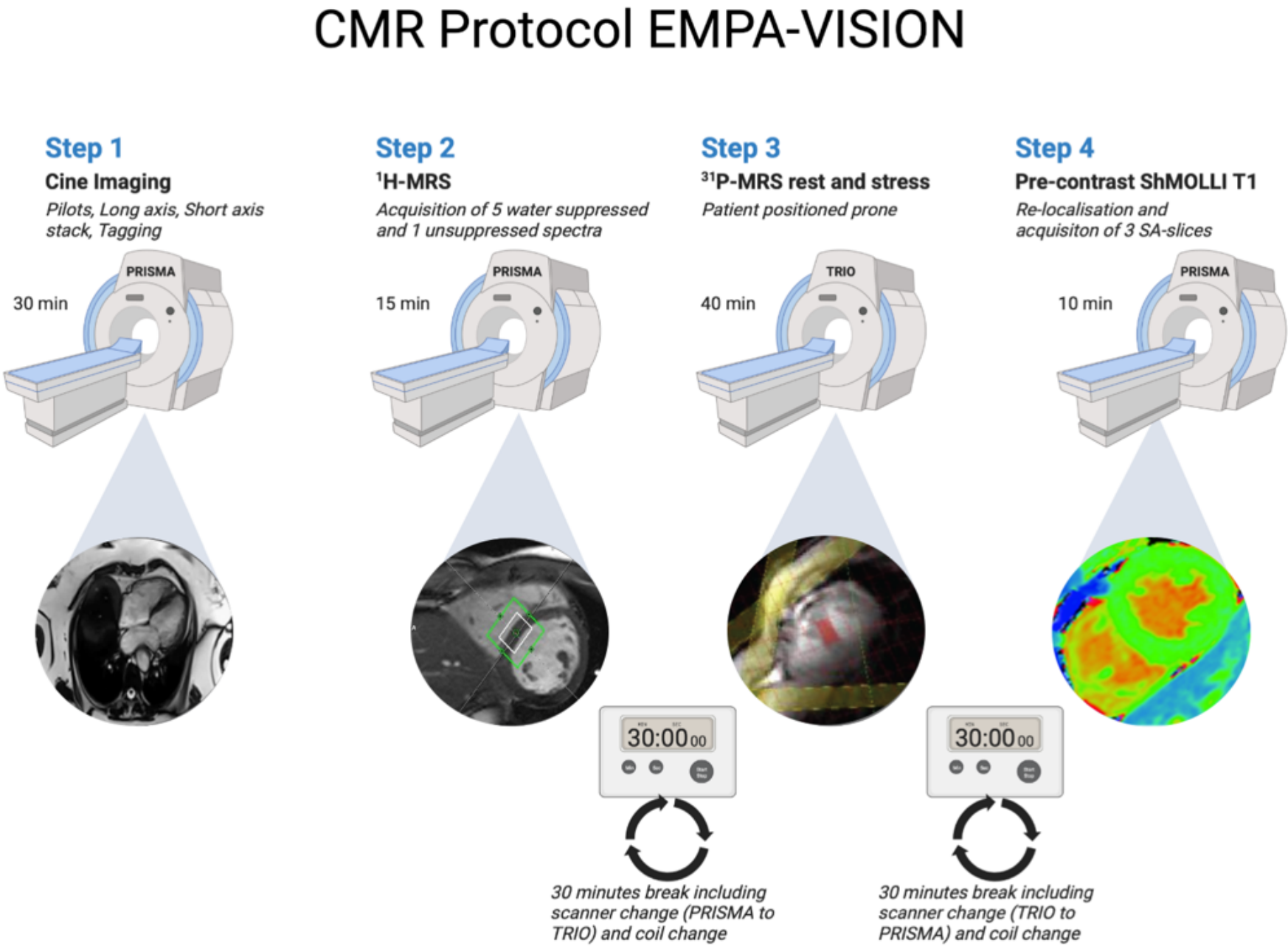

Step 5

Resting Perfusion

Myocardial Blood Flow

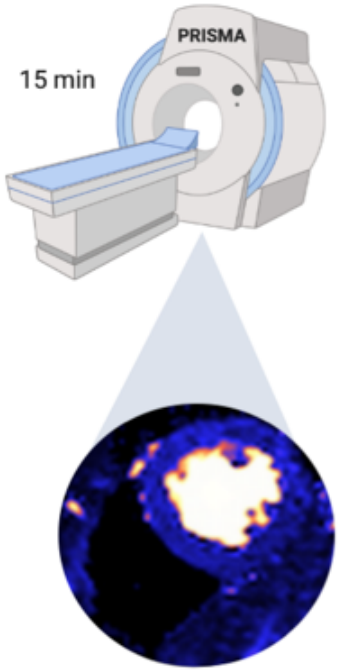

Step 6

LGE 1/2

SA-Stack

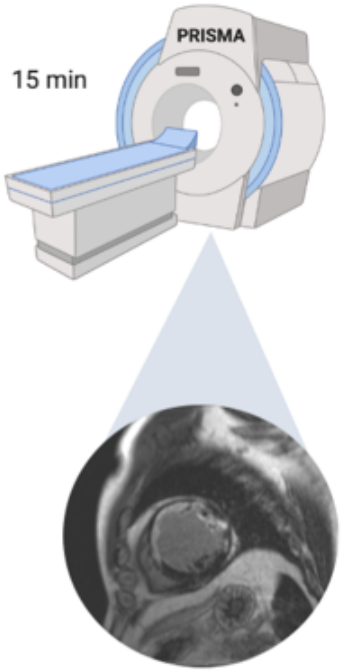

Step 7

Post-Contrast ShMOLLI-T1

Idential slice positioning as before

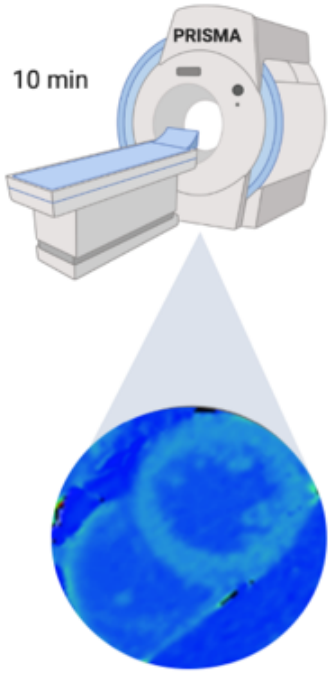

Step 8

LGE 2/2

HLA, VLA, LVOT

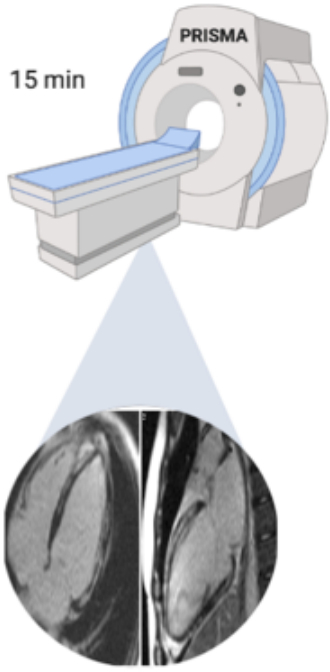

Figure 4.3: EMPA-VISION HFpEF CMR scanning protocol. *The first imaging and MRS sections were acquired on the 3T Siemens PRISMA MR-Scanner. After anatomical planning and pilot acquisition, long and short axis cines as well as myocardial tagging were performed. Then, myocardial triglyceride content (MTG) was assessed using ^{1}H-MRS. After a scanner (to the Siemens 3T TRIO) and coil change, myocardial energetics (PCr/ATP) at rest and during dobutamine stress (65% age-maximal HR) were obtained. Following another break and change back to the Siemens 3T PRISMA, native T1-mapping was performed at rest using ShMOLLI,. Rest perfusion imaging was performed immediately after gadolinium injection (0.05 mmol/kg). followed immediately by short axis (SA) late gadolinium enhancement (LGE) acquisitions. After 15min, post-contrast ShMOLLI was acquired, followed by the last missing long axis LGE-images.*

Using an 18-channel phased-array coil with the participant resting supine on the spine coil, the initial planning pilots and cine images were acquired in two long axis views (HLA, VLA) and in short axis slices covering the whole LV using retrospectively ECG-gated balanced steady-state free precession cine imaging or prospective gating in patients with atrial fibrillation (AF).[125,191] T1-maps were acquired in two matching short-axis slices based on the ShMOLLI sequence as previously described.[154]

Resting perfusion imaging was performed with an IV bolus injection of gadolinium (Gd) contrast (0.1 ml/kg, gadobutrol, Gadovist, Bayer AG, Sheffield, UK) followed by a 15-20 ml saline flush, both administered at 4-6 ml/sec. Pixel-wise perfusion maps were generated automatically using inline perfusion mapping software as previously described, to allow quantitative assessment of myocardial blood flow (MBF).[162]

Late gadolinium enhancement (LGE) imaging was performed in long and short axis views to exclude myocardial infarction or other types of scarring, as per SCMR guidelines.[125,191] **Figure 4.4** presents an overview of CMR-sequences used.

Figure 4.4: CMR Sequences EMPA-VISION HFpEF

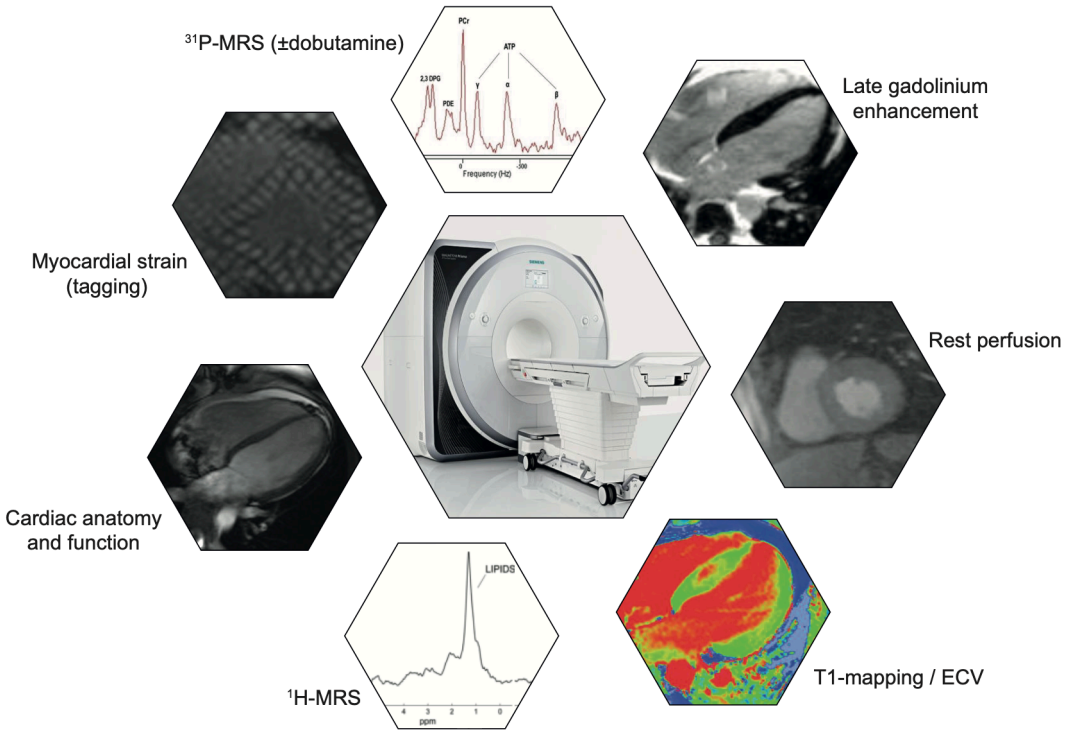

Figure 4.4: Overview of CMR Sequences EMPA-VISION HFpEF*. Cardiovascular magnetic resonance (CMR) sequences used for the EMPA-VISION trial. All sequences were performed on scanners by the same vendor (Siemens Healthineers, Erlangen, Germany) and identical field strength (3 Tesla).* ^{1}*H-MRS=proton magnetic resonance spectroscopy;* ^{31}*P-MRS=phosphorus magnetic resonance spectroscopy; ECV=extracellular volume.*

4.3.4.3 Dobutamine stress

Dobutamine was administered as a continuous intravenous infusion at incremental rates in order to achieve a significant haemodynamic effect. The infusion was commenced initially at 10 µg/kg/min but increased to a maximum of 40 µg/kg/min, depending on presence of a satisfactory haemodynamic response, which was defined as 65% of the age maximum heart rate (HR; 220-age). This elevated HR was then maintained for the duration of the acquisition. HR and blood pressure (BP)

were measured at baseline and at one-minute intervals during and after pharmacological stress until normalisation to pre-examination levels. Wherever feasible, stress cines were acquired in a mid-short axis slice as well as VLA and HLA. Due to logistical considerations, the stress-imaging was conducted as part of the ^{31}P-MRS acquisition hence used a different 3T-scanner (Magnetom TRIO, Siemens Healthineers, Erlangen, Germany) and had to be acquired using a locally created GRE-sequence by means of the integrated scanner receiver coils which resulted in a lower image quality and more susceptibility to movement artefacts.

4.3.4.4 Magnetic resonance spectroscopy

Multi-nuclear magnetic resonance spectroscopy (^{31}P- and ^{1}H-MRS) was used to assess different aspects of myocardial metabolic function. Firstly, cardiac energetics (expressed as PCr/ATP) were assessed using ^{31}P-MRS at rest and during dobutamine stress at 65% age-maximal HR (see **Chapter 2.5.1**) with patients laying in prone position over the centre of a dual-channel ^{31}P Heart/Liver coil (Siemens Healthineers, Erlangen, Germany). Furthermore, myocardial steatosis was assessed via ^{1}H-MRS (see **Chapter 2.5.3**) using an 18-channel receive array supine in end-diastole and expiration. This enabled acquisition of water suppressed and water unsuppressed lipid spectra allowing for calculation of myocardial triglycerides.

4.3.4.5 Echocardiography

Transthoracic echocardiography (TTE) was used to evaluate cardiac structure and function according to recommendations outlined by the British Society of Echocardiography.[165] The following clinical information was recorded and analysed on a Philips Healthcare ISCV analysis station:

- LVEF, LVEDV and -ESV, LVMi
- Diastolic function
- LV wall thickness and wall motion status
- Haemodynamic status (cardiac output)
- Valve status

4.3.4.6 Cardiopulmonary exercise testing and spirometry

Patients were seated on a stationary exercise bike (Ergoline GmbH, Bitz, Germany) for resting spirometry (see **Chapter 2.7**) and a cardiopulmonary exercise test (CPET) using breath-by-breath respiratory gas analysis (Metalyzer 3B, Cortex Biophysik, Leipzig, Germany). A standardised incremental exercise protocol was use, and patients encouraged to exercise until a RER of ≥1.1 was reached. SpO_2, capillary lactate and subjective exertion (Borg Scale) were assessed every 2 minutes and peak VO_2 measured at maximal exhaustion (see **Chapter 2.7** for details).

4.3.4.7 Six-minute walk test

Participants performed a six-minute walk test (6-MWT) at their own paced along a 20-meter corridor. Total distance covered, rating of perceived exertion as well as HR and BP were recorded prior to and after the test (see **Chapter 2.8**).

4.3.4.8 Blood sampling and analysis

A variety of biomarkers for assessment of safety (**Table 4.3**) and efficacy were measured in venous blood samples from patients fasting for at least 6 hours (see **Chapter 2.11**).

Table 4.3: Safety Bloods EMPA-VISION HFpEF

Haematology	
• Haematocrit • Haemoglobin • Reticulocyte count • Red blood cells (RBC) / erythrocytes	• White blood cells (WBC) / Leukocytes • Platelet count / thrombocytes • Differential automatic (relative and absolute count): Neutrophils, eosinophils, basophils, monocytes, lymphocytes
Clinical chemistry	
• Albumin • Alkaline phosphatase • GGT (gamma-glutamyl transferase) • ALT (alanine transaminase) • AST (aspartate transaminase) • Bicarbonate • Bilirubin total, fractionated if increased • Calcium • Chloride • Creatinine	• Creatine kinase (CK) • Hs Troponin I (reflex tests if CK is elevated) • Glucose • Magnesium • Phosphate • Potassium • Protein total • Sodium • Urea (BUN) • Uric acid
Lipids	
• Cholesterol (total) • HDL cholesterol • Calculated LDL cholesterol • Triglycerides (reflex test for direct measurement of LDL cholesterol triggered if triglycerides are >400 mg/dL or 4.52 mmol/L)	

Table 4.3: Safety Bloods EMPA-VISION HFpEF*. List of biochemical substances analysed for assessment of safety in EMPA-VISION's HFrEF cohort*

Biomarker efficacy assessment

- Aceto-acetate
- Aldosterone
- Angiotensin II
- Beta-hydroxybutyrate
- Brain natriuretic peptide
- Erythropoietin
- Fasting plasma glucose
- Free Fatty Acids
- HbA1c
- NT-proBNP

- Renin activity
- Direct renin concentration

Serum metabolomics

- 2,3-phosphoglycerate
- Aconitate
- Adenosine
- Adenosinemonophosphate
- Alphaketobutyrate
- Alphaketoglutarate
- Bis-phosphoglycerate
- Citrate
- Dimethylglycine
- Fructosebisphosphate
- γ-amino butyric acid (GABA)
- Glucose
- Isocitrate
- Inosine
- Lactate
- Malate
- S-Adenosylhomocystein (SAH)
- Succinate
- Pyruvate

4.3.5 Data analysis

4.3.5.1 CMR

Image analysis for cardiac indices was performed in an anonymised fashion offline in accordance with SCMR guidelines[125], using cmr42 post-processing software by an independent operator who was blinded to patient treatment status. Spectroscopic analysis for ^{31}P- and ^{1}H-MRS was performed as described in **Chapters 2.5.1** and **2.5.3** of this thesis, respectively.

4.3.5.2 Echocardiography

Analysis of TTE images was conducted on an ISCV workstation as outlined before (see **Chapter 2.6**).

4.3.5.3 CPET and spirometry

Breath-by-breath respiratory gas analysis to calculate peak VO2 and other indices as well as spirometry analysis of FEV1 and FVC was conducted on a workstation after every individual exercise test (see **Chapter 2.7**).

4.3.5.4 Biomarker and metabolomic analysis

Fasting venous bloods for efficacy and safety analyses were processed locally in keeping with official and in-house working instructions and then snap-frozen before being sent to the analysing laboratory (LabCorp, Geneva, Switzerland). Metabolomic processing from fasting serum samples was conducted in a dedicated facility with vast experience in the field (Prof. Griffin Lab, Imperial College London/University of Aberdeen, UK) while analysis and visualisation were performed in OCMR using statistical analysis software (R Core Team 2022, R Foundation for Statistical Computing, Vienna, Austria).

4.3.6 Statistical analysis

Statistical analyses of efficacy data were conducted at the Diabetes Trials Unit (The Oxford Centre for Diabetes, Endocrinology and Metabolism, University of Oxford, UK) following a prespecified statistical analysis plan (see the statistical analysis plan in the Data Supplement). Due to the lack of specific data describing the impact of SGLT2i on measures of energy metabolism in patients with HF, the sample size was calculated using an effect size based on previously published literature.[107,112,134] Consequently, detecting a treatment difference of 0.3 with a β of 0.8, an estimated effect size of 1.07 and a two-sided significance level of 0.05, the minimum sample size was determined to be a minimum number of n=30 participants. Allowing for a maximum dropout rate of 30%, it was anticipated to recruit a maximum possible number of 43 patients. The primary endpoint analysis was performed using the per protocol set (PPS) of patients with valid PCr/ATP measurements available at baseline and Week 12 and no important protocol violation relevant to the primary endpoint. Protocol violations were reviewed before the database lock. The analytical procedure included a descriptive summary and a formal (inferential) statistical summary, ANOVA, for the primary endpoint hypothesis testing.

All patients randomised to study treatment, in line with the intention-to-treat principle, were defined as the randomised set (RS) which was set to be employed for a sensitivity analysis to check for an unbiased estimation of the primary endpoint result if a substantial number of protocol violations resulted in a reduced sample size used for the primary endpoint estimates. The analysis of exploratory endpoints was performed on the RS of patients with available data using descriptive statistics

or ANCOVA. All summaries were produced for both cohorts and performed on the RS using all available data.

Subgroup analyses were performed to assess the homogeneity of treatment effects on changes in the PCr/ATP ratio in different subgroups (eGFR [<60 vs. ≥60 mL/min/1.73 m^2], diabetes mellitus [yes / no], and atrial fibrillation [yes / no] subgroups). The same ANOVA model as used for the primary endpoint was employed with the addition of subgroup term (if not already fitted) and the treatment by subgroup interaction term.

4.4 Results

Patient recruitment took place in a single centre (OCMR, Oxford, UK) from March 2018 until May 2020. A total of 101 patients performed a screening visit of which 36 patients were enrolled eventually and randomised to treatment. As mentioned above, due to the unforeseen impact of the global COVID-19 pandemic and subsequent effects on healthcare systems as well as restrictions implemented, 13 patients were unable to complete their EOT-visits (Visit 4) and thus, were excluded from the PPS. This unfortunately led to a reduction of the power from 80 % to 70 %.

.

4.4.1 Study population

Baseline data were well balanced in both treatment arms of the trial (**Table 4.4**). One patient in the placebo group was removed from the trial prematurely after experiencing cardiac arrest during the study CPET, one patient in the treatment group was removed after experiencing a UTI. Overall, 24 (11 placebo, 13 empagliflozin) of the 36 patients initially randomised to treatment completed their trial participation as defined in the per-protocol set (PPS).

Mean treatment duration was 84.7 days (SD 2.0) in the placebo and 82 days (SD 14.8) in the empagliflozin group, respectively. There were imbalances regarding the prevalence of risk factors for more severe HFpEF indicating a possibly elevated risk in the empagliflozin group. NT-proBNP, BMI, blood pressure, peak diastolic strain rate and end-diastolic volumes were all higher in the empagliflozin group. Nevertheless, HF symptom severity (NYHA class) was equally distributed. The mean eGFR of all patients was 68 ml/min/1.73m^2 (SD 19.1) while the geometric mean NT-proBNP was higher in the empagliflozin group (800.88, gSD 2.52) compared to the placebo group (643.57, gSD 2.47). **Table 4.4** summarises selected general baseline characteristics and **Table 4.5** CMR characteristics at baseline.

Table 4.4: Baseline Patient Characteristics EMPA-VISION HFpEF

Characteristic	Empagliflozin (n=18)	Placebo (n=18)	p-value
Age, mean (SD), years	69.1 (10.9)	72.1 (7.0)	
Sex, n (%)			
Male	10 (55.6)	9 (50.0)	
Female	8 (44.4)	9 (50.0)	
Race, n (%)			
White	16 (88.9)	18 (100)	
Black	1 (5.6)		
Asian	1 (5.6)		
BMI (kg/m^2), mean (SD)	30.58 (5.81)	29.4 (4.5)	
SBP (mmHg), mean (SD)	135.4 (21.8)	120.1 (16.1)	
DBP (mmHg), mean (SD)	74.2 (11.9)	74.2 (10.7)	
eGFR (ml/min/1.73 m^2), mean (SD)	72.0 (19.1)	69.1 (28.2)	
NT-proBNP (pg/ml), gMean (gSD)	800.88 (2.52)	643.57 (2.47)	
Minimum, Maximum	158.1, 6186.3	164.2, 2565.0	**ns**
ECG Parameters			
Heart rate (bpm), mean (SD)	72.57 (16.18)	72.41 (12.83)	
Sinus rhythm , n (%)	10 (55.6)	10 (55.6)	
Atrial fibrillation, n (%)	8 (44.4)	8 (44.4)	
NYHA classification, n (%)			
I	0	0	
II	15 (83.3)	14 (77.8)	
III	3 (16.7)	3 (16.7)	
IV	0	1 (5.6)	
Medical history, n (%)			
T2D	2 (11.1)	2 (11.1)	
Hypertension	7 (38.9)	5 (27.8)	
Stroke	1 (5.6)	1(5.6)	
Medications, n (%)			
β-Blockers	14 (77.8)	5 (27.8)	
ACE-I / ARB	12 (66.7)	8 (44.4)	
MRA	4 (28.6)	4 (28.6)	
Diuretics	11 (61.1)	11 (61.1)	
Anticoagulants	13 (72.2)	9 (50.0)	
Metformin	0 (0.0)	2 (11.1)	

Table 4.4: Baseline characteristics EMPA-VISION HFpEF. *Characteristics at baseline for all patients randomised to treatment. eGFR=estimated glomerular filtration rate (calculated using Cockcroft-Gault formula), ACE-i=angiotensin converting enzyme inhibitor, ARB=angiotensin II receptor blocker, bpm=beats per minute, ECG=electrocardiogram, DBP=diastolic blood pressure, MRA=mineralocorticoid receptor antagonist, β-Blockers=betablockers, T2D=type 2 diabetes, NYHA=New York Heart Association, SBP=systolic blood pressure, mmHg=millimetre mercury, pg=picogram, ml=millilitre,*

Table 4.5: Baseline CMR Characteristics EMPA-VISION HFpEF

	Placebo	Empa 10 mg
Randomised patients, N (%)	18 (100.0)	18 (100.0)
PCr/ATP ratio, mean (SD)		
At rest	1.719 (0.431)	1.896 (0.462)
Under dobutamine stress	1.645 (0.203)	1.628 (0.271)
Rest - stress	0.151 (0.321)	0.213 (0.360)
Cramer-Rao bound on PCr/ATP ratio [% of PCr/ATP], mean (SD)		
At rest	16.38 (7.57)	17.29 (9.56)
Under dobutamine stress	14.11 (5.12)	15.40 (8.38)
Myocardial triglyceride ratio (lipids / water) [%], mean (SD)	1.682 (1.071)	2.491 (2.105)
Peak systolic strain [%], mean (SD)		
Circumferential	-16.29 (2.45)	-15.75 (4.04)
Longitudinal	-12.82 (2.04)	-13.68 (3.44)
Radial	25.12 (9.94)	21.12 (7.88)
Peak diastolic strain rate [%/sec], mean (SD)		
Circumferential	70.47 (32.10)	59.82 (19.17)
Longitudinal	40.99 (21.51)	31.43 (12.38)
Torsion [degree], mean (SD)	9.57 (2.89)	8.64 (2.80)
LV end diastolic volume [mL], mean (SD)	140.92 (46.18)	183.50 (67.37)
LV end systolic volume [mL], mean (SD)	61.94 (30.70)	92.64 (45.64)
Stroke volume [mL], mean (SD)	78.98 (21.75)	90.86 (27.09)
Ejection fraction [%], mean (SD)	57.61 (9.75)	51.67 (9.89)
LV mass [g], mean (SD)	111.64 (42.95)	141.19 (56.97)
LV mass index [g/m^2], mean (SD)	54.55 (16.34)	66.42 (22.00)
Native T1 [ms], mean (SD)		
Average	1164.11 (47.89)	1194.38 (52.84)
Threshold	0.24 (0.19)	0.40 (0.26)
Lesions	1223.55 (51.17)	1243.03 (54.55)
Extracellular volume fraction [%], mean (SD)	29.60 (3.65)	28.54 (1.60)
Resting myocardial blood flow [mL/min/g], mean (SD)	1.74 (0.64)	1.77 (0.73)
Quantification of non-ischaemic pattern of LGE (fibrosis) [%], mean (SD)	6.09 (3.00)	4.77 (2.99)

Table 4.5: Baseline CMR-characteristics EMPA-VISION HFpEF*. Baseline CMR characteristics during rest and dobutamine stress in patients with HFrEF. LGE=late gadolinium enhancement; LV=left ventricular; SD=standard deviation.*

4.4.2 Primary outcome

4.4.2.1 Resting ^{31}P-MRS

In this trial, I did not observe a significant change myocardial energetics at rest in subjects with HFpEF following 12 weeks of treatment with empagliflozin. The mean change was 0.100 (SE 0.143) for empagliflozin and 0.259 (SE 0.156) for placebo, with an adjusted mean treatment difference of -0.159 (SE 0.213; 95 % CI: -0.604, 0.286; p=0.4650). This result was unchanged when including baseline PCr/ATP as a covariate in an ANCOVA model demonstrating an adjusted mean treatment difference of -0.140 (SE 0.199; 95 % CI: -0.556, 0.277; p=0.4910).

Figure 4.5: PCr/ATP at Rest EMPA-VISION HFpEF

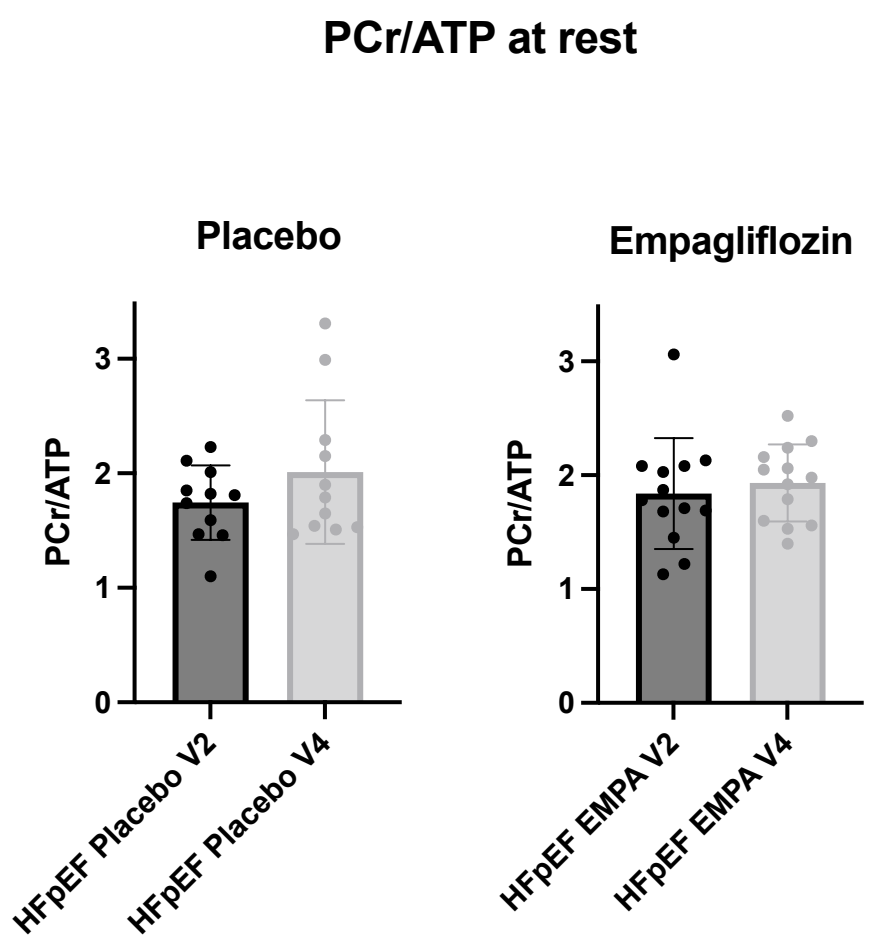

Figure 4.5: Resting PCr/ATP EMPA-VISION HFpEF. *Individual data points for the placebo (left) and empagliflozin treatment arms (right) at baseline (V2) and 12-week follow-up (V4).*

4.4.2.2 Subgroup analyses

In addition, subgroup analyses of subjects in the PPS were performed based on eGFR (< 60 ml/min/1.73m^2 vs. > 60ml/min/1.73m^2), history of T2D (yes/no) and history of AF (yes/no). Despite the limitations on sample size due to a disparate PPS of patients (COVID-19, see above), the efficacy analysis did not change the overall result in any of the subgroups.

Figure 4.6: Forest Plot EMPA-VISION HFpEF

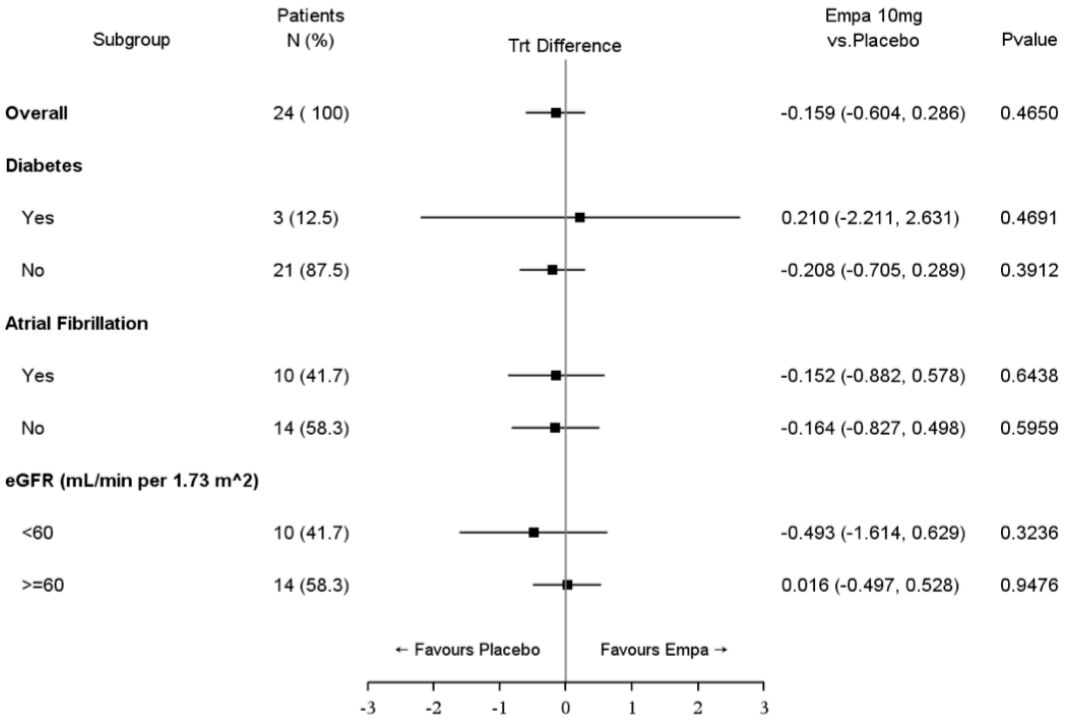

Figure 4.6: Subgroup Analysis EMPA-VISION HFpEF*. Forest plot providing a visual display of 95 % CI according to selected subgroups in the per protocol set of HFpEF patients regarding the change of resting PCr/ATP from baseline to week 12.*

4.4.3 Exploratory outcomes

4.4.3.1 Dobutamine Stress ^{31}P-MRS

Similarly to the resting PCr/ATP, results obtained during dobutamine stress (65% age maximal HR) indicated no notable difference of treatment with empagliflozin (-0.076, SE 0.138) versus placebo (0.139, SE 0.157) with an adjusted mean treatment difference of -0.215 (SE 0.211; 95 % CI: -0.659, 0.229; p=0.3219). **Figure 4.7** exhibits individual patient values separated by treatment arm (i.e. empagliflozin vs. placebo).

Figure 4.7: Dobutamine Stress PCr/ATP EMPA-VISION HFpEF

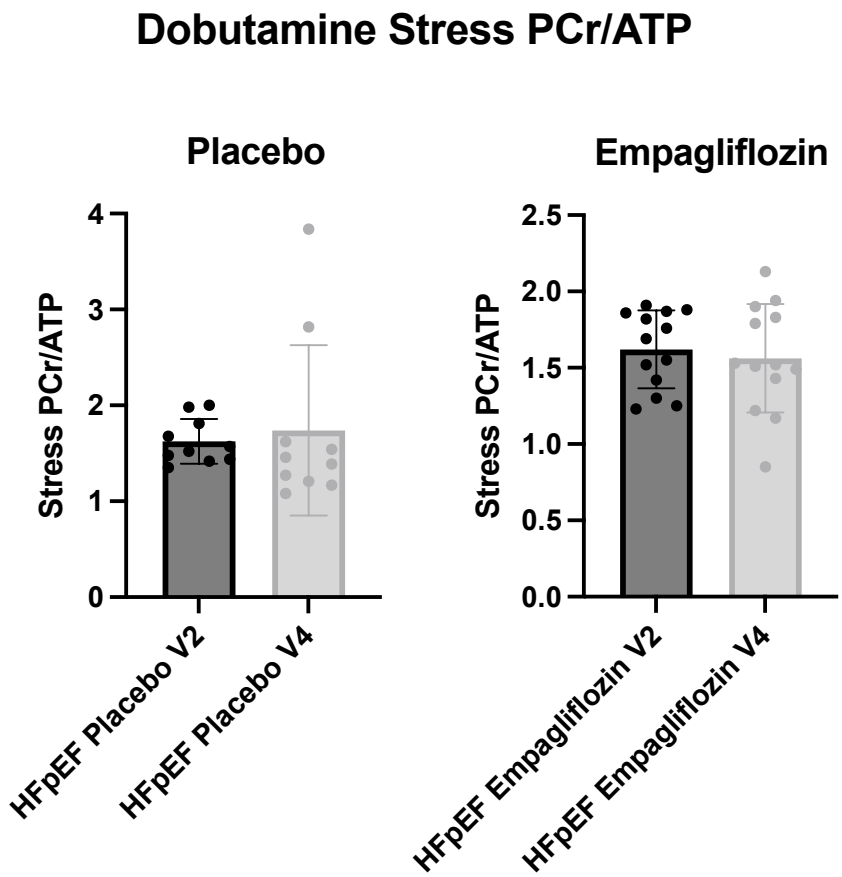

Figure 4.7: Stress PCr/ATP EMPA-VISION HFpEF. *Scatterplot of individual patient values for PCr/ATP during dobutamine stress with bar and standard errors for the placebo and empagliflozin group separately.*

Investigating the change of PCr/ATP from rest to stress (ΔPCr/ATP) elicited a similar picture as above: No marked differences were seen from baseline to week 12 with an adjusted mean change of 0.185 (SE 0.182) for empagliflozin vs. 0.113 (SE 0.208) for placebo (mean treatment difference 0.072, SE 0.279; 95 % CI: -0.514, 0.659; p=0.7983). Changes in ΔPCr/ATP for both treatment groups at baseline (V2) and EOT (V4) are shown below in **Figure 4.8.**

Figure 4.8: Delta (rest-stress) PCr/ATP EMPA-VISION HFpEF

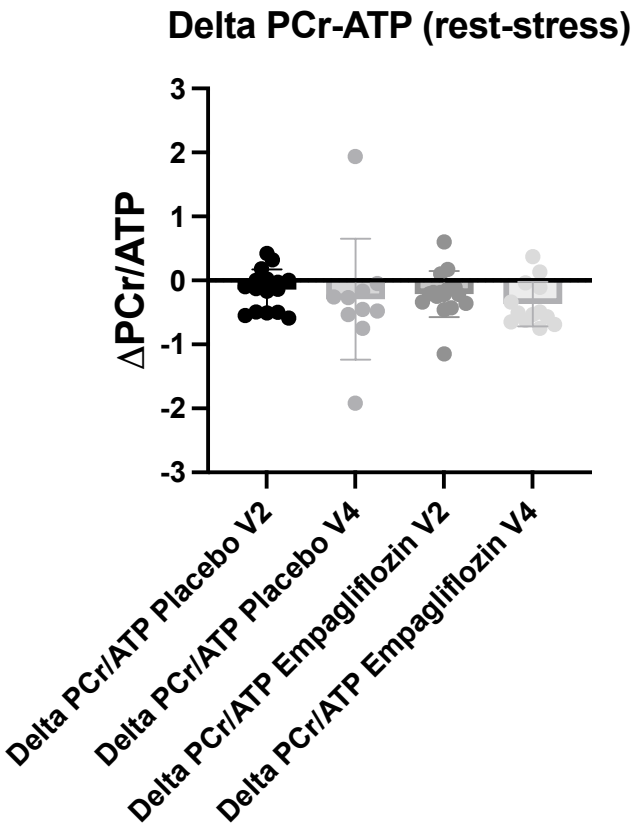

Figure 4.8: Delta PCr/ATP (rest-stress) EMPA-VISION HFpEF. *Scatterplot with bars and standard error of delta PCr/ATP (rest-stress) for individual patients in respective cohorts at baseline (V2) and end of treatment (V4).*

4.4.3.2 Assessment of myocardial steatosis via ^{1}H-MRS

As expected in a population of HFpEF patients, baseline MTG values were abnormally elevated. Empagliflozin treatment for 12 weeks resulted in a mean decrease (-0.406, SE 0.285) whereas placebo treatment increased MTG (0.020, SE 0.337). The adjusted mean treatment difference mirrored this result but did not reach statistical significance (-0.427, SE 0.451; 95 % CI: -1.393, 0.540; p=0.3599).

Figure 4.9: Myocardial Triglycerides EMPA-VISION HFpEF

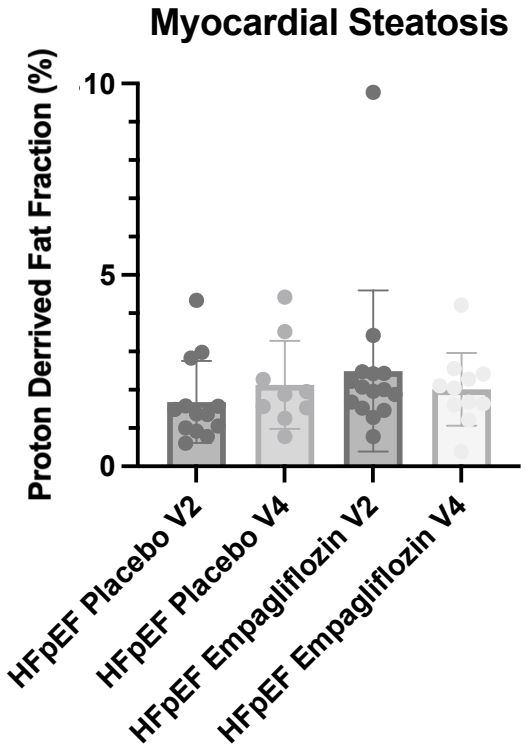

***Figure 4.9**: **Myocardial Triglycerides EMPA-VISION HFpEF**. Scatterplot with bars and standard error of myocardial triglycerides (assessed with ^{1}H-MRS) for individual patients in respective HFpEF cohorts at baseline (V2) and end of treatment (V4).*

4.4.3.3 Serum metabolomics

A snapshot analysis of targeted metabolomics entailing a panel of 19 metabolites relating to energy metabolism was investigated. Underpinning results of ^{31}P-MRS, no important change was detected following treatment with empagliflozin for 12 weeks. The metabolite panel had multiple correlations amongst the compounds (**Figure 4.10 A**) but no significant treatment difference emerged when analysing pre- and post-treatment data with Wilcoxon-ranked t-tests (**Figure 4.10 B**). No separation of metabolites was evident in a PLS-DA (**Figure 4.10 C**).

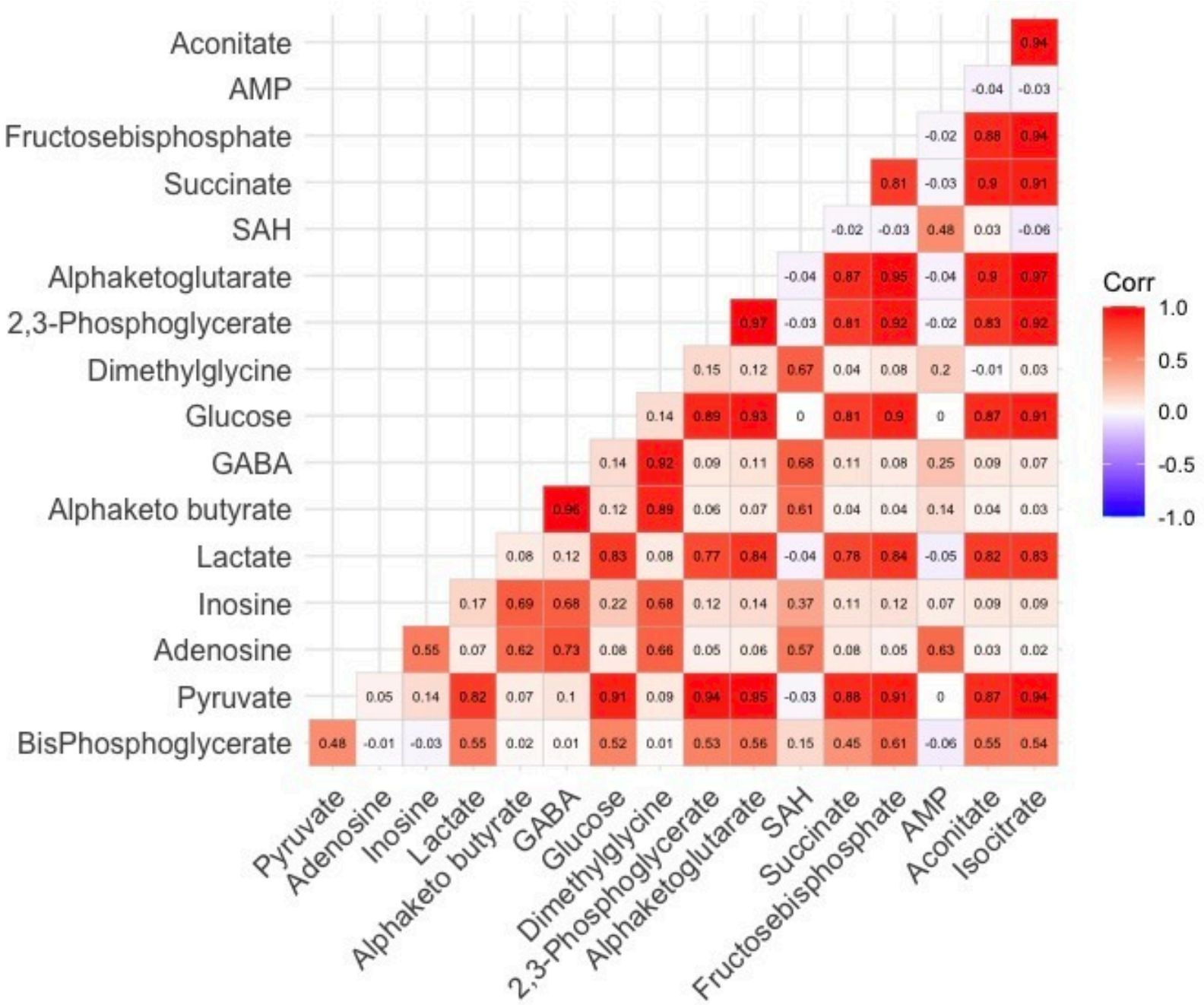

***Figure 4.10 A*: Correlation Matrix EMPA-VISION HFpEF.** *Correlation matrix visualising the degree of correlation between different metabolites with red indicating a high degree of correlation. AMP=adenosine monophosphate; GABA=γ-Aminobutyric acid; SAH=S-Adenosyl-L-homocysteine*

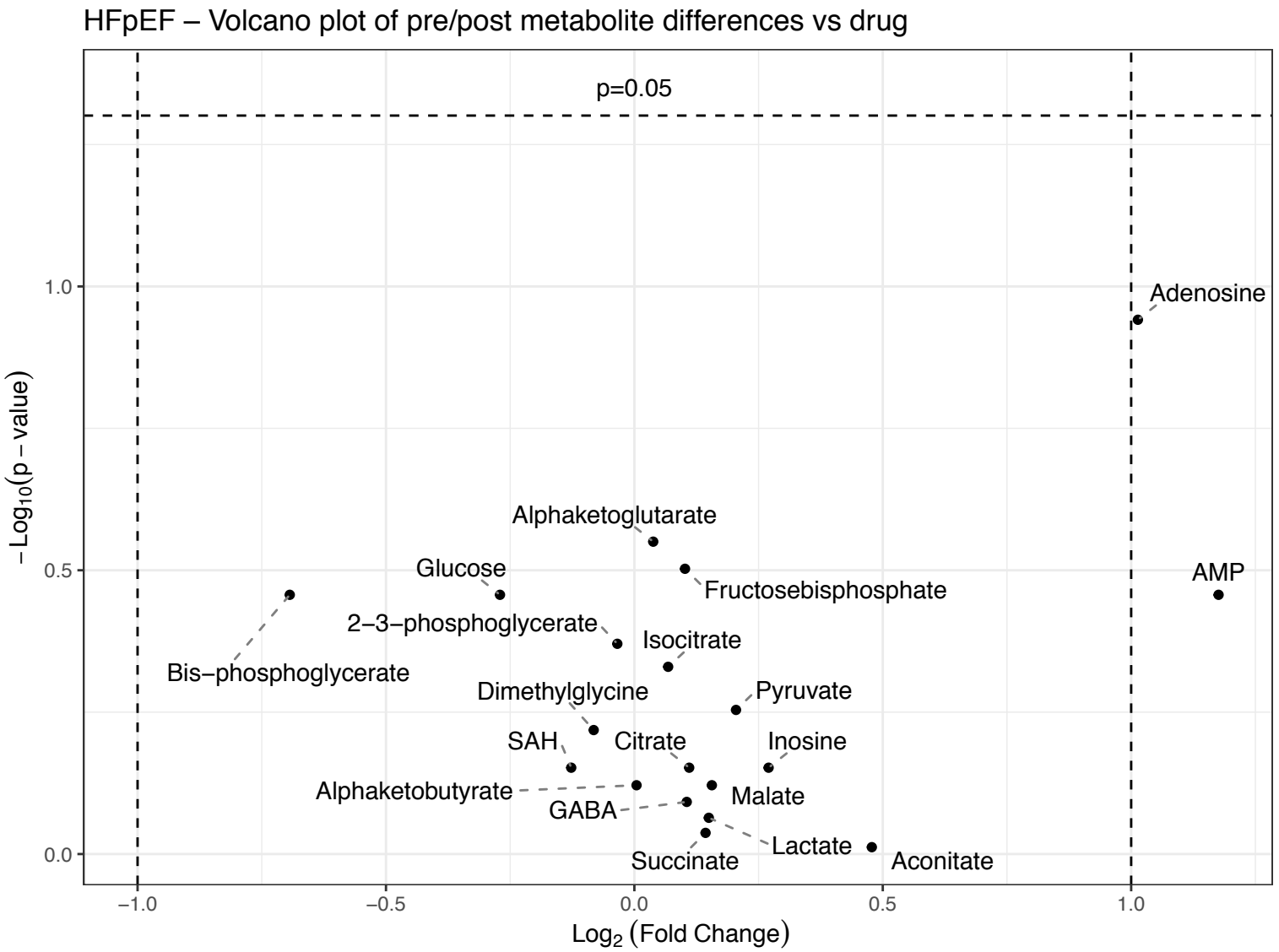

Figure 4.10 B: Volcano Plot EMPA-VISION HFpEF. *Volcano plot visualising the degree of statistical significance on the y-axis versus the magnitude of change (fold change) on the x-axis. AMP=adenosine monophosphate; GABA=γ-Aminobutyric acid; SAH=S-Adenosyl-L-homocysteine*

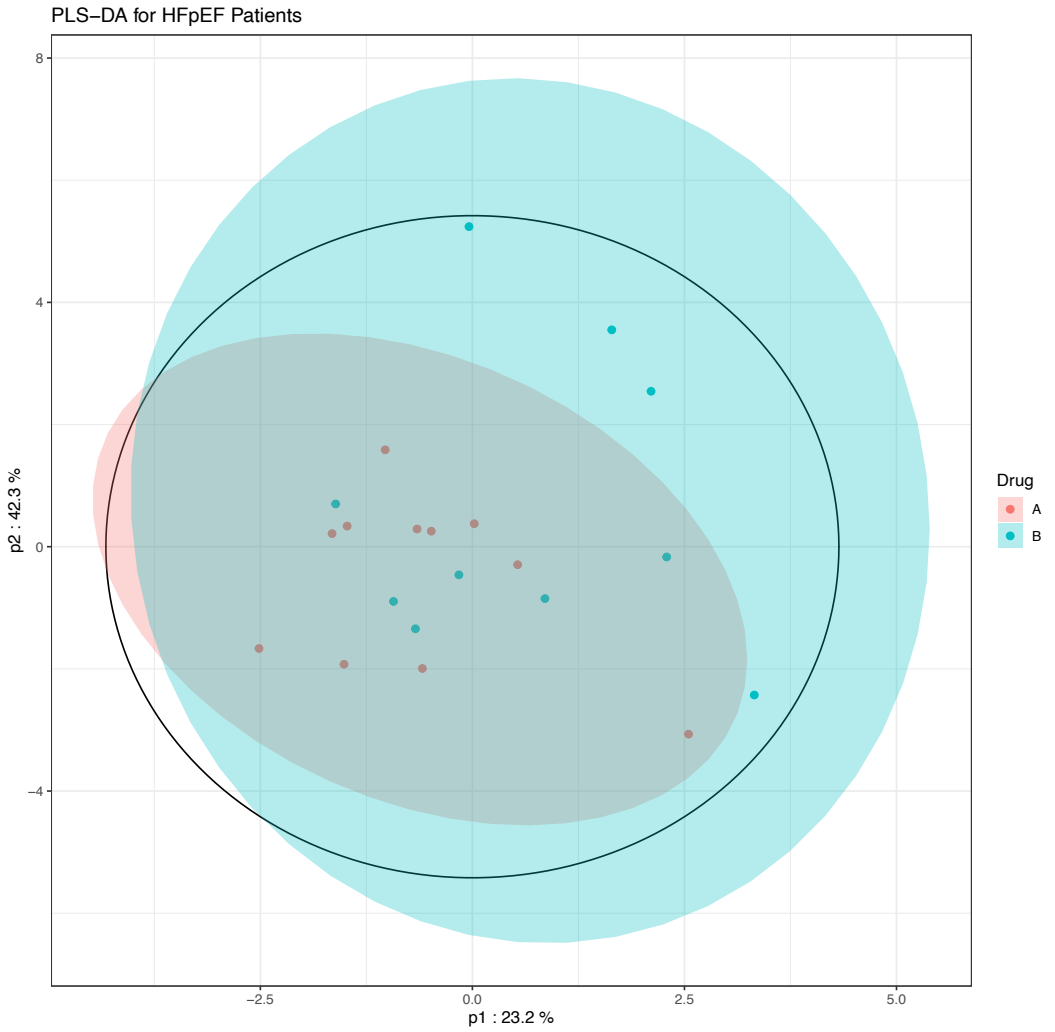

***Figure 4.10 C**: **PLS-DA EMPA-VISION HFpEF.** Partial least-squares determinant analysis (PLS-DA) showing no separation of groups when applying clustering according to treatment status (A=empagliflozin, B=placebo).*

4.4.3.4 Changes in LV structure and function

As outlined above, the significant limitations on the sample size as a result of the COVID-19 pandemic ensued in less power than anticipated.

Regardless, this trial did not demonstrate changes to LV volumes or myocardial structure after the obligatory 12-week treatment period. Interestingly, several results, despite not formally meeting the definition of statistical significance, are worth highlighting; Treatment with empagliflozin did numerically improve measures of LV contraction: Peak longitudinal systolic strain (2.18, SE 1.16; 95 % CI: -0.28, 4.64; p=0.0783), peak circumferential diastolic strain rate (7.96, SE 8.66; 95 % CI: -10.39, 26.31, p=0.37) and torsion (1.60, SE 0.91; 95 % CI: -0.32, 3.53; p=0.0968) all improved in the empagliflozin but worsened in the placebo group.

Table 4.6: Change in CMR Parameters EMPA-VISION HFpEF

Parameter Treatment	N	N analysed	Mean baseline (SE)	Adj. mean change (SE)	Adj. mean difference (95% CI)	P value
Peak systolic circumferential strain [%]						
Empagliflozin	18	13	-16.42 (1.09)	0.57 (0.70)	0.42 (-2.04, 2.88)	0.7213
Placebo	18	8	-17.21 (0.83)	0.15 (0.90)		
Peak systolic longitudinal strain [%]						
Empagliflozin	18	12	-14.16 (0.95)	1.86 (0.72)	2.18 (-0.28, 4.64)	0.0783
Placebo	18	8	-13.53 (0.59)	-0.32 (0.88)		
Peak systolic radial strain [%]						
Empagliflozin	18	13	22.94 (2.19)	-3.65 (1.76)	-0.88 (-6.89, 5.13)	0.7616
Placebo	18	9	28.27 (3.39)	-2.78 (2.14)		
Peak circumferential diastolic strain rate [%/sec]						
Empagliflozin	18	12	60.93 (5.52)	6.52 (5.52)	7.96 (-10.39, 26.31))	0.3716
Placebo	18	9	76.32 (11.58)	-1.44 (6.42)		
Peak longitudinal diastolic strain rate [%/sec]						
Empagliflozin	18	12	33.28 (3.66)	0.33 (4.80)	-6.28 (-22.59, 10.03)	0.4261
Placebo	18	9	45.17 (7.03)	6.61 (5.61)		
Torsion [degree]						
Empagliflozin	18	12	9.03 (0.87)	0.09 (0.59)	1.60 (-0.32, 3.53)	0.0968
Placebo	18	9	9.48 (1.07)	-1.51 (0.68)		
Stroke volume [mL]						
Empagliflozin	18	13	88.82 (7.43)	-2.18 (2.53)	0.58 (-7.67, 8.83)	0.8848
Placebo	18	11	70.84 (4.29)	-2.76 (2.77)		
EF [%]						
Empagliflozin	18	13	52.55 (2.90)	0.51 (1.36)	1.47 (-2.89, 5.83)	0.4885
Placebo	18	11	59.07 (2.96)	-0.96 (1.48)		
LV mass [g]						
Empagliflozin	18	13	127.72 (14.50)	-1.83 (3.21)	-0.41 (-10.86, 10.04)	0.9354
Placebo	18	11	94.40 (7.23)	-1.42 (3.52)		
LV mass index [g/m^2]						
Empagliflozin	18	13	62.24 (5.86)	-1.02 (1.81)	-1.18 (-7.06, 4.71)	0.6802
Placebo	18	11	48.74 (2.82)	0.15 (1.99)		

Table 4.6: Change from baseline to week 12 of selected CMR parameters EMPA-VISION HFrEF. *EF=LV ejection fraction*

Strain measures derived from feature tracking revealed a significant improvement of peak circumferential systolic strain (-5.28, SE; 95 % CI: -10.04, -0.53; p=0.03) and peak radial systolic strain (10.68, SE; 95 % CI: 1.16, 20.19; p=0.03) at rest. (**Table 4.7 A**) No changes were observed during peak dobutamine stress (**Table 4.7 B**).

A *Table 4.7: ANCOVA CMR Changes EMPA-VISION HFpEF*

Parameter Treatment	N	N analysed	Mean baseline (SE)	Adj. mean change (SE)	Adj. mean difference (95% CI)	P value
Peak circumferential diastolic strain rate during rest [%/sec]						
Empagliflozin	18	10	83.01 (13.70)	-0.47 (6.42)	14.76 (-7.47, 37.00)	0.1735
Placebo	18	7	85.70 (11.78)	-15.23 (7.72)		
Peak longitudinal diastolic strain rate during rest [%/sec]						
Empagliflozin	18	9	57.77 (11.99)	3.72 (8.54)	4.33 (-28.40, 37.06)	0.7714
Placebo	18	5	65.42 (11.98)	-0.61 (11.52)		
Peak circumferential systolic strain during rest [%]						
Empagliflozin	18	11	-12.18 (1.83)	-1.51 (1.31)	-5.28 (-10.04, -0.53)	0.0320
Placebo	18	7	-14.89 (2.22)	3.77 (1.67)		
Peak longitudinal systolic strain during rest [%]						
Empagliflozin	18	10	-8.89 (0.92)	-0.64 (1.11)	-0.84 (-4.98, 3.30)	0.6654
Placebo	18	6	-10.95 (1.22)	0.19 (1.45)		
Peak systolic radial strain during rest [%]						
Empagliflozin	18	11	19.56 (4.13)	4.14 (2.64)	10.68 (1.16, 20.19)	0.0306
Placebo	18	7	24.07 (4.94)	-6.54 (3.36)		
Stroke volume during rest [mL]						
Empagliflozin	18	10	76.91 (8.35)	-0.70 (4.21)	-8.04 (-24.19, 8.11)	0.2966
Placebo	18	6	57.35 (3.14)	7.34 (5.58)		
Ejection fraction during rest [%]						
Empagliflozin	18	10	48.84 (2.17)	1.86 (2.60)	0.99 (-9.38, 11.36)	0.8374
Placebo	18	6	56.13 (2.88)	0.87 (3.51)		

B

Parameter Treatment	N	N analysed	Mean baseline (SE)	Adj. mean change (SE)	Adj. mean difference (95% CI)	P value
Peak circumferential diastolic strain rate during stress [%/sec]						
Empagliflozin	18	8	84.55 (11.55)	-20.48 (11.45)	-7.17 (-63.29, 48.94)	0.7712
Placebo	18	4	136.13 (19.77)	-13.31 (17.86)		
Peak longitudinal diastolic strain rate during stress [%/sec]						
Empagliflozin	18	6	70.55 (20.06)	-8.32 (7.24)	-9.08 (-45.17, 27.02)	0.5234
Placebo	18	3	69.00 (7.92)	0.76 (10.43)		
Peak circumferential systolic strain during stress [%]						
Empagliflozin	18	8	-11.65 (1.60)	-0.11 (1.61)	0.55 (-7.33, 8.43)	0.8736
Placebo	18	4	-16.28 (0.58)	-0.66 (2.51)		
Peak longitudinal systolic strain during stress [%]						
Empagliflozin	18	6	-7.10 (1.17)	0.91 (1.84)	4.30 (-4.08, 12.67)	0.2444
Placebo	18	4	-6.50 (2.04)	-3.39 (2.35)		
Peak systolic radial strain during stress [%]						
Empagliflozin	18	8	17.06 (2.90)	0.51 (3.93)	-3.54 (-22.55, 15.47)	0.6732
Placebo	18	4	24.98 (1.20)	4.05 (6.08)		
Stroke volume during stress [mL]						
Empagliflozin	18	7	66.47 (10.03)	4.63 (9.08)	4.61 (-34.90, 44.12)	0.7847
Placebo	18	4	46.55 (5.14)	0.02 (12.39)		
Ejection fraction during stress [%]						
Empagliflozin	18	7	51.91 (4.03)	-1.02 (3.73)	-3.57 (-19.52, 12.38)	0.6040
Placebo	18	4	54.58 (6.80)	2.54 (5.05)		

***Table 4.7**: **ANCOVA of CMR Changes EMPA-VISION HFpEF**. CMR changes from baseline to week 12 in selected measures of left ventricular function and volumes during rest (A) and peak dobutamine stress (B).*

4.4.3.5 Pre-and post-contrast T1-mapping

Owing to a higher prevalence of atrial tachyarrhythmia (AF and atrial flutter) and frailty in the HFpEF patient population, acquisition of T1 maps was challenging. This in addition to the previously mentioned COVID-19 restrictions, led to fewer analysable datasets in each cohort and thus, the results presented here should be interpreted with caution.

Overall, no significant changes regarding T1-derived measures of fibrosis were observed over the 12-week period. Nonetheless, treatment with empagliflozin led

to numerically greater improvements in all ShMOLLI-T1-derived values compared to placebo (**Table 4.8**).

Table 4.8: ShMOLLI T1 EMPA-VISION HFpEF

Parameter Treatment	N	N analysed	Mean baseline (SE)	Adj. mean change (SE)	Adj. mean difference (95% CI)	P value
Native T1 - average [ms]						
Empagliflozin	18	12	1177.90 (11.27)	-5.81 (10.18)	-20.03 (-55.83, 15.77)	0.2516
Placebo	18	8	1156.42 (18.61)	14.22 (12.65)		
Native T1 - threshold [ms]						
Empagliflozin	18	12	0.33 (0.06)	-0.01 (0.08)	-0.04 (-0.33, 0.25)	0.7712
Placebo	18	7	0.18 (0.07)	0.03 (0.10)		
Native T1 - lesions [ms]						
Empagliflozin	18	6	1223.86 (15.89)	-19.52 (18.74)	-5.94 (-90.32, 78.43)	0.8634
Placebo	18	4	1208.87 (22.42)	-13.58 (23.80)		
Quantification of non-ischaemic pattern of LGE fibrosis [%]						
Empagliflozin	18	8	4.71 (1.22)	0.31 (0.81)	0.95 (-2.35, 4.24)	0.5266
Placebo	18	5	6.36 (1.56)	-0.64 (1.06)		

Table 4.8: Change from baseline to week 12 in ShMOLLI-T1 parameters in *EMPA-VISION* HFpEF.

Regrettably, only 5 datasets were eligible for analysis of change in differential ECV-fractions (i.e. cellular vs. matrix volume) in patients with HFpEF. Thus, firm conclusions are difficult to draw but generally, no change was measurable between the treatment groups (**Figure 4.11)**.

Figure 4.11: LV-Cell and -Matrix Volumes EMPA-VISION HFpEF

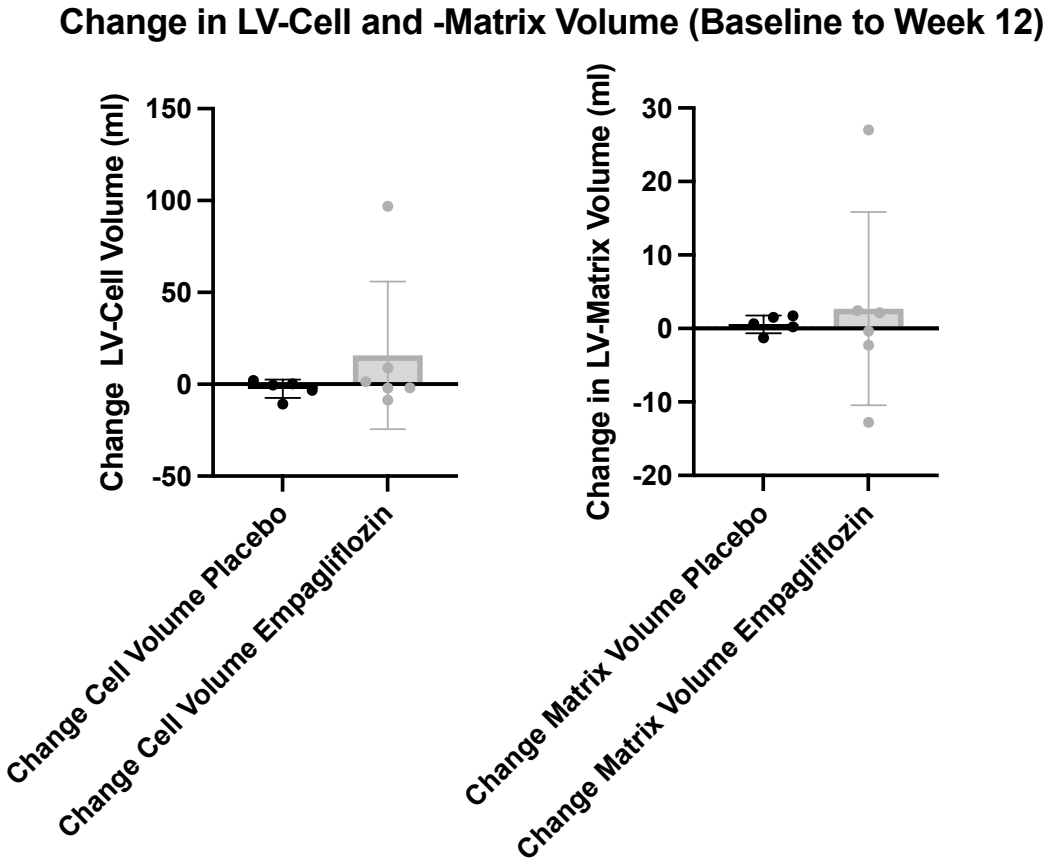

Figure 4.11: LV Cell- and Matrix Volume EMPA-VISION HFpEF*. Changes in LV-Cell and -Matrix volume (baseline to week 12) according to treatment status (placebo vs. empagliflozin).*

4.4.3.6 Echocardiography

The change in resting LVEF (biplane Simpson's method) was slightly higher in the empagliflozin (mean change: 2.6 %, SD 5.21) than the placebo group (mean change: 0.6 %, SD 7.51). No other noteworthy changes were detected (**Table 4.9**).

	Placebo						Empa 10mg				
Cohort B:HFpEF	N	Mean	SD	Q1	Median	Q3	N	Mean	SD	Q1	Median	Q3
Number of patients in the analysis set	18						18					
LVEF (%)												
Baseline	11	57.7	7.10	51.9	56.0	60.0	13	57.4	6.71	52.0	54.1	62.9
Week 12	11	58.3	5.19	53.4	59.0	62.0	13	60.1	6.89	54.0	59.2	63.0
Change from baseline at week 12	11	0.6	7.51	-2.6	-0.1	4.1	13	2.6	5.21	-1.1	2.0	5.4
LV end-diastolic volume (mL)												
Baseline	11	80.0	23.90	64.0	71.4	87.0	13	102.9	46.85	64.8	106.2	134.6
Week 12	11	78.4	27.08	60.3	65.1	93.7	13	93.3	47.66	58.6	81.8	131.7
Change from baseline at week 12	11	-1.6	13.69	-11.1	-6.4	6.7	13	-9.6	18.64	-24.4	-12.5	4.6
LV end-systolic volume (mL)												
Baseline	11	33.5	13.92	22.4	31.9	41.9	13	45.0	22.61	23.8	49.9	58.4
Week 12	11	33.0	14.85	22.2	27.3	45.7	13	38.0	21.00	23.7	35.9	53.7
Change from baseline at week 12	11	-0.5	8.03	-8.6	-2.6	7.6	13	-7.0	10.67	-11.5	-7.0	0.3
LV mass index (g/m2)												
Baseline	11	108.8	18.90	99.1	108.9	128.4	13	118.8	41.29	89.1	107.7	140.6
Week 12	11	100.2	19.84	92.7	104.4	113.3	13	117.5	40.04	88.0	112.6	145.2
Change from baseline at week 12	11	-8.6	18.00	-20.4	-8.0	5.5	13	-1.2	14.13	-8.6	2.9	8.2
E/e ratio												
Baseline	11	11.1	3.55	9.0	9.9	13.7	13	9.9	2.83	7.4	9.8	12.4
Week 12	11	10.8	4.54	7.8	9.0	14.0	13	8.9	2.80	6.6	8.1	10.6
Change from baseline at week 12	11	-0.2	2.34	-2.1	-0.3	1.0	13	-0.9	1.63	-2.0	-0.8	0.3
Left atrial volume index (mL/m2)												
Baseline	11	48.3	13.49	36.9	43.6	59.2	13	49.4	16.96	36.3	44.7	58.9
Week 12	11	49.6	13.24	39.7	50.9	55.0	13	48.2	19.28	32.4	45.5	55.3
Change from baseline at week 12	11	1.3	10.96	-8.3	1.5	11.4	13	-1.2	9.16	-5.6	-0.8	3.5
Chamber thickness (cm)												
Baseline	11	1.4	0.24	1.2	1.3	1.6	13	1.4	0.27	1.2	1.3	1.5
Week 12	11	1.4	0.16	1.3	1.3	1.5	13	1.3	0.17	1.1	1.3	1.4
Change from baseline at week 12	11	-0.0	0.35	-0.3	0.0	0.3	13	-0.1	0.33	-0.1	-0.1	0.2
Haemodynamic status (cardiac output) (L/min)												
Baseline	11	4.1	1.43	3.1	3.3	5.5	13	5.0	2.30	3.6	4.3	5.3
Week 12	11	4.4	1.04	3.7	4.3	5.3	13	5.5	2.17	4.2	4.6	6.6
Change from baseline at week 12	11	0.3	1.60	-0.7	0.3	1.5	13	0.4	1.91	-0.7	0.2	1.2
Septal e-velocity (cm/sec)												
Baseline	11	7.1	1.87	5.7	6.9	8.5	13	8.2	3.18	6.1	7.3	9.9
Week 12	11	6.9	2.20	5.4	6.9	8.1	13	6.8	1.46	5.8	7.3	7.5
Change from baseline at week 12	11	-0.2	2.02	-1.2	0.3	0.8	13	-1.4	2.99	-3.4	-1.5	0.7
Lateral e-velocity (cm/sec)												
Baseline	11	10.2	2.07	8.6	9.5	11.5	13	9.5	3.11	7.5	8.8	10.7
Week 12	11	9.9	2.63	7.7	9.1	11.7	13	10.5	3.03	8.5	9.5	12.9
Change from baseline at week 12	11	-0.3	2.95	-2.9	-0.4	1.0	13	1.1	2.84	0.0	0.6	2.9

***Table 4.9**: Baseline values, Week 12 values and changes in echocardiographic parameters over time as mean (with SD) and IQR. N=number of patients*

4.4.3.7 Cardiopulmonary exercise testing and spirometry

For patients in the HFpEF cohort, there was no significant difference between empagliflozin and placebo with regards to change from baseline to week 12 in peak $\dot{V}O_2$, Ve/VCO_2 slope, ventilatory threshold (VT), maximal workload, or any other of the parameters measured during physical exercise (CPET).

Figure 4.12: CPET Changes EMPA-VISION HFpEF

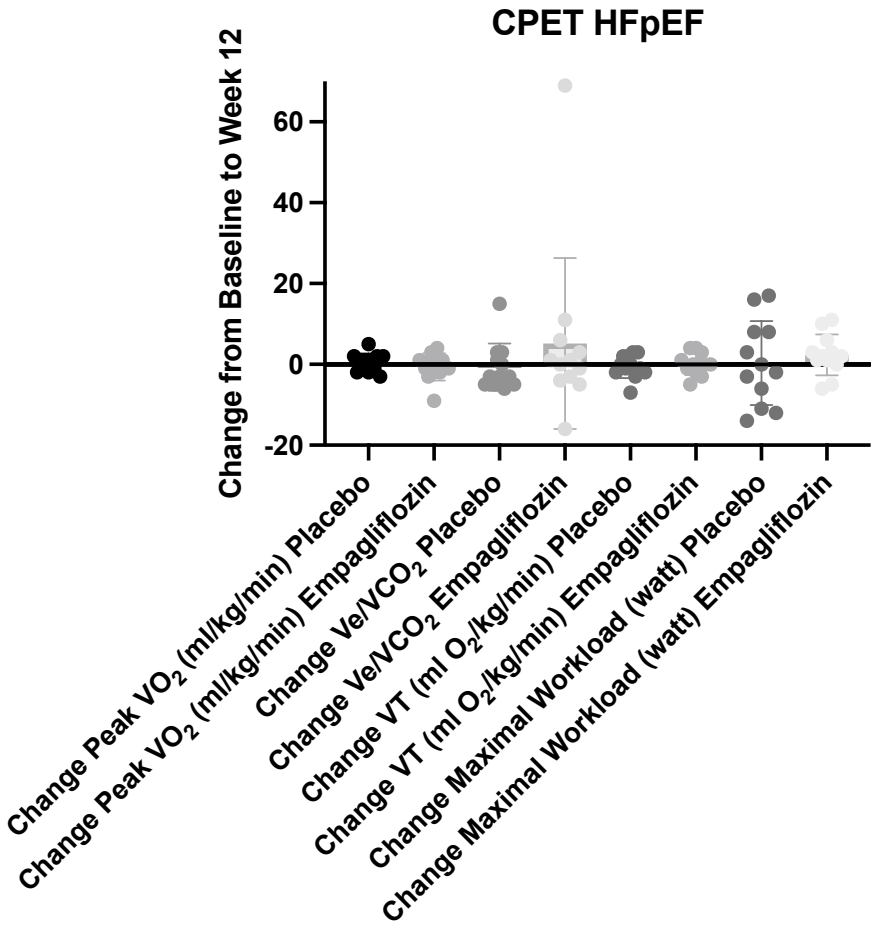

Figure 4.12: CPET Results EMPA-VISION HFpEF*. Individual data points for changes of selected CPET-measures in patients with HFpEF.*

Spirometry assessment revealed an improvement in forced vital capacity (FVC) in the empagliflozin group compared with placebo. From baseline to week 12, the adjusted mean change was 0.15 L (SE 0.10) for empagliflozin vs. -0.19 (SE 0.10) for placebo, with an adjusted mean treatment difference of 0.34 L (SE 0.15; 95 % CI: 0.03, 0.65; p = 0.0348). There was also an improvement in FEV 1 in the empagliflozin group compared with placebo. From baseline to Week 12, the adjusted mean change was 0.10 L (SE 0.07) for empagliflozin vs. -0.03 (SE 0.04) for placebo, with an adjusted mean treatment difference of 0.14 L (SE 0.06; 95 % CI: 0.00, 0.27; p = 0.0438)

4.4.3.8 Six-minute walk test

Patients on empagliflozin showed a near-significant increase of walking distance (adjusted mean difference 28.23 m, SE 14.19; 95 % CI: -1.46, 57.93; p=0.0612) with all other test items largely unchanged between empagliflozin and placebo.

4.4.3.9 Patient reported outcomes

With the exception of physical limitation in the placebo group (placebo: mean change -0.64, SD 18.69), all items of the KCCQ showed some improvement (i.e. an increased score) from baseline in both the empagliflozin and placebo treatment groups. However, the reported magnitude of change in the 3 itemised scores was consistently greater for empagliflozin than for placebo. Mean changes in the overall summary score from baseline at Week 12 were 7.15 (SD 12.36) for the empagliflozin treatment group and 3.32 (SD 12.40) for the placebo group. Mean changes in the overall clinical summary score from baseline at Week 12 followed the same pattern as changes in the overall summary score. Mean changes in the

overall clinical summary score from baseline at Week 12 were 8.65 (SD 11.51) for the empagliflozin treatment group and 4.97 (SD 14.84) for the placebo group.

Figure 4.13: KCCQ EMPA-VISION HFpEF

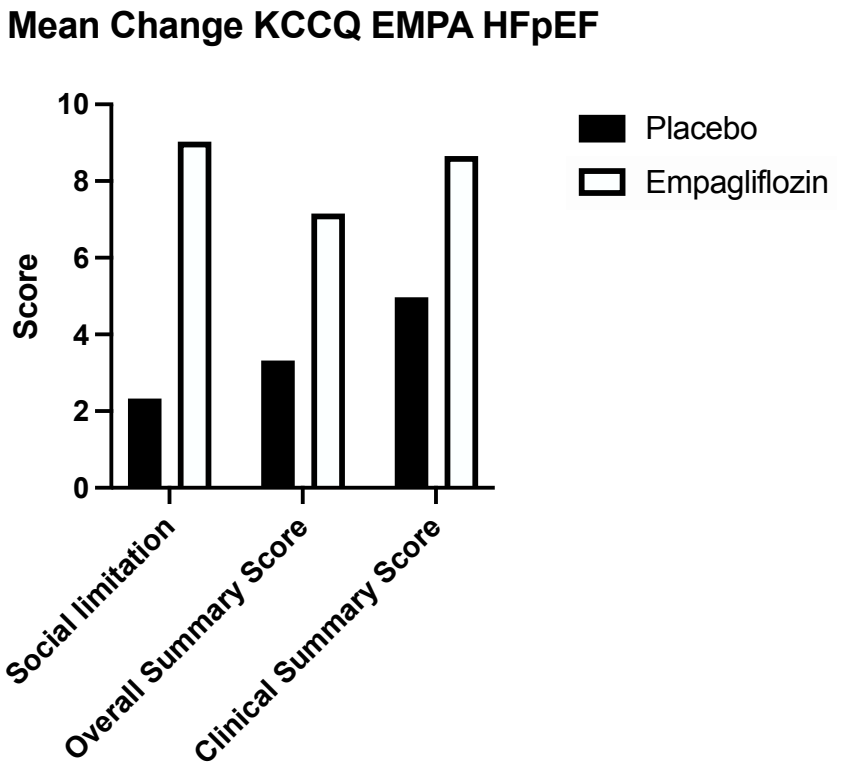

***Figure 4.13**: **Patient Reported Outcomes EMPA-VISION HFpEF.** Mean changes in the respective symptom scores of the KCCQ between the placebo and the empagliflozin groups.*

There were minor changes in the scoring of individual items of the EQ-5D based on categorical responses to items of this measure with a small number of patients showing an improvement and a small number showing a deterioration in both the empagliflozin and placebo treatment groups from baseline at Week 12. There were no notable differences in the changes in EQ-5D responses between the empagliflozin and placebo treatment groups.

4.4.3.10 Biomarker analysis

Changes to biomarkers were similar in the respective treatment groups (**Table 4.10**). As expected, markers of treatment efficacy (**Figure 4.14**) showed some group specific changes which were greater, yet not statistically significant, with empagliflozin.

Table 4.10: Biomarker Changes EMPA-VISION HFpEF

Parameter Treatment	N	N analysed	Mean baseline (SD)	Mean change (SD) at last value on treatment
Hba_{1c} [%]				
Empagliflozin	18	12	5.73 (1.02)	-0.12 (0.32)
Placebo	17	11	6.23 (1.05)	0.28 (0.66)
Acetoacetic acid [µmol/L]				
Empagliflozin	18	0	-	-
Placebo	17	2	117.6 (13.9)	-4.9 (6.9)
Beta-hydroxybutyrate [mmol/L]				
Empagliflozin	18	13	0.135 (0.053)	0.029 (0.113)
Placebo	17	12	0.196 (0.077)	-0.048 (0.099)
Fasting plasma glucose [mmol/L]				
Empagliflozin	18	13	5.76 (1.55)	-0.25 (0.49)
Placebo	17	12	6.16 (1.38)	0.40 (1.99)
Free fatty acid [mmol/L]				
Empagliflozin	18	13	0.71 (0.27)	-0.02 (0.38)
Placebo	17	12	0.79 (0.29)	-0.13 (0.39)
Aldosterone [pmol/L]				
Empagliflozin	18	13	416.052 (300.924)	-31.564 (209.094)
Placebo	17	12	380.183 (274.253)	91.787 (338.641)
Angiotensin II [ng/L]				
Empagliflozin	18	13	22.0 (7.1)	3.5 (8.3)
Placebo	17	11	34.8 (28.1)	25.1 (51.3)
Erythropoietin [U/L]				
Empagliflozin	18	13	10.3 (4.6)	2.1 (3.5)
Placebo	17	12	10.1 (6.0)	1.2 (3.5)
Renin activity [ng/L/h]				
Empagliflozin	18	12	3.91 (9.38)	-1.05 (7.76)
Placebo	17	10	3.90 (6.49)	3.86 (8.96)
Renin [ng/L]				
Empagliflozin	18	12	26.09 (40.43)	0.14 (22.04)
Placebo	17	11	52.18 (102.22)	68.92 (154.75)
			gMean (gCV %) at baseline	Relative change from baseline gMean ratio (gCV %)
BNP [ng/L]				
Empagliflozin	18	13	169.91 (84.06)	1.10 (75.38)
Placebo	17	12	100.27 (86.90)	1.49 (67.83)
NT-proBNP [pg/mL]				
Empagliflozin	18	13	768.88 (123.54)	1.12 (102.13)
Placebo	17	12	488.02 (139.24)	1.59 (96.95)

***Table 4.10**: **Biomarker Results EMPA-VISION HFpEF**. Change from baseline to week 12 (or last value on treatment) for selected exploratory biomarkers from fasting venous blood.*

Figure 4.14: Relative Biomarker Changes EMPA-VISION HFpEF

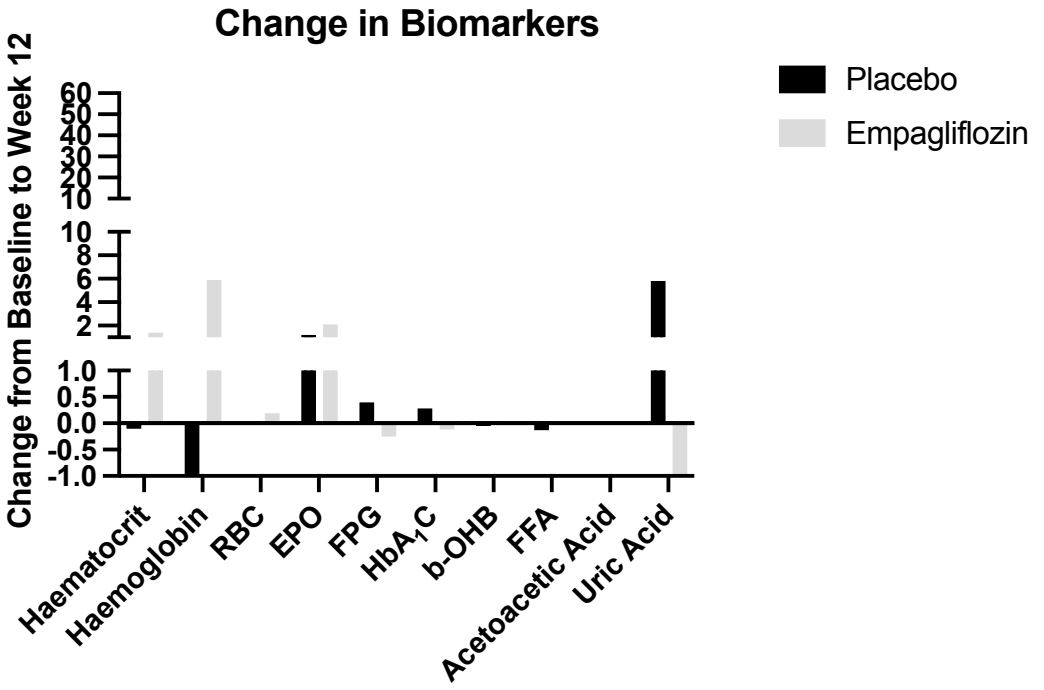

***Figure 4.14: Relative Biomarker Changes in EMPA-VISION HFpEF**. Visualised summary of changes in selected biomarkers in the empagliflozin and placebo groups, respectively.*

4.5 Discussion

This is the first randomised controlled trial investigating effects of empagliflozin treatment on measures of cardiac energy metabolism (PCr/ATP) during rest and peak dobutamine stress in patients with 'true' HFpEF (i.e. LVEF ≥ 50%). Additionally, the plethora of exploratory outcomes including imaging, metabolomic and biomarkers as well as patient reported outcomes and measures of cardiorespiratory fitness (CPET, spirometry and 6MWT) further strengthens the mechanistic understanding of treatment effects with empagliflozin in HFpEF.

Use of the SGLT2i empagliflozin (10 mg per day) did not enhance myocardial energetics (PCr/ATP) during rest or dobutamine stress. Furthermore, no noteworthy metabolic alterations were detected when conducting a snapshot metabolomic analysis of 19 targeted metabolites before and after treatment with empagliflozin or placebo for 12 weeks.

Measures of LV contraction (peak circumferential systolic strain and peak radial systolic strain) improved ($p<0.05$) while other surrogates showed numerical improvements (peak longitudinal systolic strain and torsion) for empagliflozin but not placebo, despite not reaching nominal statistical significance. Assessment of diastolic function did not show noteworthy differences.

Patient in the empagliflozin group presented with both a markedly improved walking distance (28.23 m, $p=0.06$) and improved KCCQ scores.

4.5.1 Changes in myocardial energy metabolism

Much like systolic contraction, diastolic relaxation is an active process, requiring energy in the form of ATP. Consequently, just like in HFrEF, the heart can be considered in a state of energy deficit in HFpEF. Patients with HFpEF have a lower-than-normal PCr/ATP [73] which correlates negatively with the degree of disease severity.[257]

Figure 4.15: PCr/ATP Normal vs. HFpEF

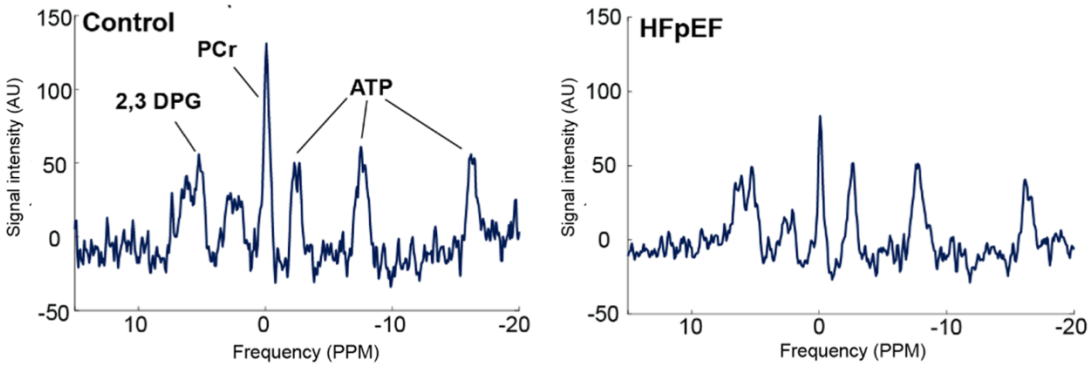

Figure 4.15 PCr/ATP Normal vs. HFpEF.*: Representative PCr/ATP spectrum from a normal control (left) compared with a patient with HFpEF (right) reveling the energetic deficit of HFpEF patients. From Burrage, M.K & Hundertmark, M.J. et. al.; Circulation 2021*[257]

In addition, it was shown that HFpEF has a distinct metabolic signature in a panel of 181 metabolites when compared to HFrEF.[84] Importantly, these metabolic/biochemical changes appear to precede structural alterations and increased humoral markers of HF hence, might be better suited to investigate patients at risk than imaging or traditional biomarkers.[258] Thus, metabolic modulation is a promising target in HFpEF.[259]

EMPA-VISION did not find notable changes to myocardial energy reserve (PCr/ATP) *in-vivo* at rest or during dobutamine stress following 12 weeks of empagliflozin. This may have several reasons; Metabolic alterations in HFpEF are poorly understood and there is a paucity of evidence regarding metabolic interventions in HFpEF. It appears to be the case that there is no uniform single 'one-fits-all' definition of HFpEF but rather many phenotypes which are currently (possibly mistakenly) summarised under one acronym.[5] Additionally, no universally accepted mouse model of HFpEF exists which makes translation of findings in rodent experiments to human physiology difficult. As a result, some rodent models, especially those with obesity and/or diabetes, show increased rates of FAO and attribute metabolic derangements in HFpEF to lipotoxicity[76,77,260], whereas others describe a reduced ability to oxidise fatty acids.[53]

Recent evidence supports our neutral results: In a murine model of hypertension-induced HFpEF, non-diabetic mice improved their diastolic function however, this was achieved without changes in expression of genes related to myocardial substrate utilization or mitochondrial biogenesis.[261] In another study using a mouse model with identical etiology for HFpEF, improvement of diastolic function was also attributed to other effects but importantly not enhanced energy production.[262] This is also highlighted by findings that in HFpEF, contrary to HFrEF, oxidation and thus utilization of ketones as a fuel for energy production was decreased despite higher levels of ketones in circulation.[260] This makes the purported mechanism of action of SGLT2i as metabolic HF treatments, focusing on induction of mild hyperketonaemia, less likely.[188] Lastly, a neural network analysis used for artificial

intelligence modelling of empagliflozin effects in HFpEF was equally more supportive of non-metabolic mechanisms of action.[263]

4.5.2 Changes in LV-structure and function

HFpEF is closely correlated to and often a consequence of hypertension and the extent of myocardial hypertrophy in patients with HFpEF is a predictor of future events and its presence an indicator of higher risk for hospitalisation.[5,264] However, conversely to patients with T2D, there is no human *in-vivo* evidence for a reducing effect of myocardial hypertrophy and/or fibrosis as a result of SGLT2i-treatment.

This trial investigated measures of LV-structure and -function via echo and CMR. In this cohort, empagliflozin treatment did not result in reduced myocardial hypertrophy or reverse remodelling. Nevertheless, measures of systolic myocardial function other than LVEF improved significantly (peak circumferential systolic strain and peak radial systolic strain;) On myocardial tagging, in keeping with the feature tracking results, there was a non-significant but consistent improvement of peak longitudinal systolic strain (p=0.0783) and torsion (p=0.0968). It has previously been established that longitudinal strain parameters are incrementally useful in HFpEF as per definition the current arbitrary phenotypisation method (LVEF), is normal (i.e.≥ 50 % minimum).[265,266] Crucially, it was further shown that strain parameters can be modified by HF treatments and thus, may represent a good imaging surrogate for trials.[266] In agreement with the results presented here, a recent prospective study in patients with T2D and a high risk for HFpEF demonstrated improved longitudinal strain measures as well.[267] Whether these changes are translated on a cellular level by reduced inflammation/cellular stress[268,269] and/or

optimised cellular electrolyte homeostasis (i.e. Ca^{2+} and Na^{+} shifting via the sodium-proton- exchanger NHE3) remains to be determined. More mechanistic trials investigating changes other than diastolic function are needed in HFpEF, but the results presented here should be taken as a blueprint in generating further, larger scale evidence.

4.5.3 Changes in cardio-respiratory fitness and patient reported outcomes

Exercise intolerance and more importantly, diminished cardiac reserve under conditions of increased demand are hallmarks of HFpEF.[5,270]

In the current study, no differences were detected in relevant measures of cardio-respiratory fitness via CPET. Interestingly, larger outcome trials assessing the phosphodiesterase-5 inhibitor Sildenafil[251] and the mineralocorticoid antagonist Aldosterone[250] likewise did not elicit differences in peak $\dot{V}O_2$ or other CPET-measures. There is considerable debate whether peak $\dot{V}O_2$ might be an equally suitable predictor of events and worse outcomes as it is in HFrEF patients and studies have demonstrated that Ve/VCO_2 might be more appropriate to phenotype HFpEF patients and identify high-risk individuals.[271-273]. No data are available on CPET effects of SGLT2i in HFpEF in human subjects. A recent exercise treadmill study in an obesity induced rat model of HFpEF demonstrated reduced rates of pulmonary hypertension during exercise, resulting in an improved exercise tolerance in animals treated with empagliflozin.[274] The reduction in PA pressures had also been observed in the *EMBRACE-HF* trial in patients with HF irrespective of LVEF measured via an implantable pressure sensor in the pulmonary artery

(CardioMEMS).[275] Nevertheless, whether or not these findings directly translate to human HFpEF is questionable but worthy of future investigation. Thus far, sacubitril/valsartan, proven to be beneficial in a selected subgroup of HFpEF patients (LVEF 45 – 57 %), equally did not exhibit any salutary effects on CPET measures.[276] Results of spirometry analysis in this trial met significance for FEV_1 and FVC. While no data exists to corroborate these findings in patient with HFpEF, it was previously shown that pulmonary function predicts outcomes and as such, may be a target worthy of future investigation.[277]

In *EMPA-VISION*, treatment with empagliflozin resulted in a numerically increased walking distance (28.23 m) and narrowly missed significance (p=0.06). The outcome observed is in agreement with other SGLT2i tested in HFpEF patients including Dapagliflozin.[2] However, in *EMPERIAL-preserved*, testing exercise capacity in patients with an LVEF > 40%, empagliflozin did not improve the 6MWT distance.[222]

Responder analysis in subjects treated with empagliflozin for KCCQ displayed a consistently greater improvement for the empagliflozin group observations confirmed by larger studies with different SGLT2i.[2,278] and importantly with a greater effect size compared to sacubitril/valsartan.[276]

4.5.4 Changes in biomarkers

In the current study, no differences were seen in neuro-humoral markers for HF which is in keeping with results from larger trials testing SGLT2i.[1,2] In general, HFpEF patients tend to have lower levels of natriuretic peptides (NP) compared to HFrEF but more importantly the phenotypic heterogeneity in patients makes risk

stratification by observing natriuretic peptide levels more challenging. In a recent study it was revealed that even patients with normal NPs and only mild diastolic dysfunction have a substantially higher risk for poor outcomes.[279] Interestingly, sacubitril/valsartan in HFpEF reduced NPs, whereas SGLT2i do not. Paradoxically however, a reduction of NP with sacubitril/valsartan did not translate to reduced hospitalisation for HFpEF whereas SGLT2i treatment did.[1,254]

4.6 Limitations and future directions

Despite the high-quality methods and broad variety of assessments, this trial has certain possible limitations. Firstly, the number of patients lost to follow-up as a result of national lockdowns (n=13, 36.1 %) meant that the trial was underpowered for investigation of the effect size previously calculated. As a result, it is possible that other outcomes might have been affected by the lower number of patients, too.

The trial treatment was provided for 12 weeks and in a single dose (10 mg) only. While hospitalisation for HF curves in *EMPEROR-preserved*[1] separate early on, the effect on CV-death develops later thus, a longer treatment duration and/or higher dose of treatment might have provided different results.

We did not interrogate effects on inflammation as part of our assessments however, recent animal models suggest that an important mechanism of action is (at least partly) mediated by the influence on SGLT2i on the inflammasome and metabolism and inflammation are deeply linked in HFpEF.[280]

4.7 Conclusions

Only very recently it was established that empagliflozin treatment is beneficial for patients with HFpEF.[1] Contrary to HFrEF, little is known about the mechanisms of how treatment with these novel drugs translate their benefits on a molecular level. Thus, this is the first mechanistic imaging trial *in-vivo* examining effects of SGLT2i in patients with true HFpEF (i.e. LVEF ≥ 50%) *EMPA-VISION* provides evidence that a direct effect on energy metabolism via enhanced ketogenesis is unlikely to be the main contributor of beneficial effects in HF patients. Furthermore, the changes observed here where partly directly affecting the heart (improved systolic function expressed by longitudinal and circumferential strain) and partly indicative of effects in other organ systems (improved pulmonary function). This indicates that benefits are likely translated differently compared to HFrEF and also may differ between phenotypes in HFpEF (e.g. diabetic, obese, hypertensive etc.) and thus, merits further investigation. Another interesting aspect is the observation that the aforementioned effects are employed independently of significantly lowered NPs and thus, quite contrary to other novel treatments licensed for certain types of HFpEF (sacubitril/valsartan). Head-to-head imaging trials, although rarely seen in the HF-community, would be contributing to increased knowledge in this syndrome.

5 Very low energy diet as a novel treatment for HFpEF

5.1 Abstract

5.1.1 Background

Heart failure with preserved ejection fraction (HFpEF) is frequent in patients with obesity and both conditions are projected to increase in prevalence even further. Whether or not obesity worsens outcomes for patients with HFpEF or if it might confer some degree of protection ('obesity paradox') in advanced stages of the syndrome remains debated. Irrespectively, it has become clear that a specific obesity-related HFpEF phenotype exists. Intentional weight loss may improve symptoms, serum markers and imaging markers in patients with HFpEF and obesity. Hence, the present study sought to investigate if weight loss is an effective treatment for patients with HFpEF and obesity.

5.1.2 Methods

14 obese HFpEF patients (BMI 33.5 kg/m^2 ± 5; NYHA I-III) were enrolled and assessed before and after a very low energy diet (VLED; 800 calories per day) for 10 weeks and compared to 10 weight-matched, obese/diabetic controls (BMI 31.8±1.5 kg/m^2). 2 subjects had to be excluded due to HFpEF unrelated medical

problems that forced them to withdraw from the VLED. We evaluated cardiac function using cardiovascular magnetic resonance (CMR) imaging at rest and following 20 watts of physiological exercise. Furthermore, we assessed diastolic function using echocardiography and cardiac energetics (PCr/ATP) using ^{31}P-MRS at rest and under dobutamine stress (65% age-maximal HR). Fasting venous bloods were collected for serum analysis of N-terminal pro-brain natriuretic peptide (NT-proBNP).

5.1.3 Results

After 10 weeks of VLED, there was a highly significant reduction in body weight (BMI -2.7 kg/m^2 ± 0.38, $p<0.001$) paralleled by a significant decrease in NT-proBNP (-239 pg/mL ± 149, $p<0.05$) and improved HF symptoms (NYHA median pre II vs. I post). Echocardiography revealed a significantly lower left atrial volume (-29 mL ± 28, $p<0.05$) and a numerically improved diastolic function (lateral E/E' -0.68 ± 0.5, $p=0.08$). CMR demonstrated a significantly lower LV mass (-9 g ± 2.9, $p<0.05$) but no changes in PCr/ATP at rest (Δ0.015±0.1, p=ns) or during dobutamine stress (Δ0.087±0.06, p=ns). Except NT-proBNP, all parameters returned to comparative levels of obese/diabetic weight-matched patients without HFpEF.

5.1.4 Conclusions

In patients with obesity and HFpEF, intentional weight loss improves prognostic serum markers for HF, decreases symptom severity, reduces atrial size and LV mass, and improves diastolic function. These findings underscore the potential for weight loss as an effective treatment for obese HFpEF and the need to investigate this underutilised treatment in larger trials.

5.2 Introduction

HFpEF is a highly heterogenous syndrome for which the ongoing difficulties to find effective treatments represents one of the biggest unmet medical needs in present cardiology. Prevalence of HFpEF is increasing steadily and estimates are predicting a further rise of this complex syndrome in future.[281] Obesity is a risk factor for the development of diastolic dysfunction and eventually development to HFpEF. Presence of both obesity and HFpEF considerably worsens the individual's prognosis[282] however, little is known about the effects of weight management in HFpEF patients, and no large trials investigated this therapeutic tool for efficacy and impact on cardiac changes. Importantly, the majority of HFpEF patients presents with marked adiposity[283] and centres with HFpEF-specific clinics report a median BMI of 40kg/m^2 in their patients.[70] Despite the aforesaid conclusions, there is still great debate around findings that a certain degree of obesity might be beneficial in HFpEF and thus, confer some protection for patients. This observation, termed the 'obesity paradox', was evident in subgroup analyses of randomised trials where HFpEF patients' mortality gradually decreased with increasing BMI and every five-unit BMI increase led to a reduction of mortality risk by 10 %.[284,285] On the other hand, a meta-analysis of dedicated studies investigating weight loss in an obese population reported a significant effect on all-cause mortality.[286] Unfortunately, modern-day HFpEF trials usually exclude patients with a BMI of more than 35 kg/m^2 hence, benefits with novel agents might not be transferrable to this specific population.[1,254]

Comparing the relatively small volume to its unalloyed need for continuous energy supply, the heart can be described as the biggest consumer of energy. Limited

storage capacity in the cardiomyocyte is reflected by the fact that around 30 % of the intracellular space is reserved for mitochondria in which the process of oxidative phosphorylation delivers the much needed ATP.[9] The healthy heart is described as metabolically flexible as this feature is important in securing incessant replenishment of the ATP pool.[287] Interestingly, obesity has been shown to alter substrate selection in favour of an over-reliance on fatty acids (FA) which promotes lipotoxicity and inflammation.[13,85] Furthermore, the overall myocardial energy reserve is reduced.[288,289] These derangements become even more obvious under increased metabolic demand, such as physical activity, where the shuttle system designed to deliver ATP from the mitochondria to the myofibrils cannot exceed its capacity and thus creates an imbalance between supply and demand.[40] This may be one of the reasons for why impaired exercise capacity is one of the major hallmarks of HFpEF and obesity alike.

Following publication of the encouraging results of the *DiRECT* trial[290], which demonstrated that weight management in the primary care setting leads to remission of T2D, very low-energy diets have resurged as an attractive treatment approach for cardio-metabolic diseases. As substantial weight loss occurs over a limited period of time, they are used as models to improve mechanistic understanding of the underlying changes that occur in weight loss in the context of HFpEF. Thus, this study sought to investigate the physiological changes that occur in patients with clinically diagnosed HFpEF and weight loss under resting conditions as well as using physiological exercise.

5.3 Methods

This prospective, longitudinal study was conducted in a single centre (OCMR, University of Oxford, Oxford, UK). Eligible patients with a clinical diagnosis of HFpEF (n=14) and obesity (BMI ≥ 28.5 kg/m^2) were enrolled and counselled to begin a very low energy diet (VLED, 800 kcal per day) with a meal replacement program following baseline assessments (**Figure 5.1** for overview). Follow-up assessments were conducted succeeding 10 weeks of VLED and results were compared to a set of 10 BMI-matched obese but otherwise healthy controls.

Figure 5.1: Study Overview VLED-HFpEF

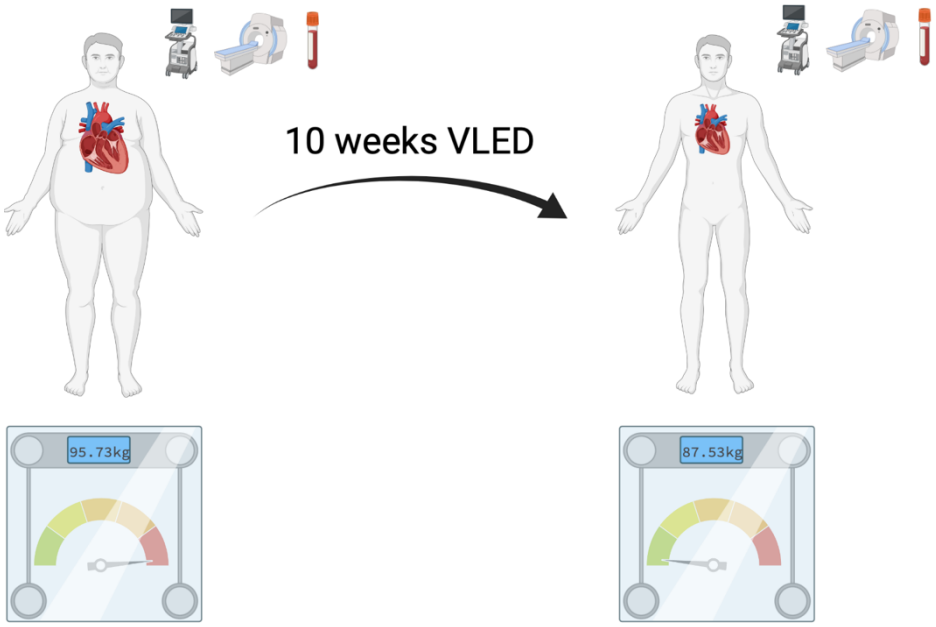

***Figure 5.1: Study Overview VLED-HFpEF**. Schematic overview of baseline and follow-up assessments of obese HFpEF patients after 10 weeks of a very low energy diet (VLED, 800kcal/day).*

The study was approved by the health research authority (IRAS ID 161729) and granted a favourable opinion by the local ethics council (South Central – Oxford B

15/SC/0004). All investigations were conducted in accordance with the Declaration of Helsinki and all participants provided written informed consent prior to any investigations.

Detailed methods are described in Chapter Two. A detailed list of in- and exclusion criteria is provided in **Table 5.1** below.

Table 5.1: Inclusion and Exclusion Criteria VLED-HFpEF

VLED in HFpEF	
Inclusion Criteria	• Participant is willing and able to give informed consent for participation in the study. • Male or Female, aged 18 – 85 years • HFpEF determined by clinical diagnosis and LVEF on echo ≥ 50 % • BMI ≥ 28.5 kg/m^2
Exclusion Criteria	• Contra-indications to MRI studies, such as metal implants, pacemakers, defibrillators • Claustrophobia (relative caution rather than total exclusion) • History or echocardiographic evidence of myocardial infarction • Significant valvular heart disease • NYHA class IV heart failure • Heart rhythm changes (other than well-controlled atrial fibrillation) • Inability or loss of ability to give informed consent • Contraindication to treatment with dobutamine, namely: • Left ventricular outflow tract obstruction • Uncontrolled hypertension • Hypersensitivity to any component of the drug • Previous reaction to dobutamine • A female who is pregnant, lactating or planning pregnancy during the course of the study. If there is any doubt, a pregnancy test will be offered, or the study deferred, or the patient will not be enrolled • Any other cause, including a significant disease or disorder which, in the opinion of the investigator, may either put the participant at risk because of participation in the study, or may influence the result of the study, or the participants ability to participate in the study

Table 5.1: In- and Exclusion Criteria VLED-HFpEF*. Detailed list of in- and exclusion criteria applying for patients enrolled in the VLED in HFpEF study. BMI=body mass index; HFpEF=heart failure with a preserved ejection fraction; LVEF=left ventricular ejection fraction; MRI=magnetic resonance imaging; NYHA=New York Heart Association; T2D=type 2 diabetes mellitus.*

5.3.1 Study population

In general, patients were considered eligible with a clinical diagnosis of HFpEF and elevated NT-proBNP (>125 pg/ml). Dose of diuretics needed to be stable for at least one week prior to enrolment. Patients with implanted devices, active ischaemia, uncontrolled hypertension or any contraindications for CMR scanning, were excluded (see **Table 5.1**).

5.3.2 Data acquisition

5.3.2.1 CMR

Cardiovascular magnetic resonance (CMR) imaging was also performed on a 3 Tesla MRI scanner (Magnetom Prisma, Siemens Healthineers, Erlangen, Germany) using a 32-channel phased array coil. Following standard planning, a retrospectively gated, highly accelerated, compressed sensing, free-breathing cine imaging sequence was used to acquire a short axis stack covering the entire heart, including both ventricles and atria, within 60 seconds.

Physiological exercise stress was then performed using a CMR-compatible stepping ergometer with the patient in supine position (Cardio Step, Ergospect GmbH, Innsbruck, Austria). The exercise protocol comprised a fixed workload of 20 W for 6 minutes. This threshold reflects the parameters commonly used for invasive hemodynamic studies in HFpEF.[291] Repeat whole-heart cine images were acquired during the final minute of the exercise period.

Figure 5.2:Study Investigations VLED-HFpEF

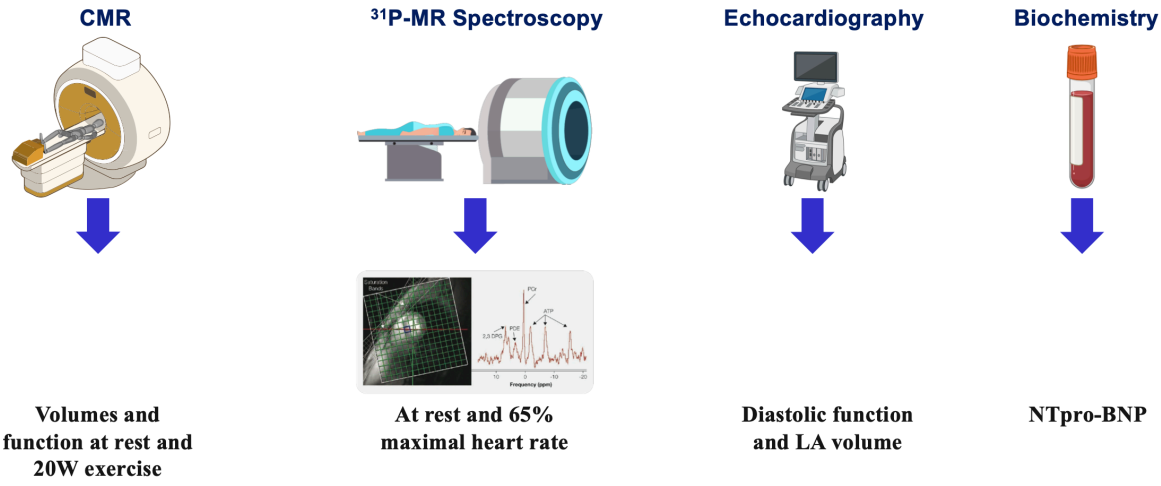

Figure 5.2: Study Investigation Overview VLED-HFpEF. *Overview of imaging methods used in this study at baseline and following 10-weeks of very low energy diet. ^{31}P-MRS=phosphorus MR spectroscopy; CMR=cardiovascular magnetic resonance; LA=left atrial; NT-proBNP=n-terminal pro brain natriuretic peptide.*

5.3.2.2 Dobutamine stress

Dobutamine was administered as a continuous intravenous infusion at incremental rates in order to achieve a significant haemodynamic effect. The infusion was commenced initially at 10 µg/kg/min but increased to a maximum of 40 µg/kg/min, depending on presence of a satisfactory haemodynamic response, which was defined as 65 % of the age maximum heart rate (HR; 220-age). This elevated HR was then maintained for the duration of the acquisition. HR and blood pressure (BP) were measured at baseline and at one-minute intervals during and after pharmacological stress until normalisation to pre-examination levels. Wherever feasible, stress cines were acquired in a mid-short axis slice as well as VLA and HLA. Due to logistical considerations, the stress-imaging was conducted as part of the ^{31}P-MRS acquisition (Magnetom TRIO, Siemens Healthineers, Erlangen,

Germany) and had to be acquired using a locally created GRE-sequence by means of the integrated scanner receiver coils which resulted in a lower image quality and more susceptibility to movement artefacts.

5.3.2.3 Magnetic resonance spectroscopy

^{31}P MRS was performed at rest on a 3 Tesla MRI scanner (Magnetom Trio, Siemens Healthineers, Erlangen, Germany). Participants were positioned prone over the centre of a 3-element dual-tuned ^{1}H/^{31}P surface coil in the isocentre of the MR system. A non-gated 3D acquisition-weighted ultra-short echo time (UTE) chemical shift imaging sequence was used with saturation bands placed over liver and skeletal muscle, as previously described.[134] All spectra were analysed using a semi-automated fitting of data from within OXSA toolbox,19 i.e. a MATLAB implementation of the AMARES fitting routine. The fitted PCr and ATP signals were corrected for partial saturation, using literature values[292], before calculating the PCr/ATP ratio as PCr/average ATP or PCr/gamma-ATP depending on spectral quality. The reported PCr/ATP was averaged over two basal septal voxels and corrected for blood signal contamination.[293] A detailed description is outlined in **Chapter Two** of this thesis.

5.3.2.4 Echocardiography

Echocardiography was performed on a GE Vivid I system (GE, Boston, USA) using a standardised protocol including parasternal long and short axis views as well as apical 2, 3, and 4-chamber views for chamber quantification. Colour Doppler assessments were performed to exclude significant valvular heart disease. Pulsed-wave Doppler assessment of mitral valve inflow was used to calculate E/A ratio.

Tissue Doppler velocities were measured at the medial and lateral mitral valve annulus to determine E/e' ratios. Continuous wave Doppler was used to assess tricuspid regurgitation velocity for estimation of systolic pulmonary artery pressure (sPAP).

5.2.3.5 Anthropometrics and biochemistry

Height and weight as well as blood pressure measurements were obtained. Fasting venous blood samples were collected at baseline and following 10 weeks of VLED to assess markers prognostic HF markers (NT-proBNP) as well as measures of insulin resistance and lipid metabolism (FFA).

5.3.3 Data analysis

5.3.3.1 CMR

Image analysis for cardiac indices was performed in an anonymised fashion offline in accordance with SCMR guidelines[125], using cmr42 post-processing software by an independent operator who was blinded to patient treatment status (see **Chapter 2.5** for details). Spectroscopic analysis for ^{31}P-MRS was performed as described in **Chapters 2.5.1** and **2.5.3** of this thesis, respectively.

5.3.3.2 Echocardiography

Analysis of TTE images was conducted on an ISCV workstation as outlined before (see **Chapter 2.6**).

5.3.3.3 Biomarker analysis

Biomarkers were analysed domestically by the Oxford University Hospital NHS Foundation Trust Hospital's clinical biochemistry laboratory according to local standard protocols.

5.3.4 Statistical analysis

Statistical analyses were performed using commercial software (SPSS 24, Chicago and GraphPad Prism 9, San Diego). All data is presented as median (IQR) unless stated otherwise. Determination of statistical significance was assessed by Wilcoxon signed-rank test. Values of $p<0.05$ were considered as statistically significant.

5.4 Results

5.4.1 Study population

Baseline characteristics are presented in **Table 5.2**.

Patient recruitment took place from September 2021 until December 2021.

All controls completed the CMR protocol without complications. Two participants in the HFpEF-VLED group had to be excluded due to incompliance with the VLED. However, this incompliance occurred due to external factors unrelated to their underlying HF diagnosis or any possible VLED side effects. The two cohorts were well balanced but the obese/diabetic controls tended to be younger (63; 59, 71) compared to obese HFpEF (69; 58, 76). As expected, there were significant differences at baseline regarding markers of cardiac function and baseline metabolic status as well as natriuretic peptides (see **Table 5.2**).

Table 5.2: Baseline Patient Characteristics VLED-HFpEF

Characteristic	**Controls n=10**	**HFpEF n=14**	**p-value**
Age (years)	63 [59, 71]	69 [58, 76]	<0.001
Male (%)	8 (80)	8 (57)	0.32
BMI (kg/m^2)	32 [30, 33]	31 [29, 38]	0.38
SBP (mmHg)	138 [125, 156]	148 [123, 158]	0.51
DBP (mmHg)	79 [75, 83]	80 [72, 88]	0.71
Resting HR (bpm)	66 [64, 78]	70 [65, 86]	0.002
Exercise HR (bpm)	96 [83, 106]	96 [84, 118]	0.49
Statin	1 (10%)	8 (57%)	
ACEi/ARB	-	9 (64%)	
Beta blocker	-	9 (64%)	
CCB	1 (10%)	3 (21%)	
MRA	-	3 (21%)	
Diuretic	1 (10%)	9 (64%)	
Aspirin	-	3 (21%)	
Anticoagulant	-	7 (50%)	
Oral hypoglycemic	-	2 (14%)	
Tafamidis	-	-	
HFA-PEFF score	2 [0, 2]	5 [4, 6]	<0.001
Atrial fibrillation	0 (0%)	7 (50%)	0.03
NYHA class:			
I	8	2	
II	1	11	
III	0	1	
IV	0	0	
HbA1c (mmol/l)	7.2 [6.9, 7.7]	5.1 [4.7, 5.6]	0.96
NT-proBNP (pg/ml)	38 [24, 80]	724 [245, 1606]	<0.001
E/e' ratio	6.1 [5.3, 9.2]	8.2 [7.2, 9.7]	<0.001
sPAP (mmHg)	9.3 [8.6, 25.3]	14.6 [12.2, 35.4]	<0.001
PCr/ATP ratio	1.93 [1.62, 2.24]	1.66 [1.39, 1.86]	<0.001

Table 5.2: Participants' baseline characteristics. *Continuous variables shown are median [interquartile range]. Categorical variables are n (%). BMI indicates body mass index; SBP, systolic blood pressure; DBP, diastolic blood pressure; ACEi, angiotensin converting enzyme inhibitor; ARB, angiotensin receptor blocker; CCB, calcium channel blocker; MRA, mineralocorticoid receptor antagonist; NYHA, New York Heart Association; HbA1c, glycated hemoglobin; NT-proBNP, N-terminal pro-brain natriuretic peptide; sPAP, systolic pulmonary artery pressure; PCr, phosphocreatine; and ATP, adenosine triphosphate. p values reported are the result of Wilcoxon-ranked t-tests.*

Within group parameters of controls showed an expected adaptation to exercise leading to augmentation of LVSV (p=0.004), RVSV (p=0.008), LVEF (p<0.001) and RVEF (p=0.004). Conversely, in the HFpEF cohort, despite some degree of adaptation to exercise, the overall response was considerably blunted.

Table 5.3: Baseline CMR Characteristics at Rest and 20w Exercise VLED-HFpEF

	Controls (n=10)			**HFpEF (n=14)**			**p†**	
	Rest	**20 W**	**p***	**Rest**	**20 W**	**p***	**Rest**	**20 W**
LVEDV (ml)	157 [119, 165]	162 [124, 191]	0.01	167 [112, 241]	177 [110, 255]	0.046	0.49	0.92
LVESV (ml)	51 [47, 54]	39 [34, 60]	0.12	64 [41, 106]	73 [39, 100]	0.95	0.11	0.003
LVSV (ml)	97 [73, 105]	111 [86, 140]	0.004	100 [71, 138]	109 [72, 143]	0.06	0.18	0.03
LVEF (%)	66 [61, 70]	73 [69, 76]	<0.001	61 [53, 69]	63 [52, 71]	0.38	0.002	<0.001
LV mass (g)	113 [81, 129]			129 [94, 190]			<0.001	
LVMi (g/m^2)	57 [49, 64]			59 [47, 87]			<0.001	
RVEDV (ml)	170 [118, 189]	183 [112, 189]	0.11	150 [107, 209]	177 [105, 227]	0.01	0.66	0.81
RVESV (ml)	61 [37, 90]	58 [31, 75]	0.02	58 [41, 86]	57 [43, 91]	0.50	0.95	0.32
RVSV (ml)	99 [74, 101]	111 [82, 134]	0.008	86 [68, 120]	101 [70, 137]	0.006	0.22	0.10
RVEF (%)	59 [53, 68]	69 [62, 71]	0.004	60 [54, 66]	65 [55, 70]	0.04	0.40	0.006

Table 5.3: Cardiac and pulmonary indices on cardiovascular magnetic resonance imaging at rest and during 20 W exercise stress at baseline. *Continuous variables shown are median [interquartile range]. LVEDV indicates left ventricular end-diastolic volume; LVESV, left ventricular end-systolic volume; LVSV, left ventricular stroke volume; LVEF, left ventricular ejection fraction; EDV/s, end-diastolic volume per second; RVEDV, right ventricular end-diastolic volume; RVESV, right ventricular end-systolic volume; RVSV, right ventricular stroke volume; RVEF, right ventricular ejection fraction; p values*

*reported are results from Wilcoxon signed-rank test (*p = rest vs 20 W within groups and $p^{\dagger}$ = between groups)*

5.4.2 Changes in anthropometrics and biomarkers

In HFpEF patients successfully completed 10-weeks of VLED there was a significant weight loss (median -7.1 kg, p=0.0005) which was mirrored in BMI and BSA. Systolic and diastolic blood pressure remained unchanged (**Figure 5.2**)

Figure 5.3: Changes in Biomarkers and Anthropometrics VLED-HFpEF

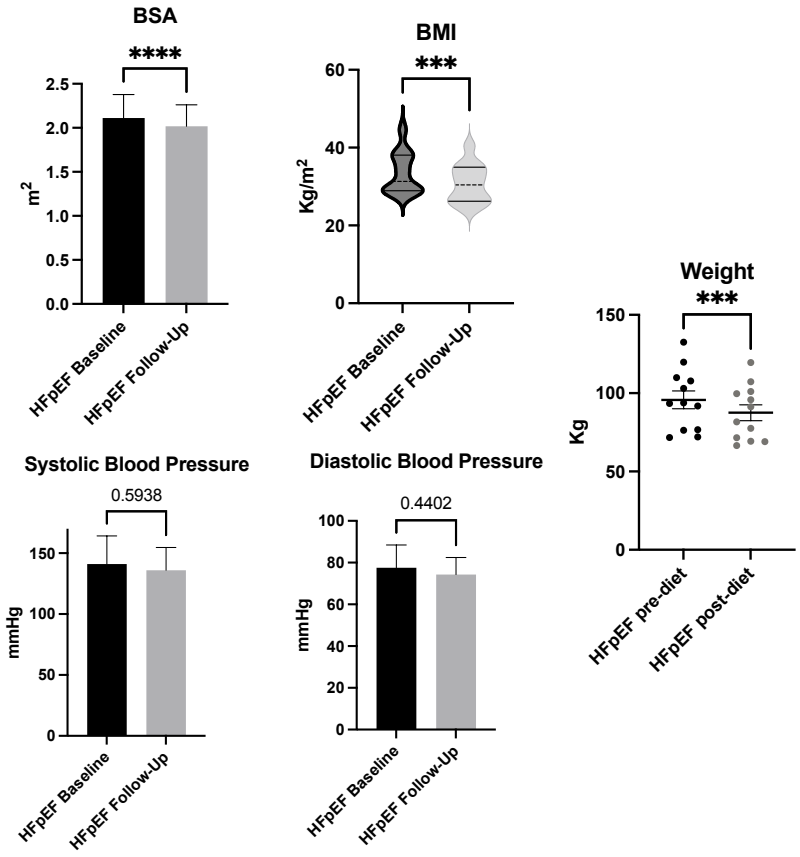

***Figure 5.3**: **Anthropometric and Biomarker Changes VLED-HFpEF**. 10 weeks of VLED in patients with HFpEF led to significant weight loss, BMI and BSA whilst no changes in blood pressure were documented.*

Interestingly, the VLED led to a marked decrease in NT-proBNP (median -268.4, p = <0.05) which was also mirrored by a decrease symptom burden (NYHA class median pre II vs. post I).

Figure 5.4: Changes in NT-proBNP and NYHA VLED-HFpEF

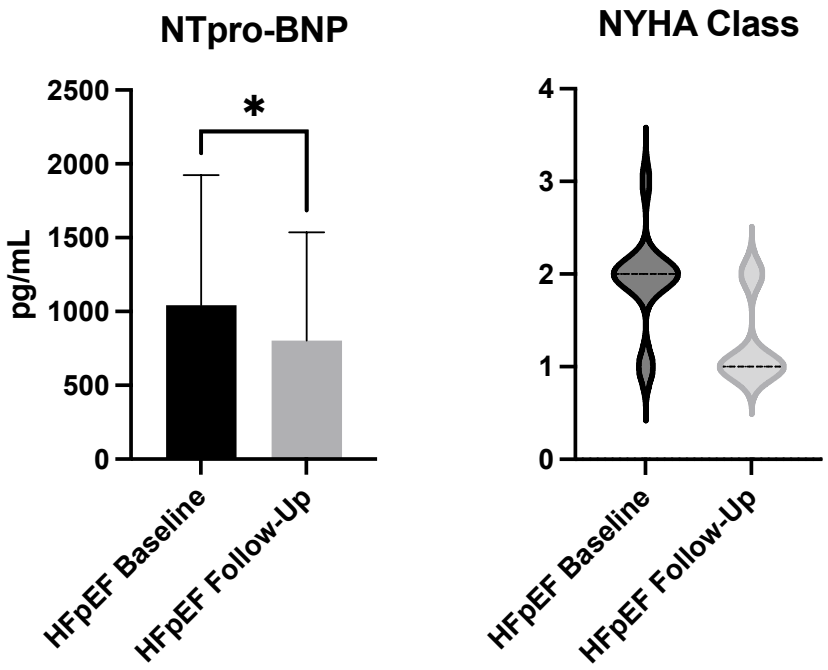

Figure 5.4: Changes in NT-proBNP and NYHA in VLED-HFpEF.

Other biomarkers of glucose tolerance decreased numerically greater following VLED while only insulin levels 60 minutes post OGTT were lowered significantly (**Figure 5.4**).

Figure 5.5: Glucose and Insulin Changes VLED-HFpEF

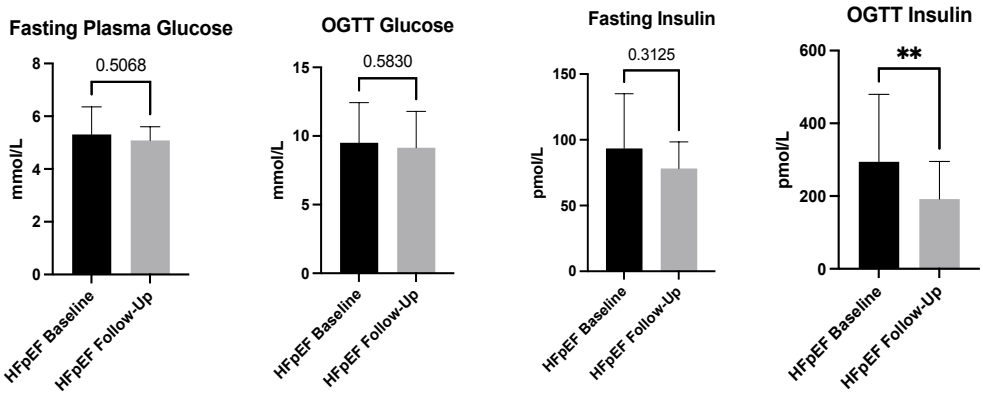

Figure 5.5: Changes in Fasting and post OGTT Glucose and Insulin in VLED-HFpEF.

5.4.3 Changes in cardiac energetics following VLED

Following 10 weeks of VLED, there was no significant difference in resting myocardial energetics (median pre VLED 1.65; 1.39, 1.86 vs. post VLED 1.64; 1.36, 2.33). Similarly, no difference on myocardial energy reserve during dobutamine stress was recorded (median pre VLED 1.57; 1.36, 2.0 vs post VLED 1.6; 1.26, 1.96). These results remained consistent when calculating the difference of PCr/ATP at rest and during stress and comparing the change (Δ PCr/ATP).

Figure 5.6: Rest and Stress Energetics VLED-HFpEF

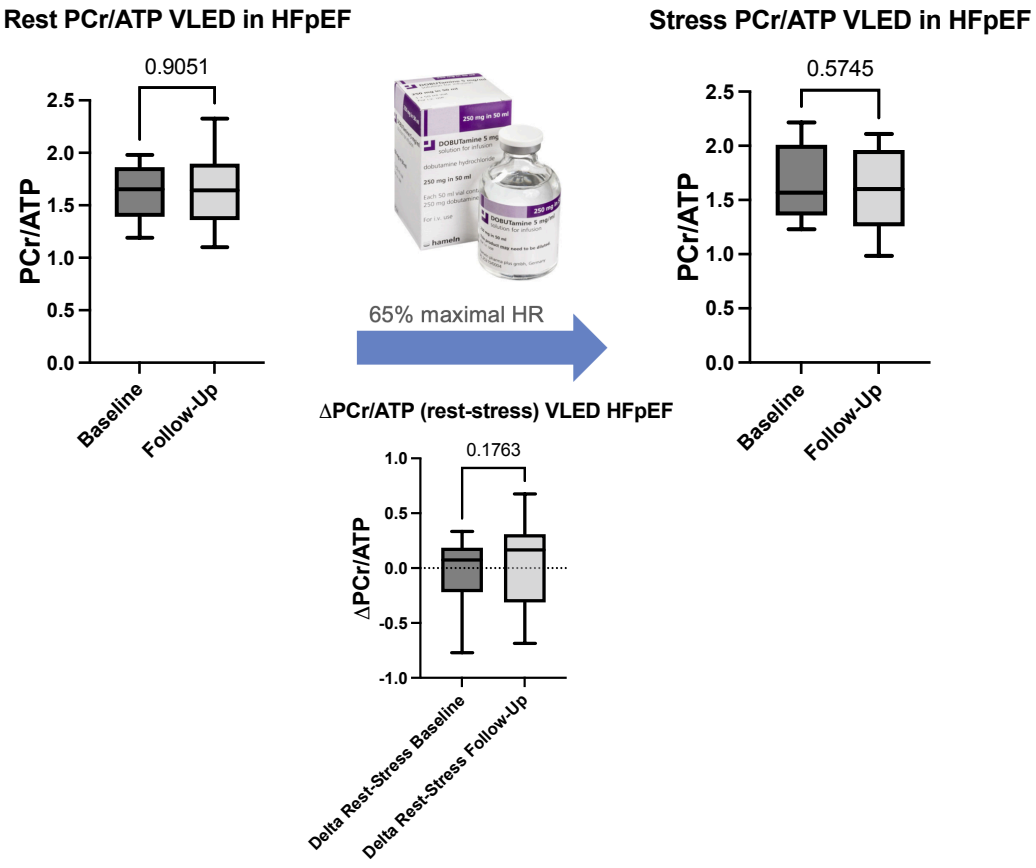

Figure 5.6 Myocardial Energetics Rest and Stress VLED HFpEF. *Boxplots with median whiskers of baseline (pre-VLED) and post-VLED myocardial energetics at rest (upper left) during dobutamine stress (upper right) and the change of the Δ (rest-stress; middle second row). HR=heart rate*

5.4.4 Cardiac structure and function

Cardiac structure and function were assessed using echocardiography (TTE) and CMR. The dietary intervention in this study did not lead to notable changes in diastolic function on TTE. However, lateral E/E', mitral valve deceleration time and early diastolic filling improved post-VLED without reaching nominal statistical significance.

Figure 5.7: Diastolic Function VLED-HFpEF

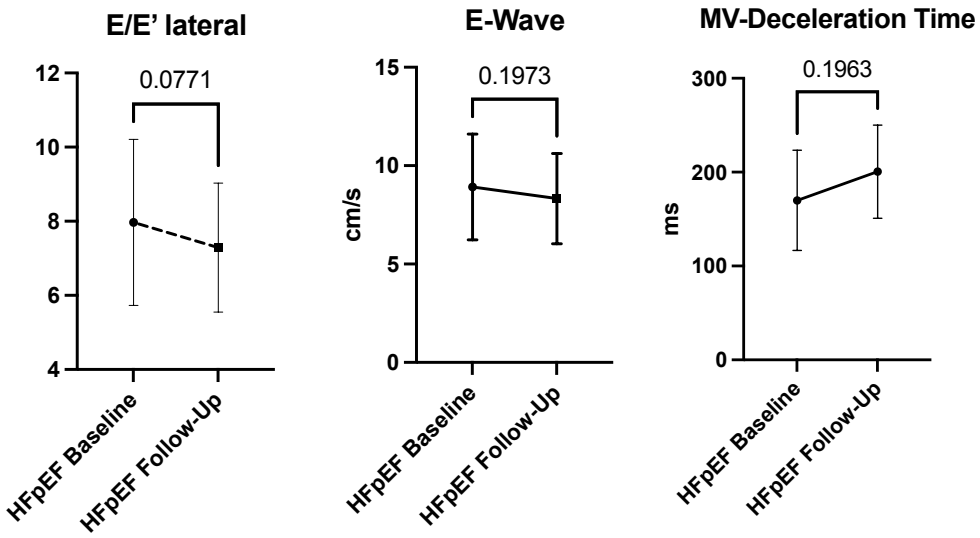

Figure 5.7: Diastolic Function TTE in VLED-HFpEF.

Equally, on TTE Left atrial (LA) biplane volume and LA-volume indexed to BSA (LAVI) were both numerically lowered by 10 weeks of VLED.

Figure 5.8: LA-Volumes VLED-HFpEF

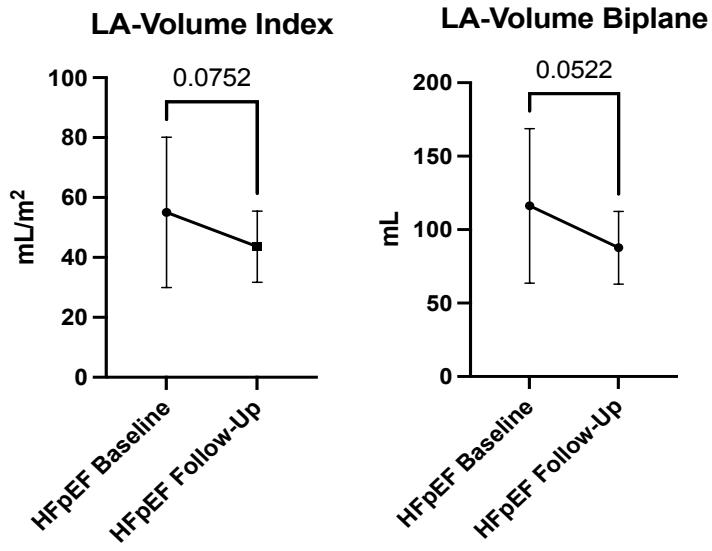

Figure 5.8: Left atrial volumes on TTE in VLED-HFpEF.

Regarding resting CMR results, LV-mass (median pre-VLED 115 g; 78.25, 198 vs. post 105 g; 77, 173; p=0.06), indexed RVEDV (median pre-VLED 134 ml/m^2;111, 219 vs/ post 84 ml/m^2; 63, 99; p = <0.001), RVEF (median pre-VLED 53 %; 50, 60 vs. post 60 %; 56, 65; p=0.0957) and RVSV (median pre-VLED 77 ml; 60, 119 vs. 71, 119; p=0.08) displayed the greatest changes. During 20 W of physiological exercise using a CMR-compatible ergometer, patients post-VLED further improved their RV-function with a markedly improved RVEDVi (median pre-VLED 74ml/m^2; 55, 95 vs. post 89 ml/m^2; 64, 112; p=0.004). higher RVEF (p=0.04) as well as RVSVi (p=0.02). Of note LVSVi also improved during exercise (p=0.05).

Table 5.4: Resting and 20W-Exercise Changes VLED-HFpEF

	Resting CMR (n=12)			**20W Exercise Stress CMR (n=12)**		
	Pre-VLED	**Post-VLED**	**p***	**Pre-VLED**	**Post-VLED**	**p***
LVEDV (ml)	167 [112, 241]	157 [102, 212]	0.05	166 [103, 216]	164 [106, 214]	0.43
LVEDVi (ml/m^2)	69 [53, 94]	73 [54, 102]	0.005	77 [54, 92]	74 [54, 101]	0.09
LVESV (ml)	64 [41, 106]	52 [31, 88]	0.52	52 [33, 87]	51 [32, 79]	0.046
LVSV (ml)	100 [71, 138]	106 [70, 124]	0.38	99 [68, 124]	107 [68, 125]	0.48
LVSVi (ml/m^2)	46 [35, 55]	49 [41, 59]	0.05	47 [37, 55]	50 [35, 62]	0.05
LVEF (%)	61 [53, 69]	66 [58, 70]	0.45	63 [58, 69]	67 [62, 70]	0.11
LV mass (g)	129 [94, 190]	115 [78, 220]	0.06	-	-	
LVMi (g/m^2)	59 [47, 87]	57 [40, 75]	0.42	-	-	
RVEDV (ml)	134 [107, 209]	162 [110,210]	0.33	159 [110, 212]	163 [133, 234]	0.21
RVEDVi (ml/m^2)	134 [111, 219]	84 [63, 99]	0.0005	74 [55, 95]	89 [64, 112]	0.004
RVESV (ml)	63 [49, 99]	67 [40, 91]	0.48	66 [53, 102]	70 [51, 101]	0.97
RVSV (ml)	77 [60, 119]	96 [71, 119]	0.08	84 [56, 127]	102 [74, 130]	0.06
RVSVi (ml/m^2)	39 [28, 50]	48 [38, 55]	0.04	39 [29, 54]	52 [39, 62]	0.02
RVEF (%)	53 [50, 60]	60 [56, 65]	0.0957	55 [51, 59]	58 [54, 66]	0.04

Table 5.4: Resting and 20W Exercise CMR Changes VLED HFpEF. *LVEDV=left ventricular end-diastolic volume; LVEF=left ventricular ejection fraction; LVESV=left ventricular end-systolic volume; LVSV=left ventricular stroke volume; RVEDV= right ventricular end-diastolic volume; RVEF=right ventricular ejection fraction; RVESV= right ventricular end-systolic volume; RVSV=right ventricular stroke volume*

5.5 Discussion

No recommendations are provided by either the European Society of Cardiology (ESC) nor the US equivalent (American Heart Association, AHA) concerning weight management strategies in obese patients with HF.[120,121] Instead, this topic is

frequently highlighted within the gaps of evidence in need of being addressed by outcome studies. Despite the existing 'obesity paradox', which is likely more attributable to HFrEF than HFpEF patients[294], an increasing number of studies reports a dedicated obesity phenotype within the spectrum of HFpEF. Hence, this prospective, longitudinal single-centre study sought to investigate patients with HFpEF and concomitant obesity before and after a VLED for 10 weeks. Detailed CMR assessments to elicit cardiac changes induced by this lifestyle intervention were augmented by biomarker analyses.

It was demonstrated that a VLED in HFpEF patients is safe and effective, resulting in substantial weight loss, enhanced insulin response and right ventricular adaptation to exercise. More importantly, prognostically relevant neuro-humoral biomarkers (NT-proBNP) and symptom burden improved substantively. Furthermore, there were numerical corrections in echocardiographic parameters of diastolic function which were near-significant. No change in resting or dobutamine stress PCr/ATP was observed.

5.5.1 Changes in anthropometrics and biomarkers

In keeping with other studies investigating dietary and pharmacological weight loss interventions in this patient cohort[117], it was confirmed that 10 weeks of VLED lead to significant weight loss (**Chapter 5.4.2**). Furthermore, and in contrast to the aforementioned studies, 10 weeks of VLED significantly lower NT-proBNP levels ($p<0.05$) and symptom burden (NYHA class) in HFpEF. This is in contrast to a RCT examining diet and exercise interventions where BNP did not reduce despite a similar mean weight loss of -7 kg in the diet group.[117] Data on natriuretic peptide

levels and their correlation to clinical outcomes is rare however, it was recently reported that weight gain leads to increased levels of NT-proBNP and this is significantly associated to cardiac decompensation.[295]

In advanced stages, HF promotes and aggravates insulin resistance and this phenomenon is equally present in patients with HFrEF and HFpEF.[296] Patients in the present study displayed improved peripheral surrogates of glucose metabolism but also significantly blunted insulin response following an OGTT with 75 g of glucose. In a cohort of non-HFpEF obese patients, weight loss decreased insulin secretion by a third although insulin sensitivity did not change.[297] Importantly, the patients had no insulin resistance at the start of the study and thus, it is unknown if insulin sensitivity might be enhanced in patients with HFpEF. The present results are encouraging and thought-provoking to investigate this in a dedicated study.

5.5.2 Changes in myocardial energetics

No data is available on the topic of effects of weight management on energy metabolism in patients with HFpEF and obesity. Thus, the present observation that PCr/ATP did not change after 10 weeks of VLED, neither at rest nor during dobutamine stress is challenging to put into context. Nevertheless, a study investigating VLED in an obese, non-HFpEF cohort recently demonstrated that myocardial function only recovered to some extent after 8-weeks [298] whereas cardiac energetics were demonstrated to be improved following 1 year of weight loss.[299] While the amount of weight loss in the aforementioned study (-8 kg) was comparable to the current study in HFpEF patients (-7 kg) these results emphasise that reversing metabolic alterations might take significantly longer than affecting

cardiac structure and function. This hypothesis is in agreement with trials of metabolic modulators (FAO inhibitor etoxomir) in cohorts of patients with hypetrophic cardiomyopathy (HCM; i.e. preserved EF and myocardial hypertrophy similar to HFpEF), where metabolic changes were only quantifiable following almost 5 months of treatment.[108]

5.5.3 Changes in cardiac structure and function

The contemporary study revealed dietary-induced changes with RV-volume adaptation to exercise being the most prominent results. It is well known that obesity in the first place and transition to overt HFpEF leads to significantly elevated pulmonary pressures which, specifically during exercise, aggravates right ventricular dysfunction.[300,301] Markedly improved RVSVi, -EDVi and -EF during exercise mirror the overall haemodynamic improvements achieved by substantial weight loss. RV-dysfunction and adverse changes in the pulmonary vasculature are predictors of worse outcomes in patients with HFpEF[302] thus, the effect of the changes presented here should be investigated in a larger outcome trial.

5.6 Conclusions

Patients with obesity and HFpEF display marked improvements of prognostic serum markers of HF, symptom burden and exercise-related RV-dysfunction. The changes presented here should be hypothesis-generating for larger trials investigating weight management as a therapeutic intervention in patients with HFpEF and likewise are evidence that the so-called ‘obesity paradox’ may not equally apply to the distinct phenotype of severely obese HFpEF patients.

6 *Investigation of Ninerafaxstat as Novel Treatment for Diabetic Cardiomyopathy*

6.1 Abstract

6.1.1 Background

T2D is a significant contributor for the development of HF and despite causing macro- and microvascular complications, also has a direct detrimental effect on the heart. The T2D heart is over-reliant on fatty acid metabolism, shows reduced glucose oxidation rates and increased inhibition of pyruvate dehydrogenase (PDH). This results in blunted ATP generation, myocardial steatosis and progressive diastolic dysfunction. We aimed to assess the effects of ninerafaxstat, a novel cardiac mitotrope designed to restore metabolic flexibility, on cardiac metabolism & function in obese T2D.

6.1.2 Methods

In this open-label, mechanistic phase 2a trial, 21 patients with T2D & obesity (HbA1c 7.0 % (6.6,7.8), 97 kg (90,102)) received 200mg ninerafaxstat twice daily for 4 or 8 weeks. Cardiac metabolism and function were assessed pre- & post-

treatment using magnetic resonance imaging (MRI), ^{31}P-, ^{1}H- magnetic resonance spectroscopy (MRS) in all patients, as well as hyperpolarized [1-^{13}C]pyruvate MRS in a subset (n=9).

6.1.3 Results

In keeping with previously published literature, T2D patients at baseline presented with reduced PCr/ATP (1.6; 1.4, 2.1), myocardial steatosis (myocardial triglycerides 2.2 %; 1.5, 3.2) and diastolic dysfunction (peak diastolic strain rate 0.86 1/s; 0.82, 1.06). Ninerafaxstat significantly improved myocardial energetics (PCr/ATP median by 32 %, $p<0.01$), reduced myocardial triglyceride content (by 34 %, $p=0.03$) and improved diastolic function (peak diastolic strain rate by 10 %, peak LV filling rate by 11 %, both $p<0.05$). PDH flux was increased in 7/9 subjects (mean 45 %, $p=0.08$). Left ventricular volumes and mass, heart rate and blood pressure were unchanged.

6.1.4 Conclusions

Treatment with ninerafaxstat significantly improved myocardial energetics, measures of steatosis and diastolic filling in patients with T2D and diabetic cardiomyopathy.

6.2 Introduction

The presence of T2D substantially increases the risk for development of HF and both HFrEF and HFpEF are worsened by concomitant T2D.[303] Even before clinically overt HF, adverse metabolic remodelling, structural alterations and development of diastolic dysfunction lead to potentially reversible changes summarised under the term 'Diabetic Cardiomyopathy' (DbCM).[87,89,304] With the rapid global increase in the prevalence of T2D, occurrence of DbCM is projected to further expand.[305] As a result, there is a substantial unmet medical need to develop novel therapeutics treating DbCM and possibly preventing progression to overt HF.[89]

The heart's exaction for continuous energy supply is unmitigated as it has the highest energy demands (measured as adenosine triphosphate (ATP) per gram of tissue) of any organ with a complete turnover of its ATP pool every ~10 seconds.[9,44] The amount of energy required to support contractile function (including active relaxation, i.e. diastolic function), basal metabolic processes, and ionic homeostasis are derived almost entirely from mitochondrial oxidative phosphorylation.[44] Given this vast demand for ATP to maintain cardiac function, it is unsurprising that there are functional consequences if ATP metabolism is deranged; and the diabetic heart is characterized by altered metabolism.[306,307]

Under physiological conditions, the heart is metabolically flexible with respect to substrate utilisation, including use of free fatty acids (FFA), glucose, ketone bodies, lactate, and several amino acids, to generate ATP.[16,89] Although T2D is characterised by both increased circulating FFA and glucose, the diabetic

myocardium heavily relies on FFA for the generation of ATP, and its metabolic flexibility to use other substrates is considerably compromised.[87] This arises due to the combination of reduced glucose uptake[89] (secondary to insulin resistance) and increased fatty acid oxidation (FAO)[305], which itself mediates an inhibition of pyruvate dehydrogenase (PDH).[9] This over-reliance on FFA in T2D results not only in a reduced efficiency of mitochondrial oxidative phosphorylation, but also increases lipotoxicity which in turn promotes inflammation and cardiac dysfunction.[308] Chronic exposure to high levels of FFA can cause excessive accumulation of substrates for non-oxidative processes, including triacylglycerol, diacylglycerol, and ceramide synthesis, which can lead to myocyte hypertrophy, dysfunction and apoptosis.[309] Consequently, the human diabetic heart is characterised by reduced PDH flux[140], impaired myocardial energetics[241], cardiac steatosis[310], left ventricular (LV) hypertrophy, and LV diastolic and/or systolic dysfunction.[311]

By partially inhibiting FAO, drugs such as trimetazidine (TMZ) aim to expand glucose oxidation by increasing PDH flux which has been shown to improve cardiac energetics and function in dilated cardiomyopathy[112]. However, despite the increased oxygen efficiency of ATP from glucose oxidation, its restricted cellular uptake due to insulin resistance[59,312], reduces the ability to recouple glucose uptake and oxidation.

Ninerafaxstat, is a novel cardiac mitotrope designed for the treatment of cardiovascular disorders characterised by abnormal cardiac energetics and/or altered cardiac metabolism. Ninerafaxstat is a structural analogue of Trimetazidine (TMZ) which undergoes rapid hydrolysis during enteral absorption and liberates

IMB-1028814 (the active moiety) and nicotinic acid in plasma. IMB-1028814 is a partial FAO inhibitor increasing glucose utilisation in myocardial tissue and is subsequently metabolised to TMZ. In addition, as nicotinic acid causes a fall in peripheral FFA levels, and increase myocardial glucose uptake (level comparable to insulin-glucose clamp[313]) this may further enhance glucose oxidation via PDH.

In order to assess the effectiveness of ninerafaxstat in DbCM, this phase 2a trial used cardiovascular magnetic resonance (CMR) to assess the hallmarks of DbCM, namely LV hypertrophy (MRI), cardiac energetics by phosphorus magnetic resonance spectroscopy (^{31}P-MRS), myocardial steatosis via proton MRS (^{1}H-MRS), PDH flux with hyperpolarized [1-^{13}C]pyruvate MRS and diastolic dysfunction with magnetic resonance imaging (MRI) and echocardiography (TTE).

6.3 Methods

IMPROVE-DiCE was a single-centre, open-label, mechanistic phase 2a, pharmacodynamic study designed to assess the effects of 200mg ninerafaxstat twice a day (BID) on myocardial energetics, metabolism, and function in patients with T2D. The trial was registered EudraCT Number: 2020-003280-26, ClinicalTrials.gov: NCT04826159 and sponsored by Imbria Pharmaceuticals, Inc. Ethical approvals for the study were granted by the Medicines and Healthcare Products Regulatory Agency (MHRA) and National Research Ethics Service (Research Ethics Committee ref 20/LO/1120). The trial was conducted according to the principles of the Declaration of Helsinki and the EU Clinical Trial Directive. All participants provided written informed consent before any investigations took place.

6.3.1 Study Visit Schedule

After testing the subject's eligibility in a screening visit, those eligible were invited to attend a baseline visit within 14 days. Following their baseline assessments, patients were asked to take the first dose of trial treatment and then invited for their EOT visits following 4 (n=5) or 8 weeks of treatment (n=16) for repeated assessments. Seven days after their individual EOT, patients were re-invited for safety assessments and their respective EOS. The general study schedule is depicted in **Figure 6.1**.

Figure 6.1: Study Structure IMPROVE-DiCE

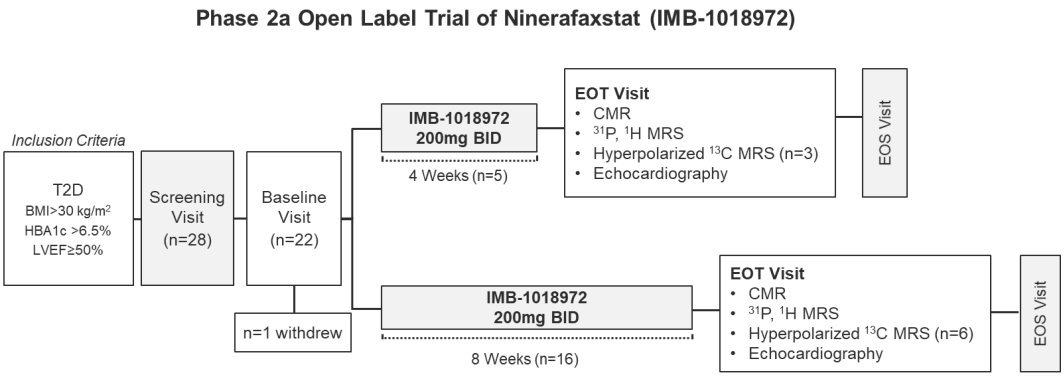

Figure 6.1: Study Structure Overview IMPROVE-DiCE. *A schematic overview of the study design and visit schedule. ^{1}H-MRS = proton magnetic resonance spectroscopy, ^{31}P-MRS = phosphorus magnetic resonance spectroscopy, BID = twice daily, BMI = Body Mass Index, CMR = cardiovascular magnetic resonance, EOS = end of study, EOT = end of treatment, LVEF = left ventricular ejection fraction, T2D = type 2 diabetes.*

6.3.2 Study population

The target population for this study were patients age ≥18 but ≤75 years with T2D (HbA1c ≥ 6.5 %), a body mass index (BMI) ≥ 30 and ≤ 40 kg/m^2 and preserved left ventricular ejection fraction (LVEF) of ≥ 50 %. Patients were excluded if they were on insulin and/or sodium glucose co-transporter 2 inhibitors (SGLT2i) therapy, had

more than moderate renal impairment (creatinine clearance < 60 mL/min/1.73m^2 of BSA), severe HF (NYHA III or IV) or any changes in their antidiabetic therapy in the last 3 months. A detailed list of in- and exclusion criteria can be found in **Table 6.1.**

Table 6.1: In- and Exclusion Criteria IMPROVE-DiCE

IMPROVE-DiCE (NCT04826159)	
Inclusion Criteria	• Provision of written informed consent before any screening procedures; • Male or female aged ≥ 18 and ≤ 75 years at screening; • Must agree to adequate contraception requirements as follows: a. WOCBP must have a negative serum pregnancy test at screening and a negative pregnancy test (serum or urine) on the day of baseline pre-dose and at the end of study (EOS)/safety follow-up visit or early termination; b. WOCBP must agree to use dual methods of contraception, including 1 highly effective and 1 effective method of contraception, from the day of first dosing until 3 months after the last administration of test product; and c. Male patients must use an effective barrier method of contraception if sexually active with a WOCBP, from the day of first dosing until 3 months after the last administration of test product; • Must agree not to donate sperm or ova from the day of first dosing until 3 months after last dosing; • Women not of childbearing potential must be either surgically sterile (hysterectomy, bilateral tubal ligation, salpingectomy, and/or bilateral oophorectomy at least 26 weeks before screening) or postmenopausal, defined as spontaneous amenorrhea for at least 2 years with follicle-stimulating hormone (FSH) in the postmenopausal range at screening; • Must be able and willing to comply with all study procedures and requirements; • Diagnosis of T2D; • Elevated HbA1c defined as ≥ 6.5 % (≥ 48 mmol/mol); • Elevated BMI defined as ≥ 30 kg/m^2; • Preserved LVEF (defined as ≥ 50 %); and • If on oral hypoglycaemic (anti-diabetic) therapy, no change in therapy over the past 3 months.

IMPROVE-DiCE (NCT04826159)	
Exclusion Criteria	• BMI > 40 kg/m^2; • Uncontrolled hypertension (defined as resting blood pressure >180/90 mmHg) at screening; • Standard contraindication(s) to magnetic resonance scanning; • More than mild to moderate valvular heart disease per Investigator's judgement; • Persistent or permanent atrial fibrillation; • History of sustained ventricular tachycardia or cardiac arrest; • Exertional angina or intermittent claudication; • Known significant obstructive coronary artery disease per Investigator's judgement;

	• Absolute or significant contraindication to dobutamine infusion, including: pheochromocytoma, LV outflow tract obstruction, untreated hyperthyroidism, severe hypotension, aortic dissection, or large aneurysm; • History of stroke, transient ischaemic attack, acute coronary syndrome, myocardial infarction, peripheral vascular disease, diagnosis of NYHA functional class III or IV heart failure, hospitalization for heart failure, or any arterial revascularisation procedure (including coronary artery bypass grafting) within 6 months before screening; • Presence of indwelling cardiac device (pacemaker, cardiac resynchronisation therapy, and/or implantable cardioverter defibrillator); • Significant hepatic impairment defined as total bilirubin and/or alanine aminotransferase and/or aspartate aminotransferase >2 × upper limit of the normal; • Moderate or severe renal impairment defined as estimated glomerular filtration rate <60 mL/min/1.73 m2 of body surface area; • History of Parkinson disease, Parkinsonian symptoms, restless leg syndrome, or other related movement disorders; • Known allergy, intolerance, or absolute contraindication to TMZ or nicotinic acid; • Concomitant use within the last 1 month of TMZ, nicotinic acid (at prescription/therapeutic dose), perhexiline, meldonium, or ranolazine; • Any use of insulin and/or SGLT2 inhibitors; • History of alcohol abuse or drug addiction within the previous 5 years; • Pregnant, or planning pregnancy or lactation; • Participation in another clinical study involving a test product or medical device within 28 days (or 5 half-lives of the test product, whichever is longer), prior to first dosing; • Any medical or surgical condition that may interfere with the patient's participation in the clinical study, significantly interfere with the interpretation of the results, or put the patient at significant risk, according to the Investigator's judgment, from study participation; or • Known hypersensitivity to IMB-1018972, mannitol, hypromellose, magnesium stearate and pre-gelatinized corn starch (other ingredients of placebo and active).

Table 6.1: In- and Exclusion Criteria for IMPROVE-DiCE*. Detailed list of in- and exclusion criteria applying for patients enrolled in the IMPROVE-DiCE trial. BMI=body mass index; FSH=follicle stimulating hormone; HbA1c=glycated haemoglobin A1c; IMB-1018972=ninerafaxstat; LVEF=left ventricular ejection fraction; SGLT2i=sodium glucose co-transporter 2 inhibitors; NYHA=New York Heart Association; T2D=type 2 diabetes mellitus; WOCBP=women of childbearing potential*

6.3.3 Data acquisition

6.3.3.1 CMR

CMR imaging was performed on a single 3T MR scanner (Magnetom TRIO, Siemens Healthineers, Erlangen Germany). A schematic overview of the scan protocol, timings and sequences used is provided in **Figure 6.2**.

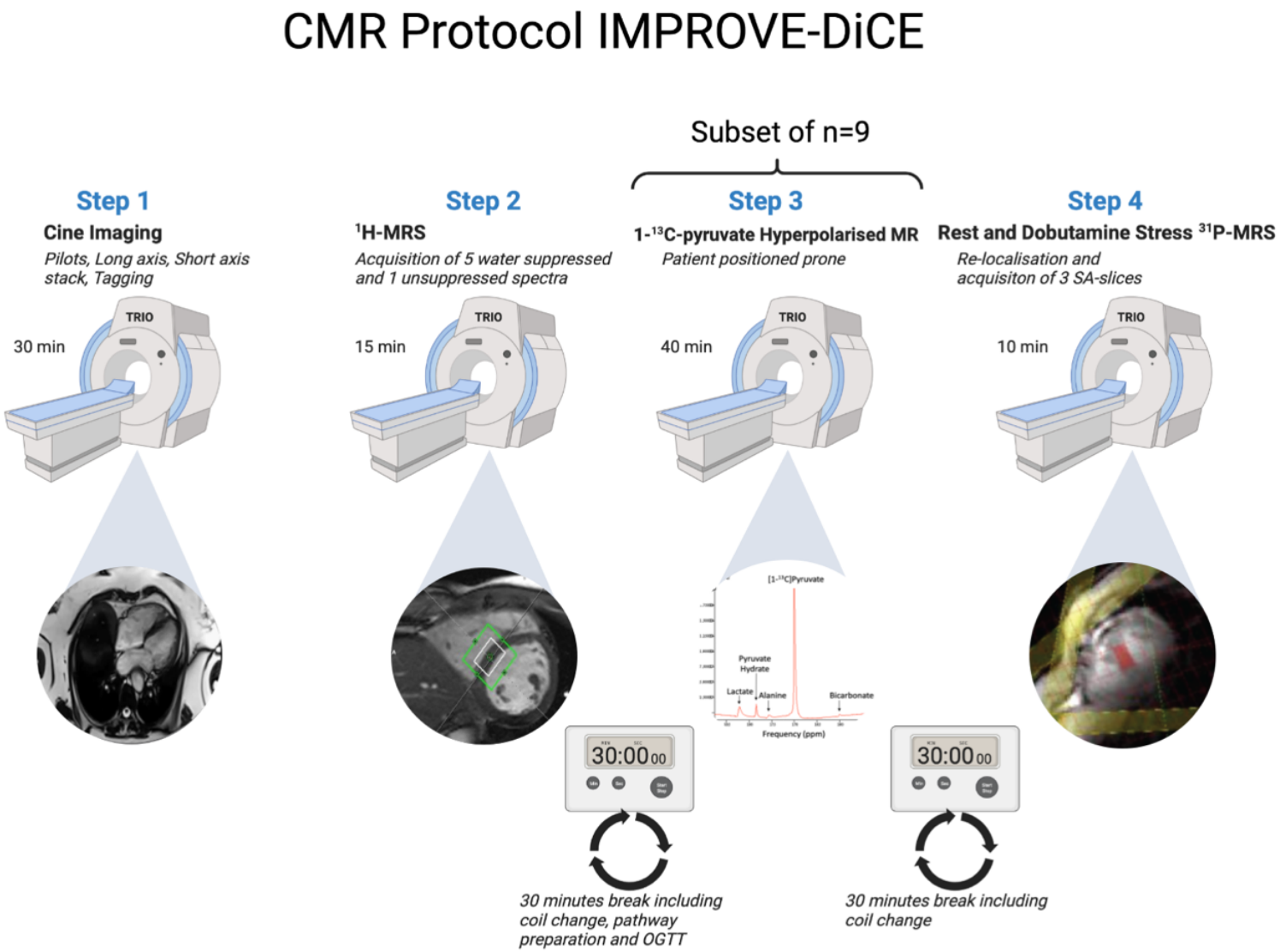

Figure 6.2: IMPROVE-DiCE CMR scanning protocol. *Firstly, anatomical and functional imaging and MRS sections were acquired. During a following break the patient was given 75 g of oral glucose as preparation for the DNP-scan and a coil change in the scanner performed. Following spectral acquisition and a quick visual quality control and coil change, myocardial energetics (PCr/ATP) at rest and during dobutamine stress (65 % age-maximal HR) were obtained.*

Using an 18-channel phased-array coil with the participant supine, the initial planning pilots and cine images were acquired in two long axis views (HLA, VLA) and in short axis slices covering the whole LV using retrospectively ECG-gated balanced steady-state free precession cine imaging or prospective gating in patients with atrial fibrillation (AF).[125,191]

6.3.3.2 Dobutamine stress

Dobutamine was administered as a continuous intravenous infusion at incremental rates in order to achieve a significant haemodynamic effect. The infusion was commenced initially at 10 µg/kg/min but increased to a maximum of 40 µg/kg/min, depending on presence of a satisfactory haemodynamic response, which was defined as 65 % of the age maximum heart rate (HR; 220-age). This elevated HR was then maintained for the duration of the acquisition. HR and blood pressure (BP) were measured at baseline and at one-minute intervals during and after pharmacological stress until normalisation to pre-examination levels. Wherever feasible, stress cines were acquired in a mid-short axis slice as well as VLA and HLA. Due to logistical considerations, the stress-imaging was conducted as part of the ^{31}P-MRS acquisition (Magnetom TRIO, Siemens Healthineers, Erlangen, Germany) and had to be acquired using a locally created GRE-sequence by means of the integrated scanner receiver coils which resulted in a lower image quality and more susceptibility to movement artefacts.

6.3.3.3 Magnetic resonance spectroscopy

Bi-nuclear magnetic resonance spectroscopy (^{31}P- and ^{1}H-MRS) was used to assess different aspects of myocardial metabolic function. Firstly, cardiac energetics (expressed as PCr/ATP) were assessed using ^{31}P-MRS at rest and during dobutamine stress at 65 % age-maximal HR with patients resting in prone position over the centre of a dual-channel ^{31}P Heart/Liver coil (Siemens Healthineers, Erlangen, Germany). Furthermore, myocardial steatosis was assessed via ^{1}H-MRS using a 18-channel receive array supine in end-diastole and expiration. This enabled acquisition of water suppressed and water unsuppressed lipid spectra allowing for calculation of myocardial triglycerides.

6.3.3.4 Hyperpolarized [1-^{13}C]pyruvate MRS

A General Electric SpinLab system (GE Healthcare, Chicago, USA) was used for the process of Dynamic Nuclear Polarization as described previously. Following sufficient polarisation of around 2 hours, sample dissolution was undertaken to produce the final hyperpolarized [1-^{13}C]pyruvate solution for injection. After quality control eligible solutions were released for human injection. Intravenous injection of the hyperpolarized pyruvate was undertaken at a dose of 0.4 ml/kg and at a rate of 5 ml per second via a power injector (MEDRAD, Bayer).

6.3.3.5 Echocardiography

TTE was used to evaluate cardiac structure and function in keeping with official recommendations by the British Society of Echocardiography. [165] The following clinical information was recorded and analysed on a Philips Healthcare ISCV analysis station:

- LVEF, LVEDV and -ESV, LVMi
- Diastolic function
- LV wall thickness and wall motion status
- Haemodynamic status (cardiac output)
- Valve status

6.3.3.6 Blood sampling and analysis

Fasting venous bloods were drawn for biochemical analysis of the following parameters at baseline and after 4- or 8 weeks of ninerafaxstat, respectively:

- Fasting plasma glucose
- Fasting plasma insulin
- HbA_1c
- HOMA-IR
- Free fatty acids (FFA)
- HDL-Cholesterol
- LDL-Cholesterol
- Total-Cholesterol
- Triglycerides
- NT-proBNP
- Hs-cTn

6.3.4 Data analysis

6.3.4.1 CMR

Image analysis for cardiac indices was performed in an anonymised fashion offline in accordance with SCMR guidelines [125], using cmr42 post-processing software by an independent operator who was blinded to patient treatment status. Spectroscopic

analysis for ^{31}P- and ^{1}H-MRS was performed as described in **Chapters 2.5.1** and **2.5.3**, respectively.

6.3.4.2 Echocardiography

Analysis of TTE images was conducted on an ISCV workstation as outlined before (see **Chapter 2.6**).

6.3.4.3 Biomarker analysis

Biomarkers were analysed domestically by OUH's clinical biochemistry laboratory according to local standard protocols.

6.3.5 Statistical analysis

Statistical analyses were performed using commercial software (SPSS 24, Chicago and GraphPad Prism 9, San Diego). All data is presented as median (IQR) unless stated. Determination of statistical significance was assessed by Wilcoxon signed-rank test. Pearson's correlation and linear regression were used. To compare the coefficient of regression between before and after the trial, dummy variable regression analysis was performed. Values of $p<0.05$ were considered as statistically significant.

6.4 Results

Patient recruitment took place between May and September 2021 and all follow-up visits were completed by December 2021. Of a total of 28 patients screened in a single centre (OCMR, Radcliffe Department of Medicine, University of Oxford), 22 were enrolled and subsequently treated. One participant withdrew from treatment during the treatment period and another one completed the treatment period but due to a panic attack did not complete the MR examination at their end of trial (EOT) visit.

6.4.1 Study population

Baseline characteristics are shown in **Table 6.2** for the 21 participants in the per protocol set. The median age for participants was 70 years (58, 72), with 57 % being male. Median HbA1c was 7.1 % (6.6 %, 7.9 %). All except one patient (95 %) were on stable doses of oral antidiabetic medication, with Metformin the most frequently prescribed agent. In agreement with a population of high CV-risk, a majority of patients were on a statin (71 %) and angiotensin converting enzyme inhibitors (ACE-I) or Angiotensin II receptor blockers (ARB) (57 %).

Table 6.2: Baseline Patient Characteristics IMPROVE-DiCE

Characteristic	**Pre-Treatment n=21**	**Post-Treatment n=21**	**p-value**
Anthropometrics, mean (SD)			
Age (years)	70 (58, 72)	70 (58, 72)	ns
Male (% of total)	12 (57)	12 (57)	ns
Weight (kg)	97 (12)	95 (12)	**<0.001**
Body mass index (kg/m^2)	33.5 (3.6)	33.1 (3.8)	**0.004**
Systolic blood pressure (mmHg)	142 (15)	140 (13)	0.42
Diastolic blood pressure (mmHg)	73 (8)	75 (8)	0.58
Resting heart rate (bpm)	75 (11)	70 (10)	**0.009**
Heart rate during stress (bpm)	112 (10)	110 (6)	0.31
Metabolic status, median (IQR)			
HbA1c (%)	7.1 (6.6, 7.9)	7.2 (6.7, 8.0)	0.41
Total cholesterol (mmol/l)	4.3 (3.4, 5.2)	4.1 (3.5, 4.8)	0.052
LDL cholesterol (mmol/l)	2.5 (1.6, 3.0)	2.3 (1.7, 2.7)	**0.01**
HDL cholesterol (mmol/l)	1.2 (1.0, 1.3)	1.2 (0.9, 1.3)	0.99
Triglycerides (mmol/l)	1.6 (1.1, 2.2)	1.3 (1.0, 2.4)	0.69
Fasting glucose (mmol/l)	8.5 (6.1, 9.1)	7.2 (5.9, 9.0)	0.65
Fasting insulin (pmol/l)	85 (57, 100)	83 (58, 107)	0.66
HOMA-IR	4.1 (2.3, 6.6)	4.2 (2.9, 6.0)	0.94
Free Fatty Acids (mmol/l)	0.9 (0.8, 1.0)	0.9 (0.5, 1.0)	0.77
Cardiac Biomarkers, median (IQR)			
NT-pro BNP (ng/ml)	82 (59, 147)	60 (40, 138)	0.70
hs-cTn (ng/l)	2 (2, 5)	2 (2, 4)	0.27
Concomitant Medications, n (%)			
Oral Hypoglycaemic	20 (95)	20 (95)	ns
ACE-I / ARB	12 (57)	12 (57)	ns
Ca^{2+}-Channel Blocker	9 (43)	9 (43)	ns
Statin	15 (71)	15 (71)	ns
Loop diuretic	4 (19)	4 (19)	ns

Table 6.2: Pre- and Post-Treatment Results IMPROVE-DiCE*. ACE-I=angiotensin converting enzyme inhibitor; ARB=angiotensin II receptor blocker; HbA1c=glycated haemoglobin A1c; HDL= high-density lipoprotein; HOMA-IR=homeostasis model*

assessment for insulin resistance; hs-cTn= highly sensitive cardiac troponin; IQR=interquartile range; kg=kilogram, LDL=low-density lipoprotein; NT-proBNP=n-terminal pro b-type natriuretic peptide;

Of the 22 participants recruited at baseline, 1 completed baseline assessment but did not complete the MRI follow up study. One participant stopped ninerafaxstat treatment early due to experiencing frequent diarrhoea and withdrew from the trial. Among the 21 patients enrolled who completed the study, adherence and side effects were assessed by weekly telephone interviews. None of the 21 patients completing the treatment experienced significant side effects. There were no significant changes to any of the patients' pre-existing medications throughout the study

6.4.2 Primary Outcome

6.4.2.1 Change in resting ^{31}P-MRS

Administration of ninerafaxstat led to significantly increased PCr/ATP in the combined 4- and 8-week cohorts (baseline median 1.6; 1.4, 2.1) to EOT 2.1 (1.7, 2.5); p = <0.01). Interestingly, when analysing the 4- and 8-week cohorts' data separately, results did not meet significance in the 4-week treatment group however, 4 out of 5 subjects normalised their myocardial energetics (baseline median 1.6; 1.2, 2.1) to EOT 2.4 (1.8, 2.7); p = 0.13). In the 8-week cohort, significance of results remained unchanged from the combined cohort (baseline median 1.8; 1.4, 2.1) to EOT median 2.0 (1.8, 2.5), p = <0.01) (**Figure 6.3**).

Figure 6.3: Resting PCr/ATP IMPROVE-DiCE

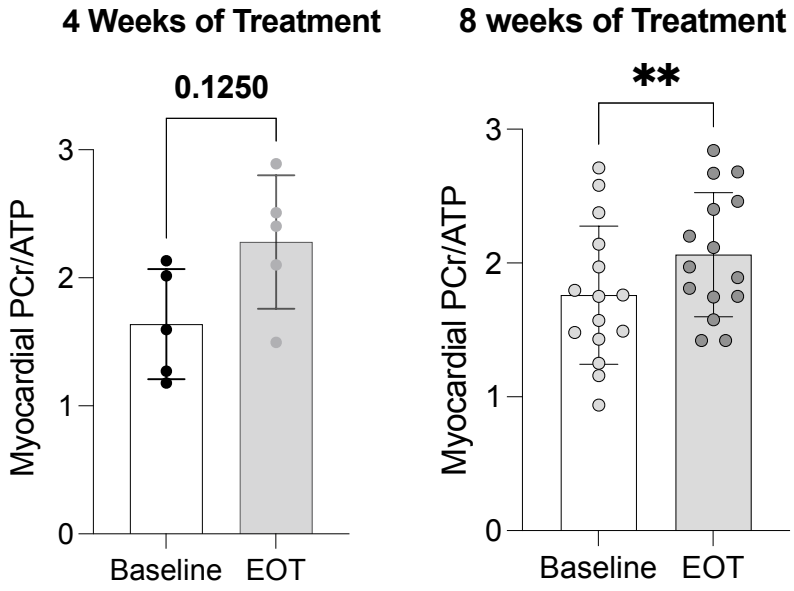

Figure 6.3: Myocardial Energetics IMPROVE-DiCE*. Scatterplots with bar graph and SD of the 4-week treatment cohort (left) and 8-week treatment cohort (right).*

6.4.3 Exploratory outcomes

6.4.3.1 Dobutamine stress ^{31}P-MRS

Due to a loss of signal to noise ratio and movement artefact as well as patient preference to omit the stress investigations, 15 of the total of 21 recorded studies were included in the analyses.

The peak heart rate (HR) achieved at baseline was very similar to the dobutamine stress response at EOT (peak HR mean before 112 /Min (±5.8) vs. 110 /Min (±6.1) after treatment, p=0.31). Myocardial energetics recorded during peak dobutamine stress were similar at baseline and following treatment with ninerafaxstat **(**PCr/ATP median during stress baseline PCr/ATP 1.7; 1.6, 2.0) vs EOT median 1.9; 1.4, 2.0), p = 0.94, **Figure 6.4 a).** Separating the 4- and 8-week treatment groups did not alter the overall result (**Figure 6.4 b and c**).

Figure 6.4: Dobutamine Stress PCr/ATP IMPROVE-DiCE

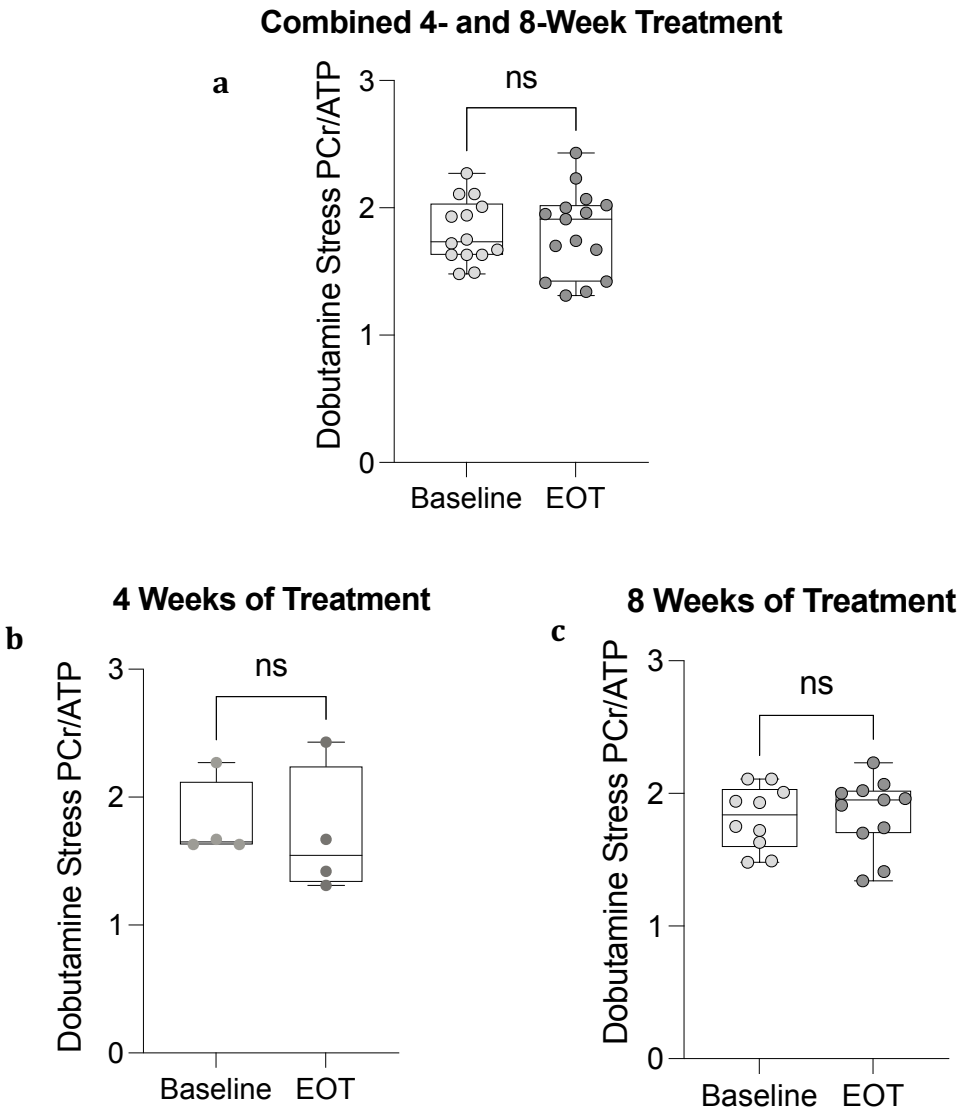

Figure 6.4: Stress PCr/ATP IMPROVE-DiCE. *Individual data points for dobutamine stress ^{31}P-MRS in the combined treatment cohort (a), 4-week treatment cohort (b) and 8-week treatment cohort (c). EOT=end of treatment, ns=not significant*

Similarly to the results for individual values of rest and stress assessments, there was a significant difference following ninerafaxstat treatment in the difference (rest-stress) PCr/ATP, the so-called 'Δ PCr/ATP' (baseline median -0.08; -0.5, 0.5), EOT median 0.5 (0.42, 0.76), p = <0.01) (**Figure 6.5**).

Figure 6.5: Delta (rest-stress) PCr/ATP IMPROVE-DiCE

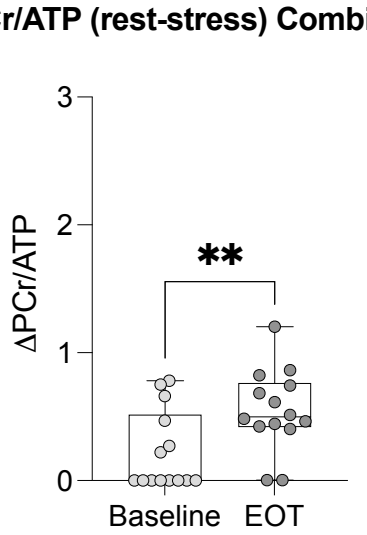

Figure 6.5: Delta PCr/ATP (rest-stress) IMPROVE DiCE*. Individual data points for the change in Δ PCr/ATP (rest-stress) from baseline (left) to EOT (right).*

6.4.3.2 Myocardial steatosis

Following the increased myocardial triglycerides (MTG) at baseline (MTG 2.2 %; 1.5, 3.2), treatment with ninerafaxstat did reduce MTG substantially in every individual patient leading to an overall significantly decreased MTG content, a surrogate of myocardial steatosis, which was reduced by 34 % overall (median MTG 2.2 %; 1.5, 3.2) to 1.5 % (1.0, 2.7), p = 0.026).

Figure 6.6: Myocardial Steatosis IMPROVE-DiCE

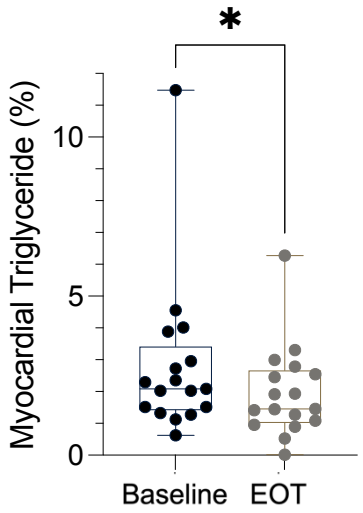

Figure 6.6: Myocardial Triglycerides IMPROVE-DiCE.

Despite FFA levels being unchanged over the treatment duration (p = 0.77), MTG content, aside being lower, remained correlated with FFA-levels (r 0.53, p = 0.03). When comparing the coefficient of regression between FFA and MTG content before and after treatment, those before treatment had a greater MTG with increasing FFA (+ 7.5 % vs + 1.6 % increase per mmol/l increase in fatty acid level, p = 0.008).

6.4.3.3 Hyperpolarized [1-^{13}C]pyruvate MRS

Dynamic nuclear polarisation was performed and [1-^{13}C]pyruvate pathways injected in a subset of 9 subjects. The [1-^{13}C]bicarbonate to [1-^{13}C]pyruvate ratio was increased (by 20 %, p=0.08) with 7 of 9 participants showing an increase in this marker of PDH flux.

Figure 6.7: PDH-Flux IMPROVE-DiCE

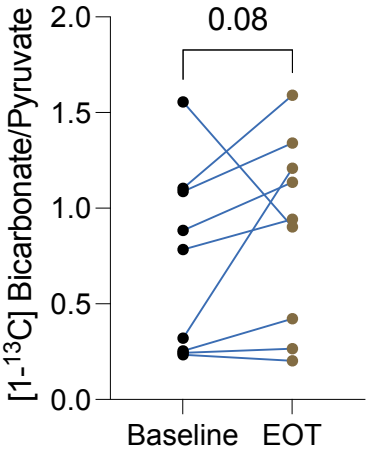

Figure 6.7: In-Vivo Bicarbonate/Pyruvate Ratio IMPROVE-DiCE

[1-^{13}C]alanine to [1-^{13}C]pyruvate ratio was reduced following treatment (by 20 %, p=0.053).

Figure 6.8: Alanine/Pyruvate IMPROVE-DiCE

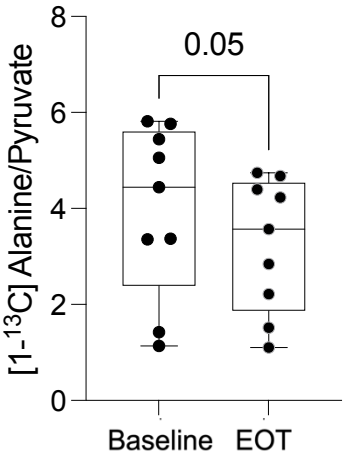

Figure 6.8: In-Vivo Alanine/Pyruvate Ratio IMPROVE-DiCE.:

The [1-^{13}C]lactate to [1-^{13}C]pyruvate ratio and the ratio of [1-^{13}C]bicarbonate and [1-^{13}C]lactate signals were both unchanged following treatment with ninerafaxstat (p=0.82, and p=0.36 respectively).

Figure 6.9: Lactate Pyruvate and Bicarbonate/Lactate IMPROVE-DiCE

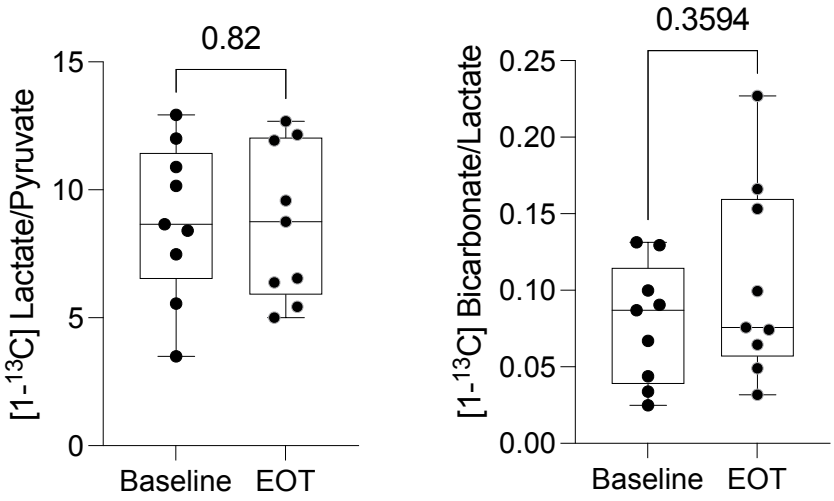

Figure 6.9: In-Vivo Lactate/Pyruvate and Bicarbonate/Lactate ratios IMPROVE-DiCE.

6.4.3.4 Changes to LV-structure and function

Treatment with ninerafaxstat was not associated with significant changes in LV-morphology. Both LVEDV, and -mass remained unchanged (**Table 6.3, Figure 6.10**). Likewise, LVEF and markers of systolic strain remained unchanged (**Table 6.3, Figure 6.10**). Whilst there was no convincing change in diastolic function recorded on TTE (**Table 6.3**), MRI analysis showed that peak diastolic circumferential strain rate (by 15 %, p=0.047, Table 3, Figure 3H), absolute LV peak filling rate (336 ml/s (290, 312) vs 373 ml/s (312, 520), p=0.03) and peak

filling rate normalised to the LVEDV (2.3 EDV/s; 2.1, 3.1 vs 2.9 EDV/s; 2.5, 3.4; p=0.02) all improved following treatment with ninerafaxstat. Left atrial size and -ejection fraction was mutually unchanged (p=0.23 and p=0.5, respectively).

Table 6.3: Imaging Results IMPROVE-DiCE

Cardiac MRI	**Pre-Treatment n=21**	**Post-Treatment n=20**	**p-value**
Left ventricle			
End-diastolic volume (ml)	135 (107, 164)	129 (103, 160)	0.83
End-systolic volume (ml)	43 (33, 58)	47 (32, 56)	0.62
Stroke volume (ml)	85 (69, 108)	83 (67, 106)	0.57
Ejection fraction (%)	65 (61, 70)	65 (60, 70)	0.89
Peak Systolic Strain Circ (%)	-18.6 (-20.5,-16.4)	-19.1 (-21.1,-16.7)	0.19
GLS (%)	-14.3 (-16.4,-11.7)	-14.7 (-16.1,-13.7)	0.39
Mass (g)	130 (98, 151)	131 (102, 144)	0.59
Left atrial volume (ml)	68 (51, 88)	62 (45, 86)	0.23
Left atrial ejection fraction (%)	60 (34, 66)	62 (49, 69)	0.5
Peak Diastolic Strain Rate Circ (1/s)	0.86 (0.82, 1.06)	0.99 (0.90, 1.09)	0.047
Peak LV Filling Rate (ml/s)	336 (290, 452)	373 (312, 520)	0.06
Normalised Peak LV Filling Rate (EDV/s)	2.5 (2.1, 3.1)	2.9 (2.5, 3.4)	0.04
Right ventricle			
End-diastolic volume (ml)	129 (115, 170)	139 (102, 155)	0.49
End-systolic volume (ml)	55 (43, 66)	59 (37, 75)	0.40
Ejection fraction (%)	57 (56, 64)	57 (54, 62)	0.19
Echocardiography	**n = 16**	**n=16**	
E/A	0.84 (0.74, 0.95)	0.77 (0.67, 0.93)	0.84
Average E/E’	8.9 (7.2, 10.0)	9.1 (7.4,12.3)	0.08

Table 6.3: Functional Imaging Parameters IMPROVE-DiCE*. Treatment with ninerafaxstat was not associated with changes in right ventricular morphology or function.*

6.4.3.5 Anthropometrics and biomarkers

Following treatment with ninerafaxstat, there was a reduction in overall body weight (by 1.5 kg, p<0.01), total serum cholesterol (4.3 mmol/L; 3.4, 5.2 to 4.1 mmol/L; 3.5, 4.8; p= 0.052) and LDL-cholesterol (2.5 mmol/L; 1.6, 3.0 to 2.1 mmol/L; 1.7, 2.7; p = 0.01). Fasting glucose, HbA1c, insulin, triglycerides as well as neurohumoral cardiac biomarkers (NT-proBNP) and markers of cardiac injury (hs-cTn) were unchanged (see **Table 6.4**).

Table 6.4: Biomarkers and Anthropometrics IMPROVE-DiCE

	Pre-Treatment n=21	**Post-Treatment n=21**	**p-value**
Anthropometrics, mean (SD)			
Age (years)	70 (58, 72)	70 (58, 72)	ns
Male (% of total)	12 (57)	12 (57)	ns
Weight (kg)	97 (12)	95 (12)	**<0.001**
Body mass index (kg/m^2)	33.5 (3.6)	33.1 (3.8)	**0.004**
Systolic blood pressure (mmHg)	142 (15)	140 (13)	0.42
Diastolic blood pressure (mmHg)	73 (8)	75 (8)	0.58
Resting heart rate (bpm)	75 (11)	70 (10)	**0.009**
Heart rate during stress (bpm)	112 (10)	110 (6)	0.31
Metabolic status, median (IQR)			
HbA1c (%)	7.1 (6.6, 7.9)	7.2 (6.7, 8.0)	0.41
Total cholesterol (mmol/l)	4.3 (3.4, 5.2)	4.1 (3.5, 4.8)	0.052
LDL cholesterol (mmol/l)	2.5 (1.6, 3.0)	2.3 (1.7, 2.7)	**0.01**
HDL cholesterol (mmol/l)	1.2 (1.0, 1.3)	1.2 (0.9, 1.3)	0.99
Triglycerides (mmol/l)	1.6 (1.1, 2.2)	1.3 (1.0, 2.4)	0.69
Fasting glucose (mmol/l)	8.5 (6.1, 9.1)	7.2 (5.9, 9.0)	0.65
Fasting insulin (pmol/l)	85 (57, 100)	83 (58, 107)	0.66
HOMA-IR	4.1 (2.3, 6.6)	4.2 (2.9, 6.0)	0.94
Free Fatty Acids (mmol/l)	0.9 (0.8, 1.0)	0.9 (0.5, 1.0)	0.77
Cardiac Biomarkers, median (IQR)			
NT-pro BNP (ng/ml)	82 (59, 147)	60 (40, 138)	0.70

	Pre-Treatment n=21	**Post-Treatment n=21**	**p-value**
hs-cTn (ng/l)	2 (2, 5)	2 (2, 4)	0.27
Concomitant Medications, n (%)			
Oral Hypoglycaemic	20 (95)	20 (95)	ns
ACE-I / ARB	12 (57)	12 (57)	ns
Ca^{2+}-Channel Blocker	9 (43)	9 (43)	ns
Statin	15 (71)	15 (71)	ns
Loop diuretic	4 (19)	4 (19)	ns

Table 6.4: Anthropometric and Biomarker Results IMPROVE-DiCE.

6.5 Discussion

IMPROVE-DiCE is the first trial assessing the effects of ninerafaxstat, a novel cardiac mitotrope, on myocardial energetics, metabolism, and function in patients with diabetic cardiomyopathy (DbCM) *in-vivo*. Major results include, but are not limited to, improved myocardial energetics, reduced MTG and ameliorated diastolic function following 4 or 8 weeks of treatment with ninerafaxstat. These findings provide evidence that ninerafaxstat is actively able to beneficially modulate the deranged metabolic machinery in the heart and suggest it has several beneficial effects in patients with DbCM.

6.5.1 Changes in myocardial energy metabolism

The T2D heart is characterised by metabolic remodelling including dominance of FAO, reduced PDH flux and glucose oxidation.[140] While there remains debate whether this metabolic remodelling is causal for impaired myocardial energetics[241], cardiac steatosis[310], LV hypertrophy, and LV diastolic dysfunction[311], it is unanimously accepted to aggravate the aforementioned. To date, several partial FAO inhibitors have aimed to restore metabolism back towards increasing glucose

oxidation by reducing PDH flux inhibition. In small studies this mechanism has been shown to improve cardiac energetics and function.[112] However, the peripheral insulin resistance[59,312] reduces the ability to recouple glucose uptake and oxidation and thus, restore physiological metabolic flexibility. Ninerafaxstat overcomes this by liberating IMB-1028814 (the active moiety) and nicotinic acid during hydrolysis in plasma. There were some safety concerns around the use of nicotinic acid in a cohort of patients with diabetes and presence of symptomatic CAD or previous MI in the HPS2-THRIVE trial.[314] Notably, there are certain differences to be taken into consideration. Firstly, patients in HPS2-THRIVE received not only a higher dose of nicotinic acid (up to 2g per day) but this was also used in a fixed combination with laropripant, a drug used to reduce the typical side effects of nicotinic acid induced by its vasodilating properties.[315] In IMPROVE-DiCE, ninerafaxstat (consisting of IMB-1028814 and nicotinic acid) is a fixed dose combination of 200mg in total thus, much less than the dose in HPS2-THRIVE. In addition, the modified release formulation used ensures liberation of IMB-1028814 and nicotinic acid occurs only after hydrolysis in plasma thus, will likely be absorbed and provide a precursor for NAD^+. Secondly, the trial population was different and interestingly, SAEs appeared to differ between ethnicities enrolled in the trial, with Chinese patients being more affected overall. The surprisingly increased rate of bleeding in HPS2-THRIVE is likely a side effect of laropriprant rather than nicotinic acid as the antagonism of the prostaglandin D_2 receptor also exhibited antagonistic effects on the thromboxane A_2 receptor hence, may affect platelet aggregation.[316]

Myocardial high-energy phosphate metabolism plays a crucial role in maintaining normal contractile function.[16] In this trial, we demonstrated that not only is T2D related to reduced PCr/ATP but also that this reduction is associated with a reduced [^{13}C]bicarbonate/ [1-^{13}C]lactate ratio. This implies that markedly reduced energetics in T2D are related to a reduction in relative carbohydrate oxidation.

The crucial importance of this increase in FA metabolism lies in the fact that the mitochondrial redox state and, as a result, the free energy of ATP-hydrolysis (ΔG) are negatively affected by a change in the balance of substrate use.[288] As such, the surge in FAO results in a loss of efficient coupling between substrate use and ATP production in the diabetic heart.[317] As the sarcoplasmic reticular Ca^{2+}-ATPase is the most energetically demanding of all enzymes involved in contractile function[318], impairment in high-energy phosphate metabolism initially affects the ability the to lower cytosolic Ca^{2+} and thus, impairs diastolic function first. In line with this, both animal[319] and human T2D[140] have shown a typical triad of reduced cardiac PDH flux, deranged myocardial energetics, and progressive diastolic dysfunction.

PDH is a key enzyme regulating the balance between carbohydrate and fat metabolism in the heart. Consequently, increasing PDH flux has previously been proposed as a novel therapeutic target in different cardiomyopathies.[319,320] Via restoration of PDH activity, a normal fuel balance may be re-established which in turn may restore cardiac energetics and function.

Following treatment with Ninerafaxstat, PCr/ATP was significantly and consistently improved. It is worthwhile noting that the magnitude of this improvement is larger than that seen with empagliflozin[189], and resulted in the

median PCr/ATP following this trial recovering to physiological ranges.[311] The numerical increase in the [1-^{13}C]bicarbonate/ [1-^{13}C]pyruvate ratio (by 20 %, p=0.08) is in keeping with the mechanism of action of as ninerafaxstat as a partial FAO inhibitor, conversely increasing glucose utilisation in myocardial tissues. Considering the study's limitations regarding sample size, the fact that 7 of 9 participants show an increase in [1-^{13}C]bicarbonate/[1-^{13}C]pyruvate ratio suggests strongly that PDH flux has increased following treatment. It is therefore reasonable to assume that the re-balancing of substrate use towards normal is likely to be a mechanism underlying the energetic benefits seen in this study. Hence, the observed improvement in diastolic function, being an active process requiring energy, is also likely to be a consequence of improved ATP metabolism.

6.5.2 Changes in LV-structure and function

The improvements seen in MTG and overall diastolic function in this study are further evidence of ninerafaxstat's metabolic mechanism of action.

Previous studies indicated that trimetazidine may cause an activation of 5′-AMP-activated protein kinase (AMPK) and inhibition of the peroxisome proliferator-activated receptor γ coactivator-1 (PGC-1α) expression.[321] This combination would result in inhibition of peroxisome proliferator-activated receptor alpha (PPARα), reducing the expression of pyruvate dehydrogenase kinase 4 and increasing PDH flux. Additionally, decreasing expression levels of genes such as fatty acid translocase (FAT/CD36) can further reduce cellular fatty acid uptake.[322] Given the active metabolite of ninerafaxstat is trimetazidine, the aforementioned mechanism

may well be why it can both reduce ectopic MTG deposition, and decrease FAO. In the present study, this was demonstrated by a reduction in MTG content without change in circulating FFA levels in combination with a stronger correlation between FFA and MTG content before treatment. Given that MTG content was correlated with diastolic function at baseline, it is also likely that this improvement is related to the amelioration in peak diastolic strain observed.

Whilst mild weight loss was noted in this trial and is known to independently improve myocardial energetics[299], myocardial steatosis[298] and diastolic function[323], the magnitude of energetic improvements and reduction in MTG seen here (~30 %) are greater than would be expected with the median 1.5 kg weight loss observed. Additionally, the time period required to detect these changes following a lifestyle intervention would need to be considerably longer.[298] Moreover, individual analysis of cases with patients maintaining their weight (data not shown), further corroborates our findings. Whether ninerafaxstat has longer term weight loss effects in addition to its metabolic effects is unknown, but worthy of future investigations.

In addition to the changes outlined above, the present trial equally observed beneficial effects on diastolic function derived from CMR. Peak filling ration normalised to EDV as well as peak filling rate individually have previously been shown to be valuable markers with high specificity and sensitivity in patients with T2D.[324] Furthermore, peak diastolic circumferential strain rate, which was abnormal at baseline and significantly improved by ninerafaxstat, is a sensitive marker of diastolic dysfunction in cardio-metabolic syndromes and thus, might be better suited in detecting this compared to echocardiography.[325]

6.6 Limitations

This study may suffer from reduced generalisability due to a small sample size in our cohort and the exclusion of patients on SGLT2i and insulin due to safety concerns. Patients with atrial fibrillation were excluded from the trial. Female and male participants were not entirely equal in our cohort and patients of minoritised ethnic were significantly underrepresented in this single-centre trial.

6.7 Conclusions

In patients with obesity (BMI $\geq$ 30 kg/m^2) and T2D, treatment with ninerafaxstat was well tolerated, safe and improved myocardial energetics, cardiac steatosis and diastolic function. This phase 2a trial strongly supports a positive effect of ninerafaxstat on myocardial metabolism and further studies are warranted to define broader patient population benefitting from this treatment as well as foster the clinical utility of this drug.

7 General conclusions and future directions

This thesis has investigated metabolic modulation by different means in a variety of HF patients. Covering the spectrum from prospective longitudinal studies to phase 2a open label and phase 3 randomised controlled trials and using gold-standard, cutting edge techniques (^{1}H-, ^{31}P and hyperpolarized MRS, serum metabolomics) the results herein provide novel insights into metabolic derangements of different phenotypes of HF and how to manipulate metabolic substrate metabolism in HF for therapeutic purposes. The principal findings of each of the experiments presented above are:

1. In a prospective double-blind RCT (*EMPA-VISION*) enrolling patients with HFrEF (**Chapter 3**), treatment with the SGLT2i empagliflozin for 12 weeks did not lead to substantial improvements in myocardial energetics at rest or during pharmacological stress (dobutamine). These findings were further corroborated by a targeted panel of myocardial metabolomics in which no overall change could be observed. However, a significant anti-hypertrophic effect including reduction of cardiomyocyte cell volume that was paralleled by a decrease in myocardial triglycerides did provide interesting new scientific approach for patient selection for treatment with SGLT2i in HFrEF. Taking the findings as a whole, it is likely that empagliflozin's

mechanism of action in HFrEF is multifactorial and that, a link of inflammation and metabolism is a worthy target to investigate in human *in-vivo* studies.

2. Despite sharing a common terminology, an increasing amount of evidence underpins the distinct differences in the development but also the aggravation of HFpEF compared to HFrEF. As such, this cohort of the randomised controlled trial *'EMPA-VISION'* sought to investigate the changes of SGLT2i treatment with empagliflozin in patients with clinically established HFpEF (**Chapter 4**). After 12 weeks, there was again no effect on cardiac energy metabolism, neither with ^{31}P-MRS nor in the serum metabolomics results, which reinforces the neutral findings in the HFrEF cohort. Importantly, similarly to HFrEF, there was again a marked reduction of myocardial steatosis in the active treatment but not in the placebo arm. Refined surrogates of systolic function (circumferential and radial strain) showed improvements which again, points to beneficial effects on cardiac structure. In addition, patients had an improved pulmonary function, reduced symptom burden (KCCQ) and an increased walking distance in the 6MWT. Of note, the original number of patients enrolled differed markedly from the number of patients completing the trial due to the far-reaching restrictions put in place as a result of the COVID-19 pandemic. Nevertheless, this was the first trial to investigate imaging endpoints and metabolism in a dedicated cohort of HFpEF patients and thus, offers more insight on selection of future endpoints for trials in this population.

3. Lifestyle modifications, contrary to pharmacological interventions, are currently largely underutilised as a treatment for established HF and mainly used for primary prevention or symptom management in selected cases. Disappointingly little is known on the potential benefits and changes induced by weight management in patients with obesity and an established diagnosis of HFpEF. As such, the study in **Chapter 5** aimed to examine the effects of weight loss with a very low energy diet (VLED) on cardiac energetics, structure and function in patients with HFpEF. The intervention led to a significantly reduced symptom burden (NYHA), level of NT-proBNP and markedly improved RV adaptation at rest and during physiological ergometer stress. As RV dysfunction and pulmonary hypertension are frequent conditions in obese HFpEF, the results are encouraging to test a dietary intervention as a treatment in a large HFpEF trial.

4. Lastly, in a phase 2a trial of ninerafaxstat, a novel cardiac mitotrope designed to enhance cardiac energy metabolism in patients with diabetes / diabetic cardiomyopathy, **Chapter 6** examined its impact on cardiac metabolism, energetics, structure and function. To do so, the novel resource of hyperpolarized MR spectroscopy was used to examine the drug's effects on pyruvate dehydrogenase (PDH), a key player in the fine regulation of balance between fatty acid oxidation (FAO) and glucose oxidation. Interestingly, treatment with this novel drug did improve PCr/ATP at rest,

reduce myocardial steatosis and in the majority of patients improve PDH-flux. Importantly, measures of diastolic function also improved significantly indicating a potential mechanism of action for other cardio-metabolic diseases related to diabetes, such as HFpEF.

Several implications for future cardio-metabolic research projects in human subjects in the context of clinical trials and drug development can be inferred from the presented data. The three major insinuations are presented below:

1. Drug development in the cardiovascular field is stagnant and lagging years behind innovative specialties such as oncology. The results of this thesis present CMR in the context of early and advanced phase clinical trials as an attractive method to reduce overall costs and improve reliability of findings. Given the mostly neutral findings on echocardiography in contrast to the widely applicable CMR findings in this thesis, early mechanistic research should increasingly focus on CMR as an imaging tool for clinical trials.

2. Hyperpolarized MR enables *in-vivo* detection of single metabolic pathways and importantly, due to the greatly improved signal strength, by use of substantially lower patient numbers compared to other techniques. Hence, a direct link between cellular biochemistry, overall metabolism and patient outcomes can achieved. This novel technique can further close the missing link between metabolism and cell-driven inflammation which is of particular importance in certain cardio-metabolic diseases like diabetes, obesity and HFpEF.

3. Despite decades of research, our understanding of cardiac physiology concerning energy metabolism is limited. More importantly, the consequences in treatment with the same drug (**Chapters 3 and 4**) may vary considerably in patient groups with different characteristics of the same syndrome (e.g. obese HFpEF vs. non-obese HFpEF). Inflammation, similar to metabolism, is a finely tuned machinery with significant multi-organ interaction and trials investigating inflammation-modulating treatments (e.g. canakimumab) depend on adequate patient selection. The same standard should be applied to mechanistic trials investigating metabolic modulators in HF.

7.1 Follow-up studies and outstanding questions

Results outlined in this thesis provide certain ideas for new experiments but likewise leave some questions unanswered. Thus, the following section intends to outline the major experiments to be performed to answer the most pertinent questions:

1. Given the effects of SGLT2i in patients with HFrEF and HFpEF (Chapters 3 and 4, respectively) on biomarkers of the RAAS as well as structural changes in the heart, it is likely that multi-organ effects of SGLT2i lead to the salutary changes observed. As such, investigating the cardio-renal axis would certainly be of value. Patients with severe kidney disease, present with reduced myocardial fibrosis and signs of reverse remodelling 6-months post kidney transplant.[326] Interestingly, these effects are similar to those observed in this Thesis (reduced T1, reduced ECV and LV-mass) following

SGLT2i treatment. Furthermore, inflammation appears to be a significant driver of fibrosis in both the kidney and the heart.[327,328] There is an increasing amount of preliminary evidence observing anti-inflammatory properties of SGLT2i.[329-331] In addition, these anti-inflammatory properties have long been known for ketone bodies and could thus present a link explaining treatment effects in HF, especially given the mild hyperketonemia induced by SGLT2i.[332,333] Assessing the effects of the two organs over a certain time frame following treatment onset (e.g. 1 month, 3 months, 6 months, 9 months) would be of great benefit to understand the mechanism of action of SGLT2i in HF but further clarify the interaction between heart and kidneys and the hierarchy of changes in HF. The experiments needed can easily be performed in a single CMR session and could be underpinned by serum biomarker and (untargeted) metabolomic as well as inflammasome analyses.

2. As outlined in **Chapter 5**, weight loss leads to favourable changes in obese patients with HFpEF. Despite the 'pilot character' of the study, its results are encouraging to pursue lifestyle related treatments for patients with chronic HF and obesity. However, important questions remaining are
    a. Can the beneficial changes be reproduced in a larger cohort?
    b. Are there differences between how weight loss is achieved (pharmacologically for example via treatment with semaglutide vs. dietary intervention) and which method is safer short and long term?
    c. Is there a BMI cut-off for patients with HFpEF over which weight loss should be a guideline recommended treatment and vice versa,

is there a lower BMI limit under which it might be harmful (i.e. obesity paradox in HFpEF)?

As diet trials are generally open-label trials[290], it would be of value designing a multi-centre trial using cluster-randomisation of the diet in question vs. pharmaceutical intervention vs. control (standard practice). Enrolling patients along the gradient of HFpEF severity and metabolic dysfunction as well as staggered BMI cut-offs (28 kg/m^2 vs. 30 kg/m^2 vs. > 34 kg/m^2) would ensure valid testing of the overall hypothesis. An imaging arm using CMR (imaging and spectroscopy) would investigate a fraction of patients in each cohort in detail in pre-determined intervals (e.g. every 3 months) while patients should generally be followed-up for at least 24 months.

3. Patients with diabetes as well as patients with obesity share common features ranging from the underlying metabolic derangements to a significantly higher prevalence of LV-hypertrophy and diastolic dysfunction, which is reflected by the neologism 'diabesity'.[334] Importantly, these alterations are largely reversible when addressing the underlying aetiology / risk factors appropriately. As demonstrated in **Chapter 6** of this thesis, metabolic and functional maladaptive changes can be significantly improved by administering ninerafaxstat, a treatment designed to re-balance substrate metabolism and addressing the energetic deficit in the heart. Most patients with HFpEF are obese and a significant proportion is diabetic, likewise. Therefore, it appears worthy to speculate if a targeted metabolic

intervention with ninerafaxstat might be suitable to rectify the functional and metabolic pathophysiological changes seen in HFpEF?

Given the effect size observed in IMPROVE-DiCE, a set of 25 HFpEF patients would suffice to investigate any metabolic and functional changes. As there continues to be debate around the definition of HFpEF in clinical trials, with many trials using a cut-off of 45 % LVEF, the patients enrolled here would need to be 'true' HFpEF with a LVEF of > 50 %, a HFA-PEFF Score[335] of > 5 and a BMI over 28 kg/m^2. Interestingly, patients with HFpEF display a muscular energetic deficit not confined to the heart muscle but likewise the skeletal muscles, leading to exercise intolerance and increased symptom burden. Using ^{31}P-MRS to measure the PCr recovery time in skeletal muscle ($\boldsymbol{\tau}$ PCr)[336] which is a good correlate of overall mitochondrial function as well as a suitable replacement for testing fitness (instead of using CPET), possibly decreasing the burden of trial participation for patients.

Bibliography

1. Anker SD, Butler J, Filippatos G, Ferreira JP, Bocchi E, Bohm M, Brunner-La Rocca HP, Choi DJ, Chopra V, Chuquiure-Valenzuela E, et al. Empagliflozin in Heart Failure with a Preserved Ejection Fraction. *N Engl J Med*. 2021;385:1451-1461. doi: 10.1056/NEJMoa2107038
2. Nassif ME, Windsor SL, Borlaug BA, Kitzman DW, Shah SJ, Tang F, Khariton Y, Malik AO, Khumri T, Umpierrez G, et al. The SGLT2 inhibitor dapagliflozin in heart failure with preserved ejection fraction: a multicenter randomized trial. *Nat Med*. 2021;27:1954-1960. doi: 10.1038/s41591-021-01536-x
3. Cook C, Cole G, Asaria P, Jabbour R, Francis DP. The annual global economic burden of heart failure. *Int J Cardiol*. 2014;171:368-376. doi: 10.1016/j.ijcard.2013.12.028
4. Groenewegen A, Rutten FH, Mosterd A, Hoes AW. Epidemiology of heart failure. *Eur J Heart Fail*. 2020;22:1342-1356. doi: 10.1002/ejhf.1858
5. Pfeffer MA, Shah AM, Borlaug BA. Heart Failure With Preserved Ejection Fraction In Perspective. *Circ Res*. 2019;124:1598-1617. doi: 10.1161/CIRCRESAHA.119.313572
6. Cohn JN, Archibald DG, Ziesche S, Franciosa JA, Harston WE, Tristani FE, Dunkman WB, Jacobs W, Francis GS, Flohr KH, et al. Effect of vasodilator therapy on mortality in chronic congestive heart failure. Results of a Veterans Administration Cooperative Study. *N Engl J Med*. 1986;314:1547-1552. doi: 10.1056/NEJM198606123142404
7. Konstam MA, Abboud FM. Ejection Fraction: Misunderstood and Overrated (Changing the Paradigm in Categorizing Heart Failure). *Circulation*. 2017;135:717-719. doi: 10.1161/CIRCULATIONAHA.116.025795
8. Mitchell P. Coupling of phosphorylation to electron and hydrogen transfer by a chemi-osmotic type of mechanism. *Nature*. 1961;191:144-148. doi: 10.1038/191144a0
9. Neubauer S. The failing heart--an engine out of fuel. *N Engl J Med*. 2007;356:1140-1151. doi: 10.1056/NEJMra063052
10. Ingwall JS. Energy metabolism in heart failure and remodelling. *Cardiovasc Res*. 2009;81:412-419. doi: 10.1093/cvr/cvn301
11. Krebs HA, Kornberg HL, Burton K. A survey of the energy transformations in living matter. *Ergeb Physiol*. 1957;49:212-298.

12. Stanley WC, Chandler MP. Energy metabolism in the normal and failing heart: potential for therapeutic interventions. *Heart Fail Rev*. 2002;7:115-130. doi: 10.1023/a:1015320423577

13. Karwi QG, Uddin GM, Ho KL, Lopaschuk GD. Loss of Metabolic Flexibility in the Failing Heart. *Front Cardiovasc Med*. 2018;5:68. doi: 10.3389/fcvm.2018.00068

14. Abumrad N, Harmon C, Ibrahimi A. Membrane transport of long-chain fatty acids: evidence for a facilitated process. *J Lipid Res*. 1998;39:2309-2318.

15. Nguyen TD, Schulze PC. Lipid in the midst of metabolic remodeling - Therapeutic implications for the failing heart. *Adv Drug Deliv Rev*. 2020;159:120-132. doi: 10.1016/j.addr.2020.08.004

16. Lopaschuk GD, Karwi QG, Tian R, Wende AR, Abel ED. Cardiac Energy Metabolism in Heart Failure. *Circ Res*. 2021;128:1487-1513. doi: 10.1161/CIRCRESAHA.121.318241

17. Meyerhof O. ENERGY RELATIONSHIPS IN GLYCOLYSIS AND PHOSPHORYLATION. *Annals of the New York Academy of Sciences*. 1944;45:377-393. doi: https://doi.org/10.1111/j.1749-6632.1944.tb47958.x

18. Cori CF. Mammalian carbohydrate metabolism. *Physiological Reviews*. 1931;11:143-275.

19. Shao D, Tian R. Glucose Transporters in Cardiac Metabolism and Hypertrophy. *Compr Physiol*. 2015;6:331-351. doi: 10.1002/cphy.c150016

20. Papandreou I, Cairns RA, Fontana L, Lim AL, Denko NC. HIF-1 mediates adaptation to hypoxia by actively downregulating mitochondrial oxygen consumption. *Cell Metab*. 2006;3:187-197. doi: 10.1016/j.cmet.2006.01.012

21. Randle PJ, Garland PB, Hales CN, Newsholme EA. The glucose fatty-acid cycle. Its role in insulin sensitivity and the metabolic disturbances of diabetes mellitus. *Lancet*. 1963;1:785-789. doi: 10.1016/s0140-6736(63)91500-9

22. Aubert G, Martin OJ, Horton JL, Lai L, Vega RB, Leone TC, Koves T, Gardell SJ, Kruger M, Hoppel CL, et al. The Failing Heart Relies on Ketone Bodies as a Fuel. *Circulation*. 2016;133:698-705. doi: 10.1161/CIRCULATIONAHA.115.017355

23. Karwi QG, Biswas D, Pulinilkunnil T, Lopaschuk GD. Myocardial Ketones Metabolism in Heart Failure. *J Card Fail*. 2020;26:998-1005. doi: 10.1016/j.cardfail.2020.04.005

24. Murashige D, Jang C, Neinast M, Edwards JJ, Cowan A, Hyman MC, Rabinowitz JD, Frankel DS, Arany Z. Comprehensive quantification of fuel use by the failing and nonfailing human heart. *Science*. 2020;370:364-368. doi: 10.1126/science.abc8861

25. Wang TJ, Larson MG, Vasan RS, Cheng S, Rhee EP, McCabe E, Lewis GD, Fox CS, Jacques PF, Fernandez C, et al. Metabolite profiles and the

risk of developing diabetes. *Nat Med*. 2011;17:448-453. doi: 10.1038/nm.2307

26. Sato K, Kashiwaya Y, Keon CA, Tsuchiya N, King MT, Radda GK, Chance B, Clarke K, Veech RL. Insulin, ketone bodies, and mitochondrial energy transduction. *FASEB J*. 1995;9:651-658.

27. Veech RL. The therapeutic implications of ketone bodies: the effects of ketone bodies in pathological conditions: ketosis, ketogenic diet, redox states, insulin resistance, and mitochondrial metabolism. *Prostaglandins Leukot Essent Fatty Acids*. 2004;70:309-319. doi: 10.1016/j.plefa.2003.09.007

28. Korvald C, Elvenes OP, Myrmel T. Myocardial substrate metabolism influences left ventricular energetics in vivo. *Am J Physiol Heart Circ Physiol*. 2000;278:H1345-1351. doi: 10.1152/ajpheart.2000.278.4.H1345

29. Veech RL. Ketone ester effects on metabolism and transcription. *J Lipid Res*. 2014;55:2004-2006. doi: 10.1194/jlr.R046292

30. ten Hove M, Lygate CA, Fischer A, Schneider JE, Sang AE, Hulbert K, Sebag-Montefiore L, Watkins H, Clarke K, Isbrandt D, et al. Reduced inotropic reserve and increased susceptibility to cardiac ischemia/reperfusion injury in phosphocreatine-deficient guanidinoacetate-N-methyltransferase-knockout mice. *Circulation*. 2005;111:2477-2485. doi: 10.1161/01.CIR.0000165147.99592.01

31. Gabr RE, El-Sharkawy AM, Schar M, Panjrath GS, Gerstenblith G, Weiss RG, Bottomley PA. Cardiac work is related to creatine kinase energy supply in human heart failure: a cardiovascular magnetic resonance spectroscopy study. *J Cardiovasc Magn Reson*. 2018;20:81. doi: 10.1186/s12968-018-0491-6

32. Nascimben L, Ingwall JS, Pauletto P, Friedrich J, Gwathmey JK, Saks V, Pessina AC, Allen PD. Creatine kinase system in failing and nonfailing human myocardium. *Circulation*. 1996;94:1894-1901. doi: 10.1161/01.cir.94.8.1894

33. Cyrus H. Fiske YS. PHOSPHOCREATINE. *Journal of Biological Chemistry*. 1929;81:629-679. doi: https://doi.org/10.1016/S0021-9258(18)63717-2

34. Gibb AA, Epstein PN, Uchida S, Zheng Y, McNally LA, Obal D, Katragadda K, Trainor P, Conklin DJ, Brittian KR, et al. Exercise-Induced Changes in Glucose Metabolism Promote Physiological Cardiac Growth. *Circulation*. 2017;136:2144-2157. doi: 10.1161/CIRCULATIONAHA.117.028274

35. Karamitsos TD, Francis JM, Myerson S, Selvanayagam JB, Neubauer S. The role of cardiovascular magnetic resonance imaging in heart failure. *J Am Coll Cardiol*. 2009;54:1407-1424. doi: 10.1016/j.jacc.2009.04.094

36. Neubauer S, Krahe T, Schindler R, Horn M, Hillenbrand H, Entzeroth C, Mader H, Kromer EP, Riegger GA, Lackner K, et al. 31P magnetic

resonance spectroscopy in dilated cardiomyopathy and coronary artery disease. Altered cardiac high-energy phosphate metabolism in heart failure. *Circulation*. 1992;86:1810-1818. doi: 10.1161/01.cir.86.6.1810

37. Ten Hove M, Neubauer S. MR spectroscopy in heart failure--clinical and experimental findings. *Heart Fail Rev*. 2007;12:48-57. doi: 10.1007/s10741-007-9003-8

38. Levelt E, Rodgers CT, Clarke WT, Mahmod M, Ariga R, Francis JM, Liu A, Wijesurendra RS, Dass S, Sabharwal N, et al. Cardiac energetics, oxygenation, and perfusion during increased workload in patients with type 2 diabetes mellitus. *European Heart Journal*. 2016;37:3461-3469a. doi: 10.1093/eurheartj/ehv442

39. Scheuermann-Freestone M, Madsen PL, Manners D, Blamire AM, Buckingham RE, Styles P, Radda GK, Neubauer S, Clarke K. Abnormal cardiac and skeletal muscle energy metabolism in patients with type 2 diabetes. *Circulation*. 2003;107:3040-3046. doi: 10.1161/01.CIR.0000072789.89096.10

40. Rayner JJ, Peterzan MA, Watson WD, Clarke WT, Neubauer S, Rodgers CT, Rider OJ. Myocardial Energetics in Obesity: Enhanced ATP Delivery Through Creatine Kinase With Blunted Stress Response. *Circulation*. 2020;141:1152-1163. doi: 10.1161/CIRCULATIONAHA.119.042770

41. Starling RC, Hammer DF, Altschuld RA. Human myocardial ATP content and in vivo contractile function. *Mol Cell Biochem*. 1998;180:171-177.

42. Beer M, Seyfarth T, Sandstede J, Landschutz W, Lipke C, Kostler H, von Kienlin M, Harre K, Hahn D, Neubauer S. Absolute concentrations of high-energy phosphate metabolites in normal, hypertrophied, and failing human myocardium measured noninvasively with (31)P-SLOOP magnetic resonance spectroscopy. *J Am Coll Cardiol*. 2002;40:1267-1274.

43. Traverse JH, Melchert P, Pierpont GL, Jones B, Crampton M, Bache RJ. Regulation of myocardial blood flow by oxygen consumption is maintained in the failing heart during exercise. *Circ Res*. 1999;84:401-408. doi: 10.1161/01.res.84.4.401

44. Ingwall JS, Weiss RG. Is the failing heart energy starved? On using chemical energy to support cardiac function. *Circ Res*. 2004;95:135-145. doi: 10.1161/01.RES.0000137170.41939.d9

45. Saupe KW, Spindler M, Hopkins JC, Shen W, Ingwall JS. Kinetic, thermodynamic, and developmental consequences of deleting creatine kinase isoenzymes from the heart. Reaction kinetics of the creatine kinase isoenzymes in the intact heart. *J Biol Chem*. 2000;275:19742-19746. doi: 10.1074/jbc.M001932200

46. Mallat Z, Philip I, Lebret M, Chatel D, Maclouf J, Tedgui A. Elevated levels of 8-iso-prostaglandin F2alpha in pericardial fluid of patients with heart failure: a potential role for in vivo oxidant stress in ventricular dilatation and progression to heart failure. *Circulation*. 1998;97:1536-1539. doi: 10.1161/01.cir.97.16.1536

47. Belch JJ, Bridges AB, Scott N, Chopra M. Oxygen free radicals and congestive heart failure. *Br Heart J*. 1991;65:245-248. doi: 10.1136/hrt.65.5.245

48. O'Rourke B, Ashok D, Liu T. Mitochondrial Ca(2+) in heart failure: Not enough or too much? *J Mol Cell Cardiol*. 2021;151:126-134. doi: 10.1016/j.yjmcc.2020.11.014

49. Tian R, Colucci WS, Arany Z, Bachschmid MM, Ballinger SW, Boudina S, Bruce JE, Busija DW, Dikalov S, Dorn GW, II, et al. Unlocking the Secrets of Mitochondria in the Cardiovascular System: Path to a Cure in Heart Failure-A Report from the 2018 National Heart, Lung, and Blood Institute Workshop. *Circulation*. 2019;140:1205-1216. doi: 10.1161/CIRCULATIONAHA.119.040551

50. Zhou B, Tian R. Mitochondrial dysfunction in pathophysiology of heart failure. *J Clin Invest*. 2018;128:3716-3726. doi: 10.1172/JCI120849

51. Tuunanen H, Engblom E, Naum A, Scheinin M, Nagren K, Airaksinen J, Nuutila P, Iozzo P, Ukkonen H, Knuuti J. Decreased myocardial free fatty acid uptake in patients with idiopathic dilated cardiomyopathy: evidence of relationship with insulin resistance and left ventricular dysfunction. *J Card Fail*. 2006;12:644-652. doi: 10.1016/j.cardfail.2006.06.005

52. Barger PM, Kelly DP. Fatty acid utilization in the hypertrophied and failing heart: molecular regulatory mechanisms. *Am J Med Sci*. 1999;318:36-42. doi: 10.1097/00000441-199907000-00006

53. Lopaschuk GD, Ussher JR, Folmes CD, Jaswal JS, Stanley WC. Myocardial fatty acid metabolism in health and disease. *Physiol Rev*. 2010;90:207-258. doi: 10.1152/physrev.00015.2009

54. Lee SH, Hadipour-Lakmehsari S, Kim DH, Di Paola M, Kuzmanov U, Shah S, Lee JJ, Kislinger T, Sharma P, Oudit GY, et al. Bioinformatic analysis of membrane and associated proteins in murine cardiomyocytes and human myocardium. *Sci Data*. 2020;7:425. doi: 10.1038/s41597-020-00762-1

55. Rosenblatt-Velin N, Montessuit C, Papageorgiou I, Terrand J, Lerch R. Postinfarction heart failure in rats is associated with upregulation of GLUT-1 and downregulation of genes of fatty acid metabolism. *Cardiovasc Res*. 2001;52:407-416. doi: 10.1016/s0008-6363(01)00393-5

56. Neglia D, De Caterina A, Marraccini P, Natali A, Ciardetti M, Vecoli C, Gastaldelli A, Ciociaro D, Pellegrini P, Testa R, et al. Impaired myocardial metabolic reserve and substrate selection flexibility during stress in patients with idiopathic dilated cardiomyopathy. *Am J Physiol Heart Circ Physiol*. 2007;293:H3270-3278. doi: 10.1152/ajpheart.00887.2007

57. Abel ED, Kaulbach HC, Tian R, Hopkins JC, Duffy J, Doetschman T, Minnemann T, Boers ME, Hadro E, Oberste-Berghaus C, et al. Cardiac hypertrophy with preserved contractile function after selective deletion of GLUT4 from the heart. *J Clin Invest*. 1999;104:1703-1714. doi: 10.1172/JCI7605

58. Sun W, Quan N, Wang L, Yang H, Chu D, Liu Q, Zhao X, Leng J, Li J. Cardiac-Specific Deletion of the Pdha1 Gene Sensitizes Heart to Toxicological Actions of Ischemic Stress. *Toxicol Sci*. 2016;151:193-203. doi: 10.1093/toxsci/kfw035

59. Swan JW, Anker SD, Walton C, Godsland IF, Clark AL, Leyva F, Stevenson JC, Coats AJ. Insulin resistance in chronic heart failure: relation to severity and etiology of heart failure. *J Am Coll Cardiol*. 1997;30:527-532. doi: 10.1016/s0735-1097(97)00185-x

60. Bedi KC, Jr., Snyder NW, Brandimarto J, Aziz M, Mesaros C, Worth AJ, Wang LL, Javaheri A, Blair IA, Margulies KB, et al. Evidence for Intramyocardial Disruption of Lipid Metabolism and Increased Myocardial Ketone Utilization in Advanced Human Heart Failure. *Circulation*. 2016;133:706-716. doi: 10.1161/CIRCULATIONAHA.115.017545

61. Ho KL, Zhang L, Wagg C, Al Batran R, Gopal K, Levasseur J, Leone T, Dyck JRB, Ussher JR, Muoio DM, et al. Increased ketone body oxidation provides additional energy for the failing heart without improving cardiac efficiency. *Cardiovasc Res*. 2019;115:1606-1616. doi: 10.1093/cvr/cvz045

62. Schugar RC, Moll AR, Andre d'Avignon D, Weinheimer CJ, Kovacs A, Crawford PA. Cardiomyocyte-specific deficiency of ketone body metabolism promotes accelerated pathological remodeling. *Mol Metab*. 2014;3:754-769. doi: 10.1016/j.molmet.2014.07.010

63. Lai L, Leone TC, Keller MP, Martin OJ, Broman AT, Nigro J, Kapoor K, Koves TR, Stevens R, Ilkayeva OR, et al. Energy metabolic reprogramming in the hypertrophied and early stage failing heart: a multisystems approach. *Circ Heart Fail*. 2014;7:1022-1031. doi: 10.1161/CIRCHEARTFAILURE.114.001469

64. Sun H, Olson KC, Gao C, Prosdocimo DA, Zhou M, Wang Z, Jeyaraj D, Youn JY, Ren S, Liu Y, et al. Catabolic Defect of Branched-Chain Amino Acids Promotes Heart Failure. *Circulation*. 2016;133:2038-2049. doi: 10.1161/CIRCULATIONAHA.115.020226

65. Neishabouri SH, Hutson SM, Davoodi J. Chronic activation of mTOR complex 1 by branched chain amino acids and organ hypertrophy. *Amino Acids*. 2015;47:1167-1182. doi: 10.1007/s00726-015-1944-y

66. Wang W, Zhang F, Xia Y, Zhao S, Yan W, Wang H, Lee Y, Li C, Zhang L, Lian K, et al. Defective branched chain amino acid catabolism contributes to cardiac dysfunction and remodeling following myocardial infarction. *Am J Physiol Heart Circ Physiol*. 2016;311:H1160-H1169. doi: 10.1152/ajpheart.00114.2016

67. Karwi QG, Zhang L, Wagg CS, Wang W, Ghandi M, Thai D, Yan H, Ussher JR, Oudit GY, Lopaschuk GD. Targeting the glucagon receptor improves cardiac function and enhances insulin sensitivity following a myocardial infarction. *Cardiovasc Diabetol*. 2019;18:1. doi: 10.1186/s12933-019-0806-4

68. Mori J, Alrob OA, Wagg CS, Harris RA, Lopaschuk GD, Oudit GY. ANG II causes insulin resistance and induces cardiac metabolic switch and inefficiency: a critical role of PDK4. *Am J Physiol Heart Circ Physiol*. 2013;304:H1103-1113. doi: 10.1152/ajpheart.00636.2012

69. Zhang L, Jaswal JS, Ussher JR, Sankaralingam S, Wagg C, Zaugg M, Lopaschuk GD. Cardiac insulin-resistance and decreased mitochondrial energy production precede the development of systolic heart failure after pressure-overload hypertrophy. *Circ Heart Fail*. 2013;6:1039-1048. doi: 10.1161/CIRCHEARTFAILURE.112.000228

70. Kass DA. Understanding HFpEF With Obesity: Will Pigs Come to the Rescue? *JACC Basic Transl Sci*. 2021;6:171-173. doi: 10.1016/j.jacbts.2020.12.010

71. Riehle C, Bauersachs J. Small animal models of heart failure. *Cardiovasc Res*. 2019;115:1838-1849. doi: 10.1093/cvr/cvz161

72. Sharp TE, 3rd, Scarborough AL, Li Z, Polhemus DJ, Hidalgo HA, Schumacher JD, Matsuura TR, Jenkins JS, Kelly DP, Goodchild TT, et al. Novel Gottingen Miniswine Model of Heart Failure With Preserved Ejection Fraction Integrating Multiple Comorbidities. *JACC Basic Transl Sci*. 2021;6:154-170. doi: 10.1016/j.jacbts.2020.11.012

73. Phan TT, Abozguia K, Nallur Shivu G, Mahadevan G, Ahmed I, Williams L, Dwivedi G, Patel K, Steendijk P, Ashrafian H, et al. Heart failure with preserved ejection fraction is characterized by dynamic impairment of active relaxation and contraction of the left ventricle on exercise and associated with myocardial energy deficiency. *J Am Coll Cardiol*. 2009;54:402-409. doi: 10.1016/j.jacc.2009.05.012

74. Mahmod M, Pal N, Rayner J, Holloway C, Raman B, Dass S, Levelt E, Ariga R, Ferreira V, Banerjee R, et al. The interplay between metabolic alterations, diastolic strain rate and exercise capacity in mild heart failure with preserved ejection fraction: a cardiovascular magnetic resonance study. *J Cardiovasc Magn Reson*. 2018;20:88. doi: 10.1186/s12968-018-0511-6

75. Djousse L, Benkeser D, Arnold A, Kizer JR, Zieman SJ, Lemaitre RN, Tracy RP, Gottdiener JS, Mozaffarian D, Siscovick DS, et al. Plasma free fatty acids and risk of heart failure: the Cardiovascular Health Study. *Circ Heart Fail*. 2013;6:964-969. doi: 10.1161/CIRCHEARTFAILURE.113.000521

76. Kenny HC, Abel ED. Heart Failure in Type 2 Diabetes Mellitus. *Circ Res*. 2019;124:121-141. doi: 10.1161/CIRCRESAHA.118.311371

77. Peterson LR, Herrero P, Schechtman KB, Racette SB, Waggoner AD, Kisrieva-Ware Z, Dence C, Klein S, Marsala J, Meyer T, et al. Effect of obesity and insulin resistance on myocardial substrate metabolism and efficiency in young women. *Circulation*. 2004;109:2191-2196. doi: 10.1161/01.CIR.0000127959.28627.F8

78. He L, Kim T, Long Q, Liu J, Wang P, Zhou Y, Ding Y, Prasain J, Wood PA, Yang Q. Carnitine palmitoyltransferase-1b deficiency aggravates pressure overload-induced cardiac hypertrophy caused by lipotoxicity. *Circulation*. 2012;126:1705-1716. doi: 10.1161/CIRCULATIONAHA.111.075978

79. Chiu HC, Kovacs A, Blanton RM, Han X, Courtois M, Weinheimer CJ, Yamada KA, Brunet S, Xu H, Nerbonne JM, et al. Transgenic expression of fatty acid transport protein 1 in the heart causes lipotoxic cardiomyopathy. *Circ Res*. 2005;96:225-233. doi: 10.1161/01.RES.0000154079.20681.B9

80. Mori J, Basu R, McLean BA, Das SK, Zhang L, Patel VB, Wagg CS, Kassiri Z, Lopaschuk GD, Oudit GY. Agonist-induced hypertrophy and diastolic dysfunction are associated with selective reduction in glucose oxidation: a metabolic contribution to heart failure with normal ejection fraction. *Circ Heart Fail*. 2012;5:493-503. doi: 10.1161/CIRCHEARTFAILURE.112.966705

81. Heather LC, Cole MA, Lygate CA, Evans RD, Stuckey DJ, Murray AJ, Neubauer S, Clarke K. Fatty acid transporter levels and palmitate oxidation rate correlate with ejection fraction in the infarcted rat heart. *Cardiovasc Res*. 2006;72:430-437. doi: 10.1016/j.cardiores.2006.08.020

82. Degens H, de Brouwer KF, Gilde AJ, Lindhout M, Willemsen PH, Janssen BJ, van der Vusse GJ, van Bilsen M. Cardiac fatty acid metabolism is preserved in the compensated hypertrophic rat heart. *Basic Res Cardiol*. 2006;101:17-26. doi: 10.1007/s00395-005-0549-0

83. Du Z, Shen A, Huang Y, Su L, Lai W, Wang P, Xie Z, Xie Z, Zeng Q, Ren H, et al. 1H-NMR-based metabolic analysis of human serum reveals novel markers of myocardial energy expenditure in heart failure patients. *PLoS One*. 2014;9:e88102. doi: 10.1371/journal.pone.0088102

84. Zordoky BN, Sung MM, Ezekowitz J, Mandal R, Han B, Bjorndahl TC, Bouatra S, Anderson T, Oudit GY, Wishart DS, et al. Metabolomic fingerprint of heart failure with preserved ejection fraction. *PLoS One*. 2015;10:e0124844. doi: 10.1371/journal.pone.0124844

85. Lopaschuk GD, Folmes CD, Stanley WC. Cardiac energy metabolism in obesity. *Circ Res*. 2007;101:335-347. doi: 10.1161/CIRCRESAHA.107.150417

86. Ruderman N, Chisholm D, Pi-Sunyer X, Schneider S. The metabolically obese, normal-weight individual revisited. *Diabetes*. 1998;47:699-713. doi: 10.2337/diabetes.47.5.699

87. Tan Y, Zhang Z, Zheng C, Wintergerst KA, Keller BB, Cai L. Mechanisms of diabetic cardiomyopathy and potential therapeutic strategies: preclinical and clinical evidence. *Nat Rev Cardiol*. 2020;17:585-607. doi: 10.1038/s41569-020-0339-2

88. Levelt E, Gulsin GS, Neubauer S, McCann GP. MECHANISMS IN ENDOCRINOLOGY: Diabetic Cardiomyopathy - Pathophysiology and Potential Metabolic Interventions. *Eur J Endocrinol*. 2018.

89. Jia G, Hill MA, Sowers JR. Diabetic Cardiomyopathy: An Update of Mechanisms Contributing to This Clinical Entity. *Circ Res*. 2018;122:624-638. doi: 10.1161/CIRCRESAHA.117.311586

90. Herrero P, Peterson LR, McGill JB, Matthew S, Lesniak D, Dence C, Gropler RJ. Increased myocardial fatty acid metabolism in patients with type 1 diabetes mellitus. *J Am Coll Cardiol*. 2006;47:598-604. doi: 10.1016/j.jacc.2005.09.030

91. Marin-Royo G, Ortega-Hernandez A, Martinez-Martinez E, Jurado-Lopez R, Luaces M, Islas F, Gomez-Garre D, Delgado-Valero B, Lagunas E, Ramchandani B, et al. The Impact of Cardiac Lipotoxicity on Cardiac Function and Mirnas Signature in Obese and Non-Obese Rats with Myocardial Infarction. *Sci Rep*. 2019;9:444. doi: 10.1038/s41598-018-36914-y

92. Wende AR, Abel ED. Lipotoxicity in the heart. *Biochim Biophys Acta*. 2010;1801:311-319. doi: 10.1016/j.bbalip.2009.09.023

93. Hardie DG. Minireview: the AMP-activated protein kinase cascade: the key sensor of cellular energy status. *Endocrinology*. 2003;144:5179-5183. doi: 10.1210/en.2003-0982

94. Graham D, Huynh NN, Hamilton CA, Beattie E, Smith RA, Cocheme HM, Murphy MP, Dominiczak AF. Mitochondria-targeted antioxidant MitoQ10 improves endothelial function and attenuates cardiac hypertrophy. *Hypertension*. 2009;54:322-328. doi: 10.1161/HYPERTENSIONAHA.109.130351

95. Mortensen SA, Rosenfeldt F, Kumar A, Dolliner P, Filipiak KJ, Pella D, Alehagen U, Steurer G, Littarru GP, Investigators QSS. The effect of coenzyme Q10 on morbidity and mortality in chronic heart failure: results from Q-SYMBIO: a randomized double-blind trial. *JACC Heart Fail*. 2014;2:641-649. doi: 10.1016/j.jchf.2014.06.008

96. Daubert MA, Yow E, Dunn G, Marchev S, Barnhart H, Douglas PS, O'Connor C, Goldstein S, Udelson JE, Sabbah HN. Novel Mitochondria-Targeting Peptide in Heart Failure Treatment: A Randomized, Placebo-Controlled Trial of Elamipretide. *Circ Heart Fail*. 2017;10. doi: 10.1161/CIRCHEARTFAILURE.117.004389

97. Lee CF, Chavez JD, Garcia-Menendez L, Choi Y, Roe ND, Chiao YA, Edgar JS, Goo YA, Goodlett DR, Bruce JE, et al. Normalization of NAD+ Redox Balance as a Therapy for Heart Failure. *Circulation*. 2016;134:883-894. doi: 10.1161/CIRCULATIONAHA.116.022495

98. Diguet N, Trammell SAJ, Tannous C, Deloux R, Piquereau J, Mougenot N, Gouge A, Gressette M, Manoury B, Blanc J, et al. Nicotinamide Riboside Preserves Cardiac Function in a Mouse Model of Dilated Cardiomyopathy.

Circulation. 2018;137:2256-2273. doi: 10.1161/CIRCULATIONAHA.116.026099

99. Abdellatif M, Trummer-Herbst V, Koser F, Durand S, Adao R, Vasques-Novoa F, Freundt JK, Voglhuber J, Pricolo MR, Kasa M, et al. Nicotinamide for the treatment of heart failure with preserved ejection fraction. *Sci Transl Med*. 2021;13. doi: 10.1126/scitranslmed.abd7064

100. Dyck GJB, Raj P, Zieroth S, Dyck JRB, Ezekowitz JA. The Effects of Resveratrol in Patients with Cardiovascular Disease and Heart Failure: A Narrative Review. *Int J Mol Sci*. 2019;20. doi: 10.3390/ijms20040904

101. Magyar K, Halmosi R, Palfi A, Feher G, Czopf L, Fulop A, Battyany I, Sumegi B, Toth K, Szabados E. Cardioprotection by resveratrol: A human clinical trial in patients with stable coronary artery disease. *Clin Hemorheol Microcirc*. 2012;50:179-187. doi: 10.3233/CH-2011-1424

102. Lewis JF, DaCosta M, Wargowich T, Stacpoole P. Effects of dichloroacetate in patients with congestive heart failure. *Clin Cardiol*. 1998;21:888-892. doi: 10.1002/clc.4960211206

103. Bersin RM, Wolfe C, Kwasman M, Lau D, Klinski C, Tanaka K, Khorrami P, Henderson GN, de Marco T, Chatterjee K. Improved hemodynamic function and mechanical efficiency in congestive heart failure with sodium dichloroacetate. *J Am Coll Cardiol*. 1994;23:1617-1624. doi: 10.1016/0735-1097(94)90665-3

104. Holubarsch CJ, Rohrbach M, Karrasch M, Boehm E, Polonski L, Ponikowski P, Rhein S. A double-blind randomized multicentre clinical trial to evaluate the efficacy and safety of two doses of etomoxir in comparison with placebo in patients with moderate congestive heart failure: the ERGO (etomoxir for the recovery of glucose oxidation) study. *Clin Sci (Lond)*. 2007;113:205-212. doi: 10.1042/CS20060307

105. Lee L, Campbell R, Scheuermann-Freestone M, Taylor R, Gunaruwan P, Williams L, Ashrafian H, Horowitz J, Fraser AG, Clarke K, et al. Metabolic modulation with perhexiline in chronic heart failure: a randomized, controlled trial of short-term use of a novel treatment. *Circulation*. 2005;112:3280-3288. doi: 10.1161/CIRCULATIONAHA.105.551457

106. Schmidt-Schweda S, Holubarsch C. First clinical trial with etomoxir in patients with chronic congestive heart failure. *Clin Sci (Lond)*. 2000;99:27-35.

107. Beadle RM, Williams LK, Kuehl M, Bowater S, Abozguia K, Leyva F, Yousef Z, Wagenmakers AJ, Thies F, Horowitz J, et al. Improvement in cardiac energetics by perhexiline in heart failure due to dilated cardiomyopathy. *JACC Heart Fail*. 2015;3:202-211. doi: 10.1016/j.jchf.2014.09.009

108. Abozguia K, Elliott P, McKenna W, Phan TT, Nallur-Shivu G, Ahmed I, Maher AR, Kaur K, Taylor J, Henning A, et al. Metabolic modulator perhexiline corrects energy deficiency and improves exercise capacity in

symptomatic hypertrophic cardiomyopathy. *Circulation*. 2010;122:1562-1569. doi: 10.1161/CIRCULATIONAHA.109.934059

109. Tuunanen H, Engblom E, Naum A, Nagren K, Hesse B, Airaksinen KE, Nuutila P, Iozzo P, Ukkonen H, Opie LH, et al. Free fatty acid depletion acutely decreases cardiac work and efficiency in cardiomyopathic heart failure. *Circulation*. 2006;114:2130-2137. doi: 10.1161/CIRCULATIONAHA.106.645184

110. Lopaschuk GD. Metabolic Modulators in Heart Disease: Past, Present, and Future. *Can J Cardiol*. 2017;33:838-849. doi: 10.1016/j.cjca.2016.12.013

111. Fragasso G, Palloshi A, Puccetti P, Silipigni C, Rossodivita A, Pala M, Calori G, Alfieri O, Margonato A. A randomized clinical trial of trimetazidine, a partial free fatty acid oxidation inhibitor, in patients with heart failure. *J Am Coll Cardiol*. 2006;48:992-998. doi: 10.1016/j.jacc.2006.03.060

112. Fragasso G, Perseghin G, De Cobelli F, Esposito A, Palloshi A, Lattuada G, Scifo P, Calori G, Del Maschio A, Margonato A. Effects of metabolic modulation by trimetazidine on left ventricular function and phosphocreatine/adenosine triphosphate ratio in patients with heart failure. *Eur Heart J*. 2006;27:942-948. doi: 10.1093/eurheartj/ehi816

113. Hirsch GA, Bottomley PA, Gerstenblith G, Weiss RG. Allopurinol acutely increases adenosine triphospate energy delivery in failing human hearts. *J Am Coll Cardiol*. 2012;59:802-808. doi: 10.1016/j.jacc.2011.10.895

114. Zamora E, Diez-Lopez C, Lupon J, de Antonio M, Domingo M, Santesmases J, Troya MI, Diez-Quevedo C, Altimir S, Bayes-Genis A. Weight Loss in Obese Patients With Heart Failure. *J Am Heart Assoc*. 2016;5:e002468. doi: 10.1161/JAHA.115.002468

115. Cohen JB, Schrauben SJ, Zhao L, Basso MD, Cvijic ME, Li Z, Yarde M, Wang Z, Bhattacharya PT, Chirinos DA, et al. Clinical Phenogroups in Heart Failure With Preserved Ejection Fraction: Detailed Phenotypes, Prognosis, and Response to Spironolactone. *JACC Heart Fail*. 2020;8:172-184. doi: 10.1016/j.jchf.2019.09.009

116. Shah SJ, Katz DH, Selvaraj S, Burke MA, Yancy CW, Gheorghiade M, Bonow RO, Huang CC, Deo RC. Phenomapping for novel classification of heart failure with preserved ejection fraction. *Circulation*. 2015;131:269-279. doi: 10.1161/CIRCULATIONAHA.114.010637

117. Kitzman DW, Brubaker P, Morgan T, Haykowsky M, Hundley G, Kraus WE, Eggebeen J, Nicklas BJ. Effect of Caloric Restriction or Aerobic Exercise Training on Peak Oxygen Consumption and Quality of Life in Obese Older Patients With Heart Failure With Preserved Ejection Fraction: A Randomized Clinical Trial. *JAMA*. 2016;315:36-46. doi: 10.1001/jama.2015.17346

118. Ramani GV, McCloskey C, Ramanathan RC, Mathier MA. Safety and efficacy of bariatric surgery in morbidly obese patients with severe systolic heart failure. *Clin Cardiol*. 2008;31:516-520. doi: 10.1002/clc.20315

119. El Hajj EC, El Hajj MC, Sykes B, Lamicq M, Zile MR, Malcolm R, O'Neil PM, Litwin SE. Pragmatic Weight Management Program for Patients With Obesity and Heart Failure With Preserved Ejection Fraction. *J Am Heart Assoc*. 2021;10:e022930. doi: 10.1161/JAHA.121.022930

120. Heidenreich PA, Bozkurt B, Aguilar D, Allen LA, Byun JJ, Colvin MM, Deswal A, Drazner MH, Dunlay SM, Evers LR, et al. 2022 AHA/ACC/HFSA Guideline for the Management of Heart Failure: A Report of the American College of Cardiology/American Heart Association Joint Committee on Clinical Practice Guidelines. *J Am Coll Cardiol*. 2022;79:e263-e421. doi: 10.1016/j.jacc.2021.12.012

121. McDonagh TA, Metra M, Adamo M, Gardner RS, Baumbach A, Bohm M, Burri H, Butler J, Celutkiene J, Chioncel O, et al. 2021 ESC Guidelines for the diagnosis and treatment of acute and chronic heart failure. *Eur Heart J*. 2021;42:3599-3726. doi: 10.1093/eurheartj/ehab368

122. Taegtmeyer H, Young ME, Lopaschuk GD, Abel ED, Brunengraber H, Darley-Usmar V, Des Rosiers C, Gerszten R, Glatz JF, Griffin JL, et al. Assessing Cardiac Metabolism: A Scientific Statement From the American Heart Association. *Circ Res*. 2016;118:1659-1701. doi: 10.1161/RES.0000000000000097

123. Grothues F, Smith GC, Moon JC, Bellenger NG, Collins P, Klein HU, Pennell DJ. Comparison of interstudy reproducibility of cardiovascular magnetic resonance with two-dimensional echocardiography in normal subjects and in patients with heart failure or left ventricular hypertrophy. *Am J Cardiol*. 2002;90:29-34. doi: 10.1016/s0002-9149(02)02381-0

124. Pennell DJ. Cardiovascular magnetic resonance: twenty-first century solutions in cardiology. *Clin Med (Lond)*. 2003;3:273-278. doi: 10.7861/clinmedicine.3-3-273

125. Schulz-Menger J, Bluemke DA, Bremerich J, Flamm SD, Fogel MA, Friedrich MG, Kim RJ, von Knobelsdorff-Brenkenhoff F, Kramer CM, Pennell DJ, et al. Standardized image interpretation and post-processing in cardiovascular magnetic resonance - 2020 update : Society for Cardiovascular Magnetic Resonance (SCMR): Board of Trustees Task Force on Standardized Post-Processing. *J Cardiovasc Magn Reson*. 2020;22:19. doi: 10.1186/s12968-020-00610-6

126. Bizino MB, Hammer S, Lamb HJ. Metabolic imaging of the human heart: clinical application of magnetic resonance spectroscopy. *Heart*. 2014;100:881-890. doi: 10.1136/heartjnl-2012-302546

127. Rial B, Robson MD, Neubauer S, Schneider JE. Rapid quantification of myocardial lipid content in humans using single breath-hold 1H MRS at 3 Tesla. *Magn Reson Med*. 2011;66:619-624. doi: 10.1002/mrm.23011

128. McGavock JM, Lingvay I, Zib I, Tillery T, Salas N, Unger R, Levine BD, Raskin P, Victor RG, Szczepaniak LS. Cardiac steatosis in diabetes mellitus: a 1H-magnetic resonance spectroscopy study. *Circulation*. 2007;116:1170-1175. doi: 10.1161/CIRCULATIONAHA.106.645614

129. Wei J, Nelson MD, Szczepaniak EW, Smith L, Mehta PK, Thomson LE, Berman DS, Li D, Bairey Merz CN, Szczepaniak LS. Myocardial steatosis as a possible mechanistic link between diastolic dysfunction and coronary microvascular dysfunction in women. *Am J Physiol Heart Circ Physiol*. 2016;310:H14-19. doi: 10.1152/ajpheart.00612.2015

130. Ordidge RJ, Mansfield P, Lohman JA, Prime SB. Volume selection using gradients and selective pulses. *Ann N Y Acad Sci*. 1987;508:376-385. doi: 10.1111/j.1749-6632.1987.tb32919.x

131. Frahm J, Bruhn H, Gyngell ML, Merboldt KD, Hanicke W, Sauter R. Localized high-resolution proton NMR spectroscopy using stimulated echoes: initial applications to human brain in vivo. *Magn Reson Med*. 1989;9:79-93. doi: 10.1002/mrm.1910090110

132. Holloway CJ, Suttie J, Dass S, Neubauer S. Clinical cardiac magnetic resonance spectroscopy. *Prog Cardiovasc Dis*. 2011;54:320-327. doi: 10.1016/j.pcad.2011.08.002

133. Bottomley PA. Noninvasive study of high-energy phosphate metabolism in human heart by depth-resolved 31P NMR spectroscopy. *Science*. 1985;229:769-772. doi: 10.1126/science.4023711

134. Tyler DJ, Emmanuel Y, Cochlin LE, Hudsmith LE, Holloway CJ, Neubauer S, Clarke K, Robson MD. Reproducibility of 31P cardiac magnetic resonance spectroscopy at 3 T. *Nmr Biomed*. 2009;22:405-413. doi: 10.1002/nbm.1350

135. Bottomley PA. MR spectroscopy of the human heart: the status and the challenges. *Radiology*. 1994;191:593-612. doi: 10.1148/radiology.191.3.8184033

136. Lamb HJ, Doornbos J, den Hollander JA, Luyten PR, Beyerbacht HP, van der Wall EE, de Roos A. Reproducibility of human cardiac 31P-NMR spectroscopy. *Nmr Biomed*. 1996;9:217-227. doi: 10.1002/(SICI)1099-1492(199608)9:5<217::AID-NBM419>3.0.CO;2-G

137. von Kienlin M, Beer M, Greiser A, Hahn D, Harre K, Kostler H, Landschutz W, Pabst T, Sandstede J, Neubauer S. Advances in human cardiac 31P-MR spectroscopy: SLOOP and clinical applications. *J Magn Reson Imaging*. 2001;13:521-527. doi: 10.1002/jmri.1074

138. Bottomley PA, Ouwerkerk R, Lee RF, Weiss RG. Four-angle saturation transfer (FAST) method for measuring creatine kinase reaction rates in vivo. *Magn Reson Med*. 2002;47:850-863. doi: 10.1002/mrm.10130

139. Ruffolo RR, Jr. The pharmacology of dobutamine. *Am J Med Sci*. 1987;294:244-248. doi: 10.1097/00000441-198710000-00005

140. Rider OJ, Apps A, Miller J, Lau JYC, Lewis AJM, Peterzan MA, Dodd MS, Lau AZ, Trumper C, Gallagher FA, et al. Noninvasive In Vivo Assessment of Cardiac Metabolism in the Healthy and Diabetic Human Heart Using Hyperpolarized (13)C MRI. *Circ Res*. 2020;126:725-736. doi: 10.1161/CIRCRESAHA.119.316260

141. Peterson LR, Gropler RJ. Radionuclide imaging of myocardial metabolism. *Circ Cardiovasc Imaging*. 2010;3:211-222. doi: 10.1161/CIRCIMAGING.109.860593

142. Osterholt M, Sen S, Dilsizian V, Taegtmeyer H. Targeted metabolic imaging to improve the management of heart disease. *JACC Cardiovasc Imaging*. 2012;5:214-226. doi: 10.1016/j.jcmg.2011.11.009

143. Dormehl IC, Hugo N, Rossouw D, White A, Feinendegen LE. Planar myocardial imaging in the baboon model with iodine-123-15-(iodophenyl)pentadecanoic acid (IPPA) and iodine-123-15-(P-iodophenyl)-3-R,S-methylpentadecanoic acid (BMIPP), using time-activity curves for evaluation of metabolism. *Nucl Med Biol*. 1995;22:837-847. doi: 10.1016/0969-8051(95)00015-p

144. Eckelman WC, Babich JW. Synthesis and validation of fatty acid analogs radiolabeled by nonisotopic substitution. *J Nucl Cardiol*. 2007;14:S100-109. doi: 10.1016/j.nuclcard.2007.02.014

145. Botker HE, Bottcher M, Schmitz O, Gee A, Hansen SB, Cold GE, Nielsen TT, Gjedde A. Glucose uptake and lumped constant variability in normal human hearts determined with [18F]fluorodeoxyglucose. *J Nucl Cardiol*. 1997;4:125-132. doi: 10.1016/s1071-3581(97)90061-1

146. Hariharan R, Bray M, Ganim R, Doenst T, Goodwin GW, Taegtmeyer H. Fundamental limitations of [18F]2-deoxy-2-fluoro-D-glucose for assessing myocardial glucose uptake. *Circulation*. 1995;91:2435-2444. doi: 10.1161/01.cir.91.9.2435

147. Prize TN. The Nobel Prize. https://www.nobelprize.org/prizes/lists/all-nobel-prizes/. 2022. Accessed 17 August.

148. Abbara S, Arbab-Zadeh A, Callister TQ, Desai MY, Mamuya W, Thomson L, Weigold WG. SCCT guidelines for performance of coronary computed tomographic angiography: a report of the Society of Cardiovascular Computed Tomography Guidelines Committee. *J Cardiovasc Comput Tomogr*. 2009;3:190-204. doi: 10.1016/j.jcct.2009.03.004

149. Leipsic J, Abbara S, Achenbach S, Cury R, Earls JP, Mancini GJ, Nieman K, Pontone G, Raff GL. SCCT guidelines for the interpretation and reporting of coronary CT angiography: a report of the Society of Cardiovascular Computed Tomography Guidelines Committee. *J Cardiovasc Comput Tomogr*. 2014;8:342-358. doi: 10.1016/j.jcct.2014.07.003

150. Purvis LAB, Clarke WT, Biasiolli L, Valkovic L, Robson MD, Rodgers CT. OXSA: An open-source magnetic resonance spectroscopy analysis toolbox in MATLAB. *PLoS One*. 2017;12:e0185356. doi: 10.1371/journal.pone.0185356

151. Tyler DJ, Emmanuel Y, Cochlin LE, Hudsmith LE, Holloway CJ, Neubauer S, Clarke K, Robson MD. Reproducibility of 31P cardiac magnetic resonance spectroscopy at 3 T. *NMR in Biomedicine*. 2009;22:405-413. doi: 10.1002/nbm.1350

152. Krafft AJ, Loeffler RB, Song R, Tipirneni-Sajja A, McCarville MB, Robson MD, Hankins JS, Hillenbrand CM. Quantitative ultrashort echo time imaging for assessment of massive iron overload at 1.5 and 3 Tesla. *Magn Reson Med*. 2017;78:1839-1851. doi: 10.1002/mrm.26592

153. Hansen MS, Sorensen TS, Arai AE, Kellman P. Retrospective reconstruction of high temporal resolution cine images from real-time MRI using iterative motion correction. *Magn Reson Med*. 2012;68:741-750. doi: 10.1002/mrm.23284

154. Piechnik SK, Ferreira VM, Dall'Armellina E, Cochlin LE, Greiser A, Neubauer S, Robson MD. Shortened Modified Look-Locker Inversion recovery (ShMOLLI) for clinical myocardial T1-mapping at 1.5 and 3 T within a 9 heartbeat breathhold. *J Cardiovasc Magn Reson*. 2010;12:69. doi: 10.1186/1532-429X-12-69

155. Ferreira VM, Wijesurendra RS, Liu A, Greiser A, Casadei B, Robson MD, Neubauer S, Piechnik SK. Systolic ShMOLLI myocardial T1-mapping for improved robustness to partial-volume effects and applications in tachyarrhythmias. *J Cardiovasc Magn Reson*. 2015;17:77. doi: 10.1186/s12968-015-0182-5

156. Ferreira VM, Piechnik SK, Dall'Armellina E, Karamitsos TD, Francis JM, Ntusi N, Holloway C, Choudhury RP, Kardos A, Robson MD, et al. T(1) mapping for the diagnosis of acute myocarditis using CMR: comparison to T2-weighted and late gadolinium enhanced imaging. *JACC Cardiovasc Imaging*. 2013;6:1048-1058. doi: 10.1016/j.jcmg.2013.03.008

157. Ferreira VM, Piechnik SK, Dall'Armellina E, Karamitsos TD, Francis JM, Choudhury RP, Friedrich MG, Robson MD, Neubauer S. Non-contrast T1-mapping detects acute myocardial edema with high diagnostic accuracy: a comparison to T2-weighted cardiovascular magnetic resonance. *J Cardiovasc Magn Reson*. 2012;14:42. doi: 10.1186/1532-429X-14-42

158. Zhang Q, Hann E, Werys K, Wu C, Popescu I, Lukaschuk E, Barutcu A, Ferreira VM, Piechnik SK. Deep learning with attention supervision for automated motion artefact detection in quality control of cardiac T1-mapping. *Artif Intell Med*. 2020;110:101955. doi: 10.1016/j.artmed.2020.101955

159. Carapella V, Puchta H, Lukaschuk E, Marini C, Werys K, Neubauer S, Ferreira VM, Piechnik SK. Standardized image post-processing of cardiovascular magnetic resonance T1-mapping reduces variability and improves accuracy and consistency in myocardial tissue characterization. *Int J Cardiol*. 2020;298:128-134. doi: 10.1016/j.ijcard.2019.08.058

160. Stuber M, Spiegel MA, Fischer SE, Scheidegger MB, Danias PG, Pedersen EM, Boesiger P. Single breath-hold slice-following CSPAMM myocardial tagging. *MAGMA*. 1999;9:85-91.

161. Kotecha T, Martinez-Naharro A, Boldrini M, Knight D, Hawkins P, Kalra S, Patel D, Coghlan G, Moon J, Plein S, et al. Automated Pixel-Wise Quantitative Myocardial Perfusion Mapping by CMR to Detect Obstructive

Coronary Artery Disease and Coronary Microvascular Dysfunction: Validation Against Invasive Coronary Physiology. *JACC Cardiovasc Imaging*. 2019;12:1958-1969. doi: 10.1016/j.jcmg.2018.12.022

162. Kellman P, Hansen MS, Nielles-Vallespin S, Nickander J, Themudo R, Ugander M, Xue H. Myocardial perfusion cardiovascular magnetic resonance: optimized dual sequence and reconstruction for quantification. *J Cardiovasc Magn Reson*. 2017;19:43. doi: 10.1186/s12968-017-0355-5

163. Cerqueira MD, Weissman NJ, Dilsizian V, Jacobs AK, Kaul S, Laskey WK, Pennell DJ, Rumberger JA, Ryan T, Verani MS, et al. Standardized myocardial segmentation and nomenclature for tomographic imaging of the heart. A statement for healthcare professionals from the Cardiac Imaging Committee of the Council on Clinical Cardiology of the American Heart Association. *Int J Cardiovasc Imaging*. 2002;18:539-542.

164. White SK, Sado DM, Fontana M, Banypersad SM, Maestrini V, Flett AS, Piechnik SK, Robson MD, Hausenloy DJ, Sheikh AM, et al. T1 mapping for myocardial extracellular volume measurement by CMR: bolus only versus primed infusion technique. *JACC Cardiovasc Imaging*. 2013;6:955-962. doi: 10.1016/j.jcmg.2013.01.011

165. Robinson S, Rana B, Oxborough D, Steeds R, Monaghan M, Stout M, Pearce K, Harkness A, Ring L, Paton M, et al. A practical guideline for performing a comprehensive transthoracic echocardiogram in adults: the British Society of Echocardiography minimum dataset. *Echo Res Pract*. 2020;7:G59-G93. doi: 10.1530/ERP-20-0026

166. Schiller NB, Shah PM, Crawford M, DeMaria A, Devereux R, Feigenbaum H, Gutgesell H, Reichek N, Sahn D, Schnittger I, et al. Recommendations for quantitation of the left ventricle by two-dimensional echocardiography. American Society of Echocardiography Committee on Standards, Subcommittee on Quantitation of Two-Dimensional Echocardiograms. *J Am Soc Echocardiogr*. 1989;2:358-367. doi: 10.1016/s0894-7317(89)80014-8

167. Galderisi M, Cosyns B, Edvardsen T, Cardim N, Delgado V, Di Salvo G, Donal E, Sade LE, Ernande L, Garbi M, et al. Standardization of adult transthoracic echocardiography reporting in agreement with recent chamber quantification, diastolic function, and heart valve disease recommendations: an expert consensus document of the European Association of Cardiovascular Imaging. *Eur Heart J Cardiovasc Imaging*. 2017;18:1301-1310. doi: 10.1093/ehjci/jex244

168. Borg G, Dahlstrom H. A pilot study of perceived exertion and physical working capacity. *Acta Soc Med Ups*. 1962;67:21-27.

169. Laboratories ATSCoPSfCPF. ATS statement: guidelines for the six-minute walk test. *Am J Respir Crit Care Med*. 2002;166:111-117. doi: 10.1164/ajrccm.166.1.at1102

170. Green CP, Porter CB, Bresnahan DR, Spertus JA. Development and evaluation of the Kansas City Cardiomyopathy Questionnaire: a new health

status measure for heart failure. *J Am Coll Cardiol*. 2000;35:1245-1255. doi: 10.1016/s0735-1097(00)00531-3

171. Roger VL. Epidemiology of Heart Failure: A Contemporary Perspective. *Circ Res*. 2021;128:1421-1434. doi: 10.1161/CIRCRESAHA.121.318172

172. Fordyce CB, Roe MT, Ahmad T, Libby P, Borer JS, Hiatt WR, Bristow MR, Packer M, Wasserman SM, Braunstein N, et al. Cardiovascular drug development: is it dead or just hibernating? *J Am Coll Cardiol*. 2015;65:1567-1582. doi: 10.1016/j.jacc.2015.03.016

173. Van Nuys KE, Xie Z, Tysinger B, Hlatky MA, Goldman DP. Innovation in Heart Failure Treatment: Life Expectancy, Disability, and Health Disparities. *JACC Heart Fail*. 2018;6:401-409. doi: 10.1016/j.jchf.2017.12.006

174. Zinman B, Wanner C, Lachin JM, Fitchett D, Bluhmki E, Hantel S, Mattheus M, Devins T, Johansen OE, Woerle HJ, et al. Empagliflozin, Cardiovascular Outcomes, and Mortality in Type 2 Diabetes. *N Engl J Med*. 2015;373:2117-2128. doi: 10.1056/NEJMoa1504720

175. Maddox TM, Januzzi JL, Jr., Allen LA, Breathett K, Butler J, Davis LL, Fonarow GC, Ibrahim NE, Lindenfeld J, Masoudi FA, et al. 2021 Update to the 2017 ACC Expert Consensus Decision Pathway for Optimization of Heart Failure Treatment: Answers to 10 Pivotal Issues About Heart Failure With Reduced Ejection Fraction: A Report of the American College of Cardiology Solution Set Oversight Committee. *J Am Coll Cardiol*. 2021;77:772-810. doi: 10.1016/j.jacc.2020.11.022

176. Kosiborod MN, Jhund PS, Docherty KF, Diez M, Petrie MC, Verma S, Nicolau JC, Merkely B, Kitakaze M, DeMets DL, et al. Effects of Dapagliflozin on Symptoms, Function, and Quality of Life in Patients With Heart Failure and Reduced Ejection Fraction: Results From the DAPA-HF Trial. *Circulation*. 2020;141:90-99. doi: 10.1161/CIRCULATIONAHA.119.044138

177. Butler J, Anker SD, Filippatos G, Khan MS, Ferreira JP, Pocock SJ, Giannetti N, Januzzi JL, Pina IL, Lam CSP, et al. Empagliflozin and health-related quality of life outcomes in patients with heart failure with reduced ejection fraction: the EMPEROR-Reduced trial. *Eur Heart J*. 2021;42:1203-1212. doi: 10.1093/eurheartj/ehaa1007

178. Packer M, Anker SD, Butler J, Filippatos G, Pocock SJ, Carson P, Januzzi J, Verma S, Tsutsui H, Brueckmann M, et al. Cardiovascular and Renal Outcomes with Empagliflozin in Heart Failure. *N Engl J Med*. 2020;383:1413-1424. doi: 10.1056/NEJMoa2022190

179. McMurray JJV, Solomon SD, Inzucchi SE, Kober L, Kosiborod MN, Martinez FA, Ponikowski P, Sabatine MS, Anand IS, Belohlavek J, et al. Dapagliflozin in Patients with Heart Failure and Reduced Ejection Fraction. *N Engl J Med*. 2019;381:1995-2008. doi: 10.1056/NEJMoa1911303

180. Bhatt DL, Szarek M, Steg PG, Cannon CP, Leiter LA, McGuire DK, Lewis JB, Riddle MC, Voors AA, Metra M, et al. Sotagliflozin in Patients with

Diabetes and Recent Worsening Heart Failure. *N Engl J Med*. 2021;384:117-128. doi: 10.1056/NEJMoa2030183

181. Zhou L, Cryan EV, D'Andrea MR, Belkowski S, Conway BR, Demarest KT. Human cardiomyocytes express high level of Na+/glucose cotransporter 1 (SGLT1). *J Cell Biochem*. 2003;90:339-346. doi: 10.1002/jcb.10631

182. Abdurrachim D, Manders E, Nicolay K, Mayoux E, Prompers JJ. Single dose of empagliflozin increases in vivo cardiac energy status in diabetic db/db mice. *Cardiovasc Res*. 2018. doi: 10.1093/cvr/cvy246

183. Abdurrachim D, Teo XQ, Woo CC, Chan WX, Lalic J, Lam CSP, Lee PTH. Empagliflozin lowers myocardial ketone utilization while preserving glucose utilization in diabetic hypertensive heart disease: A hyperpolarized (13) C magnetic resonance spectroscopy study. *Diabetes Obes Metab*. 2018. doi: 10.1111/dom.13536

184. Byrne NJ, Parajuli, N., Levasseur, J.L., Boisvenue, J., Beker, D., Masson, G., Fedak, P.W.M., Verma, S., Dyck, J.R.B. Empagliflozin Prevents Worsening of Cardiac Function in an Experimental Model of Pressure Overload-Induced Heart Failure. *JACC Basic To Translational Science*. 2017. doi: 10.1016/j.jacbts.2017.07.003

185. Santos-Gallego CG, Ibanez JAR, Antonio RS, Ishikawa K, Watanabe S, Botija MBP, Salvo AJS, Hajjar R, Fuster V, Badimon J. Empagliflozin Induces a Myocardial Metabolic Shift from Glucose Consumption to Ketone Metabolism That Mitigates Adverse Cardiac Remodeling and Improves Myocardial Contractility. *Journal of the American College of Cardiology*. 2018;71:674-674. doi: 10.1016/S0735-1097(18)31215-4

186. Verma S, Rawat S, Ho KL, Wagg CS, Zhang L, Teoh H, Dyck JE, Uddin GM, Oudit GY, Mayoux E, et al. Empagliflozin Increases Cardiac Energy Production in Diabetes: Novel Translational Insights Into the Heart Failure Benefits of SGLT2 Inhibitors. *JACC Basic Transl Sci*. 2018;3:575-587. doi: 10.1016/j.jacbts.2018.07.006

187. Ferrannini E, Muscelli E, Frascerra S, Baldi S, Mari A, Heise T, Broedl UC, Woerle HJ. Metabolic response to sodium-glucose cotransporter 2 inhibition in type 2 diabetic patients. *J Clin Invest*. 2014;124:499-508. doi: 10.1172/JCI72227

188. Ferrannini E, Mark M, Mayoux E. CV Protection in the EMPA-REG OUTCOME Trial: A "Thrifty Substrate" Hypothesis. *Diabetes Care*. 2016;39:1108-1114. doi: 10.2337/dc16-0330

189. Thirunavukarasu S, Jex N, Chowdhary A, Hassan IU, Straw S, Craven TP, Gorecka M, Broadbent D, Swoboda P, Witte KK, et al. Empagliflozin Treatment Is Associated With Improvements in Cardiac Energetics and Function and Reductions in Myocardial Cellular Volume in Patients With Type 2 Diabetes. *Diabetes*. 2021;70:2810-2822. doi: 10.2337/db21-0270

190. Gaborit B, Ancel P, Abdullah AE, Maurice F, Abdesselam I, Calen A, Soghomonian A, Houssays M, Varlet I, Eisinger M, et al. Effect of

empagliflozin on ectopic fat stores and myocardial energetics in type 2 diabetes: the EMPACEF study. *Cardiovasc Diabetol*. 2021;20:57. doi: 10.1186/s12933-021-01237-2

191. Kramer CM, Barkhausen J, Bucciarelli-Ducci C, Flamm SD, Kim RJ, Nagel E. Standardized cardiovascular magnetic resonance imaging (CMR) protocols: 2020 update. *J Cardiovasc Magn Reson*. 2020;22:17. doi: 10.1186/s12968-020-00607-1

192. Treibel TA, Kozor R, Schofield R, Benedetti G, Fontana M, Bhuva AN, Sheikh A, Lopez B, Gonzalez A, Manisty C, et al. Reverse Myocardial Remodeling Following Valve Replacement in Patients With Aortic Stenosis. *J Am Coll Cardiol*. 2018;71:860-871. doi: 10.1016/j.jacc.2017.12.035

193. Neubauer S, Horn M, Pabst T, Godde M, Lubke D, Jilling B, Hahn D, Ertl G. Contributions of 31P-magnetic resonance spectroscopy to the understanding of dilated heart muscle disease. *Eur Heart J*. 1995;16 Suppl O:115-118.

194. Murthy VL, Reis JP, Pico AR, Kitchen R, Lima JAC, Lloyd-Jones D, Allen NB, Carnethon M, Lewis GD, Nayor M, et al. Comprehensive Metabolic Phenotyping Refines Cardiovascular Risk in Young Adults. *Circulation*. 2020;142:2110-2127. doi: 10.1161/CIRCULATIONAHA.120.047689

195. Olson RE. Myocardial metabolism in congestive heart failure. *J Chronic Dis*. 1959;9:442-464. doi: 10.1016/0021-9681(59)90172-9

196. Nielsen R, Moller N, Gormsen LC, Tolbod LP, Hansson NH, Sorensen J, Harms HJ, Frokiaer J, Eiskjaer H, Jespersen NR, et al. Cardiovascular Effects of Treatment With the Ketone Body 3-Hydroxybutyrate in Chronic Heart Failure Patients. *Circulation*. 2019;139:2129-2141. doi: 10.1161/CIRCULATIONAHA.118.036459

197. Mudaliar S, Alloju S, Henry RR. Can a Shift in Fuel Energetics Explain the Beneficial Cardiorenal Outcomes in the EMPA-REG OUTCOME Study? A Unifying Hypothesis. *Diabetes Care*. 2016;39:1115-1122. doi: 10.2337/dc16-0542

198. Moreau D, Clauw F, Martine L, Grynberg A, Rochette L, Demaison L. Effects of amiodarone on cardiac function and mitochondrial oxidative phosphorylation during ischemia and reperfusion. *Mol Cell Biochem*. 1999;194:291-300. doi: 10.1023/a:1006935323491

199. Schaefer S. Cardiovascular applications of nuclear magnetic resonance spectroscopy. *Am J Cardiol*. 1989;64:38E-45E. doi: 10.1016/0002-9149(89)90733-9

200. Kappel BA, Lehrke M, Schutt K, Artati A, Adamski J, Lebherz C, Marx N. Effect of Empagliflozin on the Metabolic Signature of Patients With Type 2 Diabetes Mellitus and Cardiovascular Disease. *Circulation*. 2017;136:969-972. doi: 10.1161/CIRCULATIONAHA.117.029166

201. Doehner W, Frenneaux M, Anker SD. Metabolic impairment in heart failure: the myocardial and systemic perspective. *J Am Coll Cardiol*. 2014;64:1388-1400. doi: 10.1016/j.jacc.2014.04.083

202. Gupte AA, Hamilton DJ, Cordero-Reyes AM, Youker KA, Yin Z, Estep JD, Stevens RD, Wenner B, Ilkayeva O, Loebe M, et al. Mechanical unloading promotes myocardial energy recovery in human heart failure. *Circ Cardiovasc Genet*. 2014;7:266-276. doi: 10.1161/CIRCGENETICS.113.000404

203. Wende AR, Brahma, M.K., McGinnis, G.R., Young, M.E. Metabolic Origins of Heart Failure. *JACC Basic To Translational Science*. 2017;2:297-310.

204. Lauritsen KM, Nielsen BRR, Tolbod LP, Johannsen M, Hansen J, Hansen TK, Wiggers H, Moller N, Gormsen LC, Sondergaard E. SGLT2 Inhibition Does Not Affect Myocardial Fatty Acid Oxidation or Uptake, but Reduces Myocardial Glucose Uptake and Blood Flow in Individuals With Type 2 Diabetes: A Randomized Double-Blind, Placebo-Controlled Crossover Trial. *Diabetes*. 2021;70:800-808. doi: 10.2337/db20-0921

205. Oldgren J, Laurila S, Akerblom A, Latva-Rasku A, Rebelos E, Isackson H, Saarenhovi M, Eriksson O, Heurling K, Johansson E, et al. Effects of 6 weeks of treatment with dapagliflozin, a sodium-glucose co-transporter-2 inhibitor, on myocardial function and metabolism in patients with type 2 diabetes: A randomized, placebo-controlled, exploratory study. *Diabetes Obes Metab*. 2021;23:1505-1517. doi: 10.1111/dom.14363

206. Cameron D, Soto-Mota A, Willis DR, Ellis J, Procter NEK, Greenwood R, Saunders N, Schulte RF, Vassiliou VS, Tyler DJ, et al. Evaluation of Acute Supplementation With the Ketone Ester (R)-3-Hydroxybutyl-(R)-3-Hydroxybutyrate (deltaG) in Healthy Volunteers by Cardiac and Skeletal Muscle (31)P Magnetic Resonance Spectroscopy. *Front Physiol*. 2022;13:793987. doi: 10.3389/fphys.2022.793987

207. Verma S, Mazer CD, Yan AT, Mason T, Garg V, Teoh H, Zuo F, Quan A, Farkouh ME, Fitchett DH, et al. Effect of Empagliflozin on Left Ventricular Mass in Patients With Type 2 Diabetes Mellitus and Coronary Artery Disease: The EMPA-HEART CardioLink-6 Randomized Clinical Trial. *Circulation*. 2019;140:1693-1702. doi: 10.1161/CIRCULATIONAHA.119.042375

208. Lee MMY, Brooksbank KJM, Wetherall K, Mangion K, Roditi G, Campbell RT, Berry C, Chong V, Coyle L, Docherty KF, et al. Effect of Empagliflozin on Left Ventricular Volumes in Patients With Type 2 Diabetes, or Prediabetes, and Heart Failure With Reduced Ejection Fraction (SUGAR-DM-HF). *Circulation*. 2021;143:516-525. doi: 10.1161/CIRCULATIONAHA.120.052186

209. Santos-Gallego CG, Vargas-Delgado AP, Requena-Ibanez JA, Garcia-Ropero A, Mancini D, Pinney S, Macaluso F, Sartori S, Roque M, Sabatel-Perez F, et al. Randomized Trial of Empagliflozin in Nondiabetic Patients

With Heart Failure and Reduced Ejection Fraction. *J Am Coll Cardiol*. 2021;77:243-255. doi: 10.1016/j.jacc.2020.11.008

210. Weir RAP, Clements S, Steedman T, Dargie HJ, McMurray JJV. Prognostic value of cardiac magnetic resonance parameters and biomarkers following myocardial infarction; 10-year follow-up of the Eplerenone Remodelling in Myocardial Infarction without Heart Failure trial. *Eur J Heart Fail*. 2021. doi: 10.1002/ejhf.2402

211. Shimazu T, Hirschey MD, Newman J, He W, Shirakawa K, Le Moan N, Grueter CA, Lim H, Saunders LR, Stevens RD, et al. Suppression of oxidative stress by beta-hydroxybutyrate, an endogenous histone deacetylase inhibitor. *Science*. 2013;339:211-214. doi: 10.1126/science.1227166

212. Packer M. Autophagy stimulation and intracellular sodium reduction as mediators of the cardioprotective effect of sodium-glucose cotransporter 2 inhibitors. *Eur J Heart Fail*. 2020;22:618-628. doi: 10.1002/ejhf.1732

213. Yazaki Y, Isobe M, Takahashi W, Kitabayashi H, Nishiyama O, Sekiguchi M, Takemura T. Assessment of myocardial fatty acid metabolic abnormalities in patients with idiopathic dilated cardiomyopathy using 123I BMIPP SPECT: correlation with clinicopathological findings and clinical course. *Heart*. 1999;81:153-159. doi: 10.1136/hrt.81.2.153

214. Davila-Roman VG, Vedala G, Herrero P, de las Fuentes L, Rogers JG, Kelly DP, Gropler RJ. Altered myocardial fatty acid and glucose metabolism in idiopathic dilated cardiomyopathy. *J Am Coll Cardiol*. 2002;40:271-277. doi: 10.1016/s0735-1097(02)01967-8

215. Sharma S, Adrogue JV, Golfman L, Uray I, Lemm J, Youker K, Noon GP, Frazier OH, Taegtmeyer H. Intramyocardial lipid accumulation in the failing human heart resembles the lipotoxic rat heart. *FASEB J*. 2004;18:1692-1700. doi: 10.1096/fj.04-2263com

216. Zhou YT, Grayburn P, Karim A, Shimabukuro M, Higa M, Baetens D, Orci L, Unger RH. Lipotoxic heart disease in obese rats: implications for human obesity. *Proc Natl Acad Sci U S A*. 2000;97:1784-1789.

217. Singh JSS, Mordi IR, Vickneson K, Fathi A, Donnan PT, Mohan M, Choy AMJ, Gandy S, George J, Khan F, et al. Dapagliflozin Versus Placebo on Left Ventricular Remodeling in Patients With Diabetes and Heart Failure: The REFORM Trial. *Diabetes Care*. 2020;43:1356-1359. doi: 10.2337/dc19-2187

218. Docherty KF, Campbell RT, Brooksbank KJM, Dreisbach JG, Forsyth P, Godeseth RL, Hopkins T, Jackson AM, Lee MMY, McConnachie A, et al. Effect of Neprilysin Inhibition on Left Ventricular Remodeling in Patients With Asymptomatic Left Ventricular Systolic Dysfunction Late After Myocardial Infarction. *Circulation*. 2021;144:199-209. doi: 10.1161/CIRCULATIONAHA.121.054892

219. Plata Mosquera Cea. Reduction of extracellular volume and reverse cardiac remodeling during sacubitril/valsartan therapy assessed by cardiac magnetic

resonance in patients with heart failure (REMODELING CMR-HF). *EHJCI*. 2021.

220. Newman AA, Grimm NC, Wilburn JR, Schoenberg HM, Trikha SRJ, Luckasen GJ, Biela LM, Melby CL, Bell C. Influence of Sodium Glucose Cotransporter 2 Inhibition on Physiological Adaptation to Endurance Exercise Training. *J Clin Endocrinol Metab*. 2019;104:1953-1966. doi: 10.1210/jc.2018-01741

221. McMurray J. DETERMINE-reduced - Dapagliflozin effect on exercise capacity using a 6-minute walk test in patients with heart failure with reduced ejection fraction. In: *ESC Heart Failure 2021*. 2021.

222. Abraham WT, Lindenfeld J, Ponikowski P, Agostoni P, Butler J, Desai AS, Filippatos G, Gniot J, Fu M, Gullestad L, et al. Effect of empagliflozin on exercise ability and symptoms in heart failure patients with reduced and preserved ejection fraction, with and without type 2 diabetes. *Eur Heart J*. 2021;42:700-710. doi: 10.1093/eurheartj/ehaa943

223. Petrie MC, Lee MM, Lang NN. EMPEROR-REDUCED reigns while EMPERIAL whimpers. *Eur Heart J*. 2021;42:711-714. doi: 10.1093/eurheartj/ehaa965

224. Spertus JA, Birmingham MC, Nassif M, Damaraju CV, Abbate A, Butler J, Lanfear DE, Lingvay I, Kosiborod MN, Januzzi JL. The SGLT2 inhibitor canagliflozin in heart failure: the CHIEF-HF remote, patient-centered randomized trial. *Nat Med*. 2022;28:809-813. doi: 10.1038/s41591-022-01703-8

225. Namasivayam M, Lau ES, Zern EK, Schoenike MW, Hardin KM, Sbarbaro JA, Cunningham TF, Farrell RM, Rouvina J, Kowal A, et al. Exercise Blood Pressure in Heart Failure With Preserved and Reduced Ejection Fraction. *JACC Heart Fail*. 2022;10:278-286. doi: 10.1016/j.jchf.2022.01.012

226. Scheen AJ. Effect of SGLT2 Inhibitors on the Sympathetic Nervous System and Blood Pressure. *Curr Cardiol Rep*. 2019;21:70. doi: 10.1007/s11886-019-1165-1

227. Chilton R, Tikkanen I, Cannon CP, Crowe S, Woerle HJ, Broedl UC, Johansen OE. Effects of empagliflozin on blood pressure and markers of arterial stiffness and vascular resistance in patients with type 2 diabetes. *Diabetes Obes Metab*. 2015;17:1180-1193. doi: 10.1111/dom.12572

228. Cherney DZ, Perkins BA, Soleymanlou N, Har R, Fagan N, Johansen OE, Woerle HJ, von Eynatten M, Broedl UC. The effect of empagliflozin on arterial stiffness and heart rate variability in subjects with uncomplicated type 1 diabetes mellitus. *Cardiovasc Diabetol*. 2014;13:28. doi: 10.1186/1475-2840-13-28

229. Aimo A, Januzzi JL, Jr., Vergaro G, Ripoli A, Latini R, Masson S, Magnoli M, Anand IS, Cohn JN, Tavazzi L, et al. High-sensitivity troponin T, NT-proBNP and glomerular filtration rate: A multimarker strategy for risk stratification in chronic heart failure. *Int J Cardiol*. 2019;277:166-172. doi: 10.1016/j.ijcard.2018.10.079

230. Voors AA, Angermann CE, Teerlink JR, Collins SP, Kosiborod M, Biegus J, Ferreira JP, Nassif ME, Psotka MA, Tromp J, et al. The SGLT2 inhibitor empagliflozin in patients hospitalized for acute heart failure: a multinational randomized trial. *Nat Med*. 2022;28:568-574. doi: 10.1038/s41591-021-01659-1

231. Januzzi JL, Jr., Zannad F, Anker SD, Butler J, Filippatos G, Pocock SJ, Ferreira JP, Sattar N, Verma S, Vedin O, et al. Prognostic Importance of NT-proBNP and Effect of Empagliflozin in the EMPEROR-Reduced Trial. *J Am Coll Cardiol*. 2021;78:1321-1332. doi: 10.1016/j.jacc.2021.07.046

232. Neal B, Perkovic V, Mahaffey KW, de Zeeuw D, Fulcher G, Erondu N, Shaw W, Law G, Desai M, Matthews DR, et al. Canagliflozin and Cardiovascular and Renal Events in Type 2 Diabetes. *N Engl J Med*. 2017. doi: 10.1056/NEJMoa1611925

233. Tanaka A, Hisauchi I, Taguchi I, Sezai A, Toyoda S, Tomiyama H, Sata M, Ueda S, Oyama JI, Kitakaze M, et al. Effects of canagliflozin in patients with type 2 diabetes and chronic heart failure: a randomized trial (CANDLE). *ESC Heart Fail*. 2020;7:1585-1594. doi: 10.1002/ehf2.12707

234. Myhre PL, Vaduganathan M, Claggett B, Packer M, Desai AS, Rouleau JL, Zile MR, Swedberg K, Lefkowitz M, Shi V, et al. B-Type Natriuretic Peptide During Treatment With Sacubitril/Valsartan: The PARADIGM-HF Trial. *J Am Coll Cardiol*. 2019;73:1264-1272. doi: 10.1016/j.jacc.2019.01.018

235. Januzzi JL, Jr., Prescott MF, Butler J, Felker GM, Maisel AS, McCague K, Camacho A, Pina IL, Rocha RA, Shah AM, et al. Association of Change in N-Terminal Pro-B-Type Natriuretic Peptide Following Initiation of Sacubitril-Valsartan Treatment With Cardiac Structure and Function in Patients With Heart Failure With Reduced Ejection Fraction. *JAMA*. 2019;322:1085-1095. doi: 10.1001/jama.2019.12821

236. McMurray JJ, Packer M, Desai AS, Gong J, Lefkowitz MP, Rizkala AR, Rouleau JL, Shi VC, Solomon SD, Swedberg K, et al. Angiotensin-neprilysin inhibition versus enalapril in heart failure. *N Engl J Med*. 2014;371:993-1004. doi: 10.1056/NEJMoa1409077

237. Lawler PR, Liu H, Frankfurter C, Lovblom LE, Lytvyn Y, Burger D, Burns KD, Brinc D, Cherney DZI. Changes in Cardiovascular Biomarkers Associated With the Sodium-Glucose Cotransporter 2 (SGLT2) Inhibitor Ertugliflozin in Patients With Chronic Kidney Disease and Type 2 Diabetes. *Diabetes Care*. 2021;44:e45-e47. doi: 10.2337/dc20-2265

238. Greene SJ, Fonarow GC, Solomon SD, Subacius H, Maggioni AP, Bohm M, Lewis EF, Zannad F, Gheorghiade M, Investigators A, et al. Global variation in clinical profile, management, and post-discharge outcomes among patients hospitalized for worsening chronic heart failure: findings from the ASTRONAUT trial. *Eur J Heart Fail*. 2015;17:591-600. doi: 10.1002/ejhf.280

239. Carnethon MR, Pu J, Howard G, Albert MA, Anderson CAM, Bertoni AG, Mujahid MS, Palaniappan L, Taylor HA, Jr., Willis M, et al. Cardiovascular Health in African Americans: A Scientific Statement From the American Heart Association. *Circulation*. 2017;136:e393-e423. doi: 10.1161/CIR.0000000000000534

240. Heusch G, Libby P, Gersh B, Yellon D, Bohm M, Lopaschuk G, Opie L. Cardiovascular remodelling in coronary artery disease and heart failure. *Lancet*. 2014;383:1933-1943. doi: 10.1016/S0140-6736(14)60107-0

241. Levelt E, Rodgers CT, Clarke WT, Mahmod M, Ariga R, Francis JM, Liu A, Wijesurendra RS, Dass S, Sabharwal N, et al. Cardiac energetics, oxygenation, and perfusion during increased workload in patients with type 2 diabetes mellitus. *Eur Heart J*. 2016;37:3461-3469. doi: 10.1093/eurheartj/ehv442

242. Schroeder MA, Clarke K, Neubauer S, Tyler DJ. Hyperpolarized magnetic resonance: a novel technique for the in vivo assessment of cardiovascular disease. *Circulation*. 2011;124:1580-1594. doi: 10.1161/CIRCULATIONAHA.111.024919

243. Dougherty AH, Naccarelli GV, Gray EL, Hicks CH, Goldstein RA. Congestive heart failure with normal systolic function. *Am J Cardiol*. 1984;54:778-782. doi: 10.1016/s0002-9149(84)80207-6

244. Yusuf S, Pfeffer MA, Swedberg K, Granger CB, Held P, McMurray JJ, Michelson EL, Olofsson B, Ostergren J, Investigators C, et al. Effects of candesartan in patients with chronic heart failure and preserved left-ventricular ejection fraction: the CHARM-Preserved Trial. *Lancet*. 2003;362:777-781. doi: 10.1016/S0140-6736(03)14285-7

245. Digitalis Investigation G. The effect of digoxin on mortality and morbidity in patients with heart failure. *N Engl J Med*. 1997;336:525-533. doi: 10.1056/NEJM199702203360801

246. Flather MD, Shibata MC, Coats AJ, Van Veldhuisen DJ, Parkhomenko A, Borbola J, Cohen-Solal A, Dumitrascu D, Ferrari R, Lechat P, et al. Randomized trial to determine the effect of nebivolol on mortality and cardiovascular hospital admission in elderly patients with heart failure (SENIORS). *Eur Heart J*. 2005;26:215-225. doi: 10.1093/eurheartj/ehi115

247. Cleland JG, Tendera M, Adamus J, Freemantle N, Polonski L, Taylor J, Investigators P-C. The perindopril in elderly people with chronic heart failure (PEP-CHF) study. *Eur Heart J*. 2006;27:2338-2345. doi: 10.1093/eurheartj/ehl250

248. Massie BM, Carson PE, McMurray JJ, Komajda M, McKelvie R, Zile MR, Anderson S, Donovan M, Iverson E, Staiger C, et al. Irbesartan in patients with heart failure and preserved ejection fraction. *N Engl J Med*. 2008;359:2456-2467. doi: 10.1056/NEJMoa0805450

249. Solomon SD, Zile M, Pieske B, Voors A, Shah A, Kraigher-Krainer E, Shi V, Bransford T, Takeuchi M, Gong J, et al. The angiotensin receptor neprilysin inhibitor LCZ696 in heart failure with preserved ejection

fraction: a phase 2 double-blind randomised controlled trial. *Lancet*. 2012;380:1387-1395. doi: 10.1016/S0140-6736(12)61227-6

250. Edelmann F, Wachter R, Schmidt AG, Kraigher-Krainer E, Colantonio C, Kamke W, Duvinage A, Stahrenberg R, Durstewitz K, Loffler M, et al. Effect of spironolactone on diastolic function and exercise capacity in patients with heart failure with preserved ejection fraction: the Aldo-DHF randomized controlled trial. *JAMA*. 2013;309:781-791. doi: 10.1001/jama.2013.905

251. Redfield MM, Chen HH, Borlaug BA, Semigran MJ, Lee KL, Lewis G, LeWinter MM, Rouleau JL, Bull DA, Mann DL, et al. Effect of phosphodiesterase-5 inhibition on exercise capacity and clinical status in heart failure with preserved ejection fraction: a randomized clinical trial. *JAMA*. 2013;309:1268-1277. doi: 10.1001/jama.2013.2024

252. Pitt B, Pfeffer MA, Assmann SF, Boineau R, Anand IS, Claggett B, Clausell N, Desai AS, Diaz R, Fleg JL, et al. Spironolactone for heart failure with preserved ejection fraction. *N Engl J Med*. 2014;370:1383-1392. doi: 10.1056/NEJMoa1313731

253. Komajda M, Isnard R, Cohen-Solal A, Metra M, Pieske B, Ponikowski P, Voors AA, Dominjon F, Henon-Goburdhun C, Pannaux M, et al. Effect of ivabradine in patients with heart failure with preserved ejection fraction: the EDIFY randomized placebo-controlled trial. *Eur J Heart Fail*. 2017;19:1495-1503. doi: 10.1002/ejhf.876

254. Solomon SD, McMurray JJV, Anand IS, Ge J, Lam CSP, Maggioni AP, Martinez F, Packer M, Pfeffer MA, Pieske B, et al. Angiotensin-Neprilysin Inhibition in Heart Failure with Preserved Ejection Fraction. *N Engl J Med*. 2019;381:1609-1620. doi: 10.1056/NEJMoa1908655

255. Hahn VS, Knutsdottir H, Luo X, Bedi K, Margulies KB, Haldar SM, Stolina M, Yin J, Khakoo AY, Vaishnav J, et al. Myocardial Gene Expression Signatures in Human Heart Failure With Preserved Ejection Fraction. *Circulation*. 2021;143:120-134. doi: 10.1161/CIRCULATIONAHA.120.050498

256. Kumar AA, Kelly DP, Chirinos JA. Mitochondrial Dysfunction in Heart Failure With Preserved Ejection Fraction. *Circulation*. 2019;139:1435-1450. doi: 10.1161/CIRCULATIONAHA.118.036259

257. Burrage MK, Hundertmark M, Valkovic L, Watson WD, Rayner J, Sabharwal N, Ferreira VM, Neubauer S, Miller JJ, Rider OJ, et al. Energetic Basis for Exercise-Induced Pulmonary Congestion in Heart Failure With Preserved Ejection Fraction. *Circulation*. 2021;144:1664-1678. doi: 10.1161/CIRCULATIONAHA.121.054858

258. Tombolesi N, Altara R, da Silva GJJ, Tannous C, Zouein FA, Stenslokken KO, Morresi A, Paolantoni M, Booz GW, Cataliotti A, et al. Early cardiac-chamber-specific fingerprints in heart failure with preserved ejection fraction detected by FTIR and Raman spectroscopic techniques. *Sci Rep*. 2022;12:3440. doi: 10.1038/s41598-022-07390-2

259. Lamb HJ, Beyerbacht HP, van der Laarse A, Stoel BC, Doornbos J, van der Wall EE, de Roos A. Diastolic dysfunction in hypertensive heart disease is associated with altered myocardial metabolism. *Circulation*. 1999;99:2261-2267. doi: 10.1161/01.cir.99.17.2261

260. Deng Y, Xie M, Li Q, Xu X, Ou W, Zhang Y, Xiao H, Yu H, Zheng Y, Liang Y, et al. Targeting Mitochondria-Inflammation Circuit by beta-Hydroxybutyrate Mitigates HFpEF. *Circ Res*. 2021;128:232-245. doi: 10.1161/CIRCRESAHA.120.317933

261. Connelly KA, Zhang Y, Visram A, Advani A, Batchu SN, Desjardins JF, Thai K, Gilbert RE. Empagliflozin Improves Diastolic Function in a Nondiabetic Rodent Model of Heart Failure With Preserved Ejection Fraction. *JACC Basic Transl Sci*. 2019;4:27-37. doi: 10.1016/j.jacbts.2018.11.010

262. Byrne NJ, Matsumura N, Maayah ZH, Ferdaoussi M, Takahara S, Darwesh AM, Levasseur JL, Jahng JWS, Vos D, Parajuli N, et al. Empagliflozin Blunts Worsening Cardiac Dysfunction Associated With Reduced NLRP3 (Nucleotide-Binding Domain-Like Receptor Protein 3) Inflammasome Activation in Heart Failure. *Circ Heart Fail*. 2020;13:e006277. doi: 10.1161/CIRCHEARTFAILURE.119.006277

263. Bayes-Genis A, Iborra-Egea O, Spitaleri G, Domingo M, Revuelta-Lopez E, Codina P, Cediel G, Santiago-Vacas E, Cserkoova A, Pascual-Figal D, et al. Decoding empagliflozin's molecular mechanism of action in heart failure with preserved ejection fraction using artificial intelligence. *Sci Rep*. 2021;11:12025. doi: 10.1038/s41598-021-91546-z

264. Shah AM, Claggett B, Sweitzer NK, Shah SJ, Anand IS, O'Meara E, Desai AS, Heitner JF, Li G, Fang J, et al. Cardiac structure and function and prognosis in heart failure with preserved ejection fraction: findings from the echocardiographic study of the Treatment of Preserved Cardiac Function Heart Failure with an Aldosterone Antagonist (TOPCAT) Trial. *Circ Heart Fail*. 2014;7:740-751. doi: 10.1161/CIRCHEARTFAILURE.114.001583

265. Kraigher-Krainer E, Shah AM, Gupta DK, Santos A, Claggett B, Pieske B, Zile MR, Voors AA, Lefkowitz MP, Packer M, et al. Impaired systolic function by strain imaging in heart failure with preserved ejection fraction. *J Am Coll Cardiol*. 2014;63:447-456. doi: 10.1016/j.jacc.2013.09.052

266. Shah AM, Claggett B, Sweitzer NK, Shah SJ, Anand IS, Liu L, Pitt B, Pfeffer MA, Solomon SD. Prognostic Importance of Impaired Systolic Function in Heart Failure With Preserved Ejection Fraction and the Impact of Spironolactone. *Circulation*. 2015;132:402-414. doi: 10.1161/CIRCULATIONAHA.115.015884

267. Gamaza-Chulian S, Diaz-Retamino E, Gonzalez-Teston F, Gaitero JC, Castillo MJ, Alfaro R, Rodriguez E, Gonzalez-Caballero E, Martin-Santana A. Effect of sodium-glucose cotransporter 2 (SGLT2) inhibitors on left ventricular remodelling and longitudinal strain: a prospective observational study. *BMC Cardiovasc Disord*. 2021;21:456. doi: 10.1186/s12872-021-02250-9

268. Juni RP, Kuster DWD, Goebel M, Helmes M, Musters RJP, van der Velden J, Koolwijk P, Paulus WJ, van Hinsbergh VWM. Cardiac Microvascular Endothelial Enhancement of Cardiomyocyte Function Is Impaired by Inflammation and Restored by Empagliflozin. *JACC Basic Transl Sci*. 2019;4:575-591. doi: 10.1016/j.jacbts.2019.04.003

269. Kolijn D, Pabel S, Tian Y, Lodi M, Herwig M, Carrizzo A, Zhazykbayeva S, Kovacs A, Fulop GA, Falcao-Pires I, et al. Empagliflozin improves endothelial and cardiomyocyte function in human heart failure with preserved ejection fraction via reduced pro-inflammatory-oxidative pathways and protein kinase Galpha oxidation. *Cardiovasc Res*. 2021;117:495-507. doi: 10.1093/cvr/cvaa123

270. Guazzi M. Cardiopulmonary exercise testing in heart failure preserved ejection fraction: Time to expand the paradigm in the prognostic algorithm. *Am Heart J*. 2016;174:164-166. doi: 10.1016/j.ahj.2016.01.002

271. Yan J, Gong SJ, Li L, Yu HY, Dai HW, Chen J, Tan CW, Xv QH, Cai GL. Combination of B-type natriuretic peptide and minute ventilation/carbon dioxide production slope improves risk stratification in patients with diastolic heart failure. *Int J Cardiol*. 2013;162:193-198. doi: 10.1016/j.ijcard.2011.07.017

272. Guazzi M, Myers J, Peberdy MA, Bensimhon D, Chase P, Arena R. Exercise oscillatory breathing in diastolic heart failure: prevalence and prognostic insights. *Eur Heart J*. 2008;29:2751-2759. doi: 10.1093/eurheartj/ehn437

273. Guazzi M, Myers J, Arena R. Cardiopulmonary exercise testing in the clinical and prognostic assessment of diastolic heart failure. *J Am Coll Cardiol*. 2005;46:1883-1890. doi: 10.1016/j.jacc.2005.07.051

274. Taijyu Satoh LW, Charles F McTiernan , Andrea Levine , Jeff Baust , Yen Chun Lai and Mark T Gladwin. Abstract 11662: SGLT2 Inhibitor Improved Exercise-induced Pulmonary Hypertension (EIPH) in Heart Failure With Preserved Ejection Fraction. In: *AHA Scientific Sessions*. 2019.

275. Nassif ME, Qintar M, Windsor SL, Jermyn R, Shavelle DM, Tang F, Lamba S, Bhatt K, Brush J, Civitello A, et al. Empagliflozin Effects on Pulmonary Artery Pressure in Patients With Heart Failure: Results From the EMBRACE-HF Trial. *Circulation*. 2021;143:1673-1686. doi: 10.1161/CIRCULATIONAHA.120.052503

276. Pieske B, Wachter R, Shah SJ, Baldridge A, Szeczoedy P, Ibram G, Shi V, Zhao Z, Cowie MR, Investigators P, et al. Effect of Sacubitril/Valsartan vs Standard Medical Therapies on Plasma NT-proBNP Concentration and Submaximal Exercise Capacity in Patients With Heart Failure and Preserved Ejection Fraction: The PARALLAX Randomized Clinical Trial. *JAMA*. 2021;326:1919-1929. doi: 10.1001/jama.2021.18463

277. Andrea R, Lopez-Giraldo A, Falces C, Lopez T, Sanchis L, Gistau C, Sabate M, Sitges M, Brugada J, Agusti A. Pulmonary function predicts mortality

and hospitalizations in outpatients with heart failure and preserved ejection fraction. *Respir Med*. 2018;134:124-129. doi: 10.1016/j.rmed.2017.12.004

278. Butler J, Filippatos G, Jamal Siddiqi T, Brueckmann M, Bohm M, Chopra VK, Pedro Ferreira J, Januzzi JL, Kaul S, Pina IL, et al. Empagliflozin, Health Status, and Quality of Life in Patients With Heart Failure and Preserved Ejection Fraction: The EMPEROR-Preserved Trial. *Circulation*. 2022;145:184-193. doi: 10.1161/CIRCULATIONAHA.121.057812

279. Verbrugge FH, Omote K, Reddy YNV, Sorimachi H, Obokata M, Borlaug BA. Heart failure with preserved ejection fraction in patients with normal natriuretic peptide levels is associated with increased morbidity and mortality. *Eur Heart J*. 2022. doi: 10.1093/eurheartj/ehab911

280. Packer M, Lam CSP, Lund LH, Maurer MS, Borlaug BA. Characterization of the inflammatory-metabolic phenotype of heart failure with a preserved ejection fraction: a hypothesis to explain influence of sex on the evolution and potential treatment of the disease. *Eur J Heart Fail*. 2020;22:1551-1567. doi: 10.1002/ejhf.1902

281. Butler J, Fonarow GC, Zile MR, Lam CS, Roessig L, Schelbert EB, Shah SJ, Ahmed A, Bonow RO, Cleland JG, et al. Developing therapies for heart failure with preserved ejection fraction: current state and future directions. *JACC Heart Fail*. 2014;2:97-112. doi: 10.1016/j.jchf.2013.10.006

282. Harada T, Obokata M. Obesity-Related Heart Failure with Preserved Ejection Fraction: Pathophysiology, Diagnosis, and Potential Therapies. *Heart Fail Clin*. 2020;16:357-368. doi: 10.1016/j.hfc.2020.02.004

283. Haass M, Kitzman DW, Anand IS, Miller A, Zile MR, Massie BM, Carson PE. Body mass index and adverse cardiovascular outcomes in heart failure patients with preserved ejection fraction: results from the Irbesartan in Heart Failure with Preserved Ejection Fraction (I-PRESERVE) trial. *Circ Heart Fail*. 2011;4:324-331. doi: 10.1161/CIRCHEARTFAILURE.110.959890

284. Fonarow GC, Srikanthan P, Costanzo MR, Cintron GB, Lopatin M, Committee ASA, Investigators. An obesity paradox in acute heart failure: analysis of body mass index and inhospital mortality for 108,927 patients in the Acute Decompensated Heart Failure National Registry. *Am Heart J*. 2007;153:74-81. doi: 10.1016/j.ahj.2006.09.007

285. Kenchaiah S, Pocock SJ, Wang D, Finn PV, Zornoff LA, Skali H, Pfeffer MA, Yusuf S, Swedberg K, Michelson EL, et al. Body mass index and prognosis in patients with chronic heart failure: insights from the Candesartan in Heart failure: Assessment of Reduction in Mortality and morbidity (CHARM) program. *Circulation*. 2007;116:627-636. doi: 10.1161/CIRCULATIONAHA.106.679779

286. Kritchevsky SB, Beavers KM, Miller ME, Shea MK, Houston DK, Kitzman DW, Nicklas BJ. Intentional weight loss and all-cause mortality: a meta-analysis of randomized clinical trials. *PLoS One*. 2015;10:e0121993. doi: 10.1371/journal.pone.0121993

287. Taegtmeyer H, Golfman L, Sharma S, Razeghi P, van Arsdall M. Linking gene expression to function: metabolic flexibility in the normal and diseased heart. *Ann N Y Acad Sci*. 2004;1015:202-213. doi: 10.1196/annals.1302.017

288. Rider OJ, Cox P, Tyler D, Clarke K, Neubauer S. Myocardial substrate metabolism in obesity. *Int J Obes (Lond)*. 2013;37:972-979. doi: 10.1038/ijo.2012.170

289. Palanivel R, Fang X, Park M, Eguchi M, Pallan S, De Girolamo S, Liu Y, Wang Y, Xu A, Sweeney G. Globular and full-length forms of adiponectin mediate specific changes in glucose and fatty acid uptake and metabolism in cardiomyocytes. *Cardiovasc Res*. 2007;75:148-157. doi: 10.1016/j.cardiores.2007.04.011

290. Lean ME, Leslie WS, Barnes AC, Brosnahan N, Thom G, McCombie L, Peters C, Zhyzhneuskaya S, Al-Mrabeh A, Hollingsworth KG, et al. Primary care-led weight management for remission of type 2 diabetes (DiRECT): an open-label, cluster-randomised trial. *Lancet*. 2018;391:541-551. doi: 10.1016/S0140-6736(17)33102-1

291. Reddy YNV, Obokata M, Wiley B, Koepp KE, Jorgenson CC, Egbe A, Melenovsky V, Carter RE, Borlaug BA. The haemodynamic basis of lung congestion during exercise in heart failure with preserved ejection fraction. *Eur Heart J*. 2019;40:3721-3730. doi: 10.1093/eurheartj/ehz713

292. Tyler DJ, Hudsmith LE, Clarke K, Neubauer S, Robson MD. A comparison of cardiac (31)P MRS at 1.5 and 3 T. *Nmr Biomed*. 2008;21:793-798. doi: 10.1002/nbm.1255

293. Horn M NS, Bomhard M, Kadgien M, Schnackerz K, Ertl G. 31P-NMR spectroscopy of human blood and serum: first results from volunteers and oatients with congestive heart failure, diabetes mellitus and hyperlipidaemia. *MAGMA Magnetic Resonance Materials in Physics, Biology and Medicine*. 1993:55-60. doi: https://doi.org/10.1007/BF01760400

294. Pandey A, Patel KV, Vaduganathan M, Sarma S, Haykowsky MJ, Berry JD, Lavie CJ. Physical Activity, Fitness, and Obesity in Heart Failure With Preserved Ejection Fraction. *JACC Heart Fail*. 2018;6:975-982. doi: 10.1016/j.jchf.2018.09.006

295. Maisel AS, Shah KS, Barnard D, Jaski B, Frivold G, Marais J, Azer M, Miyamoto MI, Lombardo D, Kelsay D, et al. How B-Type Natriuretic Peptide (BNP) and Body Weight Changes Vary in Heart Failure With Preserved Ejection Fraction Compared With Reduced Ejection Fraction: Secondary Results of the HABIT (HF Assessment With BNP in the Home) Trial. *J Card Fail*. 2016;22:283-293. doi: 10.1016/j.cardfail.2015.09.014

296. Scherbakov N, Bauer M, Sandek A, Szabo T, Topper A, Jankowska EA, Springer J, von Haehling S, Anker SD, Lainscak M, et al. Insulin resistance in heart failure: differences between patients with reduced and preserved left ventricular ejection fraction. *Eur J Heart Fail*. 2015;17:1015-1021. doi: 10.1002/ejhf.317

297. van Vliet S, Koh HE, Patterson BW, Yoshino M, LaForest R, Gropler RJ, Klein S, Mittendorfer B. Obesity Is Associated With Increased Basal and Postprandial beta-Cell Insulin Secretion Even in the Absence of Insulin Resistance. *Diabetes*. 2020;69:2112-2119. doi: 10.2337/db20-0377

298. Rayner JJ, Abdesselam I, Peterzan MA, Akoumianakis I, Akawi N, Antoniades C, Tomlinson JW, Neubauer S, Rider OJ. Very low calorie diets are associated with transient ventricular impairment before reversal of diastolic dysfunction in obesity. *Int J Obes (Lond)*. 2019;43:2536-2544. doi: 10.1038/s41366-018-0263-2

299. Rider OJ, Francis JM, Tyler D, Byrne J, Clarke K, Neubauer S. Effects of weight loss on myocardial energetics and diastolic function in obesity. *Int J Cardiovasc Imaging*. 2013;29:1043-1050. doi: 10.1007/s10554-012-0174-6

300. Mohammed SF, Hussain I, AbouEzzeddine OF, Takahama H, Kwon SH, Forfia P, Roger VL, Redfield MM. Right ventricular function in heart failure with preserved ejection fraction: a community-based study. *Circulation*. 2014;130:2310-2320. doi: 10.1161/CIRCULATIONAHA.113.008461

301. Gorter TM, Obokata M, Reddy YNV, Melenovsky V, Borlaug BA. Exercise unmasks distinct pathophysiologic features in heart failure with preserved ejection fraction and pulmonary vascular disease. *Eur Heart J*. 2018;39:2825-2835. doi: 10.1093/eurheartj/ehy331

302. Nakagawa A, Yasumura Y, Yoshida C, Okumura T, Tateishi J, Yoshida J, Abe H, Tamaki S, Yano M, Hayashi T, et al. Prognostic Importance of Right Ventricular-Vascular Uncoupling in Acute Decompensated Heart Failure With Preserved Ejection Fraction. *Circ Cardiovasc Imaging*. 2020;13:e011430. doi: 10.1161/CIRCIMAGING.120.011430

303. Seferovic PM, Petrie MC, Filippatos GS, Anker SD, Rosano G, Bauersachs J, Paulus WJ, Komajda M, Cosentino F, de Boer RA, et al. Type 2 diabetes mellitus and heart failure: a position statement from the Heart Failure Association of the European Society of Cardiology. *Eur J Heart Fail*. 2018. doi: 10.1002/ejhf.1170

304. Rubler S, Dlugash J, Yuceoglu YZ, Kumral T, Branwood AW, Grishman A. New type of cardiomyopathy associated with diabetic glomerulosclerosis. *Am J Cardiol*. 1972;30:595-602. doi: 10.1016/0002-9149(72)90595-4

305. Dunlay SM, Givertz MM, Aguilar D, Allen LA, Chan M, Desai AS, Deswal A, Dickson VV, Kosiborod MN, Lekavich CL, et al. Type 2 Diabetes Mellitus and Heart Failure: A Scientific Statement From the American Heart Association and the Heart Failure Society of America: This statement does not represent an update of the 2017 ACC/AHA/HFSA heart failure guideline update. *Circulation*. 2019;140:e294-e324. doi: 10.1161/CIR.0000000000000691

306. Fukushima A, Lopaschuk GD. Cardiac fatty acid oxidation in heart failure associated with obesity and diabetes. *Biochim Biophys Acta*. 2016;1861:1525-1534. doi: 10.1016/j.bbalip.2016.03.020

307. Maack C, Lehrke M, Backs J, Heinzel FR, Hulot JS, Marx N, Paulus WJ, Rossignol P, Taegtmeyer H, Bauersachs J, et al. Heart failure and diabetes: metabolic alterations and therapeutic interventions: a state-of-the-art review from the Translational Research Committee of the Heart Failure Association-European Society of Cardiology. *Eur Heart J*. 2018;39:4243-4254. doi: 10.1093/eurheartj/ehy596

308. van de Weijer T, Schrauwen-Hinderling VB, Schrauwen P. Lipotoxicity in type 2 diabetic cardiomyopathy. *Cardiovasc Res*. 2011;92:10-18. doi: 10.1093/cvr/cvr212

309. Chiu HC, Kovacs A, Ford DA, Hsu FF, Garcia R, Herrero P, Saffitz JE, Schaffer JE. A novel mouse model of lipotoxic cardiomyopathy. *J Clin Invest*. 2001;107:813-822. doi: 10.1172/JCI10947

310. Levelt E, Pavlides M, Banerjee R, Mahmod M, Kelly C, Sellwood J, Ariga R, Thomas S, Francis J, Rodgers C, et al. Ectopic and Visceral Fat Deposition in Lean and Obese Patients With Type 2 Diabetes. *J Am Coll Cardiol*. 2016;68:53-63. doi: 10.1016/j.jacc.2016.03.597

311. Levelt E, Mahmod M, Piechnik SK, Ariga R, Francis JM, Rodgers CT, Clarke WT, Sabharwal N, Schneider JE, Karamitsos TD, et al. Relationship Between Left Ventricular Structural and Metabolic Remodeling in Type 2 Diabetes. *Diabetes*. 2016;65:44-52. doi: 10.2337/db15-0627

312. Taylor M, Wallhaus TR, Degrado TR, Russell DC, Stanko P, Nickles RJ, Stone CK. An evaluation of myocardial fatty acid and glucose uptake using PET with [18F]fluoro-6-thia-heptadecanoic acid and [18F]FDG in Patients with Congestive Heart Failure. *J Nucl Med*. 2001;42:55-62.

313. Stone CK, Holden JE, Stanley W, Perlman SB. Effect of nicotinic acid on exogenous myocardial glucose utilization. *J Nucl Med*. 1995;36:996-1002.

314. Group HTC, Landray MJ, Haynes R, Hopewell JC, Parish S, Aung T, Tomson J, Wallendszus K, Craig M, Jiang L, et al. Effects of extended-release niacin with laropiprant in high-risk patients. *N Engl J Med*. 2014;371:203-212. doi: 10.1056/NEJMoa1300955

315. Lai E, De Lepeleire I, Crumley TM, Liu F, Wenning LA, Michiels N, Vets E, O'Neill G, Wagner JA, Gottesdiener K. Suppression of niacin-induced vasodilation with an antagonist to prostaglandin D2 receptor subtype 1. *Clin Pharmacol Ther*. 2007;81:849-857. doi: 10.1038/sj.clpt.6100180

316. Lai E, Wenning LA, Crumley TM, De Lepeleire I, Liu F, de Hoon JN, Van Hecken A, Depre M, Hilliard D, Greenberg H, et al. Pharmacokinetics, pharmacodynamics, and safety of a prostaglandin D2 receptor antagonist. *Clin Pharmacol Ther*. 2008;83:840-847. doi: 10.1038/sj.clpt.6100345

317. Mazumder PK, O'Neill BT, Roberts MW, Buchanan J, Yun UJ, Cooksey RC, Boudina S, Abel ED. Impaired cardiac efficiency and increased fatty

acid oxidation in insulin-resistant ob/ob mouse hearts. *Diabetes*. 2004;53:2366-2374. doi: 10.2337/diabetes.53.9.2366

318. Lipskaia L, Chemaly ER, Hadri L, Lompre AM, Hajjar RJ. Sarcoplasmic reticulum Ca(2+) ATPase as a therapeutic target for heart failure. *Expert Opin Biol Ther*. 2010;10:29-41. doi: 10.1517/14712590903321462

319. Le Page LM, Rider OJ, Lewis AJ, Ball V, Clarke K, Johansson E, Carr CA, Heather LC, Tyler DJ. Increasing Pyruvate Dehydrogenase Flux as a Treatment for Diabetic Cardiomyopathy: A Combined 13C Hyperpolarized Magnetic Resonance and Echocardiography Study. *Diabetes*. 2015;64:2735-2743. doi: 10.2337/db14-1560

320. Lewis AJ, Neubauer S, Tyler DJ, Rider OJ. Pyruvate dehydrogenase as a therapeutic target for obesity cardiomyopathy. *Expert Opin Ther Targets*. 2016;20:755-766. doi: 10.1517/14728222.2016.1126248

321. Li YJ, Wang PH, Chen C, Zou MH, Wang DW. Improvement of mechanical heart function by trimetazidine in db/db mice. *Acta Pharmacol Sin*. 2010;31:560-569. doi: 10.1038/aps.2010.31

322. Mansor LS, Sousa Fialho MDL, Yea G, Coumans WA, West JA, Kerr M, Carr CA, Luiken J, Glatz JFC, Evans RD, et al. Inhibition of sarcolemmal FAT/CD36 by sulfo-N-succinimidyl oleate rapidly corrects metabolism and restores function in the diabetic heart following hypoxia/reoxygenation. *Cardiovasc Res*. 2017;113:737-748. doi: 10.1093/cvr/cvx045

323. Rider OJ, Francis JM, Ali MK, Petersen SE, Robinson M, Robson MD, Byrne JP, Clarke K, Neubauer S. Beneficial cardiovascular effects of bariatric surgical and dietary weight loss in obesity. *J Am Coll Cardiol*. 2009;54:718-726. doi: 10.1016/j.jacc.2009.02.086

324. Xu HY, Yang ZG, Guo YK, Shi K, Liu X, Zhang Q, Jiang L, Xie LJ. Volume-time curve of cardiac magnetic resonance assessed left ventricular dysfunction in coronary artery disease patients with type 2 diabetes mellitus. *BMC Cardiovasc Disord*. 2017;17:145. doi: 10.1186/s12872-017-0583-5

325. Chamsi-Pasha MA, Zhan Y, Debs D, Shah DJ. CMR in the Evaluation of Diastolic Dysfunction and Phenotyping of HFpEF: Current Role and Future Perspectives. *JACC Cardiovasc Imaging*. 2020;13:283-296. doi: 10.1016/j.jcmg.2019.02.031

326. Contti MM, Barbosa MF, Del Carmen Villanueva Mauricio A, Nga HS, Valiatti MF, Takase HM, Bravin AM, de Andrade LGM. Kidney transplantation is associated with reduced myocardial fibrosis. A cardiovascular magnetic resonance study with native T1 mapping. *J Cardiovasc Magn Reson*. 2019;21:21. doi: 10.1186/s12968-019-0531-x

327. Patel N, Yaqoob MM, Aksentijevic D. Cardiac metabolic remodelling in chronic kidney disease. *Nat Rev Nephrol*. 2022. doi: 10.1038/s41581-022-00576-x

328. Yaribeygi H, Butler AE, Atkin SL, Katsiki N, Sahebkar A. Sodium-glucose cotransporter 2 inhibitors and inflammation in chronic kidney disease: Possible molecular pathways. *J Cell Physiol*. 2018. doi: 10.1002/jcp.26851

329. Heerspink HJL, Perco P, Mulder S, Leierer J, Hansen MK, Heinzel A, Mayer G. Canagliflozin reduces inflammation and fibrosis biomarkers: a potential mechanism of action for beneficial effects of SGLT2 inhibitors in diabetic kidney disease. *Diabetologia*. 2019;62:1154-1166. doi: 10.1007/s00125-019-4859-4

330. Kim SR, Lee SG, Kim SH, Kim JH, Choi E, Cho W, Rim JH, Hwang I, Lee CJ, Lee M, et al. SGLT2 inhibition modulates NLRP3 inflammasome activity via ketones and insulin in diabetes with cardiovascular disease. *Nat Commun*. 2020;11:2127. doi: 10.1038/s41467-020-15983-6

331. Xie L, Xiao Y, Tai S, Yang H, Zhou S, Zhou Z. Emerging Roles of Sodium Glucose Cotransporter 2 (SGLT-2) Inhibitors in Diabetic Cardiovascular Diseases: Focusing on Immunity, Inflammation and Metabolism. *Front Pharmacol*. 2022;13:836849. doi: 10.3389/fphar.2022.836849

332. Byrne NJ, Soni S, Takahara S, Ferdaoussi M, Al Batran R, Darwesh AM, Levasseur JL, Beker D, Vos DY, Schmidt MA, et al. Chronically Elevating Circulating Ketones Can Reduce Cardiac Inflammation and Blunt the Development of Heart Failure. *Circ Heart Fail*. 2020;13:e006573. doi: 10.1161/CIRCHEARTFAILURE.119.006573

333. Youm YH, Nguyen KY, Grant RW, Goldberg EL, Bodogai M, Kim D, D'Agostino D, Planavsky N, Lupfer C, Kanneganti TD, et al. The ketone metabolite beta-hydroxybutyrate blocks NLRP3 inflammasome-mediated inflammatory disease. *Nat Med*. 2015;21:263-269. doi: 10.1038/nm.3804

334. Ng ACT, Delgado V, Borlaug BA, Bax JJ. Diabesity: the combined burden of obesity and diabetes on heart disease and the role of imaging. *Nat Rev Cardiol*. 2021;18:291-304. doi: 10.1038/s41569-020-00465-5

335. Pieske B, Tschope C, de Boer RA, Fraser AG, Anker SD, Donal E, Edelmann F, Fu M, Guazzi M, Lam CSP, et al. How to diagnose heart failure with preserved ejection fraction: the HFA-PEFF diagnostic algorithm: a consensus recommendation from the Heart Failure Association (HFA) of the European Society of Cardiology (ESC). *Eur Heart J*. 2019;40:3297-3317. doi: 10.1093/eurheartj/ehz641

336. Menon RG, Xia D, Katz SD, Regatte RR. Dynamic (31)P-MRI and (31)P-MRS of lower leg muscles in heart failure patients. *Sci Rep*. 2021;11:7412. doi: 10.1038/s41598-021-86392-y